
**The Cellular and Molecular
Mechanisms of Glucocorticoid-
Induced Growth Retardation**

Helen Catriona Owen

Thesis submitted for the degree of Doctor of Philosophy

The University of Glasgow Faculty of Medicine

2007

Abstract

Since the introduction of glucocorticoids (GCs) in the treatment of rheumatoid arthritis in 1949, GC therapy has been associated with a number of adverse effects. Long-term use of GCs can result in growth retardation during childhood due to their actions on growth plate chondrocytes, although the exact mechanisms involved are unclear. The work of this thesis has investigated the cellular and molecular mechanisms involved in mediating GC effects at the growth plate.

Affymetrix microarray has been used to identify and characterise the expression of lipocalin 2, a novel GC-responsive chondrocyte gene which may contribute to GC-induced growth retardation in the growth plate. *In vitro* and *in vivo* studies have also been used to examine the role of the cell cycle regulator, p21^{WAF1/CIP1} in GC-induced growth retardation. Finally, the growth plate sparing effects of a novel GC receptor modulator, AL-438, have also been identified. AL438, has reduced effects on bone growth compared to Dex, but maintains similar anti-inflammatory efficacy.

This work has not only determined novel mechanisms of GC-induced growth retardation, but has also advanced the search for novel GC receptor modulators with reduced adverse effects.

I declare that this thesis has been composed, along with the work described herein, by the candidate, Helen Catriona Owen. This work has not been submitted for any other degree or professional qualification. All sources of information have been acknowledged.

Helen Catriona Owen

Acknowledgements

I would firstly like to thank my supervisors, Colin Farquharson and Faisal Ahmed for their help and support throughout my PhD. I would also like to thank everyone in the Bone Biology Group here at Roslin, and in particular, Vicky Macrae for all her practical advice during my project. A thank you should also be made to the Small Animal Unit at the Roslin Institute, without whose animal husbandry, much of this project would not have been possible. I would also like to thank my funding body, the BBSRC for their financial support, without which this project would never have occurred.

A big thank you should also be made to my family and friends for their support and encouragement over the last 3 years.

Finally, a special thank you also has to be paid to my partner, Scott Roberts, not only for his invaluable advice, but also for his patience and support when things were not going to plan.

Refereed Publications

Owen HC, Miner JN, Ahmed SF, Farquharson C (2007) The growth plate sparing effects of the selective glucocorticoid receptor modulator, AL-438. *Mol Cell Endocrinol* **264**: 164-170

Owen HC, Ahmed SF, Farquharson C (2008) Dexamethasone induced expression of the glucocorticoid response gene Lipocalin 2 in chondrocytes. *Am J Physiol Endocrin Met* **In Press**

Owen HC, Miner JN, Ahmed SF, Farquharson C (2007) The role of p21WAF1/CIP1 in glucocorticoid-induced growth retardation. **Submitted**

Published Meeting Abstracts

Owen HC, Miner JN, Ahmed SF, Farquharson C (2005) Growth Plate Chondrogenesis and Longitudinal Bone Growth following Exposure to the Novel Glucocorticoid Receptor Ligand, AL-438. *Journal of Bone and Mineral Research* **20**: 1294-1294.

Owen HC, Ahmed SF, Farquharson C (2006) Glucocorticoids stimulate p21 WAF1/CIP1 expression in growth plate chondrocytes. *Journal of Bone and Mineral Research* **21**: 1165-1165.

MacRae VE, **Owen HC**, Ahmed SF, Farquharson C (2006) The role of the 11 beta HSD shuttle in modulating the effects of proinflammatory cytokines on the growth plate. *Journal of Bone and Mineral Research* **21**: S214-S214.

Owen HC, Ahmed SF, Farquharson C (2006) Glucocorticoids Induce Lipocalin 2 Gene Expression in Growth Plate Chondrocytes. *Journal of Bone and Mineral Research* **21**: S201-S201.

Owen HC, Ahmed SF, Farquharson C (2007) Identification of a Novel Glucocorticoid-Responsive Gene in Growth Plate Chondrocytes. *Journal of Bone and Mineral Research* **22**: 1116-1117.

Owen HC, Ahmed SF, Farquharson C (2007) The role of p21 WAF1/CIP1 in Glucocorticoid-Induced Growth Retardation. *Journal of Bone and Mineral Research* **22**: 1135-1136.

Unpublished Meeting Abstracts

Owen H, Miner JN, Ahmed SF, Farquharson C (2005) The Effect of the Novel Glucocorticoid Receptor Ligand, AL-438 on Growth Plate Chondrocyte Proliferation And Differentiation. *The Endocrine Society Annual Meeting, June, San Diego, USA.*

Owen H, Miner JN, Ahmed SF, Farquharson C (2005) The Growth Plate Sparing Effects of the Novel Glucocorticoid Receptor Ligand, AL-438. *Caledonian Society for Endocrinology, November, Peebles, UK.*

Owen H, Miner JN, Ahmed SF, Farquharson C (2005) The Effect of the Glucocorticoid Receptor Ligand, AL-438 on Growth Plate Chondrocytes and Longitudinal Bone Growth. *British Society for Paediatric Endocrinology and Diabetes, September, Bristol, UK*

Awards

Bone Research Society Annual Meeting - Birmingham July 2005

New Investigator Award for the abstract entitled "Growth Plate Chondrogenesis and Longitudinal Bone Growth following Exposure to the Novel Glucocorticoid Receptor Ligand, AL-438"

Bone Research Society Annual Meeting - Birmingham July 2005

Best Oral Presentation award for the presentation entitled "Growth Plate Chondrogenesis and Longitudinal Bone Growth following Exposure to the Novel Glucocorticoid Receptor Ligand, AL-438"

Roslin Institute Annual Student Poster Session - September 2005

1st Prize for the poster entitled "The Growth Plate Sparing Effects of the Novel Glucocorticoid Receptor Ligand, AL-438"

Caledonian Society for Endocrinology Annual Meeting - December 2005

Caledonian Prize Invited Lecture entitled "Longitudinal Bone Growth following Exposure to Glucocorticoids"

List of Abbreviations

ALL	Acute lymphoblastic leukaemia
ALP	Alkaline phosphatase
ANOVA	Analysis of variance
ATP	Adenosine 5'-triphosphate
BMP	Bone morphogenic protein
bp	Base pair (s)
BrdU	Bromodeoxyuridine
BSA	Bovine serum albumin
cDNA	Complementary DNA
CDK	Cyclin dependent kinase
CDKI	Cyclin dependent kinase inhibitor
CDS	Coding sequence
CEBPα	CAAT/enhancer binding protein α
CHX	Cycloheximide
Coll II	Collagen type II
Coll X	Collagen type X
Ct	Threshold cycle
CTGF	Connective tissue growth factor
DAB	Diaminobenzidine
DBD	DNA binding domain
DEPC	Diethylpyrocarbonate
Dex	Dexamethasone
DMEM	Dulbecco's modified Eagle's medium
DMSO	Dimethylsulfoxide
DMP	Dentin Matrix Protein
DNA	Deoxyribonucleic acid
DNase	Deoxyribonuclease
dNTP	Deoxyribonucleotide triphosphate

DTT	Dithiothreitol
ECM	Extracellular matrix
EDTA	Ethylenediaminetetraacetic acid
ER	Oestrogen receptor
ERE	Oestrogen response element
EtBr	Ethidium bromide
FBS	Foetal bovine serum
FGF	Fibroblast growth factor
FITC	Fluorescein isothiocyanate
GC	Glucocorticoid
GFP	Green fluorescent protein
GH	Growth hormone
GHBP	Growth hormone binding protein
GHRH	Growth hormone releasing hormone
GM-CSF	Granulocyte- macrophage colony stimulating factor
GO	Gene Ontology
GP	Growth Plate
GR	Glucocorticoid receptor
GRE	Glucocorticoid response element
GRIP1	Glutamate receptor interacting protein 1
HIF	Hypoxia-inducible factor
HPA	Hypothalamic pituitary adrenal
HSD	Hydroxysteroid dehydrogenase
HSP	Heat-shock protein
HZ	Hypertrophic zone
IGF	Insulin-like growth factor
IHC	Immunohistochemistry
Ihh	Indian hedgehog
IP	Immunoprecipitation
JIA	Juvenile Idiopathic Arthritis

kb	Kilobase (s) or 1000bp
kDa	Kilodalton (s)
LCM	Laser Capture Microscopy
LB	Lysogeny broth
LBD	Ligand binding domain
LPS	Lipopolysaccharide
MAR	Mineral apposition rate
M-CSF	Macrophage colony stimulating factor
MM	Mis-Match
MMP	Matrix metalloproteinase
MOPS	4-Morpholinepropanesulfonic acid
mRNA	Messenger RNA
NFκB	Nuclear factor κB
OD	Optical density
Oligo	Oligodeoxyribonucleotide
PAGE	Polyacrylamide gel electrophoresis
PBS	Phosphate-buffered saline
PCR	Polymerase chain reaction
PGC1	Peroxisome-proliferator activator receptor γ-coactivator
PGK	Phosphoglycerate kinase
PM	Perfect Match
Pred	Prednisolone
PTH	Parathyroid hormone
PTH1R	Parathyroid hormone type 1 receptor
PTHrP	Parathyroid hormone related peptide
PVA	Polyvinyl alcohol
PZ	Proliferative zone
qPCR	Quantitative PCR
RA	Retinoic acid
RMA	Robust multichip analysis

RNA	Ribonucleic acid
RNase	Ribonuclease
RT-PCR	Reverse transcription PCR
RZ	Resting zone
SD	Standard deviation
SDS	Sodium dodecyl sulphate
SEM	Standard error of the mean
SFRP	Secreted frizzled-related protein
SGCK	Serum and Glucocorticoid-regulated Kinase
siRNA	Short interfering RNA
SOC	Super optimal media with catabolite repression
SURE	Stops unwanted recombination events
SV40	Simian virus 40
T₃	3,5,3'-L-triiodothyronine
T₄	3,5,3',5'-L-tetraiodothyronine, thyroxine
TAE	Tris-Acetate EDTA
TBE	Tris-Borate EDTA
TBS	Tris-Buffered Saline
TBST	Tris-Buffered Saline with 0.1% Tween20
TCA	Trichloro-acetic Acid
TGF- β	Transforming growth factor β
TIMP	Tissue inhibitor of matrix metalloproteinase
TNAP	Tissue non-specific alkaline phosphatase
TRAP	Tartrate resistant acid phosphatase
Tris	Tris (hydroxymethyl)aminomethane
VEGF	Vascular endothelial growth factor
WB	Western blotting

<u>Chapter 1: Introduction and Literature Review</u>	<u>Page</u>
Preface	
1.1 Skeletal Growth	3
1.2 The Structure and Composition of Bone Tissue	3
1.2.1 Cortical Bone	4
1.2.2 Trabecular Bone	5
1.2.3 Osteoblasts	6
1.2.4 Osteocytes	7
1.2.5 Osteoclasts	8
1.3 Bone Growth	9
1.3.1 Embryonic Bone Formation	9
1.3.2 Endochondral Ossification	9
1.4 The Growth Plate	12
1.4.1 Structural Organisation of the Growth Plate	12
1.4.2 The Resting Zone	13
1.4.3 The Proliferating Zone	15
1.4.4 The Transition Zone: Proliferation to Hypertrophy	16
1.4.5 The Hypertrophic Zone	17
1.4.6 Mineralisation and the Chondro-osseous junction	17
1.4.7 The fate of the terminally differentiated chondrocyte	20
1.4.8 Extracellular Matrix Proteins	21
1.5 Longitudinal Bone Growth	24
1.5.1 The Process of Longitudinal Growth	24
1.5.2 Growth Disorders	25
1.5.3 Catch-up Growth	26
1.6 Regulation of Longitudinal Bone Growth	27
1.6.1 Systemic Regulation	27
1.6.2 Local Regulation of the Growth Plate	33
1.7 Cell Cycle Signalling	40
1.7.1 Control of Cell Cycle Gene Expression	40
1.7.2 Function of cell cycle genes in the growth plate	43
1.8 Glucocorticoids and Growth Retardation	45
1.8.1 GC Physiology	45
1.8.2 GC Receptor Pharmacology	48
1.8.3 Systemic Side Effects of GCs	51
1.8.4 Glucocorticoid Therapy and Growth during Childhood	53
1.8.5 GCs and IGF-I signalling in the growth plate	55
1.8.6 Direct effects of GCs at the Growth Plate	56
1.8.7 Glucocorticoids and catch-up growth	57
1.9 Aims and Strategy	57

Chapter 2: Materials and Methods

2.1 Reagents and Solutions	
2.1.1 Materials	60
2.1.2 Buffer Recipes	60
	60

2.2 Cell Culture	62
2.2.1 Preparation of cell culture reagents	63
2.2.2 Isolation of primary cell lines	63
2.2.3 Maintenance and differentiation of ATDC5 cells	64
2.2.4 Freezing/Thawing cells	65
2.3 In vivo methods	65
2.3.1 Production of transgenic mice	65
2.3.2 Animal Maintenance	66
2.3.3 Animal Breeding	66
2.3.4 Tail Biopsy of Animals	67
2.3.5 Isolation and culture of embryonic murine metatarsals	67
2.4 Tissue Processing and Analysis	68
2.4.1 Paraffin Embedded Tissue	68
2.4.2 RNase Free Frozen Tissue	69
2.4.3 Immunohistochemistry	73
2.4.4 Toluidine Blue Staining	73
2.4.5 Histological Assessment of Bromodeoxyuridine (BrdU) uptake	74
2.4.6 Alkaline Phosphatase and Von Kossa staining	74
2.5 RNA Methods	76
2.5.1 Isolation of Total RNA from Cells and Tissues	76
2.5.2 Isolation of RNA from LCM samples	77
2.5.3 RNA Amplification	77
2.5.4 Reverse Transcription	78
2.5.5 Polymerase Chain Reaction (PCR)	79
2.5.6 Quantitative Polymerase Chain Reaction (qPCR)	80
2.6 DNA Methods	81
2.6.1 DNA isolation from mouse tail biopsies	81
2.6.2 Genotyping transgenic mice	81
2.6.3 Agarose Gel Electrophoresis	82
2.6.4 Quantification of DNA Concentration	82
2.6.5 Restriction Endonuclease Digestion of DNA	82
2.6.6 DNA Ligation into Linearised Vectors	83
2.6.7 Isolation of DNA Fragments from Agarose gel	83
2.6.8 DNA Sequencing	84
2.6.9 Transformation of bacteria	84
2.6.10 Liquid Culture of Bacterial Clones	85
2.6.11 Minipreparation of Plasmid DNA	85
2.6.12 Endofree Maxipreparation of Plasmid DNA	85
2.7 Protein Methods	87
2.7.1 Protein Concentration Determination – Bradford Assay	87
2.7.2 SDS Polyacrylamide Gel Electrophoresis	87
2.7.3 Western Blotting	88
2.8 Microarray	89
2.8.1 Hybridisation of RNA to Affymetrix Platform	89
2.8.2 Microarray Data Analysis	92
2.9 Cell Proliferation and Differentiation Assays	93
2.9.1 [³ H]Thymidine Incorporation Assay	93
2.9.2 Alcian Blue Staining of the Cell Monolayer	93
2.9.3 Alkaline Phosphatase Assay	93

Chapter 3: Identification of Glucocorticoid-Responsive Chondrocyte Genes

3.1 Introduction	96
3.2 Hypothesis	98
3.3 Aims	98
3.4 Materials and Methods	98
3.4.1 Cell Culture	98
3.4.2 RNA Extraction and Hybridisation to the Affymetrix GeneChip	99
3.4.3 Data Normalisation	99
3.4.4 Gene Ontology Analysis	101
3.4.5 Gene Ontology Enrichment and Functional Annotation Clustering	101
3.4.6 Validation of Affymetrix Microarray Data with qPCR	101
3.5 Results	102
3.5.1 Microarray Analysis	102
3.5.2 Identification of Trends in Gene Expression	106
3.5.3 Validation of Microarray Expression Data	112
3.6 Discussion	114
3.7 Conclusions	123

Chapter 4: Functional Involvement of Lipocalin 2 in GC-Induced Growth Retardation

4.1 Introduction	125
4.2 Hypothesis	130
4.3 Aims	130
4.4 Materials and Methods	131
4.4.1 Cell Culture	131
4.4.2 Quantitative PCR	131
4.4.3 p38 MAP Kinase Assay	132
4.4.4 Western Blotting	133
4.4.5 Histological Analysis of Lipocalin 2 Expression in the Growth Plate	133
4.4.6 Isolation of Primary Murine Chondrocytes	134
4.4.7 Production of a Lipocalin 2 Expression Construct	134
4.4.8 Generation of ATDC5 Stable Transfections	135
4.4.9 Effect of Lipocalin 2 Overexpression on Chondrocyte Dynamics	136
4.4.10 Statistical Analysis	136
4.5 Results	136
4.5.1 Characterisation of Dex-induced Lipocalin 2 Expression in Chondrocytes	136
4.5.2 Immunolocalisation of Lipocalin 2 within the murine growth plate	140
4.5.3 Mechanism of Dex-induced Lipocalin 2 Expression	142
4.5.4 Involvement of the NF κ B and p38 Pathways in Lipocalin 2	143
4.5.5 Functional Effects of Lipocalin 2 on ATDC5 Proliferation and Differentiation	146
4.5.6 The Combined effects of Lipocalin 2 and Dex on ATDC5 Cells	147
4.6 Discussion	149
4.7 Conclusions	154

Chapter 5: The Role of p21^{WAF1/CIP1} in Glucocorticoid-Induced Growth Retardation

5.1	Introduction	156
5.2	Hypothesis	160
5.3	Aims	160
5.4	Materials and Methods	161
5.4.1	<i>In Vitro</i> Studies	161
5.4.1.1	Cell Culture	161
5.4.1.2	Cell Counting	161
5.4.1.3	PCR	161
5.4.1.4	Western Blotting	162
5.4.2	<i>In Vivo</i> Studies	163
5.4.2.1	p21 Null Mice Genotyping	163
5.4.2.2	<i>In Vivo</i> Treatment of Mice with Dex	163
5.4.2.3	Measurement of Organ Weights	164
5.4.2.4	Tissue Processing	164
5.4.2.5	Toluidine Blue Analysis of Growth Plate	164
5.4.2.6	Analysis of X-rays	165
5.4.2.7	Calcein Labelling	165
5.4.2.8	Laser Capture Microscopy	166
5.5	Results	167
5.5.1	<i>In Vitro</i> Studies	167
5.5.1.1	Analysis of p21 Expression during Chondrocyte Differentiation	167
5.5.1.2	p21 Expression in ATDC5 Cells following Dex Treatment	168
5.5.2	<i>In Vivo</i> Studies	169
5.5.2.1	Growth in Dex-treated Mice	169
5.5.2.2	Effect of Dex on Organ Weight	170
5.5.2.3	Effect of Dex on Growth Plate Morphology	171
5.5.2.4	Analysis of p21 expression in the Growth Plate	172
5.5.2.5	Growth in Dex-treated p21 ^{-/-} Mice	173
5.5.2.6	Skeletal Growth in Dex-treated p21 ^{-/-} Mice	174
5.5.2.7	Growth Plate Morphology in Dex-treated p21 ^{-/-} Mice	175
5.5.2.8	Calcein Labelling in Dex-treated p21 ^{-/-} Mice	177
5.6	Discussion	179
5.7	Conclusions	183

Chapter 6: The Growth Plate Sparing Effects of the Novel Glucocorticoid Receptor Ligand, AL-438

6.1 Introduction	186
6.2 Hypothesis	189
6.3 Aims	189
6.4 Materials and Methods	190
6.4.1 ATDC5 Proliferation in AL-438 treated cells	190
6.4.2 Effect of AL-438 on Proteoglycan production in ATDC5 cells	190
6.4.3 Alkaline Phosphatase Activity in AL-438 treated cells	190
6.4.4 Expression of chondrocyte marker genes with AL-438	190
6.4.5 Apoptosis in AL-438 treated ATDC5 cells	191
6.4.6 Determination of anti-inflammatory efficacy of AL-438 in ATDC5	192
6.4.7 Foetal metatarsal organ culture	193
6.4.8 Morphometric analysis	194
6.4.9 Histological assessment of bromodeoxyuridine (BrdU) uptake	194
6.4.10 Statistical Analysis	195
6.5 Results	195
6.5.1 Effect of AL-438 on ATDC5 cell number and proliferation	195
6.5.2 Differentiation in AL-438 treated chondrocytes	197
6.5.3 Effect of AL-438 on apoptosis in ATDC5 cells	198
6.5.4 Chondrocyte Marker Gene Expression in AL-438 treated ATDC5 cells	199
6.5.5 Anti-inflammatory efficacy of AL-438 in ATDC5 cells	200
6.5.6 Longitudinal bone growth and assessment of chondrocyte maturational zone sites	201
6.5.7 Effect of AL-438 on chondrocyte proliferation in metatarsals	203
6.6 Discussion	203
6.7 Conclusions	209

Chapter 7: General Discussion and Future Work

7.1 General Discussion	212
7.2 Future Work	216

Reference List	219
Appendix 1	247
Appendix 2	259
Appendix 3	260
Appendix 4	262

<u>Figure</u>		<u>Page</u>
Figure 1.1	Structure and components of long bone	5
Figure 1.2	Coll II Stained Murine Embryos	11
Figure 1.3	The Process of Endochondral Ossification	12
Figure 1.4	The Epiphyseal Growth Plate	13
Figure 1.5	Hormone action in the growth plate	32
Figure 1.6	Interaction of Ihh, PTHrP, BMP, and FGF signalling in modulating chondrocyte proliferation and differentiation	39
Figure 1.7	p21 and cyclin D1 as targets of mitogenic and antimitogenic signals in chondrocytes	43
Figure 1.8	The GC Biosynthetic Pathway	47
Figure 1.9	Mechanisms of GC-regulated gene transcription	51
Figure 2.1	Isolation of Primary Murine Chondrocytes	64
Figure 2.2	Murine Metatarsal Dissection	68
Figure 2.3	The CryoJane Tape transfer	71
Figure 2.4	The Laser Capture Microdissection Process	72
Figure 2.5	Affymetrix Microarray overview	91
Figure 3.1	Line graph of Control and Dex sample data loaded into GeneSpring	100
Figure 3.2	Scatterplot of Affymetrix micorarray results from GeneSpring analysis	103
Figure 3.3	Functional Annotation of up-regulated and downregulated genes	108
Figure 3.4	GC-responsive chondrocyte genes	113
Figure 3.5	Validation of microarray results with qPCR analysis	114
Figure 4.1	Crystal structure of NGAL	127
Figure 4.2	Characteristic features of the lipocalin fold	128
Figure 4.3	Characterisation of Lipocalin 2 expression over time	138
Figure 4.4	Dose-response of Lipocalin 2 expression with Dex	139
Figure 4.5	Lipocalin 2 Expression in Primary Chondrocytes	140
Figure 4.6	Localisation of Lipocalin 2 Expression in the Growth Plate	141
Figure 4.7	Involvement of the GR in GC-induced Lipocalin 2 expression	142
Figure 4.8	The p38 signalling pathway and Lipocalin 2 expression	144
Figure 4.9	The NFkB signalling pathway and Lipocalin 2 expression	145
Figure 4.10	The effect of increased lipocalin 2 expression on chondrocytes	147
Figure 4.11	The combined effect of lipocalin 2 and Dex on ATDC5 cells	148
Figure 4.12	The Lipocalin 2 Promoter	152
Figure 5.1	Immunohistochemical localisation of p21 in the rat growth plate	158
Figure 5.2	Genotyping of p21 null homozygous and heterozygous mice	163
Figure 5.3	LCM of proliferating and hypertrophic chondrocytes	166

Figure 5.4	Expression of CDKIs during ATDC5 differentiation	167
Figure 5.5	p21 expression with Dex treatment in ATDC5 cells	169
Figure 5.6	Skeletal growth in Dex-treated mice	170
Figure 5.7	Effect of Dex on mouse organ weights	171
Figure 5.8	Toluidine Blue staining of the Growth Plate in Dex-treated mice	172
Figure 5.9	Growth in p21 ^{-/-} Dex-treated mice	174
Figure 5.10	Skeletal growth of Dex-treated p21 null mice	175
Figure 5.11	Toluidine Blue staining of growth plates from Dex-treated p21 null mice	176
Figure 5.12	Calcein labelling in Dex-treated p21 ^{-/-} mice	178
Figure 5.13	Factors acting on the p21 promoter	181
Figure 6.1	Structural differences between AL-438 and Dexamethasone	188
Figure 6.2	Murine foetal metatarsal culture model	193
Figure 6.3	Effect of Dex, Pred and AL-438 on cell proliferation	196
Figure 6.4	Effect of AL-438 on ATDC5 differentiation	197
Figure 6.5	Effect of AL-438 on apoptosis during chondrogenesis	198
Figure 6.6	Chondrocyte marker gene expression in ATDC5 cells	199
Figure 6.7	LPS-induced IL-6 production in ATDC5 cells	200
Figure 6.8	Effect of AL-438 on the growth of murine metatarsals	202
Figure 6.9	Histological assessment of chondrocyte proliferation in metatarsals treated with Dex or AL-438	203
Figure 6.9	Proposed mechanism of action of AL-438	207
<u>Table</u>		<u>Page</u>
Table 3.1	qPCR primer sequences for confirmation of microarray results	102
Table 3.2A	Genes significantly up-regulated by 1.5-fold or more with Dex treatment.	104
Table 3.2B	Genes significantly down-regulated by 1.5-fold or more with Dex treatment	106
Table 3.3A	Functional Annotation clustering and enrichment scores for the gene ontology of genes significantly up-regulated with Dex	109
Table 3.3B	Functional Annotation clustering and enrichment scores for the gene ontology of genes significantly down-regulated with Dex	112
Table 4.1	Lipocalin protein family members and known functions	126
Table 4.2	Ct values and lipocalin 2 fold change over time with Dex	138
Table 4.3	Ct values and lipocalin 2 fold change with varying Dex concentrations	139
Table 5.1	Primer sequences and product sizes for CDKIs and chondrocyte marker genes analysed by endpoint PCR.	162
Table 6.1	Lengths of the proliferating, mineralising and hypertrophic zones in murine metatarsals treated with Dex or AL-438	202

Chapter 1

Introduction and Literature Review

Chapter Contents

Preface

1.1 Skeletal Growth

1.2 The Structure and Composition of Bone Tissue

1.2.1 Cortical Bone

1.2.2 Trabecular Bone

1.2.3 Osteoblasts

1.2.4 Osteocytes

1.2.5 Osteoclasts

1.3 Bone Growth

1.3.1 Embryonic Bone Formation

1.3.2 Endochondral Ossification

1.4 The Growth Plate

1.4.1 Structural Organisation of the Growth Plate

1.4.2 The Resting Zone

1.4.3 The Proliferating Zone

1.4.4 The Transition Zone: Proliferation to Hypertrophy

1.4.5 The Hypertrophic Zone

1.4.6 Mineralisation and the Chondro-osseous junction

1.4.7 The fate of the terminally differentiated chondrocyte

1.4.8 Extracellular Matrix Proteins

1.5 Longitudinal Bone Growth

1.5.1 The Process of Longitudinal Growth

1.5.2 Growth Disorders

1.5.3 Catch-up Growth

1.6 Regulation of Longitudinal Bone Growth

1.6.1 Systemic Regulation

1.6.1.1 GH-IGF-I system

1.6.1.2 Thyroid Hormone

1.6.1.3 Sex Steroids

1.6.2 Local Regulation of the Growth Plate

1.6.2.1 Fibroblast growth factor (FGF) signalling

- 1.6.2.2 Bone Morphogenic Protein (BMP) and Transforming Growth Factor β (TGF β) signalling
 - 1.6.2.3 Ihh/PTHrP signalling
 - 1.6.2.4 Vascular endothelial growth factor (VEGF)
 - 1.6.2.5 Sox9
 - 1.7 Cell Cycle Signalling
 - 1.7.1 Control of Cell Cycle Gene Expression
 - 1.7.2 Function of cell cycle genes in the growth plate
 - 1.8 Glucocorticoids and Growth Retardation
 - 1.8.1 GC Physiology
 - 1.8.2 GC Receptor Pharmacology
 - 1.8.3 Systemic Side Effects of GCs
 - 1.8.4 Glucocorticoid Therapy and Growth During Childhood
 - 1.8.5 GCs and IGF-I signalling in the growth plate
 - 1.8.6 Direct effects of GCs at the Growth Plate
 - 1.8.7 Glucocorticoids and catch-up growth
 - 1.9 Aims and Strategy
-
-

Preface

Since the introduction of glucocorticoids (GCs) in the treatment of rheumatoid arthritis in 1949, their therapeutic applications have broadened to encompass a large number of non-endocrine and endocrine diseases (Hench *et al.*, 1949). However, despite the intense efforts made by science and industry to maximise the efficacy and minimise the side effects of GCs, adverse reactions are still common. Impairment of childhood growth with long-term GC treatment was described nearly 50 years ago; however the mechanisms by which GCs cause this growth retardation are still unknown. With 5-10% of children requiring GC treatment at some point during childhood, it is vital that we gain a better understanding of these mechanisms to aid the development of new GCs with reduced side effects.

1.1 Skeletal Growth

Growth takes place at the epiphyseal growth plate of long bones by a finely balanced cycle of cartilage growth, matrix formation and calcification. This sequence of cellular events is known as endochondral ossification. An individual's skeletal growth rate and adult limb bone length are influenced by many factors including circulating hormones, nutritional intake, mechanical influences and disease, and growth disturbances result when there is disruption of the normal cellular activity of growth plate chondrocytes and/or the cells of bone. There is an increasing body of evidence to demonstrate that factors produced locally in bone and cartilage, or trapped within hard tissue matrix, may play a critical role in regulating normal and pathological skeletal growth and remodelling.

1.2 The Structure and Composition of Bone Tissue

1.2.1 Cortical Bone

Two types of bone structure exist; cortical (compact) and trabecular (spongy) bones (Figure 1.1A). Cortical bone makes up approximately 80% of the total skeletal mass (Sambrook *et al*, 1993), and contains few spaces. It forms the external layer of all bones in the body and the majority of the diaphyses of long bones, and provides protection and support by helping the long bones resist the stress of weight placed upon them (Skedros *et al*, 1996). Cortical bone is composed of concentric rings of bone tissue known as osteons (Figure 1.1B). Blood vessels, lymphatic vessels, and nerves from the periosteum penetrate the cortical bone through perforating (Volkmann's) canals. The blood vessels and nerves of these canals connect with those of the medullary cavity, periosteum, and central (Haversian) canals of the osteon (Havers, 1961). The central canals run longitudinally through the bone, and around the canals are concentric lamellae – rings of hard, calcified matrix. Between the lamellae are small spaces, or lacunae, which contain osteocytes. Radiating in all directions from the lacunae are minute canals known as canaliculi, which are filled with extracellular fluid. Inside these canaliculi are slender finger-like processes of osteocytes. The canaliculi connect lacunae with one another and, eventually, with the central canals. Thus, there is an intricate branching network of canals which provide a route for nutrients and oxygen to reach the osteocytes and for wastes to diffuse away. Osteocytes from neighbouring lacunae form gap junctions with one another, facilitating easy movement of materials from cell to cell. Each central canal, with its surrounding lamellae, lacunae, osteocytes and canaliculi, forms an osteon (Haversian System). Cortical bone tissue is the only connective tissue containing a basic structural unit – the osteon – associated with it.

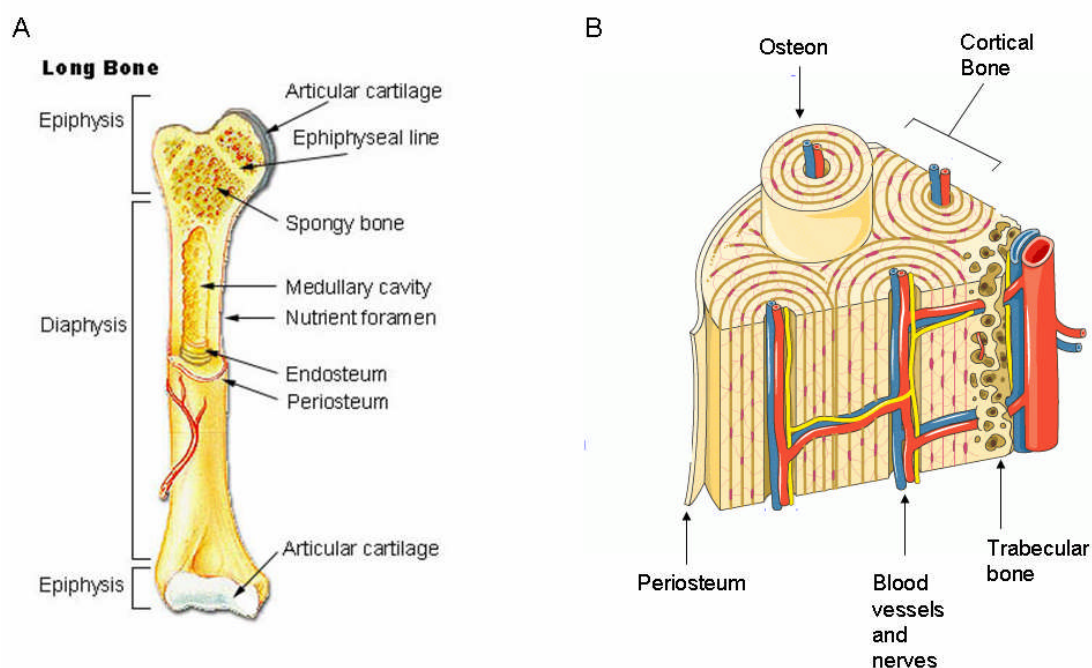


Figure 1.1 Structure and components of long bone. (A) Long bones are longer than they are wide, consisting of a long shaft (the diaphysis) plus two articular (joint) surfaces, called epiphyses. They are comprised mostly of compact bone, but are generally thick enough to contain considerable spongy bone and marrow in the hollow centre (the medullary cavity). Most bones of the limbs (including the three bones of the fingers) are long bones, except for the kneecap (patella), and the carpal, metacarpal, tarsal and metatarsal bones of the wrist and ankle (training.seer.cancer.gov) (B) A 3D representation of the structure and organisation of trabecular and compact bone (www.iofbonehealth.org).

1.2.2 Trabecular Bone

In contrast to cortical bone, trabecular (cancellous) bone does not contain true osteons, but instead consists of lamellae arranged in an irregular latticework of thin columns of bone called trabeculae. The macroscopic spaces between the trabeculae of some bones are filled with red bone marrow, which produces blood cells. Within the trabeculae are osteocytes that lie in lacunae, and radiating from the lacunae are canaliculi. Blood vessels from the periosteum penetrate through to the trabecular bone, and osteocytes in the trabeculae receive nourishment directly from the blood circulating through the marrow cavities. Osteons are not necessary in spongy bone as osteocytes are not deeply buried as they are in cortical bone, and so have access to

nutrients directly from the blood. Trabecular bone constitutes the majority of bone tissue of short, flat and irregularly shaped bones and most of the epiphyses of long bones. Trabecular bone tissue in the ribs, sternum, vertebrae and in the ends of some long bones is the only site of red bone marrow storage, and hence haemopoiesis in adults.

1.2.3 Osteoblasts

Osteoblasts are bone-forming cells that are derived from multipotent mesenchymal stem cells (stromal stem cells), are cuboidal in shape and are localised mainly to the bone surface. The gene expression profile of the osteoblast is very similar to that of a fibroblast with very few bone specific transcripts being produced. The main difference in cell function is that osteoblasts have the ability to form an extracellular matrix (osteoid) which they can subsequently mineralise (Ducy *et al*, 2000). The un-mineralised matrix is formed mainly from collagen type 1 (approximately 94%) which is laid down early in bone formation, with the remainder being taken up with embedded proteins such as osteocalcin, osteonectin, osteopontin and bone sialoprotein (Sommerfeldt and Rubin, 2001). This stage of matrix production is under strict control of growth factors such as fibroblast growth factor (FGF) and insulin like growth factor-I (IGF-I) (McCarthy *et al*, 1989; Hurley and Florkiewicz, 1996). During intramembranous ossification, mesenchymal cells differentiate into osteoblasts and bone is formed without replacing a cartilaginous model, whereas during endochondral ossification the cartilage template matrix is calcified and osteoblasts are recruited to deposit woven bone (and later lamellar bone) on the surface of the mineralised matrix residues. Following bone formation, osteoblasts can have one of four different fates: (1) they can become embedded in the bone as osteocytes, (2)

transform into inactive osteoblasts and become bone lining cells, (3) undergo apoptosis, or (4) transdifferentiate into cells that deposit chondroid or chondroid bone (Noble *et al.*, 1997; Jilka *et al.*, 1998;). Once embedded into the bone matrix the former osteoblasts, now osteocytes, cease their activity.

1.2.4 Osteocytes

Osteocytes are mature bone cells that are derived from osteoblasts, and are by far the most abundant cellular component of mammalian bones, making up 95% of all bone cells (Parfitt., 1990; Marotti *et al.*, 1996). An important role of osteocytes and their network of cell processes are to function as strain and stress sensors, signals that are vital for maintaining bone structure (Burger *et al.*, 2003). Osteocytes communicate with one another and with osteoblasts at the bone surface via a meshwork of cell processes that run through canaliculi in the bone matrix (Franz-Odenaal *et al.*, 2006). Osteocytes no longer secrete matrix minerals, but maintain daily cellular activities of bone tissue, such as the exchange of nutrients and wastes with the blood. Another function of osteocytes within the bone network is the ability to deposit and resorb bone around the osteocyte lacuna in which they are housed, thus changing the shape of the lacuna. This process, known as osteocytic osteolysis, is often not regarded as characteristic of human osteocytes, but has been observed in many vertebrates such as hamsters (Steinberg *et al.*, 1981), squirrels (Haller and Zimny 1978) and rats (Belanger 1977; Tazawa *et al.*, 2004). It has recently been proposed that the three-dimensional network of osteocytes provides the cellular basis for mechanosensing in bone, leading to adaptive bone remodelling. Mechanotransduction in bone is complex in nature, and is influenced by many modulators including PTH, prostanoids, and extracellular Ca^{2+} . It has been postulated that osteocytes transduce signals of

mechanical loading resulting in anabolic responses such as the expression of *c-fos*, IGF-I, and osteocalcin (Mikuni-Takagaki 1999).

1.2.5 Osteoclasts

Osteoclasts are multi-nucleated cells, derived from haematopoietic stem cells, which resorb mineralised bone at sites known as Howships lacunae (Sommerfeldt and Rubin, 2001). This is an essential process which allows bone repair and sequestration of calcium into the blood to maintain ion homeostasis. Bone modelling and remodelling are crucial events in skeletal development and repair, and are strictly controlled by osteoclasts. Defects in these processes lead to diseases such as hypercalcemia of malignancy and postmenopausal osteoporosis where an increase in bone resorption is the main pathological episode (Vaananen *et al*, 2000). Osteoclasts are closely related to macrophages and dendritic cells with only the final stage of differentiation altering for each cell type. This differentiation is dependent on whether the cell is stimulated by exposure to a particular receptor activator of nuclear-factor kB (NF-kB) ligand i.e. osteoclast differentiation factor, macrophage colony-stimulating factor (M-CSF) or granulocyte-macrophage colony-stimulating factor (Vaananen *et al*, 2000). Osteoclasts create a cavity at the remodelling site through the secretion of enzymes and acids such as matrix metalloproteases and tartrate resistant acid phosphatase (TRAP). Osteoblasts are then recruited to this site where they lay down a matrix which is subsequently mineralised.

1.3 Bone Growth

1.3.1 Embryonic Bone Formation

Embryonic skeletogenesis involves the sequential events of patterning, cell differentiation, and morphogenesis to give rise to cartilage and bone. The significant functional role of the skeletal structures, such as the scaffolding of the vertebrate animal, requires that skeletogenesis be under stringent regulation at multiple levels. There are two principle pathways of skeletal development: intramembranous and endochondral (Hall *et al.*, 1987). Intramembranous ossification involves direct differentiation of mesenchymal cells into osteoblasts, and is seen predominantly in craniofacial bones (Langille *et al.*, 1994). During endochondral ossification, (such as that seen in the long bones and vertebrae), mesenchymal cells condense, undergo chondrogenesis and form cartilage. This cartilage subsequently matures, undergoes hypertrophy, and is eventually replaced by bone (Caplan *et al.*, 1994).

1.3.2 Endochondral Ossification

Endochondral ossification is the process responsible for much of the bone growth in vertebrate skeletons, especially in long bones. As the name might suggest (endo - within, chondro - cartilage), endochondral ossification occurs by replacement of hyaline cartilage. Long bones of the skeleton first appear as limb buds and the earliest observable morphological event in this process (between 10.5 and 12.5 days post-coitum in the embryonic mouse) is the aggregation of committed, undifferentiated mesenchymal cells into structures known as condensations. Prechondrogenic condensation begins the process of endochondral ossification and is required for subsequent skeletal development. Chondrocytes derive from mesenchymal cells that migrate into presumptive skeletogenic sites from the cranial neural crest, paraxial

mesoderm and lateral plate mesoderm. At these skeletogenic sites, the cells become tightly packed and form cell mass condensations that prefigure the future skeletal elements (Hall and Miyake 2000). In the centre of these condensations, prechondrocytes emerge that turn off expression of mesenchymal and condensation markers, and start to express collagen type 2 (Coll II) and other early cartilage markers (Figure 1.2). Surrounding these prechondrocytes is the perichondrium, the outer layer of which becomes a connective tissue sheath while the inner cells remain pluripotential. This cartilage rudiment grows by interstitial and appositional growth, and a vascular system develops to invade the perichondrium (Figure 1.3). A collar of bone is then laid down around the mid-shaft of the bone. This ossification is a result of the inner perichondrial cells differentiating into bone forming cells, the osteoblasts. At the same time the osteoblasts, together with capillaries, invade the centre of the shaft to form a primary or diaphyseal ossification centre at a site where the cartilage cells and matrix have begun to disintegrate. Trabecular bone is then deposited on cartilaginous remnants. The embryonic bone increases in width by appositional growth, and the central cancellous bone core gradually becomes resorbed to form a marrow cavity (Figure 1.3).

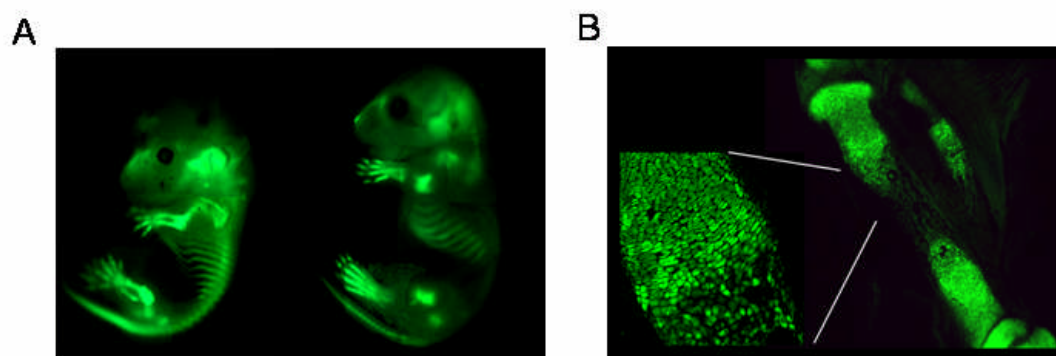


Figure 1.2 Coll II Stained Murine Embryos (A) Coll II-GFP murine embryos The GFP fluorescent reporter is expressed in cells of cartilaginous skeleton in E14.5 (left) and E17.5 (right) mouse embryos. Fluorescence is brightest in structures exhibiting the highest level of chondrogenesis, such as external ears and long bones of the extremities of the younger embryo. Some structures in the older embryo, such as most of the spine, the posterior ribs and central portions of limb bones no longer show fluorescence as the cartilage has been replaced by bone. **(B) Coll II-GFP murine embryonic tibia** Confocal optical sectioning of tibia from E17.5 embryo shows epiphyseal cartilages and growth plates on the right and a higher magnification of the proximal growth plate on the left. (www.shcc.org/growth_plate.htm)

In long bones, another centre of ossification appears at the growing cartilaginous ends, known as the secondary ossification centre (Figure 1.3). This ossification does not replace the cartilage at the articular end of the model but results in a transverse plate of cartilage extending across the epiphysis separating the secondary ossification centre from the diaphysis. This is known as the epiphyseal growth plate. Growth of cartilage in the epiphyseal plate is continuous, but the plate does not become thickened because on its diaphyseal side the cartilage matures, is calcified, resorbed and replaced by bone. This is endochondral ossification, the mechanism responsible for increasing the length of the bone. During growth this is a site of many complex cellular events; namely cartilage growth, maturation, resorption and bone formation. Disturbance of any one of these processes may be reflected in growth retardation.

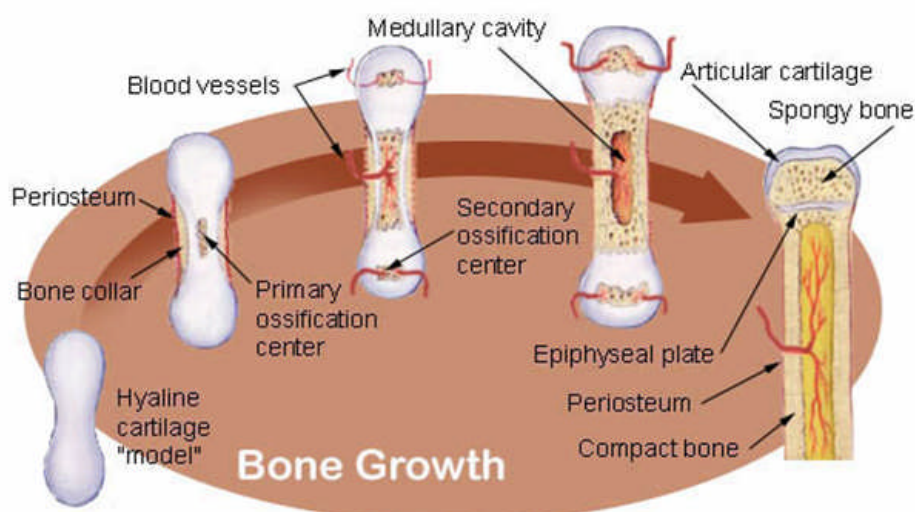


Figure 1.3 The Process of Endochondral Ossification. Following the development of a cartilage model of chondrocytes derived from mesenchymal cells, a primary ossification centre is formed in the centre of the diaphysis. This leads to the formation of the periosteum and the bone collar, and causes the chondrocytes within the primary ossification centre to hypertrophy, secrete alkaline phosphatase (ALP), and mineralise the matrix surrounding them. These chondrocytes then undergo apoptosis, and, in their place, blood vessels, lymph vessels and nerves invade the cavity they have left behind. This leads to invasion by osteoblasts, osteoclasts and haemopoietic cells. Osteoblasts use the calcified matrix as a scaffold and begin to secrete osteoid, which forms the bone trabecula. The secondary ossification centre is formed when cartilage is retained in the growth plate, located between the diaphysis (the shaft) and the epiphysis (end) of the bone. Cartilage cells undergo the same transformation as above. As growth progresses, the proliferation of cartilage cells in the growth plate slows and eventually stops (http://training.seer.cancer.gov/module_anatomy/unit3_3_bone_growth.htm).

1.4 The Growth Plate

1.4.1 Structural Organisation of the Growth Plate

The process of bone growth relies upon chondrocytes produced at the epiphyseal growth plate, which are progressively synthesised and replaced by bone with accompanying longitudinal (endochondral) bone growth (Farquharson 2003). The growth plate is a thin layer of cartilage found near the ends of long bones and vertebrae (Kronenberg *et al.*, 2003) and it comprises of both chondrocytes and their extracellular matrix (ECM). A characteristic of endochondral bone growth is the precise temporal and spatial organisation of chondrocytes within the growth plate

where they differentiate through a series of maturational stages whilst remaining in a spatially fixed location (Hunziker *et al.*, 1987). Histologically, the chondrocytes are arranged in columns similar to a stack of coins that parallel the longitudinal axis of the bone (Figure 1.4). Each column and each chondrocyte within a column are respectively separated by longitudinal and transverse septae made up of a collagenous and proteoglycan rich ECM. At the most proximal end of the growth plate are the resting chondrocytes. Directly below the resting chondrocytes are the proliferating chondrocytes, and then the pre-hypertrophic and hypertrophic chondrocytes (Figure 1.4).

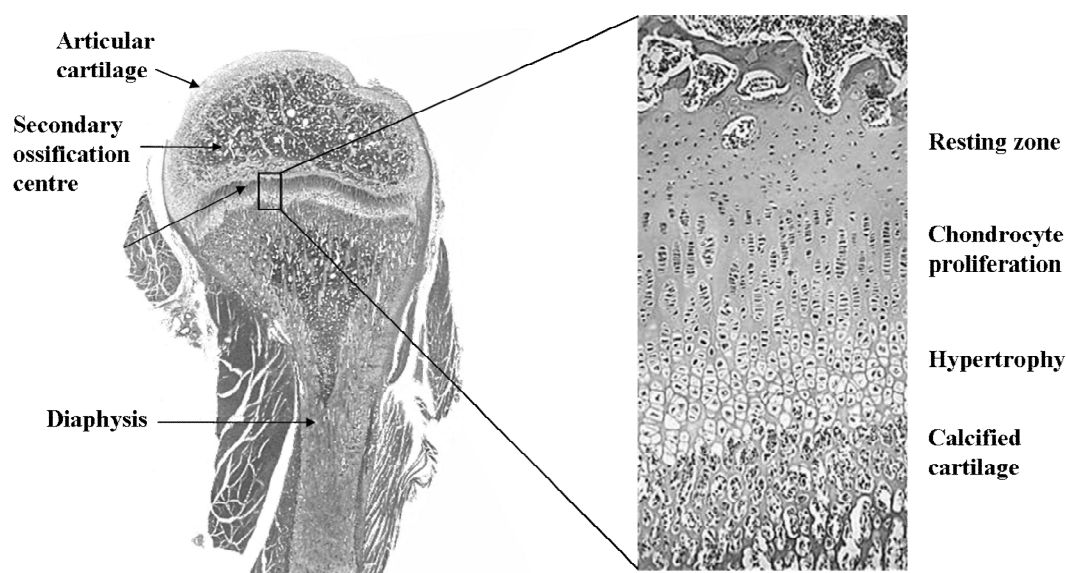


Figure 1.4 The Epiphyseal Growth Plate The growth plate is located at the end of the long bone and is contained within the epiphysis. Chondrocytes within the growth plate proceed through stages of proliferation and differentiation, ultimately leading to hypertrophy and calcification (www.kumc.edu/imstruction/medicine/anatomy/histo/web/bone/small/Bone002s.JPG and www.bu.edu/histology/p02401ooa.htm)

1.4.2 The Resting Zone

At the most proximal end of the growth plate, the reserve zone, or stem cell zone, contains the resting chondrocytes. Cells in this zone exist singly or in pairs separated by an abundant extracellular matrix, have low rates of proliferation and synthesise only low levels of proteoglycans and Coll II (Kember, 1978; Schmidt, Rodergerdts &

Buddecke, 1978; Sandell *et al.*, in press). Intuitively there is agreement that a zone of stem cells must exist proximal to the chondrocytes in the columns of the proliferative zone, and there is a significant body of experimental evidence that these stem cells can be stimulated to initiate clonal expansion as proliferative cells (Kember *et al.*, 1993). This is supported both by evidence demonstrating the responsiveness of these cells to stimulation by circulating hormones such as growth hormone (GH), and by observations with bromodeoxyuridine (BrdU) labelling that these cells have very long cell cycle times compared to cells in the proliferative pool (Isaksson *et al.*, 1982; Farnum *et al.*, 1993).

However, in most descriptions, the reserve cell zone is defined morphologically by the size and spatial orientation of the cells, and refers to all chondrocytes that do not align themselves in the columns that are characteristic of the proliferative cell zone (Seinsheimer *et al.*, 1981; Farnum *et al.*, 1986; Farnum *et al.*, 1987; Farnum *et al.*, 1993). If defined this way, the reserve zone may, in fact represent a heterogeneous zone of cells with subpopulations of chondrocytes with different physiologic functions. The size of the resting zone varies in growth plates from different bones in the same species, and, for a given growth plate, the proportional size of the resting zone relative to total growth plate size varies significantly from species to species (Ishizaki *et al.*, 1994). In humans, Kember and Sissons (1976) showed that, although the overall width of the growth plate declines as growth rate diminishes, there is no significant change in the size of the reserve cell zone. In larger species, a sizeable resting cell zone is present even after formation of the secondary ossification centre is complete. Therefore, one hypothesis is that the so-called reserve zone might serve as a mechanical support to the actively growing chondrocytes of the growth plate in

species that have relatively slow growth rates over long periods of time (Kember *et al.*, 1976; Ishizaki *et al.*, 1994).

Recently, the reserve zone chondrocytes have also been shown to be crucial for orientation of the underlying columns of chondrocytes and therefore unidirectional bone growth, and it is thought that this is due to the secretion of a growth plate-orienting factor (Abad *et al.*, 2002). It has also been suggested that resting zone chondrocytes may produce a morphogen that inhibits terminal differentiation of nearby proliferative zone chondrocytes, and therefore may be partially responsible for the organisation of the growth plate into distinct zones of proliferation and hypertrophy.

1.4.3 The Proliferating Zone

The proliferative zone contains cells from the time clonal expansion begins until the cell exits the cell cycle and begins terminal differentiation. The epiphyseal (proximal) side of the proliferative cell pool can be defined using either thymidine or BrdU labelling (Loveridge and Farquharson 1993). The number of cells in the proliferative zone correlates positively with the rate of growth, and chondrocytes in this zone are flattened, thin discs, arranged like a stack of coins (Buckwalter *et al.*, 1985). Cellular proliferation is required to maintain steady-state kinetics in a given growth plate by offsetting cellular loss at the chondro-osseous junction (Farnum *et al.*, 1989; Wilsman *et al.*, 1996a; Wilsman *et al.*, 1996b). However, the number of cells contributing to the proliferative pool changes over time and is different in growth plates growing at different rates, although the mechanism by which cellular numbers change over time is still unclear. Recent studies have shown that in one animal at one point in time,

cellular cycle times vary in growth plates growing at different rates. Cell cycle times in the proximal tibia of 4-week-old rats was shown by repeated pulse labelling of BrdU to be approximately 30 hours, compared to 76 hours in the proximal radius of the same animals. (Wilsman *et al.*, 1996b). Almost all of the difference in time was associated with the G1 phase of the cell cycle. Therefore, at one point in time, cell cycle times have an inverse relationship with the rate of growth.

Multiple mechanisms may exist by which subsets of chondrocytes regulate proliferation leading to a modulation of growth rates in different bones and in one bone over time. At separate stages of differentiation, chondrocytes may differentially respond to the same external or internal cues. One specific example is that parathyroid hormone (PTH) has different effects on collagen gene expression in chondrocytes in different maturation stages, and that these effects are exerted by distinct effector domains of the PTH molecule (Erdmann *et al.*, 1996). At any given moment, either by a finite number of cell divisions or by changes in exposure to a local mediator such as GCs, proliferating chondrocytes lose their capacity to divide and start to differentiate and become prehypertrophic, coinciding with an increase in size. These chondrocytes then further progress in the differentiation pathway to become hypertrophic chondrocytes.

1.4.4 The Transition Zone: Proliferation to Hypertrophy

When chondrocytes are examined consecutively within a growth plate column, there are cells that are spatially distal to the last chondrocytes that incorporate BrdU, but proximal to cells with a large increase in volume consistent with the hypertrophic phase. This narrow zone of transition is coordinated by a number of complex

regulatory mechanisms, and a number of unique genes involved with this transition to terminal differentiation have been identified (Wang *et al.*, 2004; Wang *et al.*, 2005), along with specific matrix markers, matrix proteins and specific receptors (Wang *et al.*, 2004; Han *et al.*, 2005).

1.4.5 The Hypertrophic Zone

The initial work demonstrating that chondrocytic hypertrophy involved a rapid increase in cell volume and change in shape was carried out by Hunziker (1987) and Buckwalter (1986). This work led to further quantitative investigations that demonstrated the strong positive correlation of final hypertrophic cell volume with rate of growth (Breur *et al.*, 1994). Although the actual rate and efficiency of volume increase varies in growth plates from different species (Barreto *et al.*, 1994; Kuhn *et al.*, 1996), the quantitative data supports the hypothesis that volume increase during hypertrophy is a major contributor to the differential rates of growth occurring in different growth plates of a given animal. In addition, a directed shape change accompanies the volume increase, so that chondrocytic height parallel to the direction of growth is increased disproportionately to width. This directed shape change accompanying the volume increase is a major determinant of overall growth. The hypertrophic chondrocytes have a round appearance and secrete large amounts of matrix proteins, a characteristic which is essential for the propagation of mineralisation, which occurs at the chondro-osseous junction.

1.4.6 Mineralisation and the Chondro-osseous junction

The chondro-osseous junction represents another transition point and is the most complex transitional zone within the growth plate. It is, in fact, a true organ-level

system in which endothelial cells of the metaphyseal vasculature, blood cells, osteoprogenitor cells, and osteoclasts are separated from the terminal hypertrophic chondrocytes only by the distance of the last transverse septum of the hypertrophic cell zone. Terminally differentiated hypertrophic chondrocytes are characterised by an increase in intracellular calcium concentration. This is essential for the production of matrix vesicles, which are small membrane-enclosed particles that are released from chondrocytes (Wang *et al.*, 2002; Anderson *et al.*, 2003). These matrix vesicles provide an environment permissive for calcium phosphate precipitation into hydroxyapatite crystals. This mineralisation process takes the form of two distinct phases; phase one occurring completely within the matrix vesicle. During this phase, phosphatases associated with the matrix vesicle (such as alkaline phosphatase and PHOSPHO1) supply the required phosphate (Roberts *et al.*, 2007), whilst calcium is captured by annexins and phosphatidyl serine, to produce mineral crystals. During phase two, these mineral crystals pierce the matrix vesicle membrane and enlarge with the addition of phosphate and calcium ions present in the extravesicular space. This results in the formation of mineral spherules which associate closely to collagen fibrils. The mineralisation process, in combination with low oxygen tension, attracts blood vessels from the underlying primary spongiosa (Schipani *et al.*, 2001). Subsequently, the remaining hypertrophic chondrocytes undergo apoptosis, leaving a scaffold for new bone formation. The apoptotic process is, among other factors, regulated by elevated intracellular calcium levels (leading to activation of proteases, lipases and nucleases), retinoic acids and vitamin D. Longitudinal and transverse septae, which keep the chondrocytes in a columnar orientation in the growth plate, are resorbed by osteoclasts from the underlying primary spongiosum (Lewinson *et al.*, 1992; Vu *et al.*, 1998). At the same time, osteoblasts enter the area to lay down new

trabecular bone (although interestingly, only the longitudinal septae are actually replaced with trabecular bone; Mitchell *et al.*, 1982). The combination of the rate of chondrocyte proliferation, the size of the proliferative pool, the enlargement of maturing chondrocytes in the hypertrophic zone and the production of ECM are the major contributors to longitudinal bone growth.

In the steady state, chondrocytic turnover at the chondro-osseous junction needs to be offset literally on a one-to-one basis by cellular proliferation in order to maintain growth plate width and constant numbers of chondrocytes in the differentiation cascade that results in longitudinal growth. Turnover not compensated for by proliferation leads first to a decrease in total cellular numbers and, ultimately, to growth plate closure. It is known that rates of chondrocytic turnover at the chondro-osseous junction can be delayed in several kinds of diseases, such as rickets or osteochondroses (Farnum *et al.*, 1984; Shapiro *et al.*, 1987). Morphologically, this delay is manifested as an accumulation of hypertrophic chondrocytes with cells continuing to be added because proliferation is not impaired. In these diseases, cellular volume increase is initiated, but the turnover events at the chondro-osseous junction do not progress. In rickets, this situation indicates that events of matrix calcification are coupled to the final hypertrophic volume increase. However, in osteochondroses, there is evidence that matrix calcification, although initially delayed, may ultimately go on and result in hypertrophic chondrocytes of abnormal morphology surrounded by highly calcified longitudinal septae (Farnum *et al.*, 1984).

1.4.7 The fate of the terminally differentiated chondrocyte

Despite the agreement on the significance of hypertrophic chondrocytes in regulating both calcification of the matrix and the final extent of growth achieved, there remains a controversy about whether the terminal chondrocyte continues to live beyond the time of erosion of the last transverse septae, or whether its fate is death at the chondro-osseous junction (Cancedda *et al.*, 1995; Kwan *et al.*, 1997; Shapiro *et al.*, 2005). There has been significant morphological evidence to suggest that terminal hypertrophic chondrocytes die by apoptosis (Galotto *et al.*, 1994), and more recently, TUNEL labelling has supported this hypothesis (Zenmyo *et al.*, 1996). Studies looking at chondrocyte apoptosis identified a number of ions (such as the Ca²⁺ and Pi ion pair), peptides, and secreted matrix metalloproteins present at the chondro-osseous junction that could act as pro-apoptotic factors (Mansfield *et al.*, 1999; Mansfield *et al.*, 2003). Interestingly, some evidence has suggested that all chondrocytes have some level of DNA fragmentation characteristic of apoptosis (Hatori *et al.*, 1995). However, others have suggested that chondrocytes can transdifferentiate into osteoblasts (Roach *et al.*, 1995; Adams and Shapiro 2002; Shapiro *et al.*, 2005). The hypothesis of transdifferentiation has been tested using cultured embryonic explants from chick femurs which were cut at the hypertrophic zone of the growth plate. Associated with the change from chondrogenic to osteogenic commitment was an asymmetric cell division with diverging fates of the two daughter cells, where one daughter cell remained viable and the other one died. This suggests that the viable daughter cell then divided and generated osteogenic cells, while the other daughter cell died by apoptosis (Roach *et al.*, 1995). More recently, the concept of chondrocyte death by autophagy has been hypothesised (Bohensky *et al.*, 2007). In this theory, it is suggested that chondrocytes express a survival phenotype in response

to changes in the cartilage microenvironment. This phenotype causes the chondrocytes to oxidise their own structural macromolecules to generate ATP, ultimately leading to tissue damage and cell death.

1.4.8 Extracellular Matrix Proteins

The chondrocytes are embedded in a surrounding ECM, which provides support to the chondrocytes, and consists of matrix molecules, remodelling enzymes and growth factors. The first group of matrix molecules are the collagens, of which types II, IX and X are expressed predominantly in the proliferating, prehypertrophic and hypertrophic zones, respectively, and are essential for the integrity of the ECM (Horton *et al.*, 2003). In addition, they play an essential role in sequestering growth factors involved in the regulation of chondrocyte proliferation and differentiation. Collagens are the most abundant proteins in mammals, and are structured in the form of a triple helix with a regular arrangement of amino acids in each of the helices (Gly-X-Pro or Gly-X-Hyp, where X may be any of various other amino acid residues). Gene mutations in type II, IX or X collagens have been associated with disturbances of the cartilage matrix causing spondyloepiphyseal dysplasia and hypochondriasis, multiple epiphyseal dysplasia, or Schmid metaphyseal chondrodysplasia, respectively (Spranger *et al.*, 1994; Muragki *et al.*, 1996; Wallis *et al.*, 1996). These dysplasias are all associated with short stature.

Another group of ECM molecules comprises the proteoglycans, including aggrecan, biglycan and glypican. Proteoglycans consist of a core protein with one or more covalently attached glycosaminoglycan chains. These glycosaminoglycan (GAG) chains are long, linear carbohydrate polymers that are negatively charged under

physiological conditions, due to the occurrence of sulphate groups. These groups are essential for the activation of proteoglycans and for cross-linking of the ECM. A common GAG chain is chondroitin sulphate, a sulphated GAG which is composed of a chain of alternating N-acetylgalactosamine and glucuronic acid. Chondroitin sulphate is a major component of the extracellular matrix, and its function largely depends on the properties of the overall proteoglycan of which it is part. It has been shown to be important in maintaining the structural integrity of the tissue, a function which is typical of the large aggregating proteoglycans such as aggrecan, versican, brevican and neurocan. As part of aggrecan, chondroitin sulphate is a major component of cartilage, and the tightly packed, highly charged sulphate groups generate electrostatic repulsion that provides much of the resistance of cartilage to compression. Loss of chondroitin sulphate from cartilage is a major cause of osteoarthritis, and consequently it is widely used as a dietary supplement for the treatment of this disease (Barnhill et al., 2006; Bruyere et al., 2007). Heparin sulphate is a linear polysaccharide which also occurs in proteoglycans, and in the ECM, the main heparin sulphate bearing proteoglycans are the multi-domain perlecan, agrin and collagen type XVIII. Heparin sulphate is also a member of the GAG family, and consists of a variably sulphated repeating disaccharide unit. Synthesis of under sulphated GAGs, for example by mutations in the diastrophic dysplasia sulphate transporter gene, causes several forms of autosomal recessive chondrodysplasias, including diastrophic dysplasia, atelosteogenesis type II, and achondrogenesis type 1B (Rossi *et al.*, 2001).

Communication exists between the ECM and cellular responses within the chondrocyte through cell surface adhesion receptors, known as integrins. They

mediate the attachment of the chondrocytes to the surrounding ECM macromolecules, thereby increasing the integrity of the growth plate (Ruoslahti *et al.*, 1991). Furthermore, there is a group of ECM-remodelling enzymes, known as matrix metalloproteinases (MMPs) and their inhibitors (tissue inhibitor of MMP; TIMP). These play a crucial role in the remodelling and degradation of the ECM and are involved in the preservation of the ECM integrity and the initiation of angiogenesis (Werb *et al.*, 1997; Ortega *et al.*, 2003). Mice lacking MMP-9 display abnormal growth plate vascularisation and bone formation (Gerber *et al.*, 1999), whereas disruption of tissue inhibitor of MMP-1 in mice increases basement membrane invasiveness of primitive mesenchyme (precursor of chondrocyte) cells *in vitro* (Alexander *et al.*, 1992). Moreover, MMP-13 (collagenase-3) has been shown to be crucial for remodelling of the matrix in the transition zone of the growth plate (Wu *et al.*, 2002). Inhibition of MMP-13 inhibits degradation of collagen II, which is predominant in the proliferating zone and suppresses the expression of collagen X, which is the major collagen of the hypertrophic zone (Wu *et al.*, 2002). The ECM also functions as a reservoir of various growth factors that may be released and influence chondrocyte function when the ECM is degraded. Moreover, the ECM may control the diffusion capacity of growth factors, including fibroblast growth factors (FGFs) and hedgehogs. The role of the ECM is crucial for the integrity of cartilage and for normal longitudinal growth, but the interaction between collagens, MMPs, integrins, and the multitude of growth factors within the ECM is still far from understood.

1.5 Longitudinal Bone Growth

1.5.1 The Process of Longitudinal Growth

Longitudinal bone growth is the result of chondrocyte proliferation and subsequent differentiation in the epiphyseal growth plate. As previously discussed, it is regulated by a multitude of genetic and hormonal factors, growth factors, environment, and nutrition (Cancedda *et al.*, 1998; Hering *et al.*, 1999; Stevens *et al.*, 1999, Robson *et al.*, 2002; Kronenberg *et al.*, 2003). All of these factors contribute to establishing the final height of an individual. There are at least three distinct endocrine phases of linear growth during postnatal life in man. A high growth rate is observed from foetal life, with a rapid deceleration up to about 3 years of age. The second phase is characterised by a period of lower, slowly decelerating growth velocity up to puberty. The last phase, puberty, is characterised by an increased rate of longitudinal growth until the age of peak height velocity has been reached. Following this, growth velocity rapidly decreases due to growth plate maturation in long bones and spine, leading to fusion of the growth plate and cessation of longitudinal growth (Drop *et al.*, 1998). Recently, the process and moment of growth plate fusion has been elegantly studied by Martin and co-workers (Martin *et al.*, 2003), who determined the number of bony bridges between the epiphysis and metaphysis by microcomputed tomography in rats between 2 and 25 months of age. Although it is generally believed that cessation of growth succeeds growth plate fusion, this has recently been disputed by Parfitt (2002). He observed cessation of growth of a metacarpal in a patient with pseudohypoparathyroidism, which was followed later by fusion of the growth plate. In support of this, a recent study in aged rats has shown that, despite cessation of growth, growth plates still exist with sporadic chondrocyte proliferation (Roach *et al.*, 2003).

1.5.2 Growth Disorders

Disturbances of longitudinal bone growth occur frequently with a high diversity in aetiology. Both short and tall stature disorders are divided into primary (defect presumed in bone/cartilage), secondary (defect located outside bone/cartilage), or idiopathic (cause unknown) (Drop *et al.*, 2001). Primary short stature disorders include chromosomal disorders such as Down and Turner syndromes, genetic disorders such as achondroplasia, hypochondroplasia and thanatophoric dysplasia, Jansen's metaphyseal chondroplasia (defects in the parathyroid hormone type 1 receptor (PTH1R)), and multiple epiphyseal dysplasia (defects in the expression of type II, IX and X collagen). Primary tall stature disorders include chromosomal disorders such as Klinefelter syndrome (or 47, XXY), and genetic syndromes such as Sotos, Marfan and Weaver syndromes. Secondary disorders of short stature include those related to GH deficiency or resistance (Pit-1, Prop-1, Larson syndrome, IGF-I deficiency), hypothyroidism, malnutrition or renal failure. Secondary disorders of tall stature include GH excess, pituitary gigantism, GH-secreting tumours such as McCune Albright syndrome and pituitary adenomas, hyperinsulinism, sex hormone resistance or deficiency, and precocious puberty. In addition to the psychological problems associated with growth retardation, a number of studies have shown that reduced growth during development can lead to disease in later life. Known as the Barker hypothesis, it is now known that slow growth during foetal life and infancy is followed by an increased risk of coronary heart disease, type 2 diabetes and hypertension during adulthood. Mechanisms underlying this are thought to include the development of insulin resistance in utero, reduced numbers of nephrons associated with small body size at birth and altered programming of the micro-

architecture and function of the liver. Slow foetal growth might also heighten the body's stress responses and increase vulnerability to poor living conditions in later life. (Barker *et al.*, 1989; Barker 2002).

1.5.3 Catch-up Growth

Many systemic diseases impair longitudinal bone growth. Interestingly, after remission, growth often accelerates beyond the normal growth rate for that particular age, a phenomenon called catch-up growth (Boersma and Wit 1997). This has been observed in many growth-retarding conditions such as Cushing's syndrome (Prader *et al.*, 1963), hypothyroidism (Boersma *et al.*, 1995), celiac disease (Damen *et al.*, 1997), anorexia nervosa/malnutrition (Prader *et al.*, 1963), and GH deficiency (Boersma and Wit 1997). To explain catch-up growth, it was originally believed that a mechanism exists in the brain that compares the actual body size with an age-appropriate set point and adjusts the growth rate accordingly, and this is termed "sizo-stat" (Onat *et al.*, 1975). This neuroendocrine hypothesis was challenged by an experimental study in the rabbit. In this experiment, the GC dexamethasone (Dex) was infused by an osmotic minipump directly in the tibial growth plate, which slowed bone growth of the treated leg but not of the contralateral vehicle-treated leg (Baron *et al.*, 1994). When Dex infusion was stopped, tibial bone growth was not just normalised but even increased compared with the contralateral leg, thereby demonstrating catch-up growth (Baron *et al.*, 1994). Based on these findings, Gafni and Baron (2000) proposed that the underlying mechanism for catch-up growth was intrinsic to the growth plate. A mechanism explaining catch-up growth may be that a maximum number of cell divisions exist for growth plate resting chondrocytes and that at each cell division the proliferation rate decreases, a process known as

senescence. Growth retardation reduces chondrocyte proliferation and thereby delays senescence. When remission takes place, the cells within the proliferating zone have a greater proliferating potential, explaining the increased growth rate compared with the unaffected growth plate. This was recently supported by intra-muscular oestrogen injections in rabbits resulting in a more rapid senescence of growth plate chondrocytes, causing proliferative exhaustion and earlier growth plate fusion compared with non-treated rabbits (Weise *et al.*, 2001). However, these studies have been performed in animals, and their pattern of catch-up growth is different from that of humans. For example, in a child who displays catch-up growth, height velocity can be four times that of normal growth, whereas in rats and rabbits the growth velocity increment is minimal. To date, additional studies are required in humans to generate a more solid and satisfactory hypothesis for the process of catch-up growth (Boersma and Wit, 1997, Wit and Boersma, 2002).

1.6 Regulation of Longitudinal Bone Growth

1.6.1 Systemic Regulation

The major systemic factors that regulate longitudinal bone growth during childhood are GH and IGF-I, thyroid hormone, and GCs, whereas during puberty, the sex steroids (oestrogens and androgens) also contribute to this process. Although the effects of these factors on longitudinal bone growth have been well reported, the mechanisms underlying these effects remain largely unknown.

1.6.1.1 GH-IGF-I system

IGF-I and -II are believed to be the key regulators of GH-independent growth before birth. This is based on findings in knockout mice, and also on the observation that in

congenital GH deficiency, birth length is only mildly diminished, whereas in congenital IGF-I deficiency birth length is severely diminished (Mehta *et al.*, 2005). Following birth, GH is an important modulator of longitudinal bone growth and, together with IGF-I, plays a major role in the hypothalamus-pituitary (HPA) growth plate axis (Figure 1.5). GH secretion from the pituitary is stimulated by Growth Hormone Releasing Hormone (GHRH) and inhibited by somatostatin, which are both released by the hypothalamus. GH is released in a pulsatile manner which is more regular and contains higher peak levels in boys, whereas in girls this secretion is more irregular (Veldhuis *et al.*, 1998). A pituitary adenoma in childhood or adulthood causes enhanced GH secretion, leading to pituitary gigantism, or acromegaly, respectively (Daughaday *et al.*, 1992; Ezzat *et al.*, 1997). Conversely, defects in the formation of GH-secreting cells (i.e. Prop-1 or Pit-1 mutations), synthesis or release of GH (i.e. by GHRH-receptor or Pit-1 mutations), or GH insensitivity can result in severe dwarfism (Wit *et al.*, 1989; Pfaffle *et al.*, 1993; Savage *et al.*, 2001).

GH acts on its target tissue directly or through IGF-I and –II. There is now substantial evidence that both IGFs have a unique and complementary role in regulating bone growth (Le Roith *et al.*, 2001). In 1957, Salmon and Daughaday postulated the somatomedin (now called IGF) hypothesis in which the growth plate chondrocytes response to GH was mediated through the hepatic production of IGF and its release into the circulation. From there, IGF-I reaches its target tissues (cartilage and bone) and interacts with its receptors, which convey a growth signal to the cell. This hypothesis is compatible with an endocrine action of IGF-I and was based on experimental evidence that the addition of GH to cartilage fragments in culture had little effect, whereas the addition of serum stimulated cellular processes associated

with chondrocyte proliferation and differentiation. However, serum from hypophysectomised animals had a lesser effect and subsequent GH therapy resulted in a serum with normal growth promoting activities. The somatomedin hypothesis has been questioned by other experiments showing that low concentrations of GH directly infused into the growth plate showed stimulated longitudinal growth in comparison to the contralateral limb (Isaksson *et al.*, 1982). These and similar studies have led to an alternative hypothesis of GH action in which GH has a direct effect on bone and other peripheral tissues resulting in the local production of IGF-I (D'Ercole *et al.*, 1984).

This hypothesis was supported by work carried out by Isaksson *et al.*, who used cultured growth plate chondrocytes to show that GH acts on resting zone chondrocytes and is responsible for local IGF-I production, stimulating the clonal expansion of proliferating chondrocytes in an autocrine/paracrine manner (Isaksson *et al.*, 1987). This hypothesis was named the dual-effector theory in analogy to the proposed dual-effector theory in adipocytes by Green *et al.*, (1985). Partly supporting the dual-effector theory, Hunziker *et al.*, (1994) showed that in hypophysectomised rats, resting cell cycle times were reduced with either GH or IGF-I administration. In addition, proliferating cell cycle time and duration of the hypertrophic phase were reduced. From these studies, it was concluded that both GH and IGF-I were capable of stimulating growth plate resting cells (Ohlsson *et al.*, 1992).

In support of direct effects of circulating GH on the growth plate, GHR has been detected in rabbit and human growth plate chondrocytes (Barnard *et al.*, 1988), and recently, both GHR and GH binding protein (GHBP) have been found in rat growth plate chondrocytes during development (Gevers *et al.*, 2002). Interestingly, the

expression of GHR and GHBP in the growth plate were shown to be regulated by thyroid hormone, GH and dexamethasone (Dex), and administration of GH into IGF-I null mice increased the width of the resting zone, supporting a direct role for GH on the growth plate. (Wang *et al.*, 1999).

IGF-I also plays an important role in longitudinal bone growth, as IGF-I null mice display severe dwarfism (Powell-Braxton *et al.*, 1993), and children with a homozygous IGF-I deletion have extremely short stature (Abuzzahab *et al.*, 2003). Mice with a double knockout for both GHR and IGF-I are smaller than mice with either a GHR or IGF-I single knockout, suggesting that both GH and IGF-I contribute significantly to longitudinal growth. In addition, mice with a double knock-out for liver IGF-I and the acid-labile subunit displayed reduced linear growth and decreased bone mineral density (Yakar *et al.*, 2002).

1.6.1.2 Thyroid Hormone

In addition to GH and IGF-I, thyroid hormone (T_3), and, to a lesser extent, its precursor thyroxine (T_4), are crucial for normal bone maturation (Shao *et al.*, 2006). In children, hypothyroidism causes growth arrest, delayed bone maturation and epiphyseal dysgenesis, with thyroxine replacement resulting in catch-up growth (Basset *et al.*, 2007). Conversely, thyrotoxicosis in children accelerates growth and advances bone age, but ultimately leads to growth retardation due to premature growth plate fusion. Many *in vitro* and *in vivo* studies have shown that T_3 regulates the transition between proliferation and terminal differentiation in the growth plate and specifically, the maturation of growth plate chondrocytes into hypertrophic cells (Figure 1.5).

In organ cultures, T_4 has been shown to stimulate chondrocyte differentiation (Miura et al., 2002), whilst in vitro, T_3 decreases chondrocyte proliferation (Ohlsson et al., 1992; Robson et al., 2000). In addition, many in vitro studies have shown that T_3 positively regulates the terminal differentiation of chondrocytes in several different species (Ohlsson et al., 1992; Bohme et al., 1995; Leboy et al., 1997; Okubo and Reddi 2003). Interestingly, mechanistic studies have shown that T_4 stimulates the expression of p21, an inhibitor of the cell cycle, in rat epiphyseal chondrocytes in vitro (Ballock et al., 2000), and also inhibits the expression of Sox-9, a transcription factor that maintains chondrocytes in an undifferentiated state (Okubo and Reddi 2003). In addition, T_3 stimulates fibroblast growth factor (FGF) receptor expression in murine chondrogenic ATDC5 cells, enhancing FGF signalling (Barnard et al., 2005).

T_3 actions are mediated through nuclear T_3 receptors (TR), which have been shown to act as ligand-controlled transcription factors (Yen et al., 2006), and a number of different isoforms of TR have been detected in the growth plate. $TR\alpha 1$ and $TR\alpha 2$ are expressed in chondrocytes and osteoblasts, as is the $TR\beta 1$ isoform. Mice lacking functional $TR\alpha 1$ and $TR\alpha 2$ display abnormal growth plate morphology and impaired mineralisation during endochondral ossification (Gauthier et al., 2001), and this is associated with reduced $FGFR1$ and $FGFR3$ expression in osteoblasts and chondrocytes (Stevens et al., 2003; Barnard et al., 2005). In contrast, mice with a mutation in $TR\beta 1$ have elevated T_4 levels, advanced bone age and short stature, resulting from a reduced width of the growth plate (O'Shea et al., 2003). A specific role for $TR\beta$ in chondrocytes has also been suggested in studies using the selective $TR\beta$ agonist GC-1 (Freitas et al., 2005). Hypothyroid rats displayed disorganised chondrocyte columns, reduced hypertrophic chondrocyte differentiation and impaired

mineralisation. These abnormalities were all rescued by the administration of T₃, and although the agonist GC-1 also rescued differentiation and mineralisation defects, normal growth plate morphology was not restored.

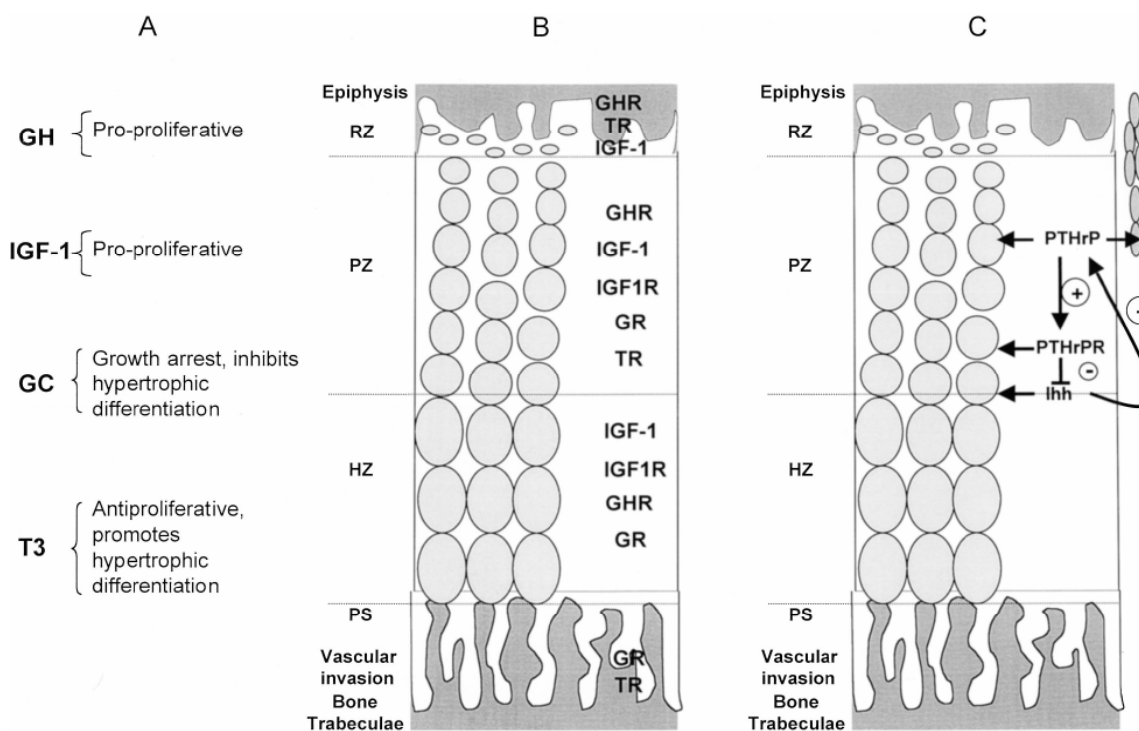


Figure 1.5 Hormone action in the growth plate. (A) The effects of GH, IGF-I, GC, and T₃ on growth plate chondrocytes. (B) Regions of the growth plate in which IGF-I and GHR, IGF-IR, GR, and TR are expressed. *RZ* indicates reserve zone; *PZ*, proliferative zone; *HZ*, hypertrophic zone; *PS*, primary spongiosum. (C) The Ihh/PTHrP feedback loop, which regulates the pace of endochondral ossification. Ihh is secreted by prehypertrophic chondrocytes and acts on perichondrial cells during development, or on proliferative chondrocytes during postnatal growth, to stimulate release of PTHrP. PTHrP acts on PTHrP receptors (*PTHrPR*) that are expressed in uncommitted prehypertrophic chondrocytes to delay differentiation and maintain cell proliferation (Robson *et al.*, 2002).

1.6.1.3 Sex Steroids

It has long been established that sex steroids are important for longitudinal growth, especially during puberty. It was generally assumed that in girls, oestrogen was the primary sex steroid regulating pubertal growth, whereas in boys this was achieved primarily by androgen. However, the finding of a male patient with an inactivation mutation in Oestrogen Receptor α ($ER\alpha$) fundamentally changed this view (Smith *et*

al., 1994). This patient, who was resistant to the actions of oestrogens, demonstrated longitudinal growth well into adulthood, resulting in tall stature due to a lack of growth plate fusion as well as severe osteoporosis, despite high levels of testosterone (Smith *et al.*, 1994). This finding led to the assumption that in both boys and girls, oestrogen is the main determinant for the puberty-associated phenomena related to longitudinal growth and bone quality (Grumbach 2001; Juul *et al.*, 2001).

In vitro studies have shown that, in the growth plate, oestrogen alters alkaline phosphatase activity, cell proliferation and proteoglycan synthesis (Schwartz *et al.*, 2002). Indeed, oestrogen has a biphasic effect on proliferation, which is stimulated by low levels and inhibited by high levels of oestrogen (Frank *et al.*, 2003). A number of studies have demonstrated the presence of the androgen receptor and both oestrogen receptors, ER α and ER β , in growth plate tissue at the mRNA and protein level in several species, including rat, rabbit, and human (Chagin and Savendahl 2007), indicating that androgens and oestrogens directly regulate processes in the growth plate. Furthermore, the growth plate possesses the ability for steroidogenesis as well as aromatisation (Van der Eerden *et al.*, 2004). However, it has been difficult to prove whether androgens have direct effects on growth plate cartilage. Non-aromatisable androgens, such as dihydrotestosterone, have been shown to regulate both the proliferation and differentiation of cultured human epiphyseal chondrocytes, probably by promoting local IGF-1 synthesis and increasing IGF-I receptor expression (Blanchard *et al.*, 1991; Krohn *et al.*, 2003).

1.6.2 Local Regulation of the Growth Plate

1.6.2.1 Fibroblast growth factor (FGF) signalling

Recent studies have shown that many of the 22 FGF genes and 4 FGF receptor (FGFR) genes are expressed by chondrocytes at every stage of endochondral bone formation. Both FGF1 and -2, as well as FGFRs 1-3 are expressed in chondrocytes (Peters *et al.*, 1992; Jinguishi *et al.*, 1995; Leach *et al.*, 1997), and in humans, mutations in the FGFR3 gene cause achondroplasia, the most common type of human dwarfism (Vajo *et al.*, 2000). In addition, overexpression of FGF2 has been shown to slow longitudinal growth (Coffin *et al.*, 1995). Mancilla *et al.* (1998) have also shown that, in a metatarsal organ culture model, FGF2 decreased growth plate chondrocyte proliferation, decreased cellular hypertrophy, and at high concentrations, decreased cartilage matrix production. However, the multiple early effects of FGFs in the development of bone have made the genetic analysis of the roles of FGF signalling during bone development a particular challenge. During the early stages of bone development, FGFs have been shown to stimulate Sox9 expression in a mesenchymal cell line (Murakami *et al.*, 2000). In proliferating chondrocytes, FGF signalling through FGFR3 inhibits proliferation (Figure 1.6) (Sahni *et al.*, 1999) by activation of the Janus kinase-signal transducer and activator of transcription-1 pathway (JAK-STAT1). In addition, activation of FGFR3 has been shown to decrease Indian hedgehog (Ihh) expression (Naski *et al.*, 1998), also leading to a decrease in chondrocyte proliferation (Figure 1.6). Accordingly, FGF signalling shortens proliferative columns both by decreasing chondrocyte proliferation directly and by suppressing Ihh expression.

1.6.2.2 Bone Morphogenic Protein (BMP) and Transforming growth factor β (TGF β) signalling

The family of BMPs is comprised of at least 15 members, which are all part of the TGF β superfamily. BMPs were originally identified as stimulators of bone formation but are now recognised as important regulators of growth, differentiation, and morphogenesis during embryology (Reddi *et al.*, 2001). Within the developing limb cartilage elements, BMP2, -4, and -7 have been detected in the perichondrium, whereas BMP6 was found in prehypertrophic and hypertrophic chondrocytes (Lyons *et al.*, 1989; Jones *et al.*, 1991; Macias *et al.*, 1997; Grimsrud *et al.*, 1999; Haaijman *et al.*, 1999). The effects of BMPs are mediated by two type I receptors, BMPRIA and -IB, which heterodimerise with the type II receptor, BMPRII. The type I receptors are differentially localised in embryonic limbs; BMPRII is detected in early mesenchymal condensations and is involved in early cartilage formation, whereas BMPRIA expression is confined to prehypertrophic chondrocytes (Zou *et al.*, 1997). Constitutive active and/or dominant negative forms of BMPRIA and -IB revealed that the type IA receptor controls the pace of chondrocyte differentiation, whereas the type IB receptor is involved in cartilage formation and apoptosis (Zou *et al.*, 1997). Mice bred with homozygous null mutations in BMP-2 and -4 do not survive (Winnier *et al.*, 1995), whereas other family members such as growth and differentiation factor 5 (GDF5) and BMP-5 are important mediators of chondrocyte differentiation in mesenchymal condensations at various sites (Mikic *et al.*, 1996, Storm *et al.*, 1999).

Several mutations in the BMP antagonist noggin result in proximal symphalangism (fusion of the joints in the carpal and tarsal bones) and multiple synostoses syndrome (premature fusion of the joints) (Gong *et al.*, 1999). Recently, BMP6 was introduced

as a possible mediator in the growth-restraining feedback loop involving Ihh and PTHrP (Grimsrud *et al.*, 1999). The fact that BMPRIA is expressed in the same region and that it has been shown to be critical for chondrocyte hypertrophy further strengthens an autocrine/paracrine role for BMP6 in prehypertrophic chondrocytes (Zou *et al.*, 1997). It has also been shown that normal chondrocyte proliferation requires parallel signalling of both Ihh and BMPs and that BMPs are capable of inhibiting chondrocyte differentiation independently of the Ihh/PTHrP pathway (Minina *et al.*, 2000) (Figure 1.6).

In humans, only a few mutations in members of the TGF β superfamily cause cartilage disorders. Genomic mutations in the human GDF5 gene have been shown to cause chondrodysplasia Grebe type, acromesomelic chondrodysplasia Hunter Thompson type, and brachydactyly type C, all of which are mainly characterised by defects of the limbs, with increasing severity towards the distal regions (Thomas *et al.*, 1996; Polinkovsky *et al.*, 1997, Thomas *et al.*, 1997). In another study, inhibition of chondrocyte differentiation by TGF β was shown to be at least partly mediated by induction of PTHrP expression (Alvarez *et al.*, 2001). These data imply that the BMPs/ TGF β and their receptors act as a signalling system, both dependently and independently of the Ihh/PTHrP feedback loop, at different levels during embryonic bone formation.

1.6.2.3 Ihh/PTHrP signalling

Ihh is a major regulator of bone development, controlling chondrocyte proliferation, chondrocyte differentiation and osteoblast differentiation. Ihh is a member of the hedgehog family of ligands, and during bone development, is synthesised by

prehypertrophic chondrocytes and by early hypertrophic chondrocytes. The binding of Ihh to its receptor (Patched-1), leads to activation of Smoothed, a membrane protein that is essential for the cellular actions of Ihh. $Ihh^{-/-}$ mice have normal bones at condensation, but later develop abnormalities of bone growth and a decrease in chondrocyte proliferation (St Jacques *et al.*, 1999). In addition, the bones of $Ihh^{-/-}$ mice have an increase in the number of hypertrophic chondrocytes versus proliferating chondrocytes. This is a result of chondrocytes leaving the proliferative pool early, and is suggested to be due to the fact that the cartilage in $Ihh^{-/-}$ mice fails to produce PTHrP.

PTHrP acts upon the G-protein coupled receptor, PTH1R, and its main function within the growth plate is to keep proliferating chondrocytes in the proliferative pool and to control the pace of chondrocyte differentiation (Figure 1.6). In $PTHrP^{-/-}$ or $PTH1R^{-/-}$ mice chondrocytes hypertrophy early and become hypertrophic close to the ends of bones (Karaplis *et al.*, 1994; Lanske *et al.*, 1996). In contrast, overexpression of PTHrP in chondrocytes delays the appearance of hypertrophic chondrocytes (Weir *et al.*, 1996). Interactions between Ihh and PTHrP were suggested when it was discovered that Ihh can stimulate the expression of PTHrP and consequently delay chondrocyte hypertrophy (Vortkamp *et al.*, 1996). It has since been hypothesised that together, Ihh and PTHrP control the decision of chondrocytes to leave the proliferative pool through a feedback loop (Figure 1.6). In this loop, Ihh is produced by prehypertrophic chondrocytes committed to hypertrophy and acting through its receptor (Ptc-1) within the perichondrium, increases the expression of PTHrP in the periarticular region. PTHrP then binds to PTH1Rs expressed on prehypertrophic chondrocytes – i.e., prior to their conversion to Ihh expressing cells – and blocks their

further differentiation. As the population of committed cells progresses to the hypertrophic phenotype, they stop expressing *Ihh*, thereby attenuating the negative feedback loop and allowing the further differentiation of uncommitted prehypertrophic cells. This feedback loop demonstrates the importance of the interactions between PTHrP and *Ihh* to determine the lengths of proliferative columns in individual bones (Kronenberg *et al.*, 2001).

1.6.2.4 Vascular endothelial growth factor (VEGF)

During chondrocyte hypertrophy, ECM surrounding the hypertrophic cells becomes calcified, which triggers the invasion of blood vessels from the underlying metaphyseal bone. This is preceded by the expression of VEGF in hypertrophic chondrocytes (Haigh *et al.*, 2000). Inactivation of VEGF by systemic administration of a soluble receptor to 24-d-old mice suppressed blood vessel invasion and trabecular bone formation concomitant with an increased width of the hypertrophic zone (Gerber *et al.*, 1999), indicating that VEGF plays an important role in the events that take place during the end-stage of endochondral bone formation such as terminal differentiation of chondrocytes, vascular invasion, chondrocyte apoptosis, and their subsequent replacement by bone (Gerber *et al.*, 1999). Other promoters or inhibitors of angiogenesis have been described in the literature, including transferrin (promoter) (Carlevaro *et al.*, 1997), chondromodulin (inhibitor) (Hiraki *et al.*, 1997), and FGFs (promoters) (Baron *et al.*, 1994). In embryonic growth plates, Schipani *et al.* (2006) described the role of hypoxia inducible factor ($\text{HIF-1}\alpha$), which is a transcription factor that regulates VEGF expression (Semenza *et al.*, 1999). Growth plate-specific targeted deletion of $\text{HIF-1}\alpha$ caused increased cell death and reduced VEGF expression (Schipani *et al.*, 2005). At the same time, cells surrounding the area of

increased cell death contained enhanced VEGF levels, suggesting that VEGF expression is regulated in an HIF-1 α -dependent and -independent manner (Schipani *et al.*, 2006).

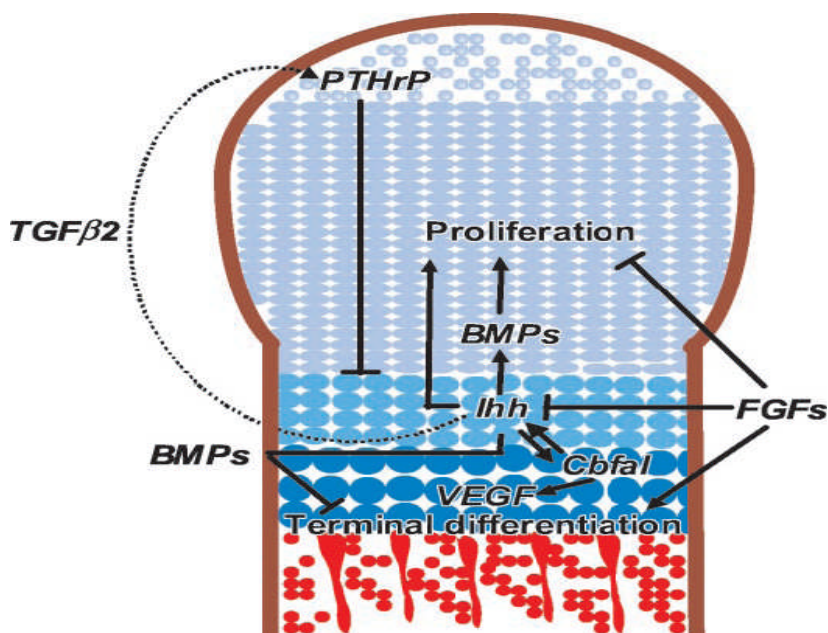


Figure 1.6 Interaction of Ihh, PTHrP, BMP, and FGF signalling in modulating chondrocyte proliferation and differentiation. Expression of Ihh in prehypertrophic chondrocytes is up-regulated by BMPs but inhibited by FGFs. Ihh activates adjacent chondrocytes and diffuses toward the lateral perichondrium, where it can bind to its receptor Patched. PTHrP production is stimulated in the periarticular perichondrium and diffuses toward the prehypertrophic zone, which expresses high levels of PTH/PTHrP receptors and inhibits the differentiation of proliferating chondrocytes. Besides modulating chondrocyte differentiation, Ihh also stimulates chondrocyte proliferation, both directly and indirectly through BMP signalling. FGFs are able to inhibit chondrocyte proliferation independently of the two stimulatory pathways. BMP signalling inhibits terminal differentiation of chondrocytes, a process that FGFs can promote. The balance between BMP and FGF signalling is crucial in regulating proliferation, Ihh expression, and terminal differentiation of chondrocytes. From Van der Eerden *et al.*, 2003.

1.6.2.5 Sox9

The main role of the transcription factor Sox9 is controlling the conversion of mesenchymal cells into chondrocytes. However, it also acts on chondrocytes through every stage of differentiation. Sox9 is expressed in cells of mesenchymal condensations and in proliferating chondrocytes, but not hypertrophic chondrocytes.

Sox9^{-/-} mesenchymal cells cannot form condensations or go on to form chondrocytes (Mori-Akiyama *et al.*, 2003), and when Sox9 was deleted from chondrocytes at later stages of development, the chondrocytes displayed decreased proliferation, decreased expression of matrix genes and decreased expression of the Ihh-PTHrP signalling pathways (Akiyama *et al.*, 2002). Sox9 is crucial for all phases of chondrocyte development, and is considered the master regulator of chondrocyte formation. Sox9 has an essential role in determining the commitment and differentiation of mesenchymal cells toward the chondrogenic lineage. Sox9 is expressed in prechondrocytic and chondrocytic cells during embryonic development, and cells lacking Sox9 fail to differentiate to a chondrocyte phenotype due to decreased activation of COL2A1 (Coll II gene), an important element of differentiation (Lefebvre *et al.*, 1997). This results in campomelic dyschondroplasia, a severe form of chondrodysplasia which is caused by a decrease in production of Coll II. Mesenchymal cells from Sox9^{-/-} knockout mice cannot differentiate into chondrocytes and cartilage cannot be formed from teratomas derived from Sox9^{-/-} embryonic stem (ES) cells (Mori-Akiyama *et al.*, 2003). Similarly, other studies have shown that the inactivation of Sox9 in mesenchymal condensations during embryonic development causes a severe decrease in differentiated chondrocytes, again resulting in severe dyschondroplasia (Akiyama *et al.*, 2002).

1.7 Cell Cycle Signalling

1.7.1 Control of Cell Cycle Gene Expression

As growth plate function is closely linked to the rates of cell cycle progression and the timing of cell-cycle exit during differentiation, it has been suggested that cell cycle genes play a crucial role in the control of longitudinal bone growth (Beier *et al.*,

1999a and b). Progression through the eukaryotic cell-cycle is controlled by cyclin-dependent kinases (CDKs) (Lundberg and Weinberg 1999), and their partner proteins, the cyclins. The activity of CDKs is highly regulated by the activity of their respective cyclins; the levels of cyclin-dependent kinase inhibitors (CKDIs) of the Cip/Kip family (p21, p27, p57), and Ink family (p15, p16, p18, p19); and inhibitory and stimulatory phosphorylation of various CDK residues. High levels of cyclins generally stimulate cell-cycle progression and proliferation through activation of CKDs, whereas high levels of CKDIs antagonise these processes. As previously mentioned, different growth plates within the same animal grow at different rates (Wilsman *et al.*, 1996). These differences are largely due to the duration of the G1 phase in proliferating chondrocytes (Wilsman *et al.*, 1996), suggesting that cell-cycle genes regulating G1 progression are of special importance in regulating endochondral bone growth. In recent years, several studies have identified G1 cell-cycle genes as targets of both extracellular signals and intracellular signalling pathways during cartilage development. Among regulators of the G1 phase of the cell-cycle, the cyclin D1 and p21^{Cip1/Waf1} genes have been shown to be regulated by numerous upstream signals, although other cyclins and CKDIs have also been identified as targets of mitogenic and anti-mitogenic signals. The D type cyclins (cyclin D1, D2, and D3) are the first cyclins to be induced in the mammalian cell-cycle and control progression through the G1 phase in complexes with CDKs 4 and 6 (Bartek and Lukas, 2001; Hulleman and Boonstra, 2001). Within the growth plate, cyclin D1 expression is specific for the proliferative zone at the mRNA and protein levels (Beier *et al.*, 2001), consistent with its role in supporting progression through the G1 phase of the cell-cycle (Figure 1.7)

p21^{Cip1/Waf1} (referred to as p21 from now on) is one of seven CDKIs. Similar to cyclin D1, expression of the p21 gene in chondrocytes is controlled by several different pathways. p21 expression is upregulated in postmitotic, differentiating chondrocytes in vivo (Stewart *et al.*, 1997; Zenmyo *et al.*, 2000). An important role of this gene in skeletal development was first suggested when it was identified as a target of activated FGF receptor 3 (FGFR3) in thanatophoric dysplasia, a severe human chondrodysplasia (Su *et al.*, 1997). Several other studies confirmed that p21 expression in chondrocytes is induced or enhanced by FGF signalling through the transcription factor STAT1 (Sahni *et al.*, 1999; Weksler *et al.*, 1999; Aikawa *et al.*, 2001; Benoist-Lasselin *et al.*, 2007). These studies suggest that induction of p21 expression and subsequent cell-cycle withdrawal likely contribute to the dwarfism caused by mutations in the FGFR3 gene (Ornitz and Marie, 2002). However, additional target genes are likely involved; for example, one study demonstrated that overexpression of an activated FGFR3 gene in transgenic mice also induces expression of the p16, p18, and p19 genes, CDK inhibitors of the INK family (Legeai-Mallet *et al.*, 2004). In addition, FGF1 induces expression of p27 and p57 in rat chondrosarcoma cells (Laplantine *et al.*, 2002). Expression of p21 and the related p27 protein in chondrocytes is also enhanced by thyroid hormone, a well-characterised inducer of chondrocyte hypertrophy (Figure 1.7) (Ballock *et al.*, 2000), and by BMP2 (Carlberg *et al.*, 2001). Finally, Sox9 (Panda *et al.*, 2001) and the c-Raf/MEK/ERK MAPK signalling cascade (Beier *et al.*, 1999; Stanton *et al.*, 2003) have also been shown to be important positive regulators of p21 expression, whereas PTH represses p21 expression in the chondrogenic cell line ATDC5 (Negishi *et al.*, 2001). In addition, chondrocyte proliferation is enhanced and p57 expression decreased in mice

with cartilage-specific inactivation of the gene encoding HIF-1a, a transcription factor involved in the cellular response to hypoxia (Schipani *et al.*, 2001).

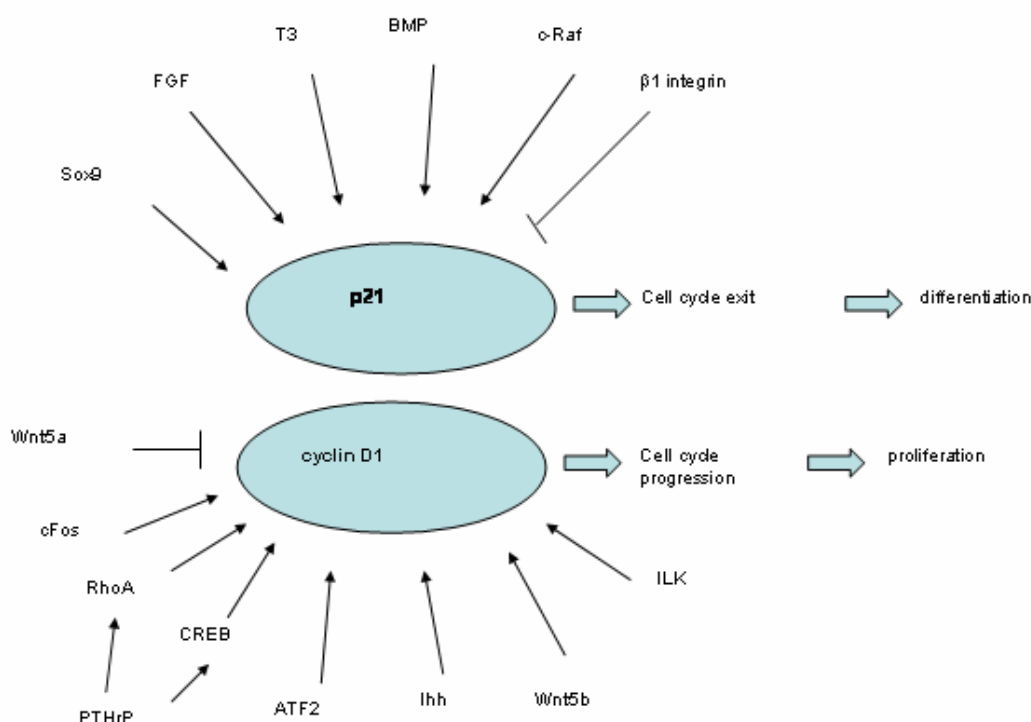


Figure 1.7 p21 and cyclin D1 as targets of mitogenic and antimitogenic signals in chondrocytes. Numerous extra- and intracellular signals target expression of cyclin D1 and p21 genes in chondrocytes, suggesting that these genes act as integrators of mitogenic and antimitogenic stimuli, respectively. *Adapted from Beier et al., 2005.*

1.7.2 Function of cell cycle genes in the growth plate

Gain- and loss-of function experiments have identified roles of multiple cell cycle genes in endochondral bone growth. Targeted inactivation of the p57Kip2 (p57) gene results in severe skeletal defects caused by delayed cell-cycle exit and disrupted hypertrophic differentiation of growth plate chondrocytes (Yan *et al.*, 1997; Zhang *et al.*, 1997). The endochondral skeleton seems to be the one of the most affected tissues, indicating that cartilage development is particularly sensitive to changes in the levels of cell-cycle proteins. Adenoviral overexpression of p57 in primary rat chondrocytes induces cell-cycle exit, but is not enough to trigger expression of Coll

X, the classical marker of hypertrophic chondrocytes (Stewart *et al.*, 2004). However, p57 cooperates with BMP2 in the induction of Coll X expression. While p21-deficient mice do not display any obvious developmental defects (Deng *et al.*, 1995), loss of p21 increases the severity of skeletal defects in p57 null mice (Zhang *et al.*, 1999). Furthermore, chondrocytes from p21 null mice show reduced antimitogenic response to FGF in organ cultures (Aikawa *et al.*, 2001), and expression of p21 antisense RNA in ATDC5 cells inhibits early chondrogenic differentiation (Negishi *et al.*, 2001).

In addition to p21, p27 has been detected immunohistochemically in hypertrophic chondrocytes in foetal and early postnatal mice (Sunters *et al.*, 1998; Horner *et al.*, 2002). p27 has also been detected in cultured rat resting zone chondrocytes where its expression is up-regulated during thyroid hormone-induced terminal differentiation (Ballock *et al.*, 2000). Targeted disruption of p27 in mice causes multi-organ hyperplasia and increased body weight, with all tissues proportionally enlarged and containing more cells (Drissi *et al.*, 1999; Nagahama *et al.*, 2001; Teixeira *et al.*, 2001), and Kiyokawa *et al.*, (1996) reported an increased size and width of tibiae and femora in p27-deficient mice compared with wild-type mice. A recent paper by Emons *et al* (2007) has gone on to study the growth plate of p27 null mice in more detail. Although the absence of p27 caused an increase in the number of proliferating chondrocytes within the growth plate, there were no obvious differences in growth plate morphology and no increase in tibial growth rate was observed. These findings suggest that p27 has modest inhibitory effects on growth plate chondrocyte proliferation but is not required for the spatial or temporal regulation of proliferation.

In contrast to the number of publications on the role of inhibitors of cell-cycle progression, fewer functional studies have been reported for positive regulators of the cell-cycle. As mentioned above, cyclin D1-deficient mice are dwarfed (Fantl *et al.*, 1995) with a smaller proliferative zone of the growth plate (Beier *et al.*, 2001). Cyclin D1 antisense oligonucleotides reduce proliferation and E2F activity, and delay cell cycle progression in chondrogenic cells (Beier *et al.*, 2001; Beier and LuValle, 2002). In contrast, defects in cyclin D2 knockout mice appear to be restricted to reproductive tissues (Sicinski *et al.*, 1996). The last few years have seen both the identification of novel regulatory mechanisms governing cell-cycle gene expression in the growth plate and progression in the functional analyses of cell-cycle genes in cartilage development. Complete elucidation of the signalling and transcriptional events involved will be necessary to understand how the cell-cycle machinery integrates multiple inputs and creates a coordinated response to the multitude of intrinsic and extrinsic signals acting on chondrocytes. In addition, further mechanistic investigations at the molecular, cellular, tissue and whole animal level will be required to obtain a comprehensive view of the role of cell-cycle genes in endochondral bone growth.

1.8 GCs and Growth Retardation

1.8.1 GC Physiology

GCs are synthesised and secreted by the adrenal cortex and are essential for the function of most systems in the body. In physiological doses, they help the body adapt to intermittent food intake by regulating blood sugar and electrolytes, promoting gluconeogenesis, mobilising fats for energy metabolism and depressing inflammatory and immune responses. Physiological GCs include the most predominant, cortisol,

cortisone and corticosterone. GCs are commonly known as the stress hormones, and, under normal circumstances are crucial for the capability of the body to respond and adapt to stress.

The main physiological stimulus for synthesis and release of GCs is adrenocorticotrophic hormone, or ACTH, secreted from the anterior pituitary gland. ACTH secretion is regulated partly by corticotrophin-releasing factor (CRF) derived from the hypothalamus and partly by the level of GCs in the blood. The release of CRF in turn is inhibited by the level of GCs and, to a lesser extent, of ACTH in the blood, and is influenced by input from the central nervous system. There is a basal release of GCs, and the concentration of endogenous GCs in the blood is higher in the morning, and low in the evening. The starting substance for the synthesis of GCs is cholesterol (Figure 1.8), which is obtained mostly from the plasma and is present in the lipid granules in the zona fasciculata of the adrenal cortex. The first step, the conversion of cholesterol to pregnenolone, is the rate limiting step and is regulated by ACTH.

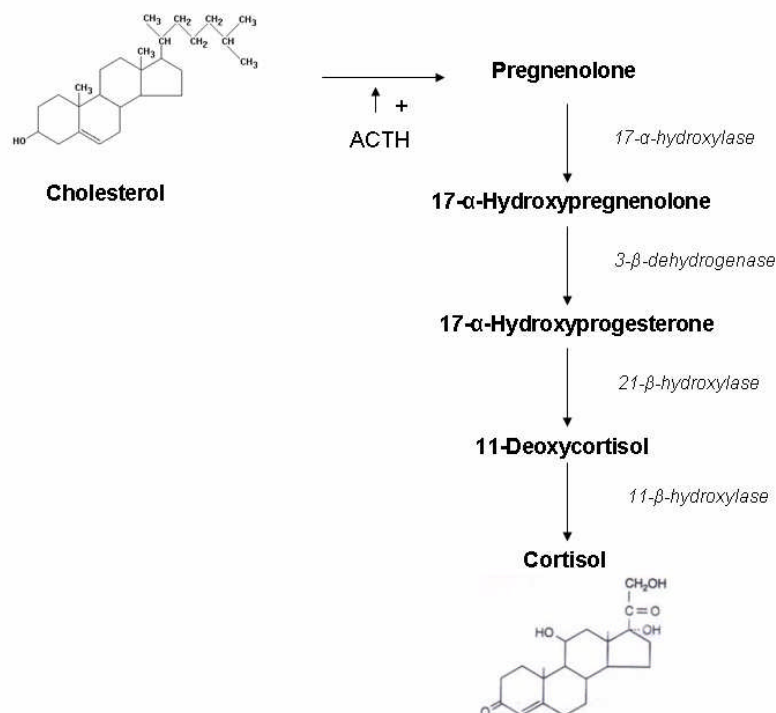


Figure 1.8 The GC Biosynthetic Pathway The first and rate-limiting step of GC synthesis is the conversion of cholesterol to pregnenolone, which is stimulated by ACTH. Pregnenolone is then converted to the GC cortisol through a series of reactions catalysed by hydroxylase and dehydrogenase enzymes (italics).

The main metabolic effects of GCs are on carbohydrate and protein metabolism. GCs cause both a decrease in the uptake and utilisation of glucose and an increase in gluconeogenesis, resulting in a tendency to hyperglycaemia. In addition, GCs cause decreased protein synthesis and increased protein breakdown, particularly in muscle, and due to an increase in lipase activation through cAMP, large doses of GCs can also result in fat redistribution as seen in Cushing's syndrome.

Both endogenous and exogenous GCs have a negative feedback effect on the secretion of CRF and ACTH. Administration of exogenous GCs depresses the secretion of CRF and ACTH, thus inhibiting the secretion of endogenous GCs and

causing atrophy of the adrenal cortex. When given therapeutically, GCs can also have powerful anti-inflammatory and immunosuppressive effects. They inhibit both the early (redness, heat, pain and swelling) and late (wound healing) manifestations of inflammation, and when used clinically to suppress graft rejection, GCs suppress the initiation of a 'new' immune response. In areas of acute inflammation, GCs cause a decreased influx and activity of leukocytes, and in areas of chronic inflammation, GCs are known to cause decreased activity of mononuclear cells, decreased proliferation of blood vessels and less fibrosis. In addition, in lymphoid tissues, GCs cause decreased clonal expansion of T and B cells, and decreased activity of cytokine-secreting T cells. GCs also act directly on inflammatory mediators, and decrease the production of cytokines including interleukins, TNF- γ and GM-CSF. These actions result in a reduction in chronic inflammation and autoimmune reactions.

1.8.2 GC Mechanisms of Action

GC effects involve interactions between the steroids and intracellular steroid hormone receptors. GCs, after entering the cell, bind to specific GC receptors (GR) in the cytoplasm, activating the receptor by causing it to undergo a conformational change exposing a DNA-binding domain. The receptor is composed of three main domains: a DNA-binding domain (DBD); a C-terminal ligand binding domain (LBD), which plays a role in ligand recognition through the ligand-dependent activation function AF-2; and an N-terminal activation domain, which plays an important role in gene regulation. The GR is capable of both positive and negative regulation of transcription, and in the absence of a ligand, is located in the cytoplasm where it is held in an inactive state by heat shock proteins (HSP). Upon the binding of a ligand, the HSP dissociate from the GR, allowing it to dimerise and translocate to the

nucleus. Once in the nucleus, the GR binds to promoters on the gene of interest known as GC response elements (GRE), resulting in the activation or repression of a specific set of transcription factors, through coactivators and corepressors, respectively (Figure 1.9) (Jantzen *et al.*, 1987; Beato *et al.*, 1996). It is thought that coactivators bind to the LBD of the GR in a ligand-dependent manner, and, consequently, although coactivators bind readily in the presence of agonists, they fail to bind in the presence of antagonist ligands, a likely mechanism of action for these antagonists (Figure 1.9). These coactivators may also play a role in the tissue-specific activity of GCs, as although many coactivators are expressed widely, some exhibit a specific tissue expression pattern (Puigserver *et al.*, 1999; Knutti *et al.*, 2001). It has also been shown that the GR is capable of binding directly to specific transcription factors such as nuclear factor- κ B (NF κ B) and activator protein-1 (AP-1) which are involved in the up-regulation of inflammatory genes. This mechanism is ligand-independent and does not require receptor dimerisation, therefore rendering it genetically separable from transcriptional activation (McKay & Cidlowski 1999) (Figure 1.9).

In humans, mutations in the GR are known to cause familial GC resistance (FGR) (Hurley *et al.*, 1991). Patients with FGR often feel fatigue, but other signs of GC insufficiency are rare as the ACTH-driven increase in cortisol compensates for receptor insensitivity. However, a consequence of this increase in ACTH is the elevation of mineralocorticoids and androgens, which can result in hypertension. In the mouse, two critical transgenic mouse models have been developed. Knockout of the GR gene in all tissues exerts minimal effects on embryonic development, but results in perinatal lethality due to underdevelopment of the lungs (Cole *et al.*, 1995).

A second mutation, GR_{dim}, uncovers an essential duality of GR function. This mutation prevents dimerisation of the receptor, and consequently prevents DNA binding. Therefore, transactivation and transrepression that require direct DNA binding of a dimeric GR are inactive, whilst transrepression involving a direct interaction between a monomeric GR and transcription factors is unaffected. Surprisingly, these mice are viable, and have no obvious defects in lung maturation or anti-inflammatory actions of the receptor, suggesting that homodimer GR-DNA binding is not essential for survival (Reichardt et al., 1998).

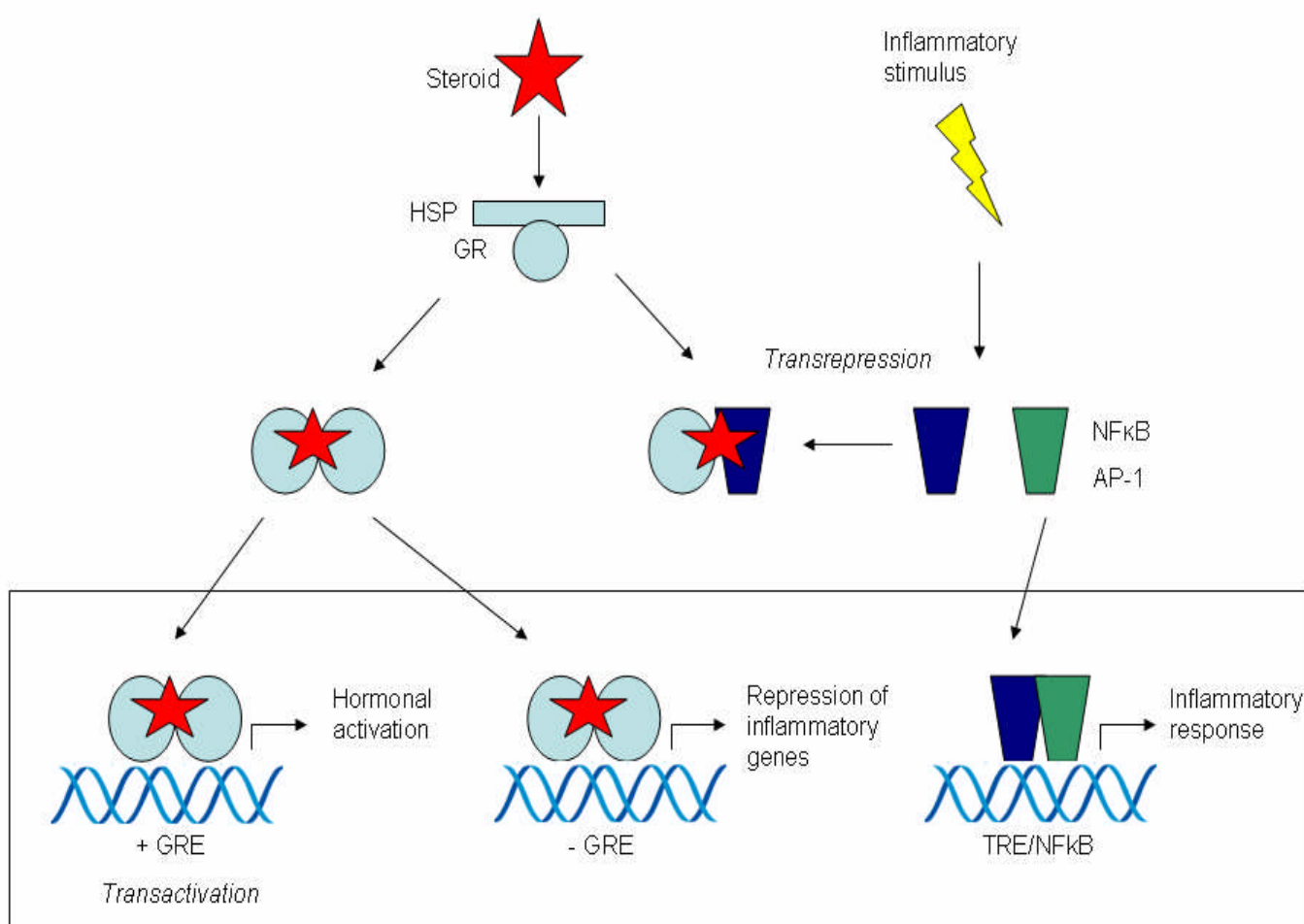


Figure 1.9 Mechanisms of GC-regulated gene transcription There are at least three distinct mechanisms by which GCs can regulate gene transcription. First, GCs bind to a cytosolic GR attached to a heat-shock protein (HSP). The HSP dissociates, and the GR dimerises and translocates to the nucleus and, in the case of positive regulation, transactivates through *cis*-activating palindromic GREs located in the promoter region of responsive genes. Second, GCs are able to bind to negative GREs resulting in the repression of gene transcription. There is now evidence to suggest that GCs may control inflammation predominantly via a third mechanism involving the transrepression of transcription factors, such as AP-1, NFκB and NF-AT that regulate inflammatory gene expression. (Figure amended from Belvisi *et al.*, 2001)

1.8.3 Systemic Side Effects of GCs

GCs affect most systems within the body. There are several situations when the carefully balanced physiological production of GCs can become unbalanced. Chronic, uncontrolled stress leads to long term activation of the HPA axis and

sustained, high GC levels. Pathological conditions in which activation of the HPA axis has been demonstrated include depression, obsessive-compulsive disorder, alcohol and drug abuse, and anorexia nervosa (Chrousos *et al.*, 2000). Imbalances in cortisol production can also occur in certain conditions that overproduce GCs. These patients present with a combination of symptoms grouped under the heading 'Cushing's syndrome'. The symptoms include central obesity, glucose intolerance, myopathy and hypertension. However, the most common way in which imbalances in the stress response system can present themselves is the administration of exogenous GCs. Exposure to high, sustained levels of corticosteroids by any mechanism uncouples the normal metabolic processes from autoregulatory feedback mechanisms and induces a stress response that cannot be maintained in the long term without severe consequences. The numerous side-effects experienced by patients undergoing long term GC treatment are a clear testament to this. Complications are time- and dose-dependent and can occur acutely with high doses or more slowly with chronic exposure and lower doses. One of the most important side effects resulting from GC therapy is osteoporosis, and this side effect alone accounts for a large degree of morbidity in patients receiving GCs. This problem is exacerbated by the fact that these patients also suffer from decreased muscle mass and are therefore more susceptible to falling. Increased susceptibility to infection is also a major problem in patients undergoing GC therapy. An additional side effect which can limit the use of GCs is hyperglycaemia due to increased gluconeogenesis, insulin resistance and impaired glucose tolerance, which can lead to diabetes. This side effect is exacerbated by the fact that, in high doses, many GCs that have affinity for the mineralocorticoid receptor (MR) can exert a mineralocorticoid effect, resulting in salt and water retention, hypertension, potassium retention and metabolic alkalosis. In

physiological GC doses, this mineralocorticoid effect is prevented by the rapid degradation of GCs by 11- β -hydroxysteroid dehydrogenase type 2 (11 β HSD2) in MR target tissues. GCs have also been known to have psychogenic effects, and approximately 5% of patients will experience some form of inappropriate euphoria, psychosis or depression. Fat redistribution and weight gain is also a concern with many patients, and facial, supraclavical and posterior cervical fat depots are particularly sensitive to GCs, resulting in the moon-face and buffalo hump characteristic of long term GC treatment (Baxter *et al.*, 1992).

1.8.4 GC Therapy and Growth During Childhood

GCs are used in the treatment in a number of chronic inflammatory, autoimmune and neoplastic diseases in children. The impairment of childhood growth with cortisone was first described over 40 years ago, and since then has been observed with other commonly used GCs such as Dex and prednisolone (Pred) (Avioli *et al.*, 1993). The increasing incidence of childhood asthma accounts for the largest group of children who are chronically exposed to steroids. Oral GC therapy in asthma is associated with a delay in growth and puberty, and there is some evidence to suggest that final height may also be compromised (Allen *et al.*, 1994). Although early studies failed to show a link between inhaled steroids and growth retardation, evidence now suggests that bone growth and collagen turnover are both reduced in children with mild asthma who use inhaled steroids (Shaw *et al.*, 1997), an effect that is most pronounced over the first few weeks of treatment.

In children with inflammatory bowel disease, growth retardation is widely reported, and seems to be related to disease activity in addition to its treatment (Markowitz *et*

al., 1993; Savage *et al.*, 1999), and vertebral fractures have also been described in children with Crohn's disease after a short period of steroid treatment (Semeao *et al.*, 1997). Impaired growth is one of the major complications of childhood renal disorders and their treatment. Children receiving GC therapy for renal disorders such as nephrotic syndrome have reduced growth and bone mineralisation (Lettgen *et al.*, 1994), and post transplantation, the dose of GC therapy is inversely related to the relative change in height of the child (Saha *et al.*, 1998). It has been suggested that alternate-day GC therapy is less detrimental to longitudinal growth however, this may still delay puberty and therefore cause a delayed growth spurt (Polito *et al.*, 1999).

GCs are widely used for treating chronic connective tissue diseases in children, and there is a considerable overlap between the inflammatory-effects and the steroid-induced effects on bone growth. A failure to maintain bone mineralisation is common in children with juvenile idiopathic arthritis (JIA), and is characterised by reduced bone formation with a subsequent failure to undergo the expected increase in bone mass during puberty (Polito *et al.*, 1999). This reduction in bone mineral density is exacerbated if GCs are used as therapy (Kotaniemi *et al.*, 1999).

GCs have consistently been the primary therapy for childhood acute lymphoblastic leukaemia (ALL). Dex is now replacing Pred as the drug of choice due to the fact that it has greater lymphocytotoxicity and higher CNS penetration. Recent studies have shown that bone mineralisation status as assessed by bone mineral density is adversely affected immediately after completion of GC treatment for ALL (Arikoski *et al.*, 1999). Previous studies at the University of Glasgow have shown alterations in bone turnover and short term growth of children during leukaemia treatment. These

changes were most marked during periods of intensive chemotherapy and high dose systemic glucocorticoid administration (Crofton *et al.*, 1998; Ahmed *et al.*, 1999; Crofton *et al.*, 1999).

1.8.5 GCs and IGF-I signalling in the growth plate

The growth-suppressing effects of GC appear multifactorial, and some GC actions in bone modify skeletal responses to GH and IGF-I (Figure 1.7). The inhibitory actions of GCs on longitudinal growth are suggested to be due, in part, to impaired action of the components of the IGF axis (Klaus *et al.*, 1998), and it has been shown that GCs reduce IGF-I mRNA in growth plate chondrocytes (Luo *et al.*, 1989). Studies of linear bone growth have shown that Dex and IGF-1 have opposite effects, with Dex decreasing and IGF-1 increasing cell proliferation (Mushtaq *et al.*, 2004). IGF-I also increases collagen synthesis and decreases collagenase 3 expression in bone, whereas GCs do the opposite. Furthermore, GCs block the activation of GH-Receptor (GHR) and IGF-I Receptor (IGF-IR) expression by GH and IGF-I in chondrocytes (Jux *et al.*, 1998), and this may account for the antagonism of the growth promoting actions of GH by GC (although children with impaired growth due to GC excess can still respond to pharmacological doses of GH therapy).

Of additional interest is the observation that GH, via IGF-I, inhibits activity of 11 β -hydroxysteroid dehydrogenase-1 (11 β HSD1) in human adipose and stromal cells (Moore *et al.*, 1999). 11 β HSD1 converts inactive cortisone to active cortisol in humans to maintain circulating levels of GCs. The type 2 enzyme, 11 β -hydroxysteroid dehydrogenase-2 (11 β HSD2) is a dehydrogenase that catalyses the inactivation of GCs to protect the nonselective mineralocorticoid receptor from GC

activation in target tissues such as the kidney. Therefore, local tissue GC concentrations are modulated by 11 β HSD2, and both 11 β HSD1 and 2 have shown to be active in osteoblasts and osteoclasts (Cooper *et al.*, 2000; Cooper *et al.*, 2003). If 11 β HSD enzymes are expressed in growth plate chondrocytes, they may act as significant GH and IGF-I-sensitive regulators of local GC concentrations in the growth plate.

1.8.6 Direct effects of GCs at the Growth Plate

Evidence for a direct effect of GC in the growth plate came from a study in which pharmacological levels (approximately 10⁻⁶M) of local Dex infusion significantly decreased tibial growth compared with the contralateral limb (Baron *et al.*, 1992). The glucocorticoid receptor (GR) has since been identified in proliferating and hypertrophic chondrocytes in the rat (Silvestrini *et al.*, 1999) and has also been found in hypertrophic chondrocytes in the human growth plate (Abu *et al.*, 2000). In rats, GC excess reduces bone growth, probably due to decreased numbers of proliferating chondrocytes and increased apoptosis of hypertrophic chondrocytes in the growth plate (Chrysis *et al.*, 2003). These results are also consistent with the Dex-induced inhibition of chondrocyte proliferation and cartilage matrix production observed in 12 week old rats in vivo (Annefeld *et al.*, 1992), supporting the hypothesis that Dex is a potent negative regulator of chondrocyte activities.

It is likely, however, that physiological levels of Dex also act as a stimulator of chondroprogenitor cell recruitment and a supporter of chondrocyte viability (Grigoriadis *et al.*, 1996). Physiological concentrations of Dex enhance expression of Sox9 (Sekiya *et al.*, 2001), which regulates expression of genes encoding markers of

commitment to chondrogenesis, including Coll X and aggrecan, which supports the hypothesis that Dex may be a maintenance factor for chondrogenic cells.

1.8.7 Glucocorticoids and catch-up growth

It is well established that the effects of GC are transient and that, after their removal, there is a period of accelerated catch-up growth. It has been proposed that the mechanism governing catch-up growth after exposure to excess GC resides in the growth plate (Baron *et al.*, 1992; Nilsson *et al.*, 2005). This proposal was based on the observation that suppression of growth within a single rabbit growth plate *in vivo* by local administration of Dex was followed by catch-up growth restricted to the affected limb. According to this model, growth inhibiting conditions of excess GC reduce the growth and maturation of growth plate stem cells (chondroprogenitors), and conserve their proliferative potential, whilst also slowing the onset of senescence (where the proliferative capacity of chondroprogenitor cells is gradually exhausted causing growth to slow and eventually stop) (Nilsson *et al.*, 2005). Studies using the ATDC5 chondrocyte cell line have also shown that Dex-treated cells retain the capacity to re-enter chondrogenesis following the withdrawal of GC (Mushtaq *et al.*, 2002). Therefore it seems that, although Dex arrests growth and differentiation of chondrocytes, the capacity for cells to undergo chondrogenesis is maintained in the presence of GC despite the fact that progenitor cells are quiescent.

1.9 Aims and Strategy

The aim of this project was to investigate and identify novel mechanisms involved in GC-induced growth retardation at the level of the growth plate chondrocyte. As previously mentioned, it is now well known that GCs reduce longitudinal growth at

the growth plate by inhibiting chondrocyte proliferation and hypertrophy. Therefore, a large portion of this project will utilise *in vitro* models of chondrocyte proliferation such as chondrocyte cell lines engineered to progress through maturational stages of chondrogenesis and differentiation, primary chondrocytes, and organ cultures. However, there are obvious limitations to such *in vitro* studies, and so murine *in vivo* studies will also be used in an attempt to gain a better understanding of the mechanisms involved in GC-induced growth retardation. My specific aims are to:

- 1) Identify novel GC-responsive chondrocyte genes using Affymetrix Microarray technology on GC-treated chondrocyte RNA. Genes identified as novel targets will then be studied in more detail using *in vitro* functional experiments.
- 2) Further characterise the expression and mechanism of action of the GC-responsive gene, lipocalin 2 in growth plate chondrocytes.
- 3) Study the effects of the CDKI p21 on GC-induced growth retardation. In order to do this, I will first carry out preliminary *in vitro* experiments to confirm previously reported data. I then plan to carry out a number of *in vivo* experiments, in which I will use p21 knock-out mice to examine the role of p21 in GC-induced growth retardation.
- 4) Examine the effects of a novel anti-inflammatory compound, AL-438, on chondrocyte proliferation and bone growth compared to Dex and Pred. This will be done through both *in vitro* and *in vivo* studies.

Chapter 2

Materials and Methods

Chapter Contents

- 2.1 Reagents and Solutions
 - 2.1.1 Materials
 - 2.1.2 Buffer Recipes
- 2.2 Cell Culture
 - 2.2.1 Preparation of cell culture reagents
 - 2.2.2 Isolation of primary cell lines
 - 2.2.3 Maintenance and differentiation of ATDC5 cells
 - 2.2.4 Freezing/Thawing cells
- 2.3 In vivo methods
 - 2.3.1 Production of transgenic mice
 - 2.3.2 Production of Knock-out Mice
 - 2.3.3 Animal Maintenance
 - 2.3.4 Animal Breeding
 - 2.3.5 Tail Biopsy of Animals
 - 2.3.6 Isolation and culture of embryonic murine metatarsals
- 2.4 Tissue Processing and Analysis
 - 2.4.1 Paraffin Embedded Tissue
 - 2.4.2 RNase Free Frozen Tissue
 - 2.4.2.1 Preparation of Hexane Freezing Bath
 - 2.4.2.2 Preparation on polyvinyl alcohol (PVA)
 - 2.4.2.3 Freezing and Cutting of Tissue
 - 2.4.2.4 Cutting Undecalcified Frozen Tissue using the CryoJane Tape transfer system
 - 2.4.2.5 Laser Capture Microdissection
 - 2.4.3 Immunohistochemistry
 - 2.4.4 Toluidine Blue Staining
 - 2.4.5 Histological Assessment of Bromodeoxyuridine (BrdU) uptake
 - 2.4.6 Alkaline Phosphatase and Von Kossa staining
- 2.5 RNA Methods
 - 2.5.1 Isolation of Total RNA from Cells and Tissues
 - 2.5.2 Isolation of RNA from LCM samples
 - 2.5.3 Reverse Transcription Polymerase Chain Reaction (RT PCR)
 - 2.5.4 Polymerase Chain Reaction (PCR)
 - 2.5.5 Real Time Quantitative Polymerase Chain Reaction (qPCR)
- 2.6 DNA Methods
 - 2.6.1 DNA isolation from mouse tail biopsies

- 2.6.2 Genotyping transgenic mice
 - 2.6.3 Agarose Gel Electrophoresis
 - 2.6.4 Quantification of DNA Concentration
 - 2.6.5 Restriction Endonuclease Digestion of DNA
 - 2.6.6 DNA Ligation into Linearised Vectors
 - 2.6.7 Isolation of DNA Fragments from Agarose gel
 - 2.6.8 DNA Sequencing
 - 2.6.9 Transformation of bacteria
 - 2.6.10 Liquid Culture of Bacterial Clones
 - 2.6.11 Minipreparation of Plasmid DNA
 - 2.6.12 Endofree Maxipreparation (Qiagen) of Plasmid DNA
 - 2.7 Protein Methods
 - 2.7.1 Protein Concentration Determination – Bradford Assay
 - 2.7.2 SDS Polyacrylamide Gel Electrophoresis
 - 2.7.3 Western Blotting
 - 2.8 Microarray
 - 2.8.1 Hybridisation of RNA to Affymetrix Platform
 - 2.8.2 Microarray Data Analysis
 - 2.9 Cell Proliferation and Differentiation Assays
 - 2.9.1 [³H]-thymidine Incorporation Assay
 - 2.9.2 Alcian Blue Staining of the Cell Monolayer
 - 2.9.3 Alkaline Phosphatase Assay
-

2.1 Reagents and Solutions

2.1.1 Materials

All chemicals were purchased from Sigma Aldrich (Dorset, UK) unless otherwise stated. PCR oligonucleotides were purchased from MWG Biotech (Ebersberg, Germany), and antibodies were purchased from SantaCruz unless otherwise stated.

2.1.2 Buffer Recipes

Cell Culture Buffers

Phosphate Buffered Saline (PBS)

140mM NaCl, 2.5mM KCl, 10mM Na₂HPO₄, 1.8mM KH₂PO₄

Cell Freezing Buffer

60% DMEM, 30% FBS, 10% Dimethyl sulfoxide; DMSO

RIPA Buffer

20mM Tris, 135mM NaCl, 10% glycerol, 1% IGEPAL, 0.1% SDS, 0.5% deoxycholic acid, 2mM EDTA

Bacterial Culture

Luria Broth (LB) media

1% bacto-tryptone, 0.5% bacto-yeast extract, 150mM NaCl, adjusted to pH 7.5

LB agar

LB supplemented with 1.5% bactoagar

Super Optimal Broth with Catabolite repression (SOC) Media

2% bacto-tryptone, 0.5% bacto-yeast extract, 10 mM NaCl, 2.5 mM KCl, 10 mM MgCl₂, 10 mM MgSO₄, 20 mM glucose

Gel Electrophoresis

Tris-Acetate-EDTA (TAE)

40mM Tris, 1mM EDTA, 0.1% acetic acid

Tris-Boric Acid-EDTA (TBE)

90mM Tris, 2mM EDTA, 90mM boric acid

Agarose Gel Loading Buffer

1.2mM bromophenol blue, 50% (w/v) glycerol, 10% (v/v) 10x TAE/TBE

Qiagen Kit Buffer Compositions

Re-suspension Buffer P1

50 mM Tris-HCl, pH 8.0; 10 mM EDTA; 100 µg/ml RNase A

Bacterial Lysis BufferP2

200 mM NaOH, 1% SDS

Elution Buffer EB

10 mM Tris-HCl, pH 8.5

Neutralisation Buffer P3

3 M Potassium Acetate, pH 5.5

Equilibration Buffer QBT

750 mM NaCl; 50 mM 3-[N-morpholino] propanesulfonic acid (MOPS), pH 7.0; 15% isopropanol (v/v); 0.15% Triton X-100 (v/v)

Column Wash Buffer QC

1M NaCl, 50mM MOPS pH7.0, 15% isopropanol (v/v) and 0.15% Triton X-100 (v/v)

Elution Buffer QN

1.6 M NaCl, 50 mM MOPS, pH 7.0, 15 % isopropanol (v/v)

DNA Re-suspension Buffer TE

10 mM Tris HCl, pH 8.0, 1 mM EDTA

PolyAcrylamide Gel Running and Staining BuffersMOPS Running Buffer

50 mM MOPS pH 7.7, 50 mM Tris, 0.1% SDS, 1mM EDTA

NuPAGE Transfer Buffer

25 mM Bicine pH 7.2 , 25 mM Bis-tris , 1 mM EDTA, 0.05 mM Chlorobutanol

LDS Sample Buffer

10% Glycerol, 141 mM Tris Base, 106 mM Tris HCl, 2% LDS, 0.51 mM EDTA, 0.22 mM SERVA® Blue G250, 0.175 mM Phenol Red, pH 8.5

Western Blotting

Tris-Buffered Saline with Tween 20 (TBST)

10mM Tris HCl pH8.0, 150mM NaCl, 0.1% Tween-20

Blocking Solution

5% (w/v) dried milk protein (Marvel) in TBST

2.2 Cell Culture

2.2.1 Preparation of Cell Culture Reagents

Dulbecco's Modified Eagle Medium/Ham's F12 (DMEM: F12), containing 4500g/L glucose and L-glutamine, was purchased from Gibco (Gibco BRL, Paisley, UK). All tissue culture reagents were prepared in a sterile category 2 hood. DMEM: F12 was supplemented with 0.5% of the antibiotic gentamycin (Gibco) and 10% heat inactivated foetal bovine serum (FBS) (Gibco) before use. All media was filter-sterilised through a 0.22 μ M filter and stored at 4°C.

2.2.2 Isolation of Primary Cell Lines

Primary chondrocytes were isolated from the rib cages of 2-day-old Swiss mice culled by cervical dislocation. Chondrocytes were isolated from the ventral parts of the rib cage in a sterile environment and incubated in a sterile petri dish in pronase (2mg/ml in PBS) for 30mins at 37°C whilst shaking. After rinsing in PBS, the rib cage was incubated in 3mg/ml collagenase in DMEM for 90mins at 37°C, and repeatedly pipetted until all soft tissues and mineralised tissues were detached from the cartilage matrix. The cartilage was washed again and incubated until completely digested (up to 3hrs) in collagenase (3mg/ml), at which point the suspension was filtered. The chondrocytes were then pelleted by centrifugation, resuspended in DMEM

supplemented with 50 μ g/ml ascorbic acid, and counted in a haemocytometer chamber. An average of 1×10^6 chondrocytes were obtained per mouse.

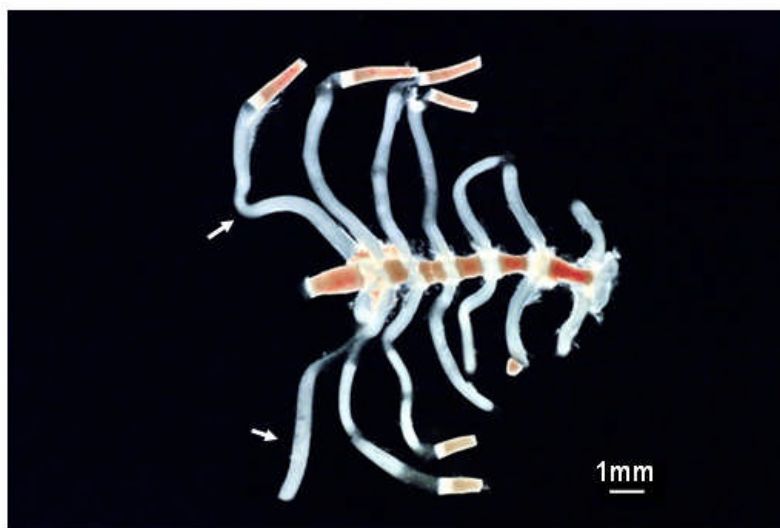


Figure 2.1 Isolation of Primary Murine Chondrocytes from the Rib Cage of 3-day-old Swiss Mice (Arrows = Chondrocytes were isolated from the ventral parts of the rib cage by digestion in pronase and then collagenase; scale bar = 1mm).

2.2.3 Maintenance and Differentiation of ATDC5 Cells

The ATDC5 cell line established by Atsumi *et al.* (1990) from the mouse teratocarcinoma cells AT805, mimics many of the events described for differentiation of epiphyseal chondrocytes. This line has less phenotypic diversity than cell cultures of primary chondrocytes, and also allows the study of the differentiation of mesenchymal cells into chondrocytes and the terminal differentiation of proliferating to hypertrophic chondrocytes (Mushtaq *et al.*, 2002). The ATDC5 chondrocyte cell line was obtained from the RIKEN cell bank (Ibaraki, Japan), and cells were cultured at a density of 6000 cells per cm^2 in multi-well plates (Costar, High Wycombe, UK). Maintenance medium (DMEM/Ham's F12; Invitrogen, Paisley, UK) was supplemented with 5% FCS (Invitrogen), 3×10^{-8} M sodium selenite and 10 μ g/ml human transferrin (Sigma, Poole, UK) and cells were grown until confluent. Adherent cells were passaged by trypsinisation at sub-confluence. The cell culture media was

removed and the monolayer washed with serum free medium. The cells were then covered with trypsin/EDTA solution and incubated at 37°C until cells became detached. Growth media containing serum was then added to the cell suspension to neutralise the trypsin, and the suspension was then pipetted repeatedly to create a single cell solution, counted using a haemocytometer, and split into fresh flasks. Differentiation was made by the addition of insulin (10µg/ml; Sigma) to the maintenance medium. Cells were incubated at 37°C in a humidified atmosphere containing 5% CO₂/95% air and the medium was changed every second day.

2.2.4 Freezing/Thawing Cells

To freeze cells a monolayer was stripped as described in 2.2.3 and counted. The cells were centrifuged at 717 x g for 5 minutes and resuspended in the appropriate volume of cell freezing buffer to give a cell concentration of between 2-4 x 10⁶ cells per ml. The cells within a cryovial (Corning, Surrey, UK) were then transferred to a temperature of -80°C for between 4-7 days and then to -150°C for longer term storage. Cells were thawed at 37°C and added drop wise to 10ml complete media. The cell suspension was then mixed and spun at 717 x g for 5 minutes to remove the DMSO. The cell pellet was resuspended in complete media and transferred to a t175 tissue culture flask.

2.3 In Vivo Methods

2.3.1 Production of Knock-Out Mice

p21^{-/-} mice were purchased from Jackson Laboratories (Massachusetts Institute for Technology, Massachusetts, USA). These mice were originally created by Hannon *et al.* (1995) at the Howard Hughes Medical Institute in Cambridge Massachusetts. The

method involved generating a null allele in 129/Sv embryonic stem (ES) cells by replacing the p21 coding sequence with a neomycin-resistance cassette (*neo^r*). Homozygous p21^{-/-} ES cells were produced by subjecting two heterozygous p21^{+/-} cell lines to selection in an increased concentration of G418. One p21^{-/-} ES cell clone was recovered from each parental p21^{+/-} line. 129/Sv cells lacking p21 were then injected into normal B6 blastocysts, creating B6-129/Sv p21^{-/-} chimaeric mice.

2.3.2 Animal Maintenance

Transgenic mice were produced as described (2.3.2) and non-transgenic mice were supplied by B&K Universal Ltd, UK. All animals were maintained under conventional housing conditions with a 12h light/dark cycle where the dark cycle consisted of 2h night light and 10h of complete darkness.

2.3.3 Animal Breeding

Mice identified as being positive for transgene incorporation (identified by PCR; section 2.6.2), were selected and bred with non-transgenic C57BL6/CBA stock mice to expand transgenic lines. Offspring carrying the transgene were maintained and negative littermates were culled. p21 null mice (strain *Cdkn1a^{tm1Tyj}*) were obtained from the Jackson Laboratory (Maine, USA). Mice identified as being heterozygous for the p21 null allele were again selected by PCR as described in 2.6.2, and were bred with other heterozygotes to obtain homozygote null mice for experimental procedures.

2.3.4 Tail Biopsy of Animals

Animals requiring tail biopsy for genotyping were anaesthetised using halothane and a 1-2cm portion of the tail was removed using a preheated scalpel. By preheating the scalpel, upon cutting, blood vessels in the tail become cauterised and bleeding is prevented.

2.3.5 Isolation and Culture of Embryonic Murine Metatarsals

The foetal mouse metatarsal explant culture provides a more physiological model for studying bone growth. It maintains cell-cell and cell-matrix interactions and the direct assessment of bone growth and histological architecture can be determined (Scheven *et al.*, 1991; Coxam *et al.*, 1996). The middle three metatarsals were aseptically dissected from 18-day-old embryonic Swiss mice that had been killed by decapitation. The experimental protocol was approved by Roslin Institute's Animal Users Committee and the animals were maintained in accordance with Home Office guidelines for the care and use of laboratory animals. Bones were individually cultured at 37°C in a humidified atmosphere of 95% air/5% CO₂ in 24-well plates (Costar) for up to 12 days. Each well contained 300µl of α -MEM without nucleosides (Invitrogen) supplemented with 0.2% BSA Cohn fraction V (Sigma), 0.1mM β -glycerophosphate (Sigma), 0.05mg/ml L-ascorbic acid phosphate (Wako, Japan), 0.292mg/ml L-glutamine (Invitrogen), 0.05mg/ml gentamicin (Invitrogen) and 1.25µg/ml fungizone (Invitrogen).

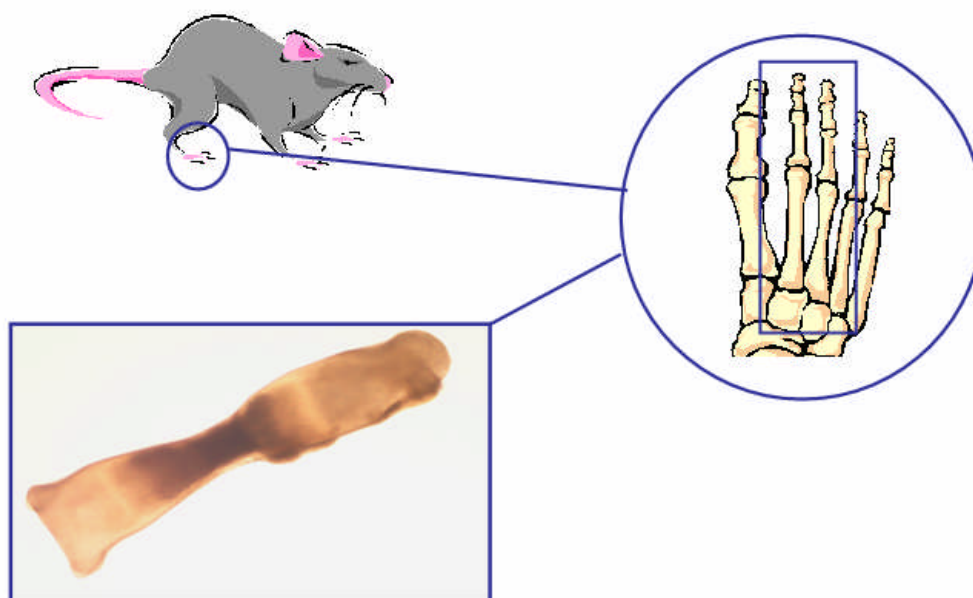


Figure 2.2 Murine Metatarsal Dissection from the hind legs of 18-day-old embryos. The middle three metatarsals are dissected and cultured for up to 12 days at 37°C.

2.4 Tissue Processing and Analysis

2.4.1 Paraffin Embedded Tissue

Bone tissue was harvested from mice culled by cervical dislocation immediately prior to use and was trimmed to the required size, before fixation in either 70% ethanol or 4% paraformaldehyde for 24h at room temperature. After removal of the fixative, the tissue was decalcified in 10% EDTA (pH 7.4) at 4°C for 4 days, with a change of EDTA on day 2. The tissue was then washed in dH₂O, and placed in 70% ethanol overnight. The following day, fresh 70% ethanol was added for 30mins, and then replaced with successive 30min incubations of 80% ethanol (twice), and 95% ethanol (twice). After a further overnight incubation in 95% ethanol, the tissue was placed in 100% ethanol for two 1h incubations, followed by two 1h incubations in xylene under a fume hood, before being placed into pre-melted wax for two 1h periods.

Once processed, the tissue was embedded in paraffin wax with a melting point of 60°C using appropriate sized plastic moulds. The wax blocks were allowed to cool, and excess wax was trimmed away on the microtome to leave the sample surface exposed for cutting. Once trimmed, the blocks were cooled on ice for 30mins before sections of 5µm thickness were cut. The sections were transferred to a 40°C water bath and left to soften for 1min before being transferred to a poly-l-lysine coated microscope slide (VWR International Ltd, Lutterworth, UK). The slides were then placed in an oven at 50°C overnight to ensure secure attachment of the sections to the slide.

2.4.2 RNase Free Frozen Tissue

2.4.2.1 Preparation of Hexane Freezing Bath

As with paraffin-embedded sections, bone tissue was harvested from mice culled by cervical dislocation immediately prior to use and was trimmed to the required size using RNase free dissection instruments. Tissues were then placed in RNA-later. In order to freeze the tissue, a large glass jar was inserted into a polystyrene base and filled 1/3 full with 100% ethanol. A small beaker was placed inside the alcohol-filled jar and dry ice chips were added to the alcohol until a saturated solution was obtained and the ethanol became viscous. The beaker was then filled with Hexane and the jar covered for 30mins to allow the hexane bath to cool to -70°C.

2.4.2.4 Preparation on Polyvinyl Alcohol (PVA)

PVA (Sigma) aids the cutting of frozen mineralised tissue. A 5% solution was prepared by gradually adding 5g of PVA to 100ml of warm DEPC treated H₂O on a

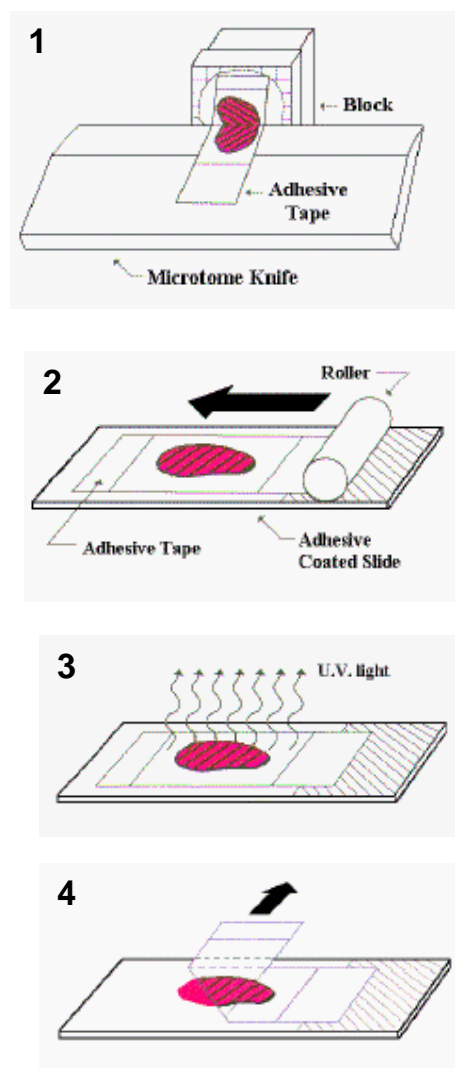
heated magnetic stirrer within an extraction hood. The solution was left stirring at a low heat for 1h, and then allowed to cool.

2.4.2.5 Freezing and Cutting of Tissue

Bone tissue samples were individually dipped in PVA and then immersed in pre-cooled hexane for 30secs, at which point they were retrieved using forceps treated with RNase zap and pre-cooled in dry ice. Tissues were then placed into pre-cooled self-sealing bags containing a piece of tissue to absorb any remaining hexane. The tissue was stored at -80°C until use. Using optimal cutting temperature compound (Brights, Huntingdon, UK) to attach the tissue to a metal chuck, sections of 10µm were cut at -30°C (Brights, OT model cryostat), and picked up on poly-l-lysine coated microscope slides. The sections were then air dried at RT.

2.4.2.6 Cutting Undecalcified Frozen Tissue - CryoJane Tape transfer system

The CryoJane tape transfer system (Instrumedics Inc, St Louis, MO, USA) has been specifically designed for sectioning tissues that are notorious for losing their morphology or shredding upon cutting. Undecalcified bone tissue is especially difficult to cut due to the presence of mineralised tissue, and sections often shred upon cutting. Sections were cut using this technique by capturing the frozen section on a cold tape window as it was being cut. The tape window attached-section was then placed onto an adhesive-coated slide and transferred by applying a flash of ultraviolet (UV) light through the slide. The UV light polymerises the adhesive layer on the slide into a hard, solvent-resistance plastic, tightly attaching the section to the slide. The tape was then peeled away leaving the frozen section tightly bonded to the plastic layer (Figure 2.4.1).



1. Cutting

After the block is trimmed, a cold adhesive tape is adhered to the block face. The tape supports and captures the section as it is being cut

2. Transfer to Slide

A cold adhesive-coated slide is placed on a temperature-controlled pad. The adhesive tape is placed section-side-down on the adhesive-coated slide, and is laminated to the adhesive layer using a cold roller.

3. Curing the Adhesive Coating

A flash of ultraviolet light passes through the slide to polymerize the adhesive layer on the slide into a hard, solvent-resistant plastic, tightly anchoring the section to the slide.

4. Removal of Tape

The tape is peeled away leaving the still frozen section tightly bonded to the plastic layer.

Figure 2.3 The CryoJane Tape transfer System This system was specifically designed for cutting tissues such as undecalcified bone which can often tear upon cutting (www.cryojane.com)

2.4.2.7 Laser Capture Microdissection

Laser capture microdissection (LCM) has been developed to provide a fast one step method of isolating specific cell populations from a complex heterogeneous tissue. This technique uses a standard histological tissue section of stained tissue under a microscope. The section is covered in part by a cap covered with a thermal polymer. Upon identification of the desired cells a Class IIIb invisible infrared laser is pulsed, melting the polymer film directly above the cells of interest. The film drips onto the desired cells in the section, solidifying and retaining the cells when the cap is removed

(Figure 2.4). By repeating this process of cell identification and laser pulsing it is possible to capture a homogeneous cell population from a tissue section. Using the PixCell II LCM microscope in combination with Arcturus software and CapSure HS LCM caps (Arcturus), specific cells within frozen sections were captured and the RNA extracted. Before LCM commenced, a ‘before manipulation’ picture of the section was taken. The laser was set to the desired size depending on the cell type to be captured, and then focused to ensure accurate capture. Desired cells were captured by pulsing the laser and moving the slide platform with the manipulator to guide the laser over the relevant cells. The LCM cap was removed and an ‘after manipulation’ picture was taken of both the section and the captured cells. Following capture, each cap was removed and placed in the incubation block, before attaching the CapSure adapter and a 0.5ml eppendorf. The samples were then stored in a dry environment until analysis.

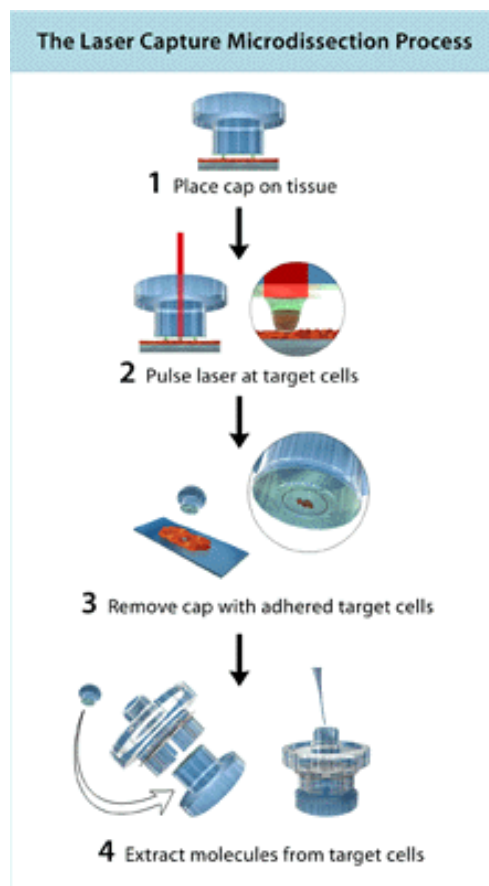


Figure 2.4 The Laser Capture Microdissection Process. Individual cells are isolated from frozen tissue sections by pulsing a laser directly over the required cells, and collecting the cells on the surface of a specially designed cap containing an adhesive polymer. Picture from www.Arcturus.com.

2.4.3 Immunohistochemistry

Paraffin sections were dewaxed in xylene and rehydrated through a graded series of alcohol solutions as follows; 100% xylene, 2x5mins; 100% ethanol, 2x1min; 70% ethanol, 1x2mins; 50% ethanol, 1x2mins; tap water, 1x30secs; dH₂O, 1x5mins. To obtain antigen retrieval, samples were submerged in 0.1M sodium citrate for 90 minutes at 70 °C and then washed in PBS. Endogenous peroxidases were blocked by incubating the sections with 3% hydrogen peroxide (in methanol), followed by 3 washes in PBS. Unspecific protein binding was blocked by normal goat serum (1:5) diluted in PBS for 30 min at RT. Specific primary antibodies were diluted to the recommended concentration (Appendix 4) in PBS/5% FCS, and sections were covered with diluted antibody solution and incubated in a humidified chamber overnight at 4°C. Control sections received a similar dilution of normal serum or IgG specific to the primary antibody used. Following this the sections were washed in PBS, and incubated with a 1:100 dilution of secondary antibody for 60 min at RT (Appendix 4). DAB substrate reagent (0.06% DAB, 0.1% H₂O₂ in PBS) was incubated for 8 minutes at RT, rinsed in PBS and counterstained with Meyer's haematoxylin (Sigma) for 5 min. The sections were dehydrated through alcohols and mounted in DePeX (DPX) for visualisation under a light microscope.

2.4.4 Toluidine Blue Staining

Toluidine blue is a metachromatic dye that stains cartilage, and is therefore useful for staining the growth plate, and in particular, defining the proliferative and hypertrophic zones. Sections were dewaxed through graded alcohols as previously described (2.4.3), and sections immersed in 1% Toluidine blue in 50% isopropanol for 2mins at room temperature (RT). The sections were then rinsed twice with isopropanol, and

placed in 2 changes of fresh isopropanol for 30secs each, before being cleared in xylene for 2mins and mounted in DPX.

2.4.5 Histological Assessment of Bromodeoxyuridine (BrdU) Uptake

BrdU was added to the culture medium of metatarsals for the last 6h of culture. At the end of the incubation period, the tissue was washed in PBS and fixed in 70% ethanol, dehydrated, and embedded in paraffin wax. Sections 10 μ m in thickness were cut along the longitudinal axis, and chondrocyte nuclei with incorporated BrdU were detected using an indirect immunofluorescence procedure. Briefly, sections were denatured with 1.5 M HCl for 30 min before incubation with an antibody to BrdU (DAKO, Ely, UK; Appendix 4) diluted 1:50 in PBS for 1 h. After washing, the sections were incubated for an additional 1 h in fluorescein isothiocyanate-labeled (FITC) goat anti-mouse IgG (Sigma) diluted 1:50 in PBS (Appendix 4). The sections were finally mounted in PBS/glycerol (Citifluor, Agar Scientific, Essex, UK). Sections were examined using a Leica BMRB fluorescent microscope, and the total number of BrdU positive chondrocytes within both the proximal and distal growth regions was counted. To determine the proliferation index, the total number of BrdU positive cells were divided by the total area of the metatarsal section.

2.4.6 Von Kossa and ALP Staining

Wax sections (10 μ m in thickness) were reacted for ALP activity for the demarcation of the hypertrophic and proliferating zones within the growth plate. This procedure is a simultaneous coupling azo dye method utilising sodium α -naphthyl phosphate as substrate for ALP in the presence of fast blue RR (a diazonium salt). When the α -naphthyl phosphate is hydrolysed by ALP the α -naphthyl couples with the diazonium

salt, forming an insoluble, visible pigment at sites of phosphatase activity. Sections were dewaxed as previously described (2.4.3), and incubated in sodium barbitone buffer with fast blue salt for 2mins at 37°C (100ml sodium barbitone; 400µl 10% MgCl₂, 50mg α-naphthylphosphate; 100mg fast blue salt). The reaction was stopped with 0.1M acetic acid and the sections washed twice with distilled water, and mounted in aqueous mounting solution. Sections were also stained with von Kossa and haematoxylin and eosin using standard protocols to identify the zone of cartilage mineralisation (Mushtaq *et al.*, 2004). This stain is used to detect the presence of calcium salt deposits in cell monolayers. It utilises silver nitrate in the staining solution (silver ion carries a positive charge) binding with the anionic (negative charge) region of the salt (in this case phosphate). As the major calcium salt found in mineralising cells is calcium phosphate this stain will show regions where crystals of calcium phosphate (hydroxyapatite) are present. The growth media was removed from the cell monolayer and the cells washed 3x with distilled H₂O. The cell monolayer was then immersed in 5% silver nitrate for 30 minutes under strong light, this actively reduces the calcium and replaces it with silver thus creating black deposits. The monolayer was then washed 3x in distilled H₂O and incubated with 2.5% sodium thiosulphate for 5 minutes to remove unreacted silver ions. The monolayer was then stored under distilled H₂O until a digital image was taken. The sections were then counterstained and mounted as previously described (2.4.3). Images of the stained metatarsals were captured and the size of the ALP-negative proliferating zone was determined (proliferating zone = total length – (hypertrophic zone + mineralizing zone). The size of the hypertrophic zone was determined by subtracting the von Kossa stained mineralizing zone from the ALP-positive zone, and the size of the mineralizing zone was determined directly from the von Kossa-stained sections.

2.5 RNA Methods

2.5.1 Isolation of Total RNA from Cells and Tissues

Ultraspec RNA isolation reagent was used to isolate RNA from both cell monolayers and tissues. When isolating RNA from a cell monolayer the cells were scraped directly in ultraspec (1ml per 25cm²) and transferred to a nuclease free universal. Similarly for tissue the dissected organ was immersed in ultraspec (approx 1ml/g tissue). The tissue/cells were homogenised using an electric homogeniser in five 10-second bursts. The universal was returned to ice between each of the bursts to prevent heat build up. The homogenised lysate was then passed through a 25G needle ten times to ensure the production of a uniform lysate. Chloroform (200µl per ml) was added and vortexed for 15 seconds, the sample was then incubated on ice for 5 minutes, before centrifuging at 12,000g (4°C) for 15 minutes; this separates the sample into two phases – the upper, aqueous phase and the lower organic phase. The RNA is contained in the aqueous phase and proteins/DNA in the organic phase. The aqueous phase was removed and transferred to a sterile tube, and 0.5x the volume of isopropanol added to the RNA. 50µl RNA Tack resin was added to the RNA and vortexed for 30 seconds. The mixture was spun for 1 minute at 12,000g and supernatant discarded. The pellet was then washed twice with 75% ethanol by serial vortexing and centrifugation. The pellet was then left to air dry for 30 minutes. The RNA was eluted from the resin pellet by the addition of 100µl nuclease free H₂O. To each 100µl of RNA, 10µl 10x DNase 1 Buffer (Ambion, Huntingdon, UK) was added along with 2.5µl RNase inhibitors (Promega, Southampton, UK). This was vortexed before 5µl DNase (Ambion) was added. The RNA was mixed and incubated at 37°C

for 60 minutes. The DNase was inactivated using 0.2 x the volume of inactivation reagent (Ambion).

2.5.2 Isolation of RNA from LCM Samples

Using the RNeasy micro extraction kit (Qiagen), 40µl of RLT buffer was placed into the cap within the eppendorf tube (see section 2.4.2.5) at RT for 30mins. The cap/eppendorf assembly was then centrifuged at 12000g for 1min, and an additional 35µl RLT buffer added. After addition of 75µl ethanol, the contents were loaded into an RNeasy MiniElute Spin column (Qiagen), centrifuged at 8000g for 30secs and the flow-through discarded. The spin column was then washed with 350µl buffer RW1 (Qiagen; 8000g for 30secs) and the flow through discarded. Any contaminating genomic DNA was removed with the addition of DNase I (80µl; 15mins at RT) to the spin column. This was then washed through with 350µl buffer RW1 centrifuged at 8000g for 30secs, and the flow through discarded. 500µl of RPE buffer was added to the spin column and centrifuged (8000g; 30secs), the flow through discarded, and 500µl of 80% ethanol was then passed through the column and discarded (8000g; 2mins). To elute the RNA, 14µl of nuclease-free water was added to the column, and centrifuged at 12000g for 1min. The RNA was stored at -80°C until analysis.

2.5.3 RNA Amplification

RNA amplification was carried out using the RiboAmp RNA amplification kit (Ambion, TX, USA). This procedure consists of reverse transcription with an oligo(dT) primer bearing a T7 promoter and in vitro transcription of the resulting DNA with T7 polymerase. This generates hundreds to thousands of antisense RNA copies of each mRNA in a sample. For first strand cDNA synthesis, the RNA was

mixed with the oligo(dT) primer up to a volume of 12µl and incubated at 70°C, before being placed on ice. 8 µl of reverse transcription master mix (2µl 10X First Strand buffer; 1µl Ribonuclease inhibitor; 4µl dNTP mix; 1µl Reverse Transcriptase) was added to the cDNA/oligo(dT) mix, and incubated at 42°C for 2h. For the second strand cDNA synthesis, 80µl of second strand master mix (63µl NFW; 10µl 10X second strand buffer; 4µl dNTP mix; 2µl DNA Polymerase; 1µl RNase H) was added to each 20µl sample, and incubated for 2h at 16°C. The cDNA was then purified by equilibrating the cDNA filter cartridge, and adding 250µl of cDNA Binding Buffer to each cDNA sample. The mixture was applied to an equilibrated cDNA filter cartridge, and the cartridge washed with 500µl cDNA Wash Buffer. The cDNA was eluted with 2 x 10µl NFW. To synthesise amplified RNA (aRNA), *in vitro* transcription was carried out. Firstly, a 24µl transcription reaction mix was made containing the following: 4µl T7 ATP solution (75mM); 4µl T7 CTP solution (75mM); 4µl T7 GTP solution (75mM); 4µl T7 UTP solution (75mM); 4µl T7 10X reaction buffer; 4µl T7 enzyme mix. This was added to 16µl of the eluted cDNA, and incubated for 24h at 37 °C. Following this, 2µl DNase I was added to the mix and incubated for 30min at 37°C, and 60µl of Elution Solution was then added to each aRNA sample. To purify the aRNA, 350µl of aRNA Binding Buffer and 250µl of 100% ethanol were added to the sample, which was then passed through an aRNA Filter Cartridge. This was washed with 650µl aRNA Wash Buffer, and the aRNA eluted with 2 x 50µl 50°C Nuclease-free Water.

2.5.4 Reverse Transcription

Reverse transcriptase is a RNA-dependent DNA polymerase which is encoded by retroviruses. Their viral function is to copy the viral RNA genome into DNA prior to

its integration into host cells. This can be exploited to allow production of DNA (cDNA) from any RNA template and is known as reverse transcription PCR. The Superscript - First Strand synthesis system for RT-PCR was used for reverse transcription (Invitrogen) along with Oligo dT (Roche, East Sussex, UK). 5µg RNA sample and 500ng Oligo dT were mixed and incubated at 70°C for 10 min to denature the RNA, this was subsequently incubated on ice for 1 minute. 2µl 10 x RT buffer, 2mM MgCl₂, 10mM DTT and 0.5mM dNTP's were added to each RNA sample and mixed, finally 200units (u) Superscript enzyme was added and mixed. The following PCR cycle was used; 25°C for 10 min, 42°C for 50 min and 70°C for 15 min for annealing, elongation and termination respectively. The cDNA was stored at -20°C until required.

2.5.5 Polymerase Chain Reaction (PCR)

PCR was performed on either cDNA produced from reverse transcription or on genomic DNA, as a diagnostic tool or to allow the amplification of a gene for functional studies. In a typical 50µl PCR reaction the following quantities of reactants were used; 0.2 mM dNTP mix (Promega), 5µl 10x PCR Buffer (Roche), 5 units Taq polymerase (Roche), 0.5µM of the forward and reverse primers, 4µl DNA (at appropriate concentration) and nuclease free H₂O up to 50µl. This was then cycled in a ThermoHybaid Px2 Thermal Cycler under the following conditions: 94°C for 5 minutes for one cycle, thirty cycles of 94°C for 30 seconds 55-60°C (depending on the melting temperature of the primers) for 30 seconds and 72°C for 1 minute and finally one step of 72°C for 10 minutes. The PCR products were then run on an agarose gel, as outlined in section 2.6.3. For all PCRs, Classic 18S (Ambion) was

used as an internal standard (Primer sequences unknown). Because of its invariant expression across tissues and treatments, 18S ribosomal RNA is an ideal internal control for RNA analysis.

2.5.6 Quantitative Polymerase Chain Reaction (qPCR)

RNA was isolated by phenol/chloroform extraction and used directly in a quantitative PCR reaction. The Platinum[®] SYBR[®] Green qPCR SuperMix Kit (Invitrogen) method was utilised to allow quantification by fluorescence during the PCR reaction. Briefly 40µl SYBR green mastermix was added to 10ng RNA along with 0.2µM of the required forward and reverse primers. The qPCR reaction was cycled in a Stratagene Mx3000P qPCR system as follows: 1 cycle of 50°C for 2mins, 95°C for 2mins (RT step), then 45 cycles of 95°C for 15secs, 55°C for 30secs and 72°C for 30secs. Each tissue sample was tested in triplicate and compared to GAPDH RNA (Primers: forward 5' TGAGGCCGGTGCTGAGTATGTCG 3'; reverse 5' CCACAGTCTTCTGGGTGGCAGTG 3') as an external control which allowed normalisation of results. An identical PCR was carried out on a dilution series of RNA using both gene of interest and external to allow estimation of PCR efficiency. The raw data is in the form of a C_t value which is the cycle number at which the fluorescence in the tube passed above a predefined threshold. This C_t value is used in the calculations to show relative differences in gene expression in different samples. Briefly the difference in C_t values between the gene of interest and the control was calculated and used to determine relative quantification by expressing the values as $2^{-\Delta C_t}$.

2.6 DNA Methods

2.6.1 DNA isolation from mouse tail biopsies

Tail biopsies were carried out on halothane anaesthetised mice, and the tail biopsy placed into a labelled tube containing 750 μ l tail digest buffer (0.3M sodium acetate, 10mM TrisHCl pH 7.9, 1mM EDTA pH 8, 1% SDS and 200 μ g/ml Proteinase K. Samples were incubated overnight at 37°C and frozen at -20°C for storage until needed. Prior to PCR analysis, samples were centrifuged at 16000g at 4°C for 15mins, and frozen. This process was repeated twice, and ensured the sodium dodecyl sulphate (SDS) present in the tail digest buffer was sedimented and did not interfere with the PCR reaction.

2.6.2 Genotyping Transgenic Mice

PCR reactions were carried out as described in section 2.5.4. Tail digests were spun at 16000g for 15mins at 4°C and stored on ice to prevent SDS in the digest buffer from floating in the supernatant. The supernatant was then diluted 1:10 to minimise the risk of SDS interfering with the PCR reaction. A master mix containing nuclease-free H₂O, 10xPCR buffer, 2mM dNTP, 25mM MgCl₂, 10 μ M primers and Taq was made, and 18 μ l of master mix was added to 2 μ l of 1:10 diluted DNA. This was then cycled in a ThermoHybaid Px2 Thermal Cycler under the following conditions: 94°C for 5 minutes for one cycle, thirty cycles of 94°C for 30 seconds 55-60°C (depending on the melting temperature of the primers) for 30 seconds and 72°C for 1 minute and finally one step of 72°C for 10 minutes. The PCR products were then run on an agarose gel, as outlined in section 2.6.3

2.6.3 Agarose Gel Electrophoresis

DNA fragments were separated by horizontal agarose gel electrophoresis on 1.5 - 2% Agarose gels. The gels were produced by dissolving powdered agarose in TAE buffer by heating to the point of boiling. Ethidium bromide (EtBr) was added to a final concentration of 0.5µg/ml to allow visualisation of the DNA under UV light. The gel was then poured into a cassette with slot former and allowed to set. The DNA samples were mixed with loading buffer and loaded onto the submerged gel. The fragments were separated according to size by applying a voltage of 120V across the gel for 1-2 hours. DNA bands were visualised using a UV transilluminator and photographed using attached camera.

2.6.4 Quantification of DNA Concentration

DNA concentration was calculated by UV spectroscopy. Readings were taken at 260nm and 280nm. The concentration of DNA was automatically calculated by the biowave reader using the following equation: $A_{260} \times 50 \times \text{dilution factor}$. The ratio of: A_{260} / A_{280} gives an indication to how pure the DNA is, proteins have an absorbance at around A_{280} therefore the lower the number the less pure the DNA preparation is.

2.6.5 Restriction Endonuclease Digestion of DNA

Digestion of DNA using restriction endonucleases was carried out both as a diagnostic tool and to allow the formation of a DNA fragment to engineer into plasmid DNA. Roche restriction endonucleases were used for this process along with their optimised buffer. A typical 20µl digest contained 1µg DNA, 1 unit of the restriction enzyme and 2µl 10x reaction buffer, made up to 20µl with distilled H₂O.

The restriction reaction was carried out at 37°C for 1-2 hours, and 1 unit of each enzyme was used per 1 µg of DNA in a 20 µl reaction.

2.6.6 DNA Ligation into Linearised Vectors

The vector of choice was linearised by restriction enzyme digestion using enzyme sites contained within the vector multiple cloning site. The insert will also have complementary sites at either terminus making “sticky ends” for ligation. A molar ratio of 3:1 insert to plasmid was used for all ligations of this nature. The Roche rapid ligation kit was used and manufacturer’s instructions followed. Briefly both insert and vector were diluted in DNA dilution buffer so that the final volume equalled 10 µl, reaction buffer (10 µl) was then added and mixed. Finally 1 µl DNA ligase was added to the reaction which was incubated at 4°C overnight. This ligation mixture was used directly for transformation of supercompetent SURE 2 cells.

2.6.7 Isolation of DNA Fragments from Agarose gel

DNA was separated as detailed in section 2.6.3. The DNA band was visualised over UV light (due to EtBr intercalation) and excised using a scalpel blade, taking care to trim all unstained gel from the slice. The agarose gel slice was weighed and then subjected to the DNA extraction protocol set out in the QiaQuick gel extraction kit (Qiagen). Briefly 300 µl of QG buffer was added per 100mg of agarose and heated to 50°C for 10 minutes to dissolve the gel. 100 µl isopropanol per 100mg agarose was added to the mixture to help increase the DNA yield. The mixture was then applied to a spin column and centrifuged at 17,900 x g for 1 minute. This allows the DNA to bind to the silica membrane of the column. The DNA was then washed with 750 µl

wash buffer (PE) by applying it to the spin column and centrifuging at 17,900 x *g* for 1 minute. The empty spin column was then spun for an additional minute to remove traces of ethanol. The DNA was eluted by the addition of 50µl buffer EB or nuclease free H₂O and centrifuging at 17,900 x *g* for 1 minute. The DNA was stored at -20°C until needed.

2.6.8 DNA Sequencing

DNA sequencing was carried out commercially at the DNA sequencing facility at Dundee University.

2.6.9 Transformation of Bacteria

SURE 2 (Stop Unwanted Rearrangement Events) supercompetent *Escherichia coli* cells (*E.coli*) (Stratagene, The Netherlands) were used for transformations in this study, due to the fact that these cells have been engineered to lack components of pathways that cause the rearrangement and deletion of non-standard secondary and tertiary structures. This property makes these cells ideal for the cloning of DNA segments that are difficult to clone in conventional *E.coli* strains. For transformations, 100µl SURE 2 cells were incubated with 2µl β-mercaptoethanol on ice for 10mins. Approximately 20ng plasmid DNA was then added to the cells, mixed, and incubated on ice for 30mins, at which point the cells were subjected to exactly 30secs heat shock at 42°C, before being placed back on ice for a further 2mins. 900µl SOC (Hanahan, 1983) media (Invitrogen, Paisley, UK) was added to the cells and incubated at 37°C for 1 hour with constant agitation. Aliquots of the

transformation mixture were spread on LB (Bertani, 2004) agar plates containing 100µg/ml ampicillin and incubated overnight at 37°C.

2.6.10 Liquid Culture of Bacterial Clones

Individual colonies were picked from the agar plates of transformed bacteria into a 10ml LB culture media containing 100µg/ml ampicillin. This was incubated overnight at 37°C with constant agitation. 2ml of the bacterial culture was spun at 6,000g and pelleted bacteria resuspended in 1ml LB containing 50% glycerol. These glycerol stocks were stored at -20°C until required.

2.6.11 Minipreparation of Plasmid DNA

The remaining 8ml of bacterial culture was used for plasmid DNA production utilising the Qiagen miniprep spin kit (West Sussex, UK). Briefly the 8ml of culture was spun at 8950 x g for 15 minutes and resuspended in 250µl buffer P1. The cells were then lysed by addition of 250µl buffer P2, and incubated at room temperature for 5 minutes. The genomic DNA and proteins were precipitated from the lysate by addition of 350µl buffer N3 and centrifuged at 17,900 x g for 15 minutes to clear the lysate. The supernatant was centrifuged through a Qiagen column containing a silica membrane to selectively adsorb plasmid DNA in the high salt buffer. The membrane was washed with buffer PE and plasmid DNA eluted by centrifugation at 17,900 x g with 50µl buffer EB or distilled water.

2.6.12 Endofree Maxipreparation (Qiagen) of Plasmid DNA

Endotoxin-free DNA improves the efficiency of transfection into sensitive or immunologically active cells, and Endofree Maxi Prep kits remove endotoxin

generated from gram-negative bacteria such as *E. coli*. A 10ml liquid culture was set up as detailed above and grown for 8 hours at 37°C with vigorous shaking. The 10ml *E. coli* culture was then transferred into a flask containing 200ml LB (with 100µg/ml ampicillin) and grown overnight at 37°C with vigorous shaking. The bacterial cells were harvested by centrifugation at 6000 x *g* for 15 min at 4°C. The supernatant was removed and bacterial pellet resuspended in 10ml buffer P1. The cells were then lysed through addition of 10 ml buffer P2 which was mixed thoroughly by inverting and incubated at room temperature for 5 minutes. The genomic DNA, proteins, cell debris, and SDS were precipitated by addition of 10 ml chilled buffer P3, which was mixed by inverting 4–6 times. The lysate was poured into the barrel of the QIAfilter cartridge and incubated at room temperature for 10 min. The lysate was then passed into a sterile tube and 2.5 ml buffer ER was added to remove endotoxin and incubated on ice for 30 minutes. The filtered lysate was applied to a QIAGEN-tip equilibrated with buffer QBT and allowed to enter the resin by gravity flow. The QIAGEN-tip was washed with 2 x 30 ml buffer QC, and the DNA was eluted by addition of 15 ml buffer QN and precipitated by the addition of 0.7 volumes of room temperature isopropanol. This was mixed and centrifuged at 15,000 x *g* for 30 min at 4°C to pellet the plasmid DNA. The supernatant was decanted and pellet washed with 5 ml of endotoxin-free 70% ethanol and centrifuged at 15,000 x *g* for a further 10 min. The supernatant was decanted and the pellet left to air dry for 10 min. The DNA pellet was then re-dissolved in 100µl endotoxin-free buffer TE and stored at -20°C until required.

2.7 Protein Methods

2.7.1 Protein Concentration Determination – Bradford Assay

The Bio-Rad protein assay kit used is based on the method described by Bradford (Bradford, 1976). The Bradford protein assay is a simple procedure for determination of protein concentrations in solutions and utilises the change in absorbance of Coomassie Blue upon binding to protein. The Bradford protein assay is not sensitive to interference by chemicals in the lysis buffer, however high concentrations of detergent do cause anomalies in results. The method employed uses gamma-globulin as a standard. Nine standards of gamma globulin were prepared ranging from 10µg/ml to 90µg/ml. 160µl of each standard was pipetted in duplicate into a 96 well plate along with a buffer blank. The protein that was to be measured was diluted in the same buffer as gamma-globulin and also added to the individual wells in duplicate. 40µl of dye reagent concentrate (Bio-Rad, Herts., UK) was added to each well and mixed. The plate was incubated at room temperature for 5 minutes and the absorbance read at 595 nm. The absorbencies of the samples were compared to a standard curve generated from the absorbencies from the standards.

2.7.2 SDS Polyacrylamide Gel Electrophoresis (SDS PAGE)

Cells were scraped in RIPA buffer containing 1.6 mg/ml of Complete[®] protease inhibitor cocktail (Roche), and proteins were separated according to weight on Novex Bis-Tris gels (Invitrogen). The comb was removed from the pre-cast gel and the wells rinsed with distilled water. The gel was then placed in to a tank filled with 1x MOPS running buffer (Invitrogen), and the centre of the tank was filled with an anti-oxidant to maintain reduced proteins their reduced state. Protein samples in 1x LDS sample buffer (containing DTT reducing agent) were heated to 70°C for 15 minutes and

cooled on ice. The samples were then centrifuged at 17,900 x g for 30 seconds. The samples (containing 50µg lysate protein) and a pre-stained molecular weight marker (See Blue plus 2; Invitrogen) were loaded onto the gel, and the gel was run at 200V for 60 minutes.

2.7.3 Western Blotting

Following electrophoresis, the gel was removed from the cassette and immersed in transfer buffer. An individual sheet of nitrocellulose membrane was washed in dH₂O for 5mins, and then washed in transfer buffer along with two 3M papers, cut slightly larger than the gel, and four foam pads. The nitrocellulose was laid on top of the gel and sandwiched between the two 3M papers, ensuring exclusion of any air bubbles. This sandwich was placed in the X-blot module (Invitrogen) between the four foam pads. The module was then clamped onto the gel tank and topped up with ice-cold transfer buffer. The proteins in the gel were electro-blotted on to the nitrocellulose at 30V for 90 minutes on ice. The nitrocellulose was then blocked for 1h in 5% milk protein (Marvel) in TBST (blocking solution) at RT to reduce non-specific antibody binding. The primary antibody was added at an appropriate dilution (Appendix 4) in blocking solution and incubated at 4°C, with gentle agitation overnight. The nitrocellulose was subsequently washed 3 times in 50ml TBST to remove any unbound antibody, and then incubated at RT for 60 minutes with anti-IgG-peroxidase diluted in blocking solution (specificity dependent on primary antibody). The blot was again washed 3 times in 50ml TBST and the immune complexes then visualised by enhanced chemiluminescence (ECL) (Amersham, Buckinghamshire, UK). This kit operates using an acridan-based substrate which when in close proximity to peroxidase releases light. The position of the immune complexes were visualised by

exposure of the membrane to ECL film (Amersham), which was subsequently developed in a Kodak automatic developer. To assess equal loading the proteins on the blot were stained with Indian ink after alkali pre-treatment, as described by Sutherland and Skerrit (1986). Briefly the membranes were washed in TBST before incubation with 0.2M NaOH for 5 minutes. The membrane was then submerged in 10% India ink solution for 120 minutes and finally washed repeatedly in TBST until only the protein bands were visible.

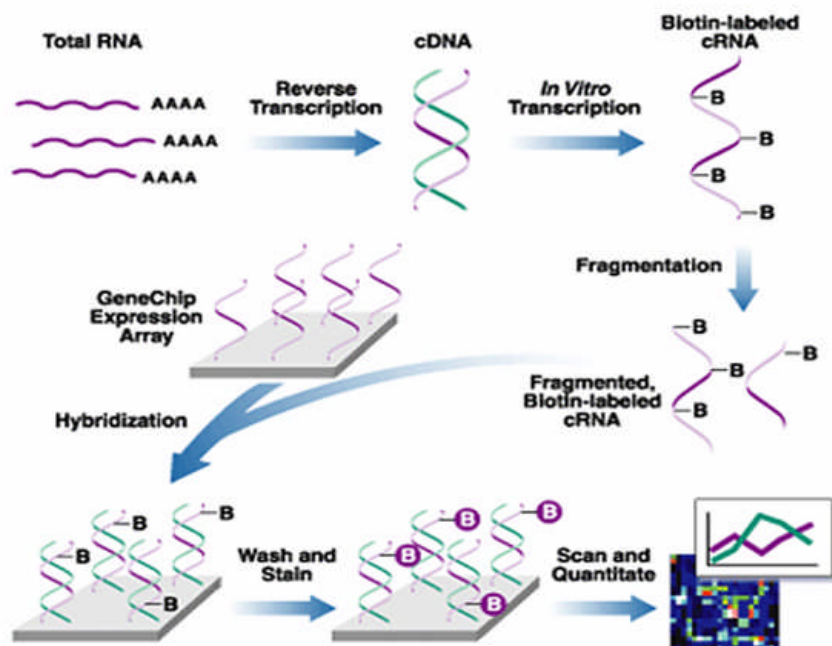
2.8 Microarray

2.8.1 Hybridisation of RNA to Affymetrix Platform

The fundamental basis of DNA microarrays is the process of hybridisation. Two DNA strands hybridise if they are complementary to each other, and one or both strands of the DNA hybrid can be replaced by RNA and hybridisation will still occur. Affymetrix microarrays use a photolithographic mask to control synthesis of oligonucleotides on the surface of a chip (Figure 2.5). The masks control the synthesis of several hundred thousand squares, each containing many copies of an oligo. For expression analysis, up to 40 oligos are used for the detection of each gene. From a region of each gene, 11-20 oligos are chosen as perfect matches (PM; i.e. perfectly complementary to the mRNA of that gene), and another 11-20 oligos are chosen as mismatch oligos (MM). The MM oligos are identical to the PM oligos except for at position 13, where one nucleotide has been exchanged to its complementary nucleotide. The MM oligos will detect non-specific and background hybridisation, which is important for quantifying weakly expressed mRNAs. Hybridisation of ATDC5 RNA to the Affymetrix Genechip was carried out at the Human Genome Mapping Project (HGMP) Gene Service (Cambridge, UK).

Following extraction of total RNA from ATDC5 cells, mRNA was converted to cDNA using reverse transcriptase and a poly-T primer. The resulting cDNA was amplified using T7 RNA polymerase in the presence of biotin-CTP, so each cDNA produced 50-100 copies of biotin-labelled cRNA. The cRNA was then incubated at 94 degrees in fragmentation buffer to produce cRNA nucleotide fragments of 35 to 200 nucleotides in length. These fragments were hybridised to the Affymetrix chip, and any non-hybridised material washed away. The hybridised biotin-labelled cRNA was then stained with Streptavidin-Phycoerythrin and washed, and the chip scanned in a confocal laser scanner. The signal on the chip was then amplified with goat IgG and biotinylated antibody, before being scanned again. The absolute expression value for each transcript was then calculated from the combined PM-MM differences of all the pairs in the probe set by Affymetrix software

A



B

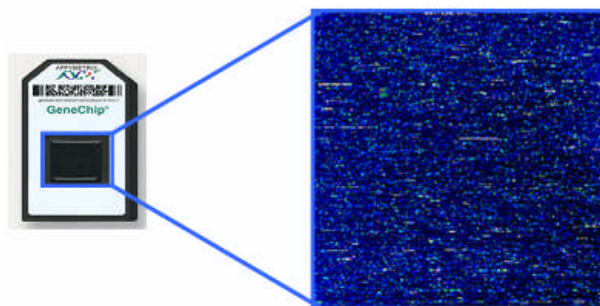


Figure 2.5 Affymetrix Microarray overview. (A) Affymetrix microarray involves the reverse transcription of total RNA into cDNA. This cDNA then undergoes in vitro transcription into cRNA, during which point a biotin label is attached. The labeled RNA is then fragmented, and hybridised to a GeneChip containing thousands of oligonucleotide probes for specific genes. The hybridised chip is then washed and stained, and can then be scanned for the detection of specific genes. (B) Affymetrix GeneChip showing a hybridised sample. This chip can then be scanned and analysed for the expression of genes of interest. Diagram taken from www.affymetrix.com.

2.8.2 Microarray Data Analysis

The data obtained from the Affymetrix hybridisation was pre-processed using the Robust Multichip Analysis (RMA) algorithm in GeneSpring 7.0 (Silicon Genetics, CA, USA). The Robust Multichip Analysis algorithm (RMA; Irizarry *et al.*, 2003) is commonly used to normalise Affymetrix data, and uses the PM value only, ignoring the expression value obtained for the MM probe. RMA analysis involves calculating the average background for the entire chip (*BG), and then subtracting this from the PM of a given probe. Intensity dependent normalisation of this value (PM-*BG) is carried out, and then log transformed. RMA normalisation is carried out on all probe pairs within a given set, and a single value is obtained using Tukey's median polishing procedure. RMA normalisation is an effective method for normalising microarray data, as, by ignoring the MM value, less 'noise' is produced, therefore reducing the chance of false positives. The uploaded data was first separated into 2 groups according to treatment type, and then normalised. Measurements of less than 0.01 were set to 0.01, and each chip (i.e. sample) was normalised to the 50th percentile (i.e. all of the measurements on each chip were divided by a percentile value of 50%). Per Chip normalisations control for chip-wide variations in intensity. Such variations may be due to inconsistent washing, inconsistent sample preparation, or other microarray production or microfluidics imperfections. Each gene was then normalised to the control sample. In this normalisation, each gene is divided by the average intensity of that gene in the control samples. To assess differential gene expression between treatments, expression values were further filtered by retaining only those probe sets with a fold change of at least 1.5 in Dex samples compared with Controls. A two-sample t-test was then carried out, resulting in a list of genes whose expression was significantly changed by 1.5-fold or more in Dex-treated samples.

2.9 Cell Proliferation and Differentiation Assays

2.9.1 [³H] Thymidine Incorporation

Chondrocyte proliferation was assessed by incubating the cells with 0.2 μ Ci/ml [³H]thymidine (37MBq/ml; Amersham Pharmacia Biotech, Bucks, UK) for the last 2h of the incubation period. Following removal of the [³H]thymidine, the cells were fixed in ice-cold TCA (5%) for 15mins, washed, and lysed in 0.1M NaOH for up to 30mins. Scintillation fluid was then added, and the amount of radioactivity incorporated into trichloroacetic acid insoluble precipitates was measured using a scintillation counter.

2.9.2 Alcian Blue Staining of the Cell Monolayer

Proteoglycan synthesis was evaluated by staining with Alcian Blue. In brief, cells were washed twice with PBS, fixed in 95% methanol for 20 min and stained with 1% Alcian Blue 8 GX (Sigma) in 0.1 M HCl overnight and rinsed with distilled water. Alcian Blue-stained cultures were extracted with 1 ml 6M guanidine-HCl for 6 h at room temperature and the optical density (O.D.) was measured at 630 nm using a Jenway 6105 spectrophotometer.

2.9.3 Alkaline Phosphatase Assay

Cell layers were rinsed with PBS and lysed with 0.9% NaCl and 0.2% Triton X-100 and centrifuged at 12000g for 15 min at 4°C. The supernatant was assayed for protein content and ALP activity as a measure of cell number and chondrocyte differentiation respectively. The protein content of the supernatant was measured using the Bio-Rad protein assay reagent (Bio-Rad Laboratories) as previously described (2.7.1). Enzyme

activity was determined by measuring the cleavage of 10 mM p-nitrophenyl phosphate (pNPP) at 410 nm. Total ALP activity was expressed as nmoles pNPP hydrolysed/min/mg protein.

Chapter 3

Identification of Novel Glucocorticoid-Responsive Chondrocyte Genes

Chapter Contents

- 3.1 Introduction
 - 3.2 Hypothesis
 - 3.3 Aims
 - 3.4 Materials and Methods
 - 3.4.1 Cell Culture
 - 3.4.2 RNA Extraction and Hybridisation to the Affymetrix GeneChip
 - 3.4.3 Data Normalisation
 - 3.4.4 Gene Ontology Analysis
 - 3.4.5 Gene Ontology Enrichment and Functional Annotation Clustering
 - 3.4.6 Validation of Affymetrix Microarray Data with qPCR
 - 3.5 Results
 - 3.5.1 Microarray Analysis
 - 3.5.2 Identification of Trends in Gene Expression
 - 3.5.3 Validation of Microarray Expression Data
 - 3.6 Discussion
 - 3.7 Conclusions
-
-

3.1 Introduction

GCs are used extensively for the treatment of autoimmune and inflammatory diseases, including arthritis, asthma, multiple sclerosis, inflammatory bowel disease and chronic active hepatitis. In addition, GCs are also used in combination with other drugs to reduce inflammation associated with leukaemia, and to suppress the immune system following transplantation. GCs are also used extensively in paediatric practice for the treatment of chronic inflammatory, autoimmune and neoplastic diseases, and it is estimated that 10% of children may require some form of GC therapy during childhood (Warner 1995).

Impairment of childhood growth with GCs was first described over 40 years ago (Blodgett *et al.*, 1956), and since then, a number of studies in experimental animal models have also shown that high levels of GCs have a suppressive effect on longitudinal bone growth (Rooman *et al.*, 1999; Stevens *et al.*, 1999; Silvestrini *et al.*, 2000).

Multiple mechanisms have been proposed to explain the growth-suppressing effect of supraphysiological GCs, and it is now known that GCs act locally to inhibit longitudinal bone growth, suggesting a mechanism intrinsic to the growth plate (Baron *et al.*, 1992). In rats, GC excess reduces bone growth, probably due to decreased numbers of proliferating chondrocytes and increased apoptosis of hypertrophic chondrocytes in the growth plate (Chrysis *et al.*, 2003). These results are also consistent with the Dex-induced inhibition of chondrocyte proliferation and cartilage matrix production observed in 12 week old rats *in vivo* (Annefeld *et al.*, 1992), and with *in vitro* models of chondrocyte growth, which show that

pharmacological doses of Dex reduce the proliferation of murine chondrogenic ATDC5 cells (Mushtaq *et al.*, 2002). GCs have also been shown to promote apoptosis and reduce proliferation through suppression of the phosphatidylinositol 3-kinase (PI3K) pathway (Chrysis *et al.*, 2003; Chrysis *et al.*, 2005; Macrae *et al.*, 2007), and down-regulate chondrocyte marker genes Coll II, Coll X and aggrecan (Owen *et al.*, 2007; also see 6.5.4). Other GC-target genes that have been recently identified include C-type natriuretic peptide (Agoston *et al.*, 2006) and vascular endothelial growth factor (VEGF) (Koedam *et al.*, 2002). The IGF-I/GH system is also thought to play a major role in GC-regulation of the growth plate and it has been shown that GCs cause antagonism of growth hormone (GH) secretion and action. It has also been shown that GCs inhibit pulsatile GH release (Wehrenber *et al.*, 1992; Giustina *et al.*, 1992; Giustina *et al.*, 1998), reduce GH receptor expression, and inhibit IGF-I activity (Unterman *et al.*, 1985).

Although many of the molecular factors involved in GC-induced growth retardation have been identified, a comprehensive understanding of the mechanisms governing GC effects at the growth plate has not been achieved. The advent of functional genomics in combination with systems biology and integrative physiology approaches has equipped us with the tools to overcome some of the challenges associated with understanding these complex interactions. In this study, comprehensive gene expression profiling of the murine chondrogenic ATDC5 cell line by Affymetrix microarray has been used to systematically investigate the modulation of factors that modulate GC-induced growth retardation. This study identified numerous genes that undergo significant changes in expression with GCs. One of these genes, lipocalin 2, was then selected for further functional analysis.

3.2 Hypothesis

The hypothesis of this study was that a pharmacological dose of the commonly used GC, Dex, would up- or down- regulate genes not previously linked with GC-induced growth retardation at the growth plate.

3.3 Aims

- I. Carry out an Affymetrix microarray on Dex-treated ATDC5 cells and identify novel genes involved in GC-induced growth retardation by gene ontology analysis.
- II. Identify novel pathways involved in growth retardation by bioinformatics methods such as Functional Annotation Clustering.
- III. Confirm changes in expression of selected genes with q-PCR.

3.4 Materials and Methods

3.4.1 Cell Culture

The ATDC5 chondrocyte cell line was obtained from the RIKEN cell bank (Ibaraki, Japan), and cells were cultured at a density of 6000 cells per cm² in differentiation medium as described in section 2.2.3. ATDC5 cells were differentiated for 15 days, by which point the cells are considered to be in the chondrocytic phenotype, with the expression of chondrocyte marker gene aggrecan, and the formation of nodules. At day 15, the cells were incubated with 10⁻⁶M Dex (Sigma; water soluble) (in differentiation medium), for 24h, and control cells received differentiation medium only.

3.4.2 RNA Extraction and Hybridisation to the Affymetrix GeneChip

Total RNA was extracted from duplicate control and Dex-treated cultures at 24h following treatment using the phenol/chloroform extraction method as described in section 2.5.1. RNA integrity and quantity was assessed using the Agilent 2000 Bio analyzer system, and RNA samples were subsequently hybridised to the Affymetrix Mouse Genome 430 2.0 Gene Chip array for 16h (2.8.1). This GeneChip contains 45101 probe sets, and can analyse the expression level of over 39000 transcripts and variants from 34000 characterised mouse genes. Following hybridisation, the GeneChip arrays were stained, washed and scanned. Bio analysis, microarray hybridisation and scanning were completed at the Human Genome Mapping Resource Centre (HGMP) in Cambridge. A detailed description of the hybridisation protocol can be found in section 2.8.1.

3.4.3 Data Normalisation

The data obtained from the Affymetrix hybridisation was pre-processed using the RMA algorithm in GeneSpring 7.0 (Silicon Genetics, CA, USA) (2.8.2). Each gene was then normalised to the control sample. In this normalisation, each gene is divided by the average intensity of that gene in the control samples (Figure 3.1). To assess differential gene expression between treatments, expression values were further filtered by retaining only those probe sets with a fold change of at least 1.5 in Dex samples compared with Controls. Due to the fact that there were only 2 replicates per treatment, a two-sample t-test was carried out for each sample. This test looks for differentially expressed genes between each condition, and is applied to the mean of each of the 2 normalised values for each treatment against the baseline value of 0 (in log scale). (All genes are centred around 0 after normalisation in GeneSpring, which

represents the baseline expression level where genes do not show any differential expression compared to controls). Therefore, genes associated with a p-value lower than 0.05 were regarded as statistically significant (i.e up- or down-regulated compared to an expression baseline of 0). This analysis resulted in a gene list of 96 transcripts, whose expression was significantly changed by 1.5-fold or more in Dex-treated samples.

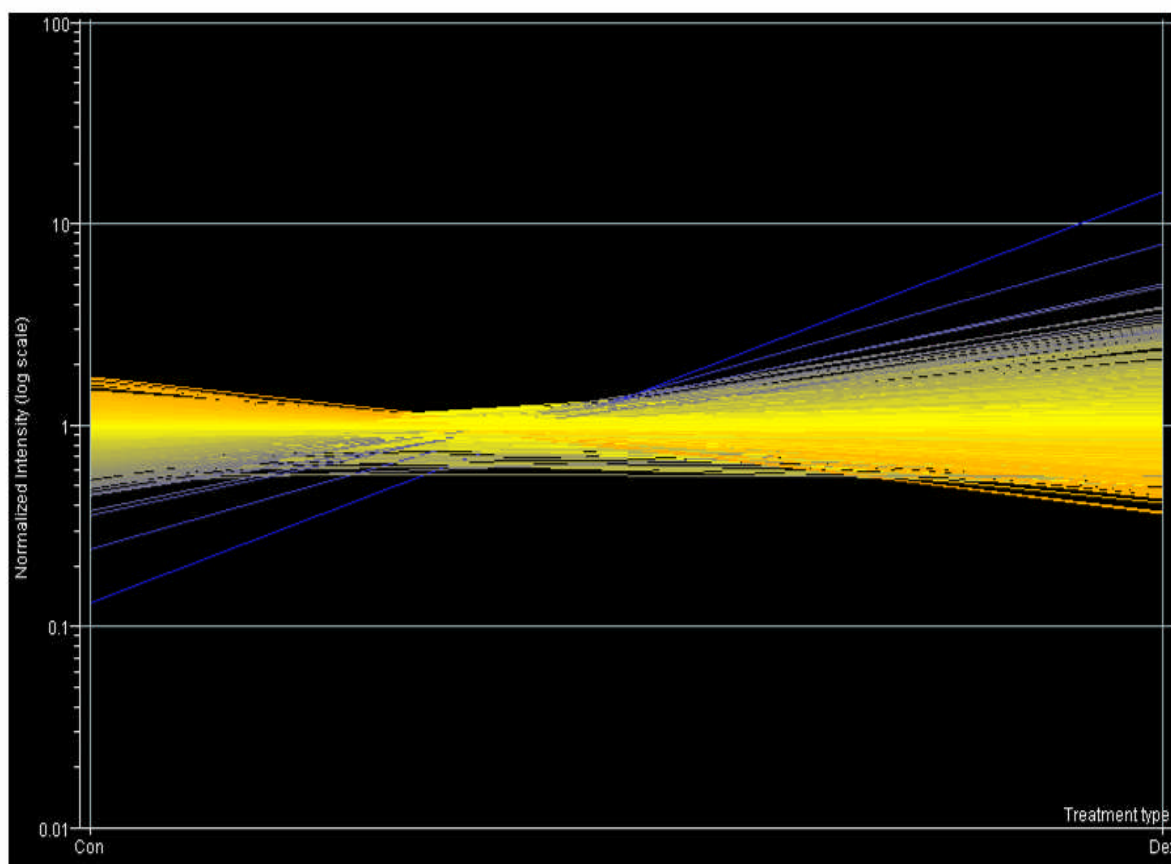


Figure 3.1 Line graph of Control and Dex sample data loaded into GeneSpring. Gene expression values were pre-normalised with the RMA algorithm, and log transformed. Average gene expression values for control (Con) samples are represented by the left y-axis and values for Dex samples by the right y-axis.

3.4.4 Gene Ontology Analysis

Probe set lists resulting from the comparison of Control versus Dex samples filtered using a 1.5-fold cutoff were assigned a molecular function with the NetAffx annotation programme (<http://www.affymetrix.com/analysis>).

3.4.5 Gene Ontology Enrichment and Functional Annotation Clustering

Gene sets were created using the Functional Annotation Analysis option on the Database for Annotation, Visualisation, and Integrated Discovery (DAVID; The National Institute of Allergy and Infectious Diseases) (Dennis *et al.*, 2003). Gene ontology (GO) is a method for describing (annotating) gene terms, and the most significant annotated terms can be found by looking at the probabilities that the terms are counted by chance. This is done by GO enrichment analysis, which gives an enrichment score associated to each term. A list of the most significant GO terms can then be created by ordering the enrichment scores.

3.4.5 Validation of Affymetrix Microarray Data with qPCR

Total RNA was extracted from triplicate control and Dex-treated ATDC5 cultures at 24h following Dex (10^{-6} M) treatment using the phenol/chloroform extraction method as described in section 2.5.1. RNA quantity and integrity was assessed using the Bioanalyzer 2000 system (Agilent). RNA samples or blanks (containing nuclease-free water in place of RNA) were reverse transcribed in 20 μ l reactions with 200ng random hexamers and 200U Superscript II reverse transcriptase using the Superscript preamplification protocol (2.5.4) (Invitrogen). qPCR was performed using the Stratagene Mx3000P real-time QPCR system (Stratagene, California, USA) as previously described (2.5.5). Primers were designed using the software programme

Primer3 (Whitehead Institute for Biomedical Research), and were made to span at least one intron to prevent any amplification from contaminating genomic DNA by semi-quantitative PCR. Genes selected for further analysis by qPCR were as follows: Lipocalin 2, Secreted frizzled-related protein 2 (SFRP2), connective tissue growth factor (CTGF), IGF-I, Lumican, integrin α 10, dentin matrix protein 1 (DMP1) and serum-glucocorticoid regulated kinase (SGCK). Primer sequences are displayed in Table 3.1, and amplicon locations in Appendix 5. Fold changes were normalised for the expression of GAPDH, and calculated using the comparative method as previously described (section 2.5.5).

Table 3.1 Primer sequences for qPCR confirmation of Microarray data

Gene Name	Forward (5'-3')	Reverse (5'-3')	Amplicon Size
Lipocalin 2	CAGAAGGCAGCTTTACGATG	CCTGGAGCTTGGAACAAATG	134
SFRP	TACCACGGAAGCCTCTAAGC	CTCGCTTGCACAGAGATGTT	100
CTGF	CCACCCGAGTTACCAATGAC	GACAGGCTTGCGATTTTAG	146
IGF-I	GTGGACCGAGGGGCTTTTACTT	TTTGCAGCTTCGTTTTCTTGTTTG	246
Lumican	TGCTCGAGCTTGATCTCTCC	CAGTGGTCCCAGGATCTTACA	156
Integrin α 10	CTGAGGCTGGTTCACAATGA	CGGGAGGCTTCATTCACTAG	138
DMP1	AAAGTCAAGCTAGCCCAGAGG	CCGGTCCCCGTACTCTTAG	129
SGCK	GATGGGCCTGAACGATTTTA	GAGGAGAGGGGTAGCGTTC	111
GAPDH	TGAGGCCGGTGCTGAGTATGTCTG	CCACAGTCTTCTGGGTGGCAGTG	302

3.5 Results

3.5.1 Microarray Analysis

Quality control analysis revealed that all RNA samples were of a suitable quality for hybridisation to the Affymetrix gene chip. Analysis in GeneSpring 6.0 software demonstrated that from a total of 45101 probe sets, 614 genes were changed by 1.5-fold or more (Figure 3.2). Significance testing of these genes with student's t-test ANOVA analysis then identified 96 genes whose expression was significantly changed by 1.5-fold or more with Dex treatment (Table 3.1A and B, and Appendix 1

for full details of gene ontologies). 82.2% of these genes were significantly up-regulated with Dex treatment, leaving 17.7% of down-regulated genes in response to Dex. A distribution of fold differences between Control and Dex samples showed that the majority of gene expression changes did not exceed 1.5-fold.

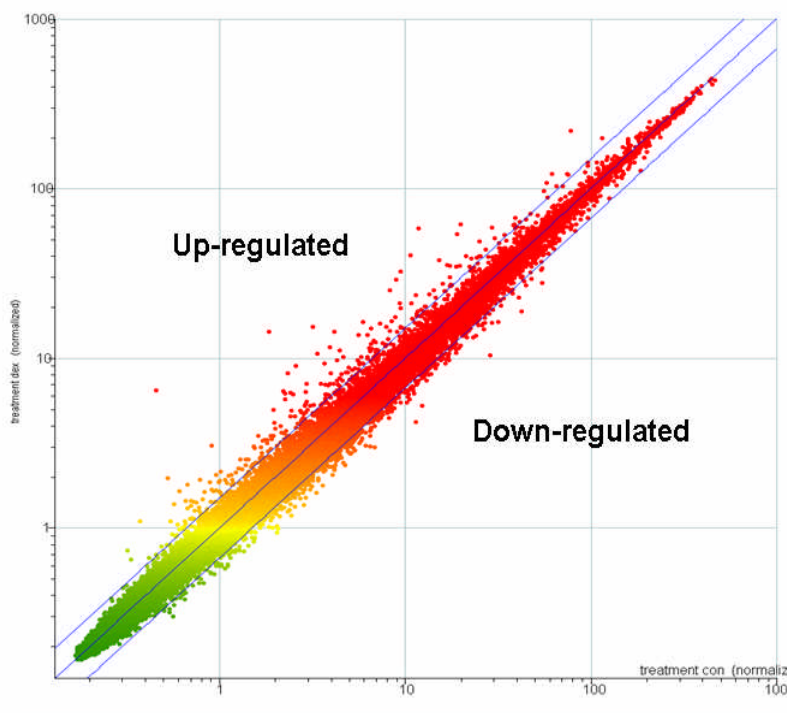


Figure 3.2 Scatterplot of Affymetrix micorarray results from GeneSpring analysis. Analysis in GeneSpring 6.0 software demonstrated that from a total of 45101 probe sets, 614 genes were changed by 1.5-fold or more. Genes to the left of the outer blue line are up-regulated by 1.5-fold or more, and genes to the right of the outer blue line are down-regulated by 1.5-fold or more.

Table 3.2A Genes significantly up-regulated by 1.5-fold or more with Dex treatment.

Affymetrix ID	Fold Change	Gene Name	Assoc. with Bone Growth/Remodelling	Assoc. with GCs
1427747_a_at	14.53	lipocalin 2	*	*
1448550_at	7.98	lipopolysaccharide binding protein		*
1428942_at	5.064	metallothionein 2	*	
1416125_at	3.877	FK506 binding protein 5		
1442025_a_at	3.839	similar to promyelotic leukaemia zfp		
1434202_a_at	3.607	hypothetical protein MCG58343		
1418187_at	3.583	calcitonin receptor activity modifying protein		*
1448881_at	3.44	haptoglobin acute phase response		*
1416953_at	3.324	connective tissue growth factor	*	
1425281_a_at	3.19	delta sleep inducing peptide		
1423233_at	3.131	CCAAT/enhancer binding protein delta		*
1449851_at	3.035	chemokine ligand 2		
1419874_x_at	2.983	promyelotic leukaemia zinc finger protein		
1420772_a_at	2.893	delta sleep inducing peptide		
1422557_s_at	2.847	metallothionein 1	*	
1418091_at	2.731	transcription factor CP2 like 1		
1440235_at	2.69	Integrin alpha 10	*	
1422878_at	2.591	synaptotagmin 12		
1416041_at	2.56	serum/glucocorticoid regulated kinase	*	*
1428471_at	2.53	sorbin and SH3 domain containing 1		
1450826_a_at	2.508	serum amyloid A 3		
1455048_at	2.475	immunoglobulin superfamily member 2		
1423274_at	2.365	DEAD-H		
1443745_s_at	2.332	dentin matrix protein 1	*	
1426236_a_at	2.32	glutamate ammonia ligase		
1422573_at	2.108	AMP deaminase 3		
1449254_at	2.02	secreted phosphoprotein 1		
1418269_at	2.005	lysyl oxidase-like 3		
1448830_at	2.003	dual specificity phosphatase 1		
1417507_at	1.999	cytochrome b-561		
1434203_at	1.973	hypothetical protein MCG58343		
1438953_at	1.935	c-fos induced growth factor		
1435943_at	1.905	dipeptidase 1		
1434642_at	1.9	dehydrogenase/reductase member 8		
1448842_at	1.894	Cysteine dioxygenase 1		
1439755_at	1.837	signal-induced proliferation-associated 1 like 1		
1416383_a_at	1.835	pyruvate carboxylase		
1451596_a_at	1.834	sphingosine kinase 1		
1424051_at	1.823	procollagen type IV	*	
1436789_at	1.818	similar to FLJ14166 protein		
1460011_at	1.793	cytochrome p450		

Table 3.2A Continued

Affymetrix ID	Fold Change	Gene Name	Assoc. with Bone Growth/Remodelling	Assoc. with GCs
1452141_a_at	1.788	selenoprotein P		
1433832_at	1.782	expressed sequence AI551766		
1418932_at	1.768	Interleukin 3		
1426195_a_at	1.756	Cystatin C		
1422620_s_at	1.736	phosphatidic acid phosphatase 2a		*
1422478_a_at	1.668	acetyl coenzyme A synthetase 2		
1417936_at	1.666	chemokine ligand 9		
1454675_at	1.665	nuclear receptor subfamily 1 group D		
1449731_s_at	1.657	nuclear factor of kappa light chain gene enhancer		
1448489_at	1.651	platelet activating factor 2		
1447602_x_at	1.646	sulfatase 2 metabolism		
1424671_at	1.645	pleckstrin homology domain containing F		
1437820_at	1.642	forkhead-like 18		
1451939_a_at	1.635	sushi-repeat containing protein		
1435254_at	1.627	plexin B1		
1456312_x_at	1.62	Gelsolin		
1454849_x_at	1.619	Clusterin		
1441926_x_at	1.616	transmembrane inner ear		
1430388_a_at	1.615	sulfatase 2 metabolism		
1459978_x_at	1.6	similar to FLJ14166 protein		
1448321_at	1.6	SPARC related modular calcium binding 1		
1455078_at	1.593	protein pdb:1LBG		
1416825_at	1.579	synotrophin acidic 1		
1450678_at	1.565	Integrin beta 2		*
1425894_at	1.565	cDNA sequence BC019711		
1452296_at	1.554	slit homolog 3		
1426947_x_at	1.553	procollagen type IV alpha 2		
1417872_at	1.544	Sprouty homolog 1		
1428164_at	1.531	nudix type motif 9		
1415874_at	1.525	period homolog 1		
1420834_at	1.522	vesicle-associated membrane protein 2		
1455768_at	1.516	Niemann pick type C2		
1437865_at	1.507	spermatogenesis associated 13		
1455158_at	1.504	Integrin alpha 3	*	
1427038_at	1.501	preproenkephalin 1		
1421037_at	1.5	neuronal PAS domain protein 2		
1421921_at	1.498	Cysteine protease inhibitor		

Table 3.2B Genes significantly down-regulated by 1.5-fold or more with Dex treatment

Affymetrix ID	Fold Change	Gene Name	Assoc. with Bone Growth/Remodelling	Assoc. with GCs
1418174_at	2.681	D site albumin promoter binding protein		
1423607_at	2.232	lumican	*	
1451191_at	1.984	cellular retinoic acid binding protein II		
1423294_at	1.923	CPG2_Human coatomer gamma 2 subunit		
1449855_s_at	1.887	ubiquitin thiolesterase		
1449486_at	1.876	carboxylesterase 1		
1448201_at	1.718	secreted frizzled-related sequence protein 2		*
1450243_a_at	1.692	down syndrome critical region gene 1		
1428950_s_at	1.664	nucleolar protein 8		
1454888_at	1.639	prefoldin 4		
1425357_a_at	1.618	cysteine knot superfamily1		
1450756_s_at	1.61	cullin 3		
1425806_a_at	1.546	SRB7		
1417394_at	1.531	Kruppel-like factor 4 (gut)		
1431056_a_at	1.529	lipoprotein lipase		
1436993_x_at	1.524	four and a half LIM domains1		
1437401_at	1.506	IGF-1	*	*

3.5.2 Identification of Trends in Gene Expression

The enrichment score tells users how important a specific gene annotation is in terms of the results obtained from an individual microarray, and therefore, higher enrichment scores mean that particular gene annotations are biologically more important. The enrichment score of a gene group is determined from the minus log transformation on the geometric mean of p-values from the annotation terms associating with one or more of the gene group members. Of 79 genes up-regulated in the presence of Dex, 23% were involved in extracellular signalling (Table 3.2A; Figure 3.3A), and a relatively high enrichment score of 5.1 displayed that extracellular matrix proteins are important following GC exposure in chondrocytes. Unsurprisingly, 5% of genes were associated with bone formation and remodelling. An enrichment score of 2.4 confirmed that these genes played an important role in the cell's response to GCs. 7% of genes had links with cell-matrix communication

(enrichment score = 2.4), and 5% of genes were associated with cell motility and adhesion. A number of genes involved in differentiation (12%) and proliferation (5.5%) were also up-regulated (enrichment scores: 1.9 and 1.4, respectively), as were genes associated with ion binding (13%; 1.2 enrichment) and membrane proteins (13%; 1.1 enrichment). Interestingly, a number of genes involved in apoptosis were also up-regulated (6.8%, 1.1 enrichment) (Figure 3.3A). As a smaller number of genes were down-regulated with Dex treatment, only 4 gene ontologies were associated with the gene list produced. Again, extracellular signalling was the most important ontology after Dex treatment, with 24% of down-regulated genes having some extracellular signalling association (enrichment score: 1.3) (Figure 3.3B; Table 3.2B). Interestingly, 24% of down-regulated genes had some known enzyme actions (enrichment score = 1.1), and genes associated with cell metabolism were also important (34%, enrichment score: 0.7). A number of genes involved in the development process were also down-regulated (17%), although this ontology was the least important (enrichment score: 0.25).

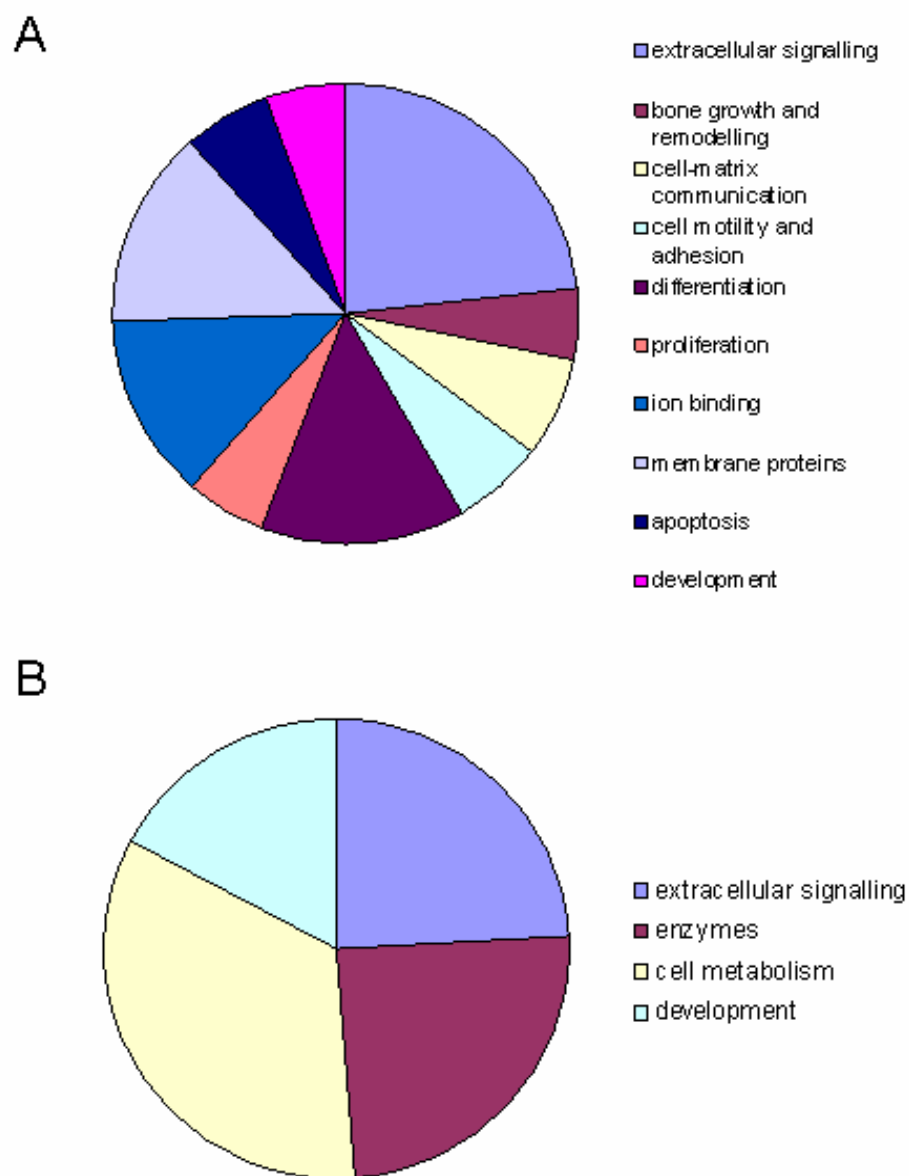


Figure 3.3 Functional Annotation of up-regulated (A) and down-regulated (B) genes in ATDC5 cells following Dex treatment. In both groups, extracellular signalling seems to be the most important gene ontology following Dex treatment.

Table 3.3A Functional Annotation clustering and enrichment scores for the gene ontology of genes significantly up-regulated with Dex treatment

Gene Ontology	Enrichment	Affymetrix ID	Gene Name
Extracellular signalling	5.1	1443745_s_at	dentin matrix protein 1
		1450678_at	integrin beta 2
		1435254_at	plexin b1
		1451939_a_at	sushi-repeat-containing protein
		1423274_at	dead/h (asp-glu-ala-asp/his) box polypeptide 26
		1427747_a_at	lipocalin 2
		1448321_at	sparc related modular calcium binding 1
		1422620_s_at	hydrogen peroxide inducible protein 53
		1417936_at	chemokine (c-c motif) ligand 9
		1455768_at	niemann pick type c2
		1424051_at	procollagen, type iv, alpha 2
		1430388_a_at	sulfatase 2
		1418269_at	lysyl oxidase-like 3
		1448881_at	haptoglobin
		1455158_at	integrin alpha 3
		1450826_a_at	serum amyloid a 3
		1425894_at	mas-related gpr, member f
		1427038_at	preproenkephalin 1
		1449254_at	osteopontin
		1456312_x_at	gelsolin
		1426195_a_at	cystatin c
		1454849_x_at	clusterin
		1438953_at	c-fos induced growth factor
		1448489_at	platelet-activating factor acetylhydrolase 2
		1452296_at	slit homolog 3 (drosophila)
		1416953_at	connective tissue growth factor
		1426947_x_at	procollagen, type vi, alpha 2
		1435943_at	dipeptidase 1 (renal)
		1418187_at	receptor calcitonin activity modifying protein 2
		1452141_a_at	selenoprotein p, plasma, 1
		1441926_x_at	transmembrane inner ear
		Bone formation	2.4
1450678_at	integrin beta 2		
1448321_at	sparc related modular calcium binding 1		
1449254_at	osteopontin		
1416953_at	connective tissue growth factor		
1424051_at	procollagen, type iv, alpha 2		
1440235_at	integrin, alpha 10		
1426947_x_at	procollagen, type vi, alpha 2		
Cell/ECMcommunication	2.4	1428471_at	sorbin and sh3 domain containing 1
		1438953_at	c-fos induced growth factor
		1455158_at	integrin alpha 3
		1443745_s_at	dentin matrix protein 1
		1449254_at	osteopontin
		1452296_at	slit homolog 3 (drosophila)
		1416953_at	connective tissue growth factor
		1452141_a_at	selenoprotein p, plasma, 1
1438953_at	c-fos induced growth factor		
1441926_x_at	transmembrane inner ear		

Table 3.3A continued

Gene Ontology	Enrichment	Affymetrix ID	Gene Name
Cell motility and adhesion	2.1	1450678_at	integrin beta 2
		1452296_at	slit homolog 3 (drosophila)
		1449254_at	secreted phosphoprotein 1
		1416953_at	connective tissue growth factor
		1424051_at	procollagen, type iv, alpha 2
Proliferation	1.4	1440235_at	integrin, alpha 10
		1426947_x_at	procollagen, type vi, alpha 2
		1451596_a_at	sphingosine kinase 1
		1450678_at	integrin beta 2
		1435254_at	plexin b1
		1422620_s_at	hydrogen peroxide inducible protein 53
		1449254_at	secreted phosphoprotein 1
		1419874_x_at,	zinc finger and btb domain containing 16
		1438953_at	c-fos induced growth factor
		1449731_s_at	nuclear factor of kappa light chain gene enhancer in b-cells inhibitor, alpha
Differentiation	1.9	1460011_at	cytochrome p450, family 26, subfamily b, polypeptide 1
		1443745_s_at	dentin matrix protein 1
		1450678_at	integrin beta 2
		1435254_at	plexin b1
		1449254_at	secreted phosphoprotein 1
		1419874_x_at,	zinc finger and btb domain containing 16
		1415874_at	sprouty homolog 1 (drosophila)
		1438953_at	c-fos induced growth factor
		1449731_s_at	nuclear factor of kappa light chain gene enhancer in b-cells inhibitor, alpha
		1451596_a_at	sphingosine kinase 1
		1416825_at	syntrophin, acidic 1
		1452296_at	slit homolog 3 (drosophila)
		1416953_at	connective tissue growth factor
		1417872_at	four and a half lim domains 1
		1454675_at	thyroid hormone receptor alpha
		1452141_a_at	selenoprotein p, plasma, 1
		1455158_at	integrin alpha 3
Ion binding	1.2	1441926_x_at	transmembrane inner ear
		1460011_at	cytochrome p450, family 26, subfamily b, polypeptide 1
		1416383_a_at	pyruvate carboxylase
		1448842_at	cysteine dioxygenase 1, cytosolic
		1419874_x_at,	zinc finger and btb domain containing 16
		1456312_x_at	gelsolin
		1423274_at	dead/h (asp-glu-ala-asp/his) box polypeptide 26
		1424671_at	pleckstrin homology domain containing, family f (with fyve domain) member 1
		1451596_a_at	sphingosine kinase 1
		1448321_at	sparc related modular calcium binding 1
		1452296_at	slit homolog 3 (drosophila)
1416825_at	syntrophin, acidic 1		
1428164_at	nudix (nucleoside diphosphate linked moiety x)-type motif 9		

Table 3.3A continued

Gene Ontology	Enrichment	Affymetrix ID	Gene Name
Ion binding (cont.)	1.2	1417507_at	cytochrome b-561
		1435943_at	dipeptidase 1 (renal)
		1418269_at	lysyl oxidase-like 3
		1417872_at	four and a half lim domains 1
		1422557_s_at	metallothionein 1
		1428942_at	metallothionein 2
		1450678_at	integrin beta 2
Membrane proteins	1.1	1425894_at	mas-related gpr, member f
		1435254_at	plexin b1
		1449254_at	secreted phosphoprotein 1
		1419874_x_at	zinc finger and btb domain containing 16
		1456312_x_at	gelsolin
		1455078_at	slingshot homolog 2 (drosophila)
		1437820_at	forkhead-like 18 (drosophila)
		1440235_at	integrin, alpha 10
		1448489_at	platelet-activating factor acetylhydrolase 2
		1422620_s_at	hydrogen peroxide inducible protein 53
		1416953_at	connective tissue growth factor
		1424051_at	procollagen, type iv, alpha 2
		1426947_x_at	procollagen, type vi, alpha 2
		1418187_at	receptor (calcitonin) activity modifying protein 2
		1418269_at	lysyl oxidase-like 3
		1428471_at	sorbin and sh3 domain containing 1
		1454675_at	thyroid hormone receptor alpha
		1418091_at	transcription factor CP2-like 1
		1455158_at	integrin alpha 3
		1451596_a_at	sphingosine kinase 1
Apoptosis	1.1	1435254_at	plexin b1
		1422620_s_at	hydrogen peroxide inducible protein 53
		1449254_at	osteopontin
		1419874_x_at	zinc finger and btb domain containing 16
		1454849_x_at	clusterin
		1420772_a_at	tsc22 domain family 3
		1449731_s_at	nuclear factor of kappa light chain gene enhancer in b-cells inhibitor, alpha
		1424671_at	pleckstrin homology domain containing, family f (with fyve domain) member 1
		1416041_at	serum/glucocorticoid regulated kinase

Table 3.3B Functional Annotation clustering and enrichment scores for the gene ontology of genes significantly down-regulated with Dex treatment

Gene Ontology	Enrichment	Affymetrix ID	Gene Name
Extracellular signalling	1.3	1423607_at	lumican
		1437401_at	insulin-like growth factor 1
		1431056_a_at	lipoprotein lipase
		1423294_at	mesoderm specific transcript
		1449486_at	carboxylesterase 1
		1448201_at	secreted frizzled-related sequence protein 2
		1425357_a_at	gremlin 1
Enzyme action	1.1	1436993_x_at	profilin 2
		1425806_a_at	suppressor of RNA polymerase B
		1431056_a_at	lipoprotein lipase
		1423294_at	mesoderm specific transcript
		1449486_at	carboxylesterase 1
		1449855_s_at	ubiquitin thiolesterase
Cell metabolism	0.7	1454888_at	prefoldin 4
		1431056_a_at	lipoprotein lipase
		1425806_a_at	suppressor of RNA polymerase B
		1451191_at	cellular retinoic acid binding protein ii
		1423294_at	mesoderm specific transcript
		1450756_s_at	cullin 3
		1417394_at	kruppel-like factor 4 (gut)
		1418174_at	d site albumin promoter binding protein
Development	0.25	1449855_s_at	ubiquitin thiolesterase
		1437401_at	insulin-like growth factor 1
		1450243_a_at	down syndrome critical region gene 1-like 1
		1451191_at	cellular retinoic acid binding protein ii
		1448201_at	secreted frizzled-related sequence protein 2
		1425357_a_at	gremlin 1

3.5.3 Validation of Microarray Expression Data

From a list of 96 genes, a short-list of 8 genes were chosen for further analysis. The choice of candidates from the short-list that were initially prioritised for future study were based on reviews of function, likely relationship to GC action and association with chondrocytes and bone growth (Figure 3.4). Lipocalin 2 was chosen for the exceptionally large fold change (14-fold) compared to other genes, and for the fact that it has previously been shown to be expressed in chondrocytes (Ulivi *et al.*, 2006). Serum GC-regulated kinase (SGCK) was chosen as it is known to be an important signalling molecule in growth factor and insulin dependent signalling pathways, and has previously been shown to be up-regulated in osteoblasts in response to Dex

(Leclerc *et al.*, 2002). Connective tissue growth factor (CTGF), Lumican, Integrin α 10, and dentin matrix protein 1 (DMP-1) were chosen for their links with growth plate chondrogenesis, and IGF-I and secreted frizzled-related protein (SFRP) are both important signalling molecules at the level of the growth plate and in GC actions.

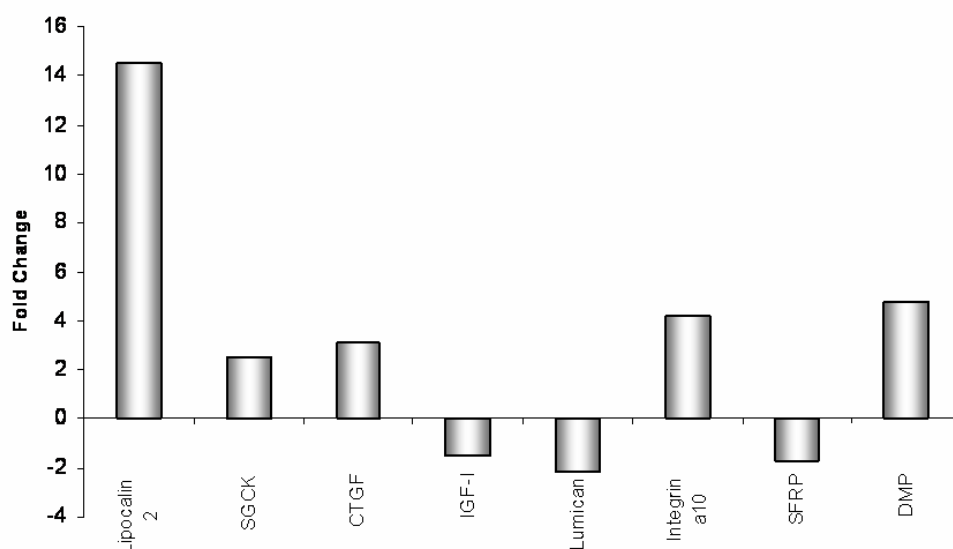


Figure 3.4 GC-responsive chondrocyte genes as determined by Affymetrix microarray analysis. A short list of 8 genes were chosen for further analysis based on reviews of function, likely relationship to GC action and association with chondrocytes and bone growth.

To validate microarray data using independent methods, the genes were analysed for changes in expression with qPCR. Gene expression patterns for Lipocalin 2, SGCK, CTGF, IGF-I, Integrin α 10, and DMP-1 all mirrored expression patterns observed in the microarray, with significant fold changes of 42-fold, 2.5-fold, 4.2-fold, -6.5-fold, 4.2-fold and 4.8-fold, respectively ($p < 0.01$) (Figure 3.5). Interestingly, the fold changes obtained for qPCR analysis were notably higher than those obtained in the microarray. The expression of Lumican and SFRP were not changed when analysed by qPCR.

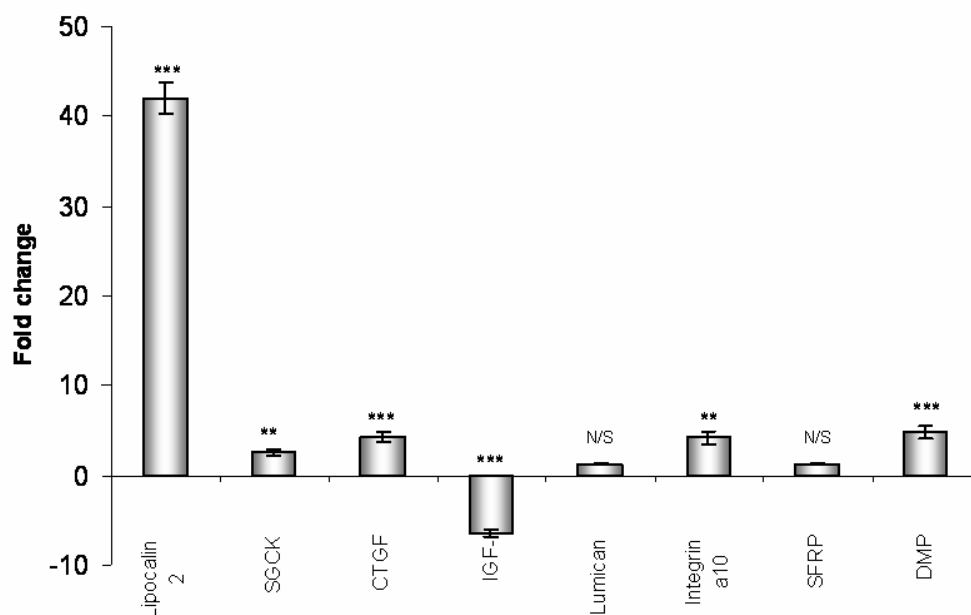


Figure 3.5 Validation of microarray results with qPCR analysis. Gene expression patterns for lipocalin 2, SGCK, CTGF, IGF-I, Integrin α 10, and DMP-1 all mirrored expression patterns observed in the microarray, although the fold-changes in expression were notably larger with qPCR analysis. All data are expressed as mean \pm SEM (n=3 replicates each run in triplicate; ***p<0.001 vs. control samples; **p<0.01 vs. control samples; ^{N/S}not significant).

3.6 Discussion

Glucocorticoids are the most effective anti-inflammatory agents known. However, in children, their long-term use leads to growth retardation through a combination of systemic effects through the GH/IGF axis, and direct effects on the growth plate (Baron *et al.*, 1992; Ahmed and Mushtaq, 2002). The exact mechanisms by which GCs exert their effects at the growth plate are still unclear, but may be related to a reduction in chondrocyte proliferation combined with an increase in apoptosis, in addition to alterations in IGF-I signalling mechanisms (Mushtaq *et al.*, 2004, Chrysis *et al.*, 2005). Murine *in vivo* studies have demonstrated that after one week of Dex treatment, the total width of the growth plate in 3-week-old mice is significantly decreased due to a decrease in the width of the proliferative zone (Smink *et al.*, 2003; Owen *et al.*, unpublished). In addition the murine chondrogenic ATDC5 cell line has

previously been used to show that, *in vitro*, Dex causes a significant reduction chondrocyte proliferation and an increase in ALP activity, a known marker of terminally differentiating chondrocytes (Mushtaq *et al.*, 2002; Owen *et al.*, 2007).

This study provides an extensive profile of the alterations in gene expression that occur in GC-treated chondrocytes. While some of the disclosed genes have previously been described as GC-responsive in chondrocytes (IGF-I, SGCK, CTGF), the response of many others, such as lipocalin 2, SFRP2 and DMP-1 are described here for the first time.

Microarrays are a powerful method for the global analysis of gene or protein content and expression, however, due to the fact that the technology is so sensitive to change, and the fact that such large data sets are produced, it is critical that all steps of the process are accurately and consistently performed, to maximise the reliability and significance of results. In addition, the experimental design must take into account the biological question under study, and should include statistical input to permit the required level of statistical significance to be obtained. Consequently, experiments should be well controlled and replicated. In this study, two control replicates and two Dex replicates were used to identify differentially expressed genes in Dex-treated ATDC5 cells. Although increasing the replicate number or pooling samples may have improved the statistical power of the results obtained, changes in gene expression were confirmed by qPCR, suggesting that the results did not contain a large number of false positives. However, there is a possibility that some interesting genes were overlooked due to the occurrence of false negatives.

In any gene expression analysis, technological problems and biological variation can make it difficult to distinguish signal from noise (Vingron *et al.*, 2001). A major caveat of microarray analysis is the generation of large data sets, and the quantification of expression levels observed for any given chip (Barash *et al.*, 2004). There are large variations in PM and MM intensities for a probe set (2.8.1), and the MM is an extremely complex measure of unspecific hybridisation. In addition, GeneChips can display expression level independent effects at the probe level. Therefore, it is important that expression levels are scaled before comparing expression data between GeneChips and between probes on the same chip. Selecting the correct normalisation algorithm is critical in obtaining robust data, however, unfortunately, a consensus has yet to be reached regarding the selection of optimal normalisation algorithms, and there are many different normalisation algorithms available. The RMA algorithm (2.8.2) is commonly used to normalise Affymetrix data, and uses the PM value only, ignoring the expression value obtained for the MM probe. RMA normalisation is an effective method for normalising microarray data, as, by ignoring the MM value, less 'noise' is produced, therefore reducing the chance of false positives. In this study, data was normalised with the RMA algorithm using the microarray data analysis programme GeneSpring, and was then filtered for significant changes in expression of 1.5-fold or more. Higher stringency normalisation and filtering reduces the frequency of false positives, but can also limit the amount of meaningful data obtained. It is therefore important to establish a balance between excluding biologically meaningful data by using restrictive analysis criteria and using permissive parameters, which could also reduce the biological value of the data by increasing the number of artefacts. Consequently, although a two-sample t-test was carried out to determine significant changes in gene expression

compared to baseline values in this study, both the cross-gene error model and multiple testing corrections were considered too stringent and were not used.

From this analysis, a list of 76 up-regulated and 19 down-regulated genes were then annotated and clustered according to function. Traditional microarray analysis methods are useful for the identification of probe sets exhibiting transcriptional responses to Dex-treatment, but are limited in certain capacities. Alternate statistical methods such as student's t-tests produce transcript lists that, while effectively reducing the dimensionality or sample size of the data set, can increase the rate of false negatives. In addition, Gene Ontology annotations alone are not always sufficiently robust to detect differences in the representation of specific molecular categories. Accordingly, it can be difficult to grasp a clear concept of the central pathways and biological categories affected by Dex treatment. Functional annotation clustering is an algorithm that is designed to effectively evaluate the effect of a specific experimental condition on known biological pathways and functional categories. These analyses show whether a given treatment (e.g. Dex stimulation) results in enrichment of genes sets involved in the regulation of a specific phenotype. Enriched gene sets were identified for both up- and down-regulated transcripts.

The highest correlation for both the up- and down-regulated Dex phenotype was extracellular signalling, which contained 32 and 7 genes, respectively. Interestingly, a recent paper studying the effect of irradiation on the expression of genes within the growth plate has also found that extracellular signalling genes are up-regulated in both the proliferative and hypertrophic zones following irradiation (Zhang *et al.*, 2007). The authors hypothesise that this is due to the premature terminal differentiation of

proliferating chondrocytes following irradiation, and results in increased matrix production. The theory that GCs cause premature differentiation of chondrocytes has previously been postulated (Mushtaq *et al.*, 2002), and would explain the reduction in proliferation and increase in alkaline phosphatase activity commonly observed in GC-treated chondrocytes (Mushtaq *et al.*, 2002; Owen *et al.*, 2007). The finding that a large number of up-regulated genes were also associated with differentiation also supports this hypothesis. Not surprisingly, genes involved in bone formation and remodelling were important in the response to Dex-treatment, and a large number of genes involved in apoptosis were also up-regulated. A number of previous studies have shown that GCs increase chondrocyte apoptosis *in vitro* and *in vivo*, although this response seems to vary between cell types. In the HCS2-8 cell line, Dex increased apoptosis partly by suppression of the Akt-(PI3K) signalling pathway (Chrysis *et al.*, 2004), and in ATDC5 cells in the terminally differentiated phenotype, Dex increased apoptosis, although no increases were observed during the proliferative phase (Mushtaq *et al.*, 2002). In pre-pubertal mice treated daily with Dex for 7 days, TUNEL staining displayed a significant increase in apoptotic hypertrophic chondrocytes (Smink *et al.*, 2003). Although functional annotation clustering is a useful method for extracting meaningful data from microarrays, it does have some limitations. The enrichment score obtained in functional annotation clustering is a measure of the importance of a particular annotation term within a gene group, however, due to the complexity of biological systems, this score is only a guideline and should be used in combination with the expected biology for the samples in question.

Following data analysis, a short-list of 8 genes were chosen for further study based on links with bone tissue or GC action. The Wnt-antagonist SFRP-2, the proteoglycan Lumican, and IGF-I were all down-regulated by Dex, although only IGF-I was confirmed as being down-regulated after qPCR analysis. Variations in results between microarray and qPCR analysis have been widely reported and is caused by a number of factors including the microarray normalisation technique used, measurement of spot intensity in the microarray, and tissue preparation between experiments (Morey *et al.*, 2006). The IGF-I signalling system is one of the major regulators of endochondral ossification, and previous studies have shown that GCs reduce IGF-I mRNA in growth plate chondrocytes (Luo *et al.*, 1989), and inhibit basal and IGF-I induced DNA synthesis (Itagane *et al.*, 1991). It has been suggested that some skeletal effects of GCs may be mediated via decreased IGF-I expression, with reduced expression of IGF-I, IGF-I receptor and growth hormone receptor in GC-treated chondrocytes (Jux *et al.*, 1998, Klaus *et al.*, 2000). Interestingly however, work at the Roslin Institute previously shown that IGF-I ameliorates Dex-induced growth retardation in murine metatarsal cultures (Mushtaq *et al.*, 2004), suggesting that IGF-I may in fact have a protective role against GC in the growth plate.

Up-regulated genes included CTGF, integrin $\alpha 10$, lipocalin 2, SGCK, and DMP1. CTGF is a secreted, extracellular matrix-associated protein that regulates diverse cellular functions in different cell types, and is a critical growth factor for chondrocyte proliferation and differentiation. Endogenous overexpression of CTGF in human chondrocytic HCS-2/8 cells, achieved by using recombinant adenoviruses that generated CTGF mRNA, resulted in enhanced cellular proliferation and expression of aggrecan and type X collagen (Nakanishi *et al.*, 2000). It also increased the

proteoglycan synthesis and gene expressions of aggrecan and collagen type II, in maturing HCS-2/8 cells. Furthermore, CTGF overexpression effectively stimulated the gene expression of collagen type X, a marker of chondrocyte hypertrophy, in RGC cells in over-confluent culture where the cells were in the prehypertrophic stage (Nakanishi *et al.*, 2000). Moreover, the CTGF overexpressing HCS-2/8 cells stimulated ALP activity, a marker of calcification, and indeed induced matrix calcification of HCS-2/8 cells in culture (Nishida *et al.*, 2002). In another study, during the healing of experimental bone fracture, CTGF was expressed in periosteal cells and hypertrophic chondrocytes (Kanaan *et al.*, 2006). These results indicate that CTGF directly promotes the proliferation and differentiation of growth cartilage cells toward endochondral ossification. Interestingly, in this study, CTGF expression was increased with Dex, which is a known inhibitor of chondrocyte proliferation both *in vitro* and *in vivo*, a finding which contradicts the hypothesis that CTGF is a promoter of chondrocyte proliferation. However, CTGF has previously been shown to be upregulated by Dex in both the chondrocytic HCS-2.8 cell line (Kubota *et al.*, 2003), and in primary chondrocytes (James *et al.*, 2007), and interestingly, a recent study has shown that CTGF is upregulated in growth plate chondrocytes undergoing recovery following irradiation (Wang *et al.*, 2007). This finding, along with the fact that both Dex and irradiation cause an increase in the expression of other ECM components, suggests that both treatments are working in a similar way to cause growth retardation at the level of the growth plate.

Chondrocyte function crucially depends on the interaction of chondrocytes with the surrounding ECM. These interactions are primarily mediated by members of the integrin family of cell surface receptors. The up-regulation of integrin $\alpha 10$ suggests

that these receptors in particular are important in the chondrocyte response to GCs. Expression of integrin alpha10 is initiated at the beginning of chondrogenesis and continues throughout cartilage development in adult cartilage (Wenke *et al.*, 2006). It has recently been shown that Integrin α 10 null mice display growth retardation due to increased apoptosis of growth plate chondrocytes (Bengtsson *et al.*, 2005). The finding that Dex induces Integrin α 10 expression has previously been unreported, and provides a novel target for investigation in GC-induced effects.

Closer examination of the genes contributing to the enrichment scores for the extracellular signalling gene set revealed that DMP1 was the top ranking gene. DMP1 belongs to the SIBLING family of matrix molecules and has been linked to chondrocyte differentiation. A study analysing the skeletal phenotype of DMP(-/-) mice found that their long bones were shorter and wider, with highly expanded growth plates (Ye *et al.*, 2005). This phenotype appeared to be due to increased cell proliferation in the proliferating zone and reduced apoptosis in the hypertrophic zone. Interestingly, a recent paper documenting an Affymetrix microarray of GC-treated primary chondrocytes also found that DMP-1 was the top ranking gene when analysing gene enrichment for extracellular signalling (James *et al.*, 2007), suggesting that DMP1 plays an important role in GC-induced growth retardation.

SGCK is a serine kinase that has a catalytic domain homologous to that of Akt, and can be activated by PI3 Kinase, making it an important signalling molecule in growth factor and insulin dependent signalling pathways. SGCK has been shown to play an important role in the maintenance of cells within the cell cycle, by phosphorylating and consequently inhibiting the activation of Foxo3a, a member of the Forkhead

family of transcription factors (Brunet *et al.*, 2001). Under normal circumstances, Foxo3a targets the activation of the CDKI p27, causing cells to exit the cell cycle and progress towards terminal differentiation and apoptosis. By inhibiting Foxo3a activity, SGCK causes the cells to continue proliferating, indicating that SGCK is a regulator of cell survival (Tessier *et al.*, 2006). The role of SGCK as a stress response protein has been widely reported. A variety of environmental stresses such as UV irradiation, heat shock, oxidative stress, and hyper-osmotic stress induce SGCK protein levels through the p38/MAPK pathway and SGCK phosphorylation through the PI3K pathway in non-tumourigenic mammary epithelial cells (Leong *et al.*, 2003). SGCK has previously been shown to be upregulated in osteoblasts in response to Dex (Leclerc *et al.*, 2004), however, there have been no previous reports of SGCK expression within the growth plate. The fact that SGCK expression is increased in response to environmental and toxicological stresses, and inactivates proteins involved in the exit from the cell cycle, suggests that SGCK may be acting as a survival factor in response to Dex in this study.

From a list of 79 genes up-regulated following Dex treatment, lipocalin 2 expression was increased by the greatest amount in this study (14-fold microarray response and 40-fold qPCR response). Lipocalin 2, also known as Neutrophil-associated gelatinase lipocalin (NGAL), was originally identified as a 25kDa protein which binds to small lipophilic substances such as bacteria-derived lipopolysaccharide (LPS), and is thought to act as a modulator of inflammation. It has been shown to be expressed in the liver, spleen, lung, muscle, heart and tibia of embryonic mice (Garay-Rojas *et al.*, 1996; Ulivi *et al.*, 2006). Within the tibia of embryonic rats, the rat homologue of lipocalin 2, neu-related lipocalin (NRL) is localised to the prehypertrophic

chondrocytes (Zerega *et al.*, 2000). Differences in lipocalin 2 expression between adult and foetal tissue have previously been described (Garay-Rojas *et al.*, 1996) and, as lipocalin 2 is known to induce the differentiation of mesenchymal cells to epithelial cells (Yang *et al.*, 2002), a role for lipocalin 2 in the control of cellular differentiation has been proposed (Ulivi *et al.*, 2006).

3.7 Conclusions

As previously mentioned, it has been hypothesised that Dex may cause growth retardation by causing premature differentiation of proliferative chondrocytes within the growth plate. This hypothesis is supported by the finding that Dex causes an increase in the expression of ECM genes, such as CTGF and DMP1, and an increase in ALP activity (Mushtaq *et al.*, 2002; Owen *et al.*, 2007). The fact that lipocalin 2 is known to induce differentiation and reduce proliferation (Yang *et al.*, 2002; Devireddy *et al.*, 2001) suggests that increased lipocalin 2 expression is a possible mechanism for GC-induced growth retardation. The expression of lipocalin 2 in response to Dex, and the effect of lipocalin 2 on chondrocyte dynamics requires further study.

Chapter 4

Functional Involvement of Lipocalin 2 in Glucocorticoid-Induced Growth Retardation

Chapter Contents

- 4.1 Introduction
 - 4.2 Hypothesis
 - 4.3 Aims
 - 4.4 Materials and Methods
 - 4.4.1 Cell Culture
 - 4.4.2 Quantitative PCR
 - 4.4.3 p38 MAP Kinase Assay
 - 4.4.4 Western Blotting
 - 4.4.5 Histological Analysis of Lipocalin 2 Expression in the Growth Plate
 - 4.4.6 Isolation of Primary Murine Chondrocytes
 - 4.4.7 Production of a Lipocalin 2 Expression Construct
 - 4.4.8 Generation of ATDC5 Stable Transfections
 - 4.4.9 Lipocalin 2 Overexpression
 - 4.4.10 Statistical Analysis
 - 4.5 Results
 - 4.5.1 Characterisation of Dex-induced Lipocalin 2 Expression in Chondrocytes
 - 4.5.2 Immunolocalisation of Lipocalin 2 within the murine growth plate
 - 4.5.3 Mechanism of Dex-induced Lipocalin 2 Expression
 - 4.5.4 Involvement of the NF κ B and p38 Pathways in Lipocalin 2
 - 4.5.5 Functional Effects of Lipocalin 2 on ATDC5 Proliferation and Differentiation
 - 4.5.6 The Combined effects of Lipocalin 2 and Dex on ATDC5 Cells
 - 4.6 Discussion
 - 4.7 Conclusions
-
-

4.1 Introduction

The mechanisms by which GCs exert control over chondrocyte dynamics are presently unclear. It is likely that GCs affect a wide range of complex regulatory and signalling networks involving cell-matrix and intercellular interactions to mediate chondrocyte proliferation and differentiation. In Chapter 3, Affymetrix Microarray gene expression profiling of ATDC5 cells was used to identify novel glucocorticoid-responsive chondrocyte genes in an attempt to further our understanding of the processes involved in GC-induced growth retardation. It was confirmed that CTGF, Integrin α 10, DMP-1, SGCK, and lipocalin 2 were upregulated by Dex in ATDC5 cells. One gene in particular, lipocalin 2, stood out due to the fact that it was upregulated by 40-fold in the presence of Dex, and was therefore selected for further analysis.

Lipocalin 2 was originally identified as an acute phase protein released in the immune response, and is a member of the lipocalin family of binding proteins. Members of this family are typically small secreted proteins which are characterised by a range of different molecular-recognition properties: their ability to bind small, principally hydrophobic molecules (such as retinol); their binding to specific cell-surface receptors and their formation of macromolecular complexes. The lipocalins are a large and ever-expanding group of proteins exhibiting great structural and functional diversity, both within and between species. Although they have, in the past, been classified primarily as transport proteins, it is now clear that members of the lipocalin family fulfil a variety of different functions (Table 4.1) These include roles in retinol transport, olfaction, pheromone transport, immune responses and the enzymatic

synthesis of prostaglandins. In addition the lipocalins have also been implicated in the regulation of the immune response and the mediation of cell homeostasis.

Table 4.1 Lipocalin protein family members and known functions

Name	Abbreviation	Common Names and Acronyms	Known Functions	References
Extracellular fatty acid-binding lipocalin	Ex-FABP	Ch21, P20K, quiescence-specific protein	Mediator of cell cycle regulation	Bedard <i>et al.</i> , 1989; Flower 1994
Retinol-binding protein	RBP	serum retinol binding protein	Sole retinol transporter in plasma from liver to peripheral tissues	Blomhoff <i>et al.</i> , 1990
β -Lactoglobulin	Blg	BLG	Major component of whey from milk, may be a carrier of insoluble molecules from mother to child	Said <i>et al.</i> , 1989; Hambling <i>et al.</i> , 1992
Glycodelin	Glc	pregnancy protein 14, human pregnancy-associated endometrial protein, α 2-globulin, α -uterine protein	Major component of rat urine; pheromone transporter	Roy <i>et al.</i> , 1966; Roy <i>et al.</i> , 1983
Apolipoprotein D	apoD	apocrine secretion odour-binding protein (ASOB2)	Cholesterol metabolism; mediator of proliferation and differentiation	Francone <i>et al.</i> , 1989; Lopez-Boado <i>et al.</i> , 1994
Epididymal retinoic acid-binding protein	E-RABP	B/C protein, epididymal secretory protein (ESP1), lipocalin 5	Sperm maturation, epididymal function	Ong <i>et al.</i> , 2000; Fouchecourt <i>et al.</i> , 2003
Odourant binding protein	OBP	frog Bowman's gland protein	Odour molecule transporter	Lee <i>et al.</i> , 1987; Cavaggianni <i>et al.</i> , 1987; Snyder <i>et al.</i> , 1988
Tear prealbumin	TP	protein migrating faster than albumin, specific tearalbumin, tear lipocalin, lipocalin 1, LCN1	Scavenger of hydrophobic harmful molecules and bacterial growth inhibitor; present in tears	Fluckinger <i>et al.</i> , 2004
Probasin	PB	pM-40	Cell cycle regulation	Matuo <i>et al.</i> , 1984; Spence <i>et al.</i> , 1989
Prostaglandin D synthase	PGDS	β -trace	Synthesises prostaglandin D2 (major neuromodulator) in the brain	Urade <i>et al.</i> , 1989; Nagata <i>et al.</i> , 1991
Neutrophil gelatinase-associated lipocalin	NGAL	SIP24, 24p3, uterocalin, Neu-related lipocalin, lipocalin 2	Acute phase protein released in the immune response and after partuition	Hraba-Renevey <i>et al.</i>, 1989; Meheus <i>et al.</i>, 1993; Lui <i>et al.</i>, 1995

Despite common characteristics and common functions, the lipocalin family has been defined largely on the basis of structure and sequence. In contrast with their low conservation at the sequence level, analysis of available lipocalin crystal structures shows that the overall folding pattern common to the lipocalins is highly conserved (Figure 4.1). The lipocalin fold is a highly symmetrical all- β protein dominated by a single eight-stranded antiparallel β -sheet closed back on itself to form a continuously hydrogen-bonded β -barrel, which, in cross-section, has a flattened or elliptical shape and encloses an internal ligand-binding site (Goetz *et al.*, 2000). The eight β -strands of the barrel are linked by a succession of loops. These seven loops, are all typical of short β -hairpins, except loop L1 which is a large Ω loop which forms a lid folded back to partially close the internal ligand-binding site found inside the closed barrel (Figure 4.2).



Figure 4.1 Crystal structure of the human homologue of lipocalin 2, neutrophil gelatinase associated lipocalin (NGAL). The crystal structure of NGAL displays a single eight-stranded continuously hydrogen-bonded antiparallel β -barrel, which encloses an internal ligand-binding site. β -strands are shown as smoothly curving arrows, and α -helices are shown as spiral ribbons. Fatty acid ligand molecules are shown using a coloured all-atom representation. *From Goetz et al., 2000*

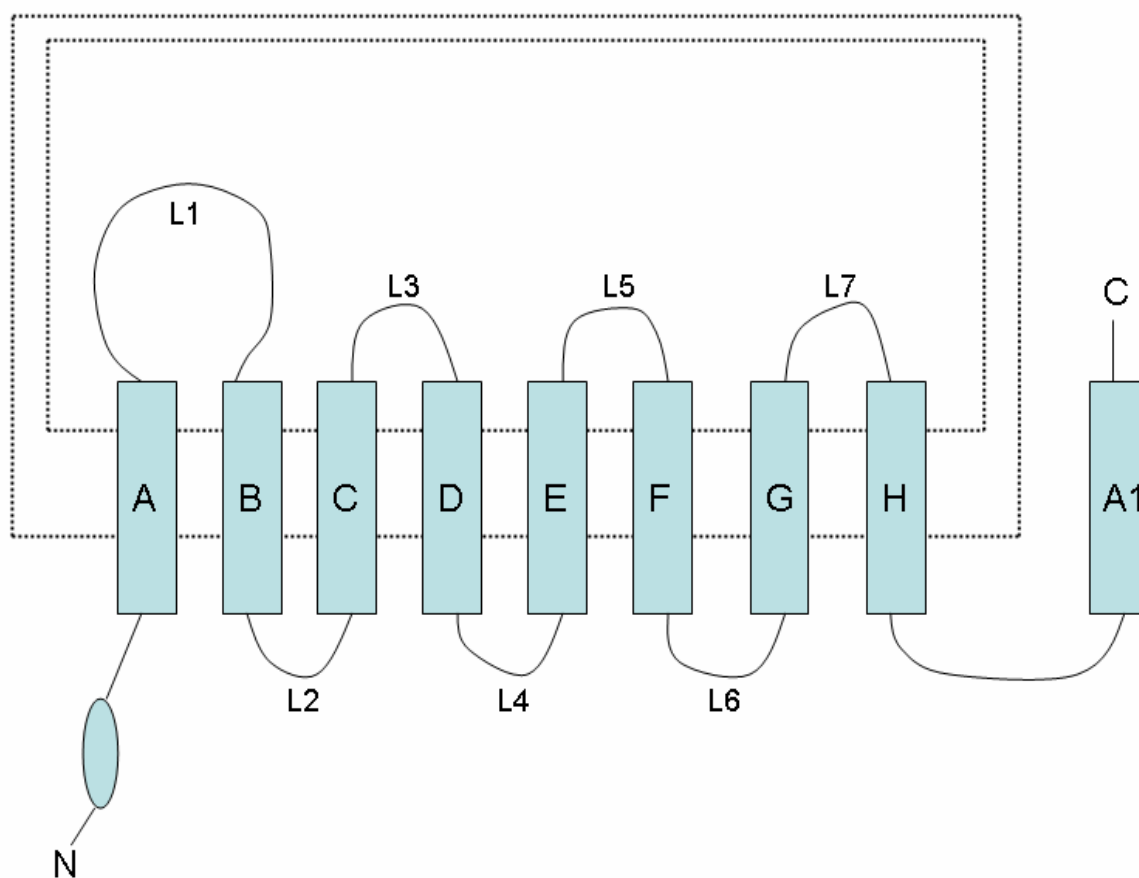


Figure 4.2 Characteristic features of the lipocalin fold. An unwound view of the lipocalin fold orthogonal to the axis of the barrel. The eight β -strands of the antiparallel β -sheet are shown as arrows and labelled A-H. The N-terminal helix (N) and C-terminal α -helix (labelled A1) are also marked. The hydrogen-bonded connection of two strands is indicated by a pair of dotted lines between them. Connecting loops are shown as solid lines and labelled L1-L7. The two ends of the β -barrel are topologically distinct. One end has four β -hairpins (L1, L3, L5 and L7) and is called the ‘open end’ as the internal ligand-binding site is located here. The other has three β -hairpin loops (L2, L4 and L6). At this section, the N-terminal polypeptide chain crosses the end of the barrel to close it, and is therefore termed the closed end of the molecule. *Adapted from Flower et al., 1996.*

Lipocalin 2 is a secreted glycoprotein that was identified and characterised in quiescent Balb/c3T3 cells in the late 1980's. Originally known as superinducible protein 24 (SIP24), its expression can be induced by a number of factors including serum, FGF, prostaglandin F2a, phorbol ester, and Dex. It is also a major secretory protein of cultured mouse macrophages which have been stimulated with lipopolysaccharide (LPS) (Meheus *et al.*, 1993). Lipocalin 2 is the protein product of the murine gene named 24p3, whose cDNA was originally cloned from mouse kidney primary cell cultures (Hraba-Renevey *et al.*, 1989). The role of Lipocalin 2 in inflammation was further hypothesised when it was discovered that lipocalin 2 knock-out mice had increased susceptibility to infection (Berger *et al.*, 2006) and as lipocalin 2 is known to induce the differentiation of mesenchymal cells to epithelial cells (Yang *et al.*, 2002), a role for lipocalin in the control of cellular differentiation has also been proposed (Ulivi *et al.*, 2006).

The tissue expression of lipocalin 2 has been well documented, and it has been shown to be expressed in the liver, spleen, lung, muscle, heart and tibia of embryonic mice (Garay-Rojas *et al.*, 1996; Ulivi *et al.*, 2006). Within the tibia of embryonic rats, the rat homologue of lipocalin 2, neu-related lipocalin (NRL), is localised to the prehypertrophic chondrocytes (Zerega *et al.*, 2000), and in cultured MC615 chondrocytes, lipocalin 2 expression is detected in hypertrophic chondrocytes only (Ulivi *et al.*, 2006). Lipocalin 2 has previously been shown to be regulated by Dex in a number of cell types (Garay-Rojas *et al.*, 1996; Vizzardelli *et al.*, 2006), however, its stimulation in ATDC5 cells has not previously been reported, and may provide a novel mechanism for GC-induced growth retardation in chondrocytes.

4.2 Hypothesis

The hypothesis of this study was that the acute-phase binding protein lipocalin 2 could mediate the effects of Dex on growth plate chondrocytes, therefore providing a potential novel mechanism for GC-induced growth retardation.

4.3 Aims

- I. Characterise lipocalin 2 expression in ATDC5 cells and primary chondrocytes through timecourse and dose response experiments.
- II. Confirm increases in lipocalin 2 expression are GR dependent and do not involve the synthesis of other proteins.
- III. Investigate the involvement of the p38 and NF κ B signalling pathways in Dex-induced lipocalin 2 expression.
- IV. Analyse the effect of lipocalin 2 over-expression on chondrocyte dynamics through stable transfection of ATDC5 cells.

4.4 Materials and Methods

4.4.1 Cell Culture

The ATDC5 chondrocyte cell line was maintained and differentiated as previously described (Section 2.2.3) for 8 days, at which point Dex (final concentration 10^{-6} M) was added to the cells for the stated period. Control cells received vehicle only. Total RNA was extracted from chondrocytes as previously described (2.5.2). The protein synthesis blocker, cycloheximide (CHX; $8\mu\text{g/ml}$), and the GC-receptor antagonist RU486 (10^{-5} M) were added to ATDC5 cells to investigate the mechanisms involved in Dex-induced lipocalin 2 expression, and the involvement of the p38/NF κ B pathway was assessed using specific inhibitors of p38 (SB203580; $20\mu\text{M}$; Calbiochem, CA, UAS) and NF κ B (TLCK; $0.5 - 50\mu\text{M}$ (Sigma); SN50; $18\mu\text{M}$, Calbiochem). Recombinant lipocalin 2 was added to the cells at a range of concentrations ($5 - 20\mu\text{g/ml}$; R&D Systems, Abingdon, UK) to analyze the effect of lipocalin 2 on cell proliferation.

4.4.2 QPCR

QPCR was used to confirm changes in the expression of selected genes. ATDC5 cells at day 8 of culture were incubated with 10^{-6} M Dex for 1h to 7-days and RNA extracted as previously described (2.5.2). RNA samples or blanks (containing nuclease-free water in place of RNA) were reverse transcribed in $20\mu\text{l}$ reactions with 200ng random hexamers and 200U Superscript II reverse transcriptase using the Superscript preamplification protocol as previously described (2.5.4) (Invitrogen). qPCR was performed using the Stratagene Mx3000P real-time QPCR system as previously described (2.5.6) (Stratagene, California, USA). Primers were designed using the software programme Primer3 (Whitehead Institute for Biomedical Research),

and were made to span at least one intron to identify any amplification from contaminating genomic DNA by semi-quantitative PCR (See Appendix 5). cDNA (10ng) derived from each of 3 control and 3 Dex treated cultures at each time point was amplified in triplicate using the Platinum SYBR Green qPCR SuperMix (Invitrogen, Paisley, UK) under the following conditions: cDNA was denatured for 2 minutes at 95 °C, followed by 40 cycles consisting of 15 s at 95°C and 30 s at 60°C and 1 cycle consisting of 1 min at 95°C and 30 s at 60 °C. Each reaction contained 10µl cDNA, 25µl Platinum SYBR Green qPCR Super-Mix, 1µl ROX Reference Dye, and 250nM primer in a total volume of 50µl. A dilution series of both gene of interest and external control (GAPDH) were carried out and subjected to an identical PCR to allow estimation of PCR efficiency, and fold changes normalised for the expression of GAPDH, were calculated using the comparative method (Livak *et al.*, 2001).

4.4.3 p38 MAP Kinase Assay

The nonradioactive p38 MAPK assay (Cell Signalling Technology, Boston, USA) was used to determine the level of active p38 in SB203580 treated ATDC5 cells according to the manufacturer's instructions. Briefly, treated cells were lysed and p38 MAPK was immunoprecipitated from the lysate using beads coated with phospho-p38 MAPK (Thr-180/Tyr-182) monoclonal antibody overnight at 4°C with constant agitation. After washing in the lysis buffer and kinase buffer provided, the immunoprecipitated p38 MAPK was incubated for 30min at 30 °C in kinase buffer containing 200µM ATP and 2µg of GST-ATF-2 fusion protein as substrate. The reaction was terminated by adding 2x Laemmli buffer and heating the samples to 95°C for 5min. The samples were separated on a 4-12% SDS-PAGE gel and

immunoblotted for phosphorylated ATF-2 and total p38 MAPK (Cell Signalling Technology).

4.4.4 Western Blotting

Cells were lysed in RIPA buffer as previously described and amount of protein quantified using the Bradford assay as previously described (2.7.1). Protein lysates (15µg) were loaded onto 10% Bis-Tris Gels, fractionated and electroblotted onto nitrocellulose membranes (2.7.2). After blocking with 5% non-fat milk powder and 0.1% Tween, the membranes were incubated overnight with Anti-Lipocalin 2 primary antibody (1:500; R&D Systems) at 4°C, washed and incubated at room temperature for 1h with rabbit anti-goat peroxidase labelled secondary antibody (1:2000; DAKO, Cambridge, UK). Beta-actin expression was also measured as a loading control (anti beta-actin clone AC15; Sigma A5441; 1:5000) on membranes stripped with Stripping Reagent (Pierce, IL, USA) for 1.5h at RT. The immune complexes were then visualised by enhanced chemiluminescence (ECL) (GE Healthcare, Buckinghamshire, UK) (2.7.3).

4.4.5 Histological Analysis of Lipocalin 2 Expression in the Growth Plate

Tibiae were dissected from 10-day-old and 5-week-old saline and Dex treated mice (5mg/kg Dex daily for 7 days), that had been euthanised by cervical dislocation. Metatarsals were dissected from 17-day-old normal foetal mice euthanised by cervical dislocation. The tissues were then processed as previously described (2.4.1), and sections cut at 6µm. For histological analysis, sections were dewaxed and demasked for 30min in 10mM citrate buffer, and immunohistochemistry carried out (2.4.3) with an overnight incubation at 4°C of 2µg/ml goat anti-lipocalin 2 (R & D systems)

followed by rabbit anti-goat IgG peroxidase (1:100 dilution; DAKO) for 60 min. Specific background staining was inhibited by incubating control sections with 0.2mg/ml Goat IgG (concentration if IgG content in primary antibody) in place of goat anti-lipocalin 2 under the same conditions. Ideally, specific background staining should also be blocked by the adsorption of a primary antibody with the purified antigen prior to use, however, at this time, no purified lipocalin 2 antigen was available. Another useful negative control in this study would have been growth plates from lipocalin 2 null mice, however, again, these mice were not readily available and so could not be used.

4.4.6 Isolation of Primary Murine Chondrocytes

Primary cultures of chondrocytes from rib growth plates of 1-day-old mice were prepared using the isolation procedure and culture system developed by Lefebvre *et al.* (1994), as detailed in section 2.2.2. Chondrocytes were seeded in 6-well plates at a density of 100,000 cells per well in DMEM with antibiotics, ascorbic acid, and 10% FBS, and were grown for 24h, at which point Dex was added (10^{-6} M; 6h, 24h, or 72h incubation).

4.4.7 Production of a Lipocalin 2 Expression Construct

Lipocalin 2 cDNA (see Appendix 3 for sequence details) was first ligated into the pGEM-T Easy vector (Promega, WI, USA) for cloning as detailed in sections 2.6.5-2.6.12, inclusive (see Appendix 2 for vector details). The digested pGEM-Lipocalin 2 clone was run on a 1.5% agarose gel, and the lipocalin 2 fragment purified using the Qiagen QiaQuick gel extraction kit as outlined in 2.6.7. Amplified lipocalin 2 cDNA was then inserted into the EcoRI site of the pWGB10 overexpression vector

(Appendix 2) as described in sections 2.6.5 – 2.6.12 (a kind gift from Dr. Wei Cui, Imperial College, London). pWGB10 contains a phosphoglycerate kinase (PGK) promoter, which drives recombinant protein expression, and a simian virus 40 (SV40) small t intro/polyA, and SV40/Puromycin to allow cell selection. To stop re-circularisation of the empty vector, the pWGB10 plasmid was first dephosphorylated with shrimp alkaline phosphatase (SAP) in a reaction containing 100ng vector DNA, 2 units SAP (Roche), and 1x reaction buffer for 10mins at 37°C. This was then heat killed at 70°C for 15mins. Following lipocalin 2 ligation into the linearised pWGB10 vector, the ligation reaction was used to transform SURE2 competent cells as described in 2.6.9. Liquid cultures and plasmid minipreparations of individual clones were subsequently carried out (2.6.10 and 2.6.11, respectively). The clones were then analysed by multiple restriction digestions with enzymes EcoRI, NcoI and PstI to assess insert orientation. A clone containing the insert in the correct orientation (in respect to the PGK promoter) was then purified as detailed in 2.6.12.

4.4.8 Generation of ATDC5 Stable Transfections

1µg of pWGB10/Lipocalin2 was transfected into 80% confluent ATDC5 cells using FuGene6 according to the manufacturer's instructions (Roche Diagnostics, Basel, Switzerland). Control cell lines were generated using the same procedure after transfection of an empty pWGB10 vector. After 48 hours, cells were selected in media containing 2µg/ml puromycin, and after 2 weeks, when no sign of cellular death was evident, clones were isolated and lipocalin 2 expression evaluated by PCR and Western blotting (2.5.4 and 2.7.3).

4.4.9 Effect of Lipocalin 2 Overexpression on Chondrocyte Proliferation and Differentiation

To understand more fully the functional effects of lipocalin 2 overexpression on chondrocyte function, chondrocyte proliferation ($[^3\text{H}]$ thymidine uptake) and chondrocyte differentiation (Coll X expression) was assessed as previously described (2.9.1 and 2.5.5, respectively). Additional experiments determined if the response of ATDC5 cells to Dex treatment (10^{-6}M for 48h) was modified in the presence of lipocalin 2 overexpression.

4.4.9 Statistical Analysis

Analysis of variance (ANOVA) was performed to determine the significance of a given result. General Linear Model analysis incorporating pair-wise comparisons using Tukeys test was used to compare groups within the ANOVA models. All data are expressed as the mean \pm SEM. Statistical analysis was performed using Minitab 14. Statistical significance was accepted at $p < 0.05$.

4.5 Results

4.5.1 Characterisation of Dex-induced Lipocalin 2 Expression in Chondrocytes

The temporal effect of 10^{-6}M Dex on lipocalin 2 expression was studied, and although no effect was seen at 1h, Dex significantly ($p < 0.001$) increased lipocalin 2 expression at all other time points studied (6-168h), with an apparent plateau at 48h (75-fold) (Figure 4.3; Ct values in Table 4.2). Consequently, 48h Dex incubation was used for all future ATDC5 experiments. Dex-induced lipocalin 2 expression in ATDC5 cells was also found to be concentration-dependent (Figure 4.4A-C). At 10^{-6}M Dex, lipocalin 2 expression was 71-fold higher than control samples. This response was

reduced to 44-fold and 13-fold at 10^{-7} and 10^{-8} Dex, respectively ($p < 0.001$), whereas no response was observed with 10^{-9} M Dex (Ct values in Table 4.3) Western blotting confirmed that 10^{-6} M Dex increased lipocalin 2 protein expression at 48h in ATDC5 cells (Figure 4.5). Primary chondrocytes also expressed lipocalin 2 and this expression was increased with 10^{-6} M Dex treatment (3-fold at 6h, $P < 0.001$), and this increased expression was maintained for up to 72h (Figure 4.3C). Taken together, the results indicate that Dex regulates chondrocyte lipocalin 2 expression at both the mRNA and protein level and that the regulation of gene expression is both time and concentration dependent.

Table 4.2 Ct values and corresponding fold change in expression of Lipocalin 2 following exposure to 10^{-6} M Dex for varying timecourses

Sample	Lipocalin 2 Ct	GAPDH Ct	Change in Ct	$2^{\text{change in Ct}}$	Fold Change
Control 1h	33.47	15.2	-18.27	3.16E-06	
Dex 1h	32.1	14.9	-17.2	6.64E-06	2.1 ± 0.24
Control 6h	32.29	15.34	-16.95	7.90E-06	
Dex 6h	26.85	15.29	-11.56	3.31E-04	41.8 ± 1.45
Control 24h	32.12	15.06	-17.06	7.32E-06	
Dex 24h	26.25	14.55	-11.7	3.01E-04	41.1 ± 1.67
Control 48h	32.19	14.62	-17.57	5.14E-06	
Dex 48h	26.58	15.24	-11.34	3.86E-04	75.1 ± 3.1
Control 96h	31.41	15.01	-16.4	1.16E-05	
Dex 96h	25.5	15.46	-10.04	9.50E-04	81.9 ± 2.7
Control 168h	29.33	16.19	-13.14	1.11E-04	
Dex 168h	24.2	17.19	-7.01	7.76E-03	69.9 ± 1.78

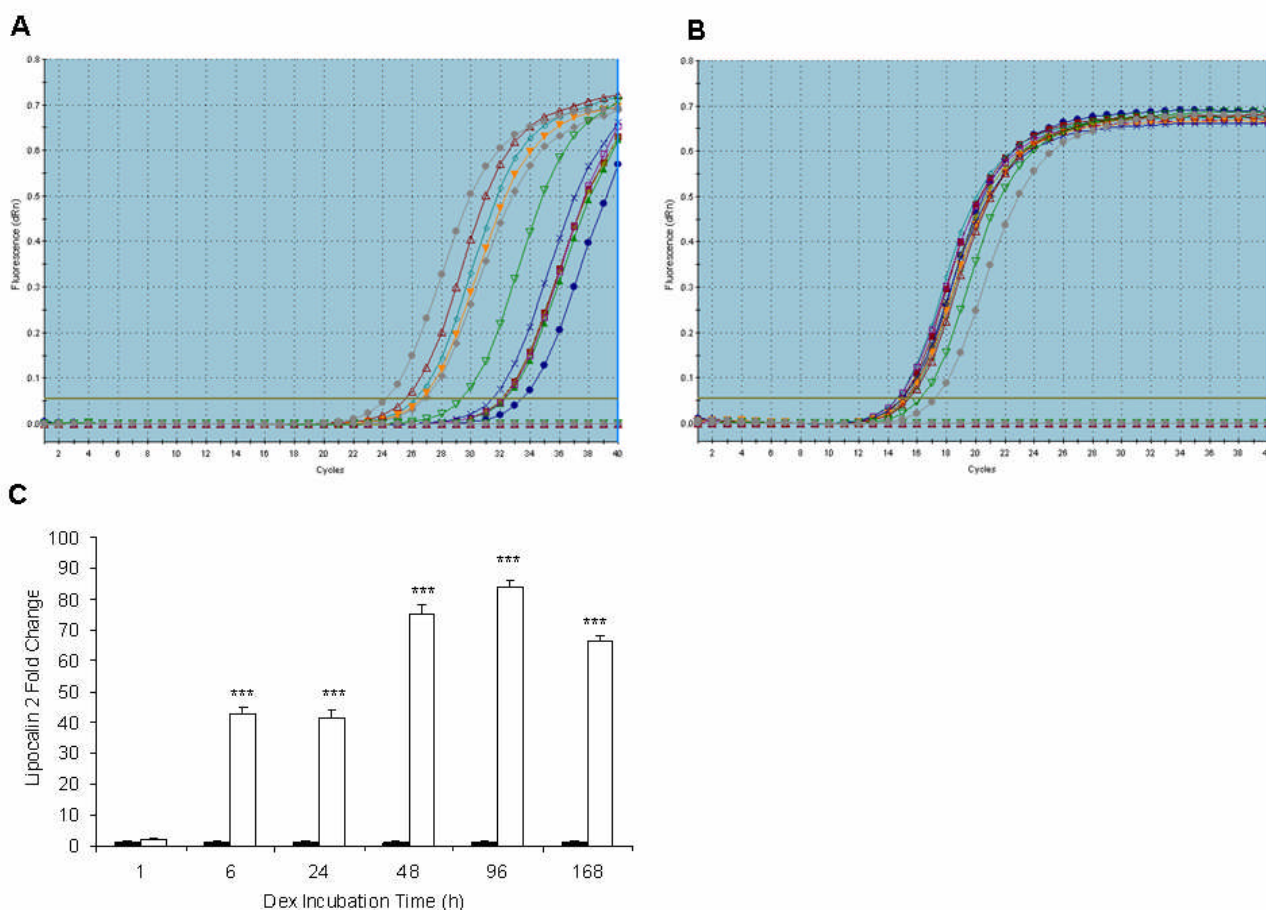
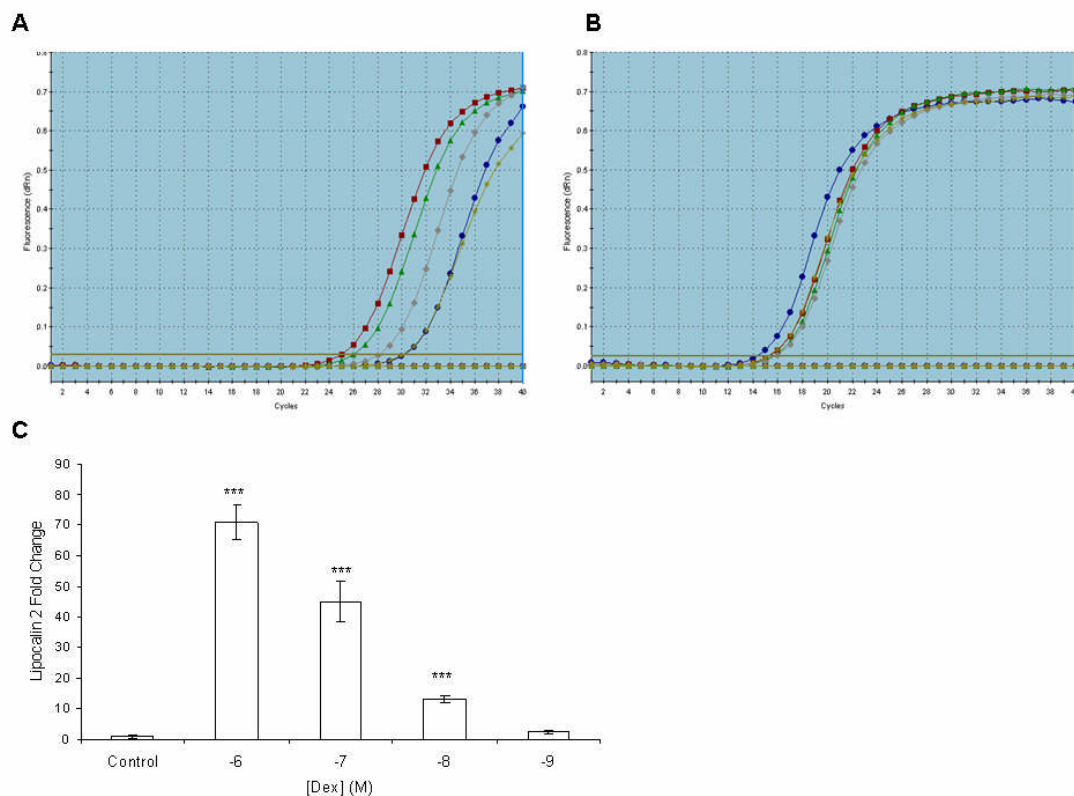
**Figure 4.3 Lipocalin 2 Expression following Dex exposure over time** A) Lipocalin 2 amplification in ATDC5 cells treated with 10^{-6} M Dex for 1-168h (1h control, blue circles, Dex, purple open squares; 6h control, green triangles, Dex, grey diamonds; 24h control, purple open squares, Dex, blue open diamonds; 48h control, red squares, Dex, orange inverted triangles; 96h, control, blue crosses, Dex, red triangles; 168h control, green open triangles, Dex, grey circles). C) GAPDH amplification in ATDC5 cells treated with 10^{-6} M Dex for 1-168h. D) Fold change in lipocalin 2 expression with Dex (10^{-6} M) over time (data are expressed as mean ± SEM). For all data, n=3 cell culture replicates run in triplicate.

Table 4.3 Ct values and corresponding fold change in expression of Lipocalin 2 following exposure to varying concentrations of Dex for 48h.

Sample	Lipocalin 2 Ct	GAPDH Ct	Change in Ct	$2^{\text{change in Ct}}$	Fold Change
Control	32.38	16.61	-15.77	1.79E-05	
Dex 10^{-6} M	27.32	17.68	-9.64	1.25E-03	69.8 ± 5.5
Dex 10^{-7} M	28.34	17.99	-10.35	7.66E-04	42.7 ± 6.7
Dex 10^{-8} M	30.29	18.21	-12.08	2.31E-04	12.9 ± 1.27
Dex 10^{-9} M	32.03	17.54	-14.49	4.35E-05	2.4 ± 0.25

**Figure 4.4** Dose-responsive change in lipocalin 2 expression in ATDC5 cells with Dex over 48h. A) Amplification of lipocalin 2 treated with 10^{-6} M (red closed squares), 10^{-7} M (green closed triangles), 10^{-8} M (grey diamonds) and 10^{-9} M (blue circles) Dex for 48h (controls = yellow asterisk). B) Amplification of GAPDH following exposure to Dex (10^{-6} M- 10^{-9} M) for 48h. C) Dose-responsive change in lipocalin 2 expression following exposure to Dex (data are expressed as mean ± SEM). For all data, n=3 cell culture replicates run in triplicate.

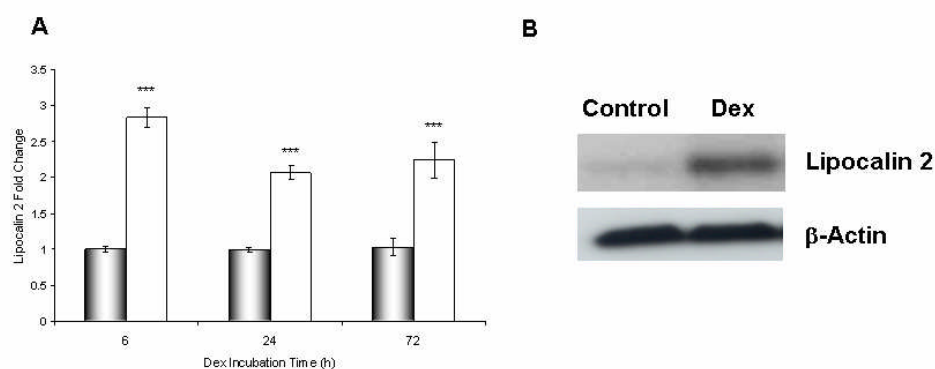


Figure 4.5 Lipocalin 2 Expression in Chondrocytes A) Primary murine chondrocytes treated with 10^{-6} M Dex for 6, 24 or 72h. B) Lipocalin 2 protein expression in ATDC5 cells as analysed by Western blotting, after exposure to 10^{-6} M Dex for 48h.

4.5.2 Immunolocalisation of Lipocalin 2 Expression in the Murine Growth Plate

Immunohistochemistry revealed that in metatarsals from 17-day old foetal mice, lipocalin 2 was poorly expressed in both the proliferating and mineralising chondrocytes, situated on either side of the strongly positive staining prehypertrophic/hypertrophic chondrocytes (Figure 4.6A). The pattern of lipocalin distribution appeared to change in the post-natal growth plate. In the 10-day-old epiphysis, greater lipocalin 2 expression was localised to the proliferating chondrocytes (Figure 4.6B) and this was more clearly seen in the 5-week-old growth plate where intense lipocalin 2 staining was observed in both the proliferating and hypertrophic zones (Figure 4.6C). No obvious difference in lipocalin 2 localisation or staining intensity was observed between the growth plates of 5-week-old Dex-treated and control mice (data not shown). High levels of expression were also observed in the articular chondrocytes, and within the hypertrophic chondrocytes of the developing secondary ossification centre (Figure 4.6D) of the 10-day-old tibias. All control sections incubated with pre-immune serum were negative (Figure 4.6E). The immunolocalisation results clearly show that lipocalin 2 is expressed by murine

growth plate chondrocytes and this confirms our qPCR data (Figure 4.5A). In the epiphyses from older animals lipocalin 2 appears to be present in all growth plate maturational zones whereas in the younger growth plates it is more restricted to the maturing hypertrophic cells.

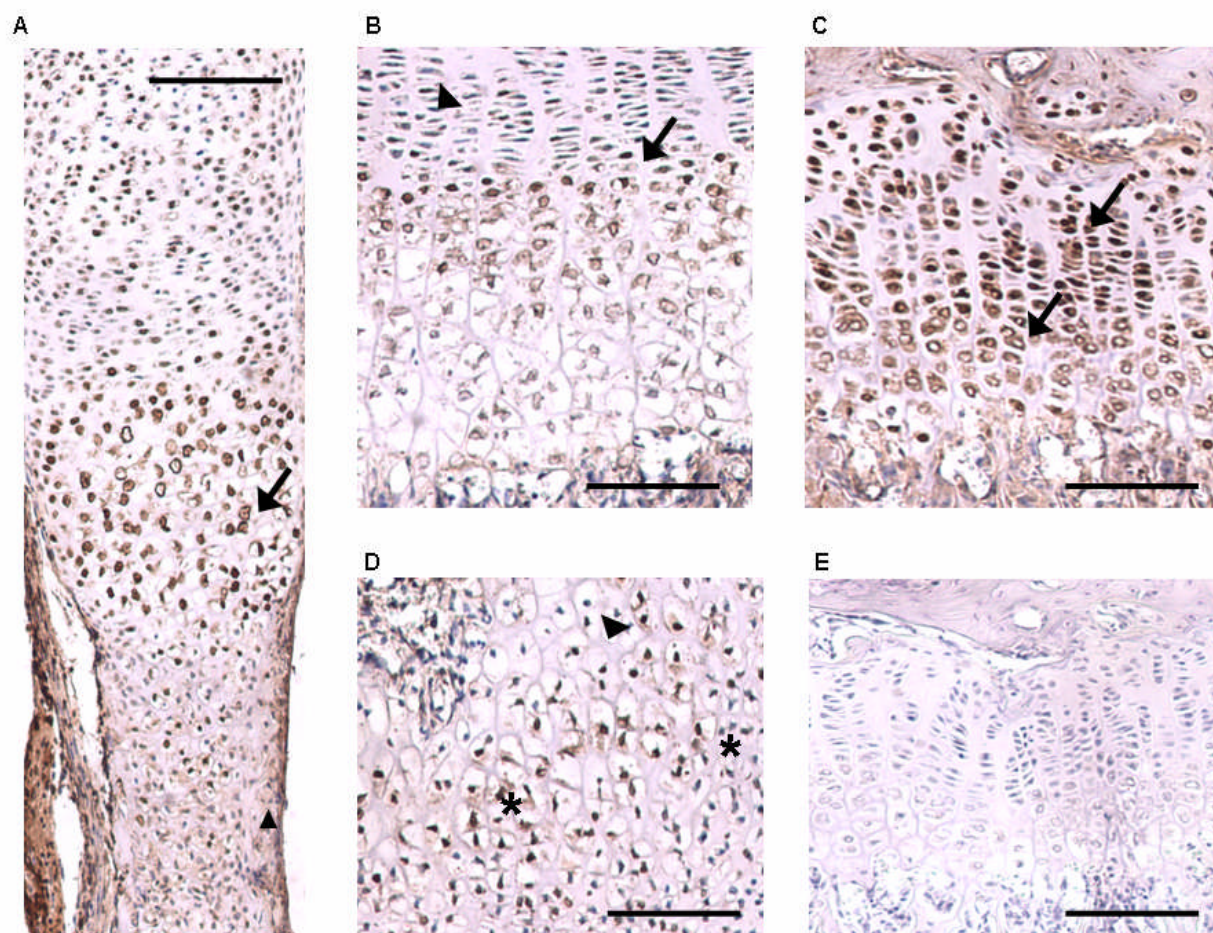


Figure 4.6 Lipocalin 2 localisation in the murine proximal tibia and metatarsal. (A) In metatarsals from 17-day old foetal mice, lipocalin 2 is poorly expressed in the proliferating and mineralising chondrocytes (arrowheads), however strong positive staining is present in the prehypertrophic and hypertrophic chondrocytes (arrows) (scale bar = 400 μ m). (B) In the 10-day-old lipocalin 2 expression is localised to the proliferating chondrocytes and this can also be seen in the 5-week-old growth plate (scale bar = 200 μ m) (arrows) (C), where intense lipocalin 2 staining is present in both the proliferating and hypertrophic zones (arrows). (D) Lipocalin is also present in the chondrocytes of the developing secondary ossification centre (*) (scale bar = 200 μ m). (E) All control sections incubated with Goat IgG are negative.

4.5.3 Mechanism of Dex-induced Lipocalin 2 Expression in Chondrocytes

Incubating ATDC5 cells with CHX did not block Dex-induced lipocalin expression (Figure 4.7A), but instead caused a further significant increase in lipocalin 2 expression. RU486 caused lipocalin 2 expression to return to basal levels in the presence of Dex (Figure 4.7B) (13-fold change in the presence of RU486 and Dex compared to 39-fold change with Dex alone; $p < 0.01$). As with most steroidal competitive antagonists, RU486 exhibits partial agonist properties under certain conditions (Leonhardt and Edwards, 2002), and this could explain the small 13-fold increase in lipocalin 2 expression with RU486 alone (Figure 4.7B).

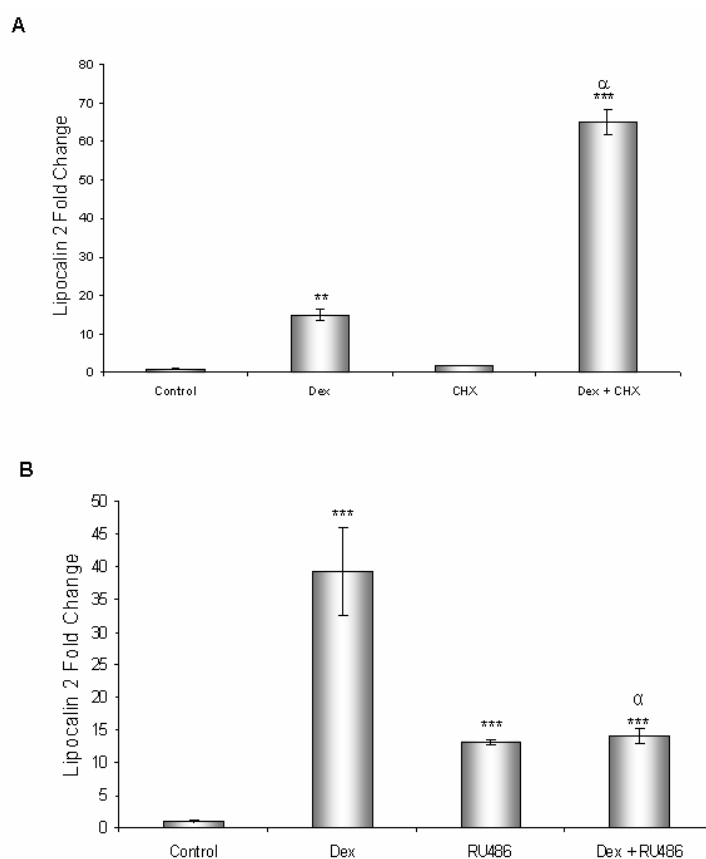


Figure 4.7 Involvement of the GR in GC-induced Lipocalin 2 expression in ATDC5 cells. (A) Lipocalin 2 expression with Dex plus the protein synthesis blocker CHX. ATDC5 cells were incubated with 10^{-6} M Dex for 6h, with CHX ($8\mu\text{g/ml}$) added 30mins before the addition of Dex. (B) Lipocalin 2 expression with Dex plus the GR antagonist, RU486. ATDC5 cells were incubated with 10^{-6} M Dex plus RU486 (10^{-5} M) for 48h. All data are expressed as mean \pm SEM ($n=3$ cell culture replicates run in triplicate; *** $p < 0.001$ vs. control; α $p < 0.05$ vs. Dex).

4.5.4 Involvement of the NF κ B and p38 pathways in Dex-induced Lipocalin 2 Expression

The addition of SB203580 blocked p38 activity but did not block the increase in lipocalin 2 expression observed with Dex (Figures 4.8A and 4.8B). However, TLCK caused a concentration-dependent reduction in lipocalin 2 expression compared to Dex alone (Figures 4.9A and 4.9B). Both 5 and 50 μ M TLCK significantly reduced Dex induced lipocalin 2 expression but only 50 μ M TLCK brought lipocalin 2 expression back to non-induced levels (Figure 4.9B). It was next determined if TLCK could, in part, inhibit the antiproliferative effects of Dex on ATDC5 proliferation (Mushtaq *et al* 2002; Owen *et al.* 2007). Dex (10^{-6} M) caused a significant reduction (46.5%; $p < 0.001$) which was partly reversed by co-incubation with 50 μ M TLCK (Figure 4.7C). Co-incubation, however, only increased proliferation by 20% ($p < 0.05$) compared to cells incubated with Dex alone, and this proliferation remained significantly lower ($p < 0.001$) lower than control cells. These data indicate that the Dex effects on lipocalin 2 expression are not dependent on protein synthesis or p38 activity. The transcription factor, NF κ B, however appeared to mediate the Dex effects on chondrocyte lipocalin 2 expression. To confirm that this was, in fact the case, a specific peptide inhibitor for NF κ B, SN50, was also incubated in the presence of Dex in ATDC5 cells. Interestingly, this inhibitor had no effect on Dex-induced lipocalin 2 expression, suggesting that the inhibitory effects seen with TLCK were not specific to NF κ B (Figure 4.9D).

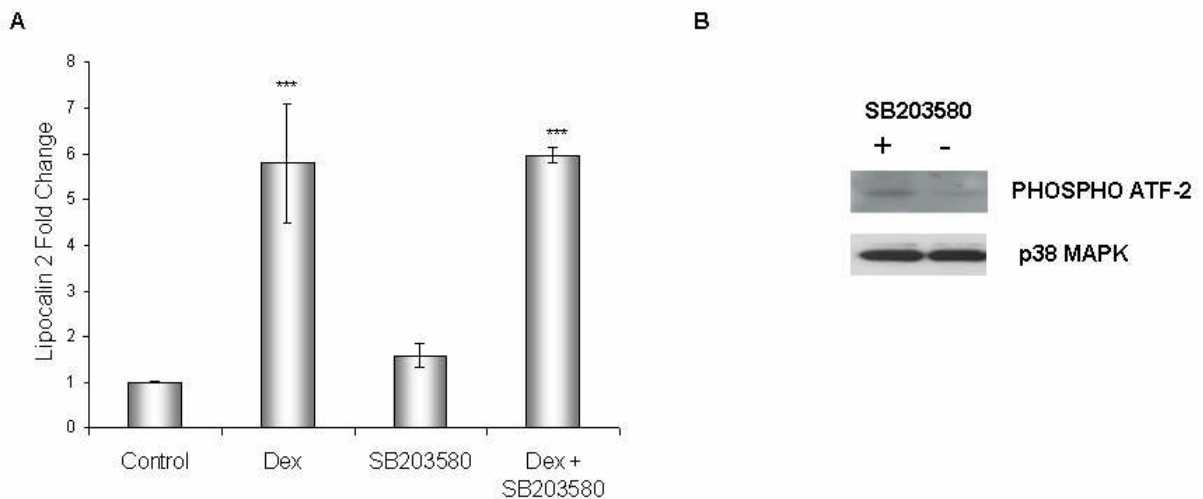


Figure 4.8 The p38 signalling pathway and GC-induced Lipocalin 2 expression. (A) Lipocalin 2 expression with Dex (10^{-6} M) and the p38 inhibitor SB203580 (20 μ M). ATDC5 cells were incubated with SB203580 for 2h, before the addition of Dex for the remaining 48h. All data are expressed as mean \pm SEM (n=3 separate cell culture replicates run in triplicate; ***p<0.001 vs. control). (B) p38 activity in SB203580 treated ATDC5 cells. A kinase assay for p38 MAPK activity was carried out using ATF-2 fusion protein as phosphorylation substrate. Total p38 protein was determined by Western blotting.

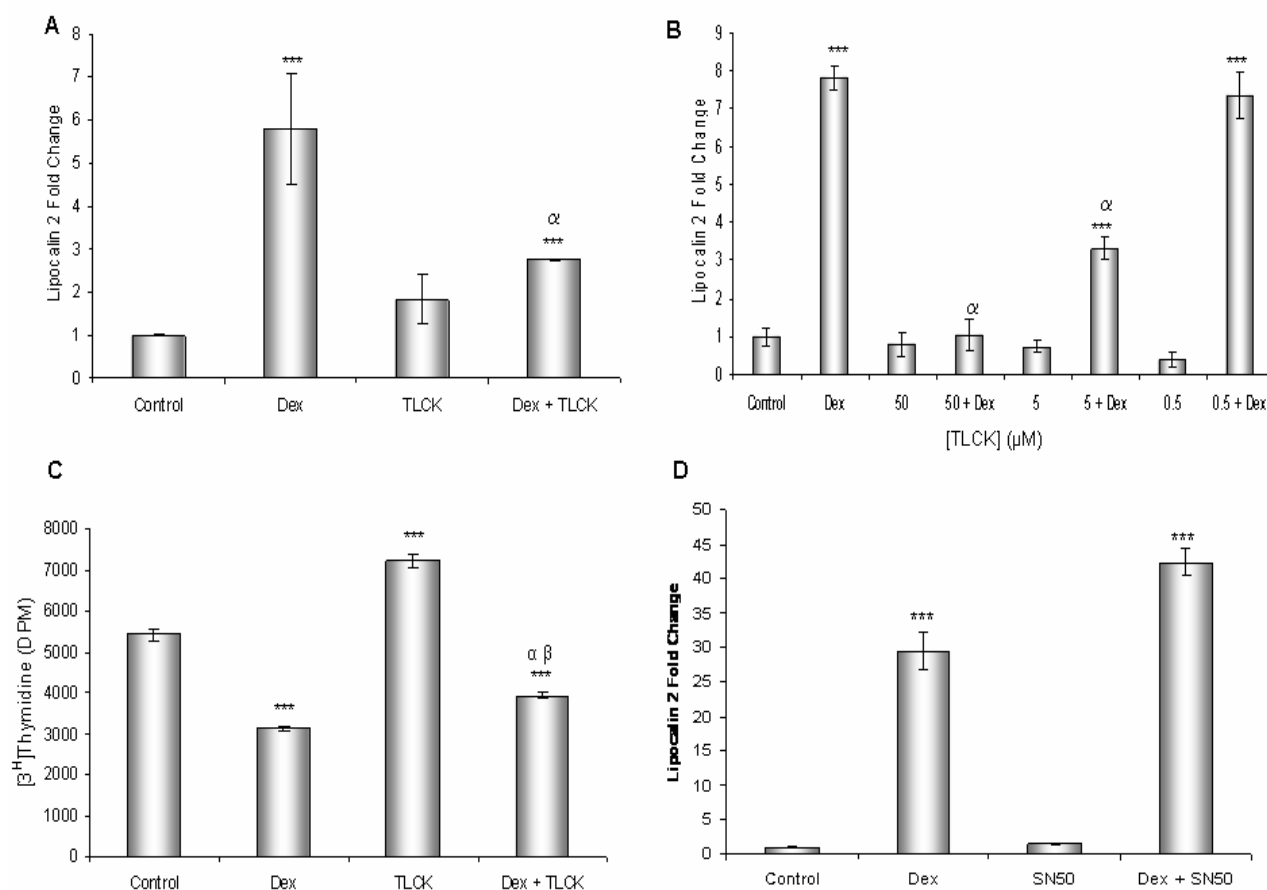


Figure 4.9 The NFκB signalling pathway and GC-induced Lipocalin 2 expression. The NFκB inhibitor TLCK (50μM) TLCK was incubated with ATDC5 cells for an initial period of 4h before the addition of Dex for another 48h. (B) Lipocalin expression with varying concentrations of TLCK. ATDC5 cells were incubated with 50, 5 or 0.5μM TLCK for 4h before the addition of 10⁻⁶M Dex for the remaining 48h. (C) Proliferation of ATDC5 cells treated with TLCK (50μM) and/or Dex (10⁻⁶M) for 48h. (D) Lipocalin 2 expression with Dex (10⁻⁶M) and the selective NFκB inhibitor SN50 (18μM). ATDC5 cells were incubated with SN50 for 2h, before the addition of Dex for the remaining 48h. All data are expressed as mean ± SEM (n=3 separate cell culture replicates run in triplicate; ***p<0.001 vs. control; ^αp<0.05 vs. Dex, ^βp<0.01 vs. TLCK).

4.5.5 Functional Effects of Lipocalin 2 on ATDC5 Cell Dynamics

To identify the possible physiological effect of Dex-induced lipocalin 2 expression on chondrocyte dynamics, in initial studies, the effects of both lipocalin 2 overexpression (Figure 4.10A) and recombinant lipocalin 2 on ATDC5 proliferation was analysed. Proliferation was significantly reduced ($p < 0.001$) in overexpressing cells (Figure 4.10B) and those treated with recombinant lipocalin 2 (Figure 4.10C). The reduction in proliferation by recombinant lipocalin 2 was modest (23.1% at 10 μ g/ml) and similar at all concentrations tested, whereas a more dramatic effect (49.1%) was noted in the overexpressing cells. This difference is likely to be due to the unstable nature of synthetic recombinant proteins, and therefore over-expressing cells were used for further analysis.

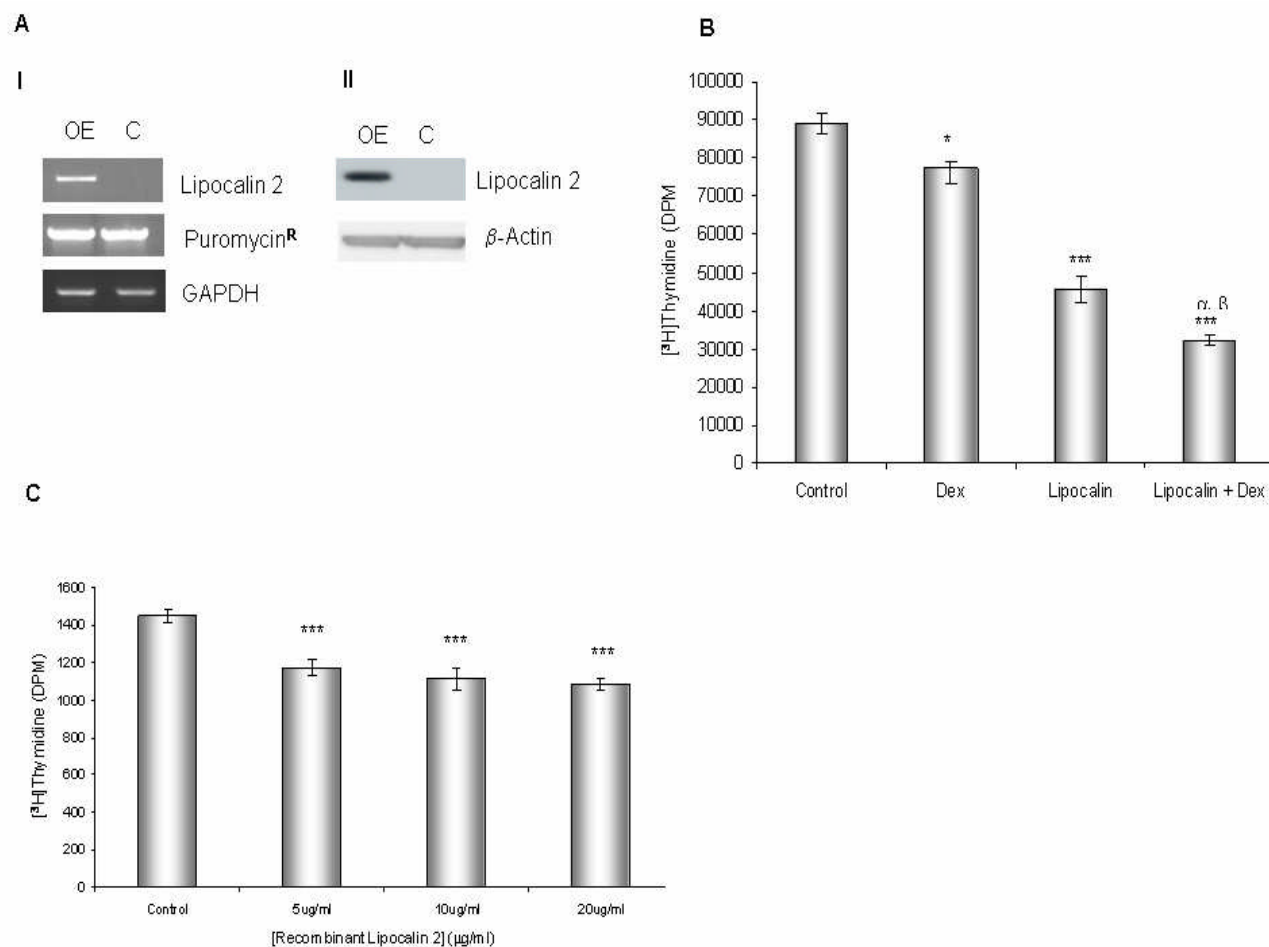


Figure 4.10 The effect of increased lipocalin 2 expression on chondrocyte dynamics. (A) Lipocalin 2 over-expression in ATDC5 cells was confirmed by (I) PCR of Lipocalin 2, puromycin resistance gene, and GAPDH; and (II) Western blotting for lipocalin 2 and beta-actin loading control. (OE = Lipocalin over-expressing; C = Control cells containing empty vector only). (B) Proliferation of lipocalin 2 over-expressing cells as measured by [³H]-thymidine incorporation. Transfected ATDC5 cells were incubated with or without 10⁻⁶M Dex for 24h. (n=3 cell culture replicates; ***p<0.001 vs. control; **p<0.01 vs. control; ^αp<0.05 vs. Dex, ^βp<0.01 vs. Lipocalin). (C) ATDC5 proliferation as measured by [³H]thymidine incorporation following 48h incubation with recombinant lipocalin 2 protein (5-20 μ g/ml; R&D systems) (n = 6 cell culture replicates; ***p<0.001 vs. control).

4.5.6 The Combined Effect of Lipocalin 2 and Dex on ATDC5 Cells

Lipocalin-2 overexpression caused an increase in collagen type-X expression (4-fold, p<0.001; Figure 4.11A). The effects of lipocalin-2 overexpression on chondrocyte proliferation (64% reduction vs. control cells, p<0.001) and collagen type-X

expression (8-fold increase vs. control, $p < 0.001$) were further amplified by the addition of 10^{-6} M Dex (Figures 4.11A and 4.11). This apparent synergistic effect of Dex and lipocalin 2 on proliferation and collagen type X expression may be in response to the further increase in lipocalin 2 expression (140-fold, $p < 0.001$) noted in the Dex treated overexpressing cells (Figure 4.11B).

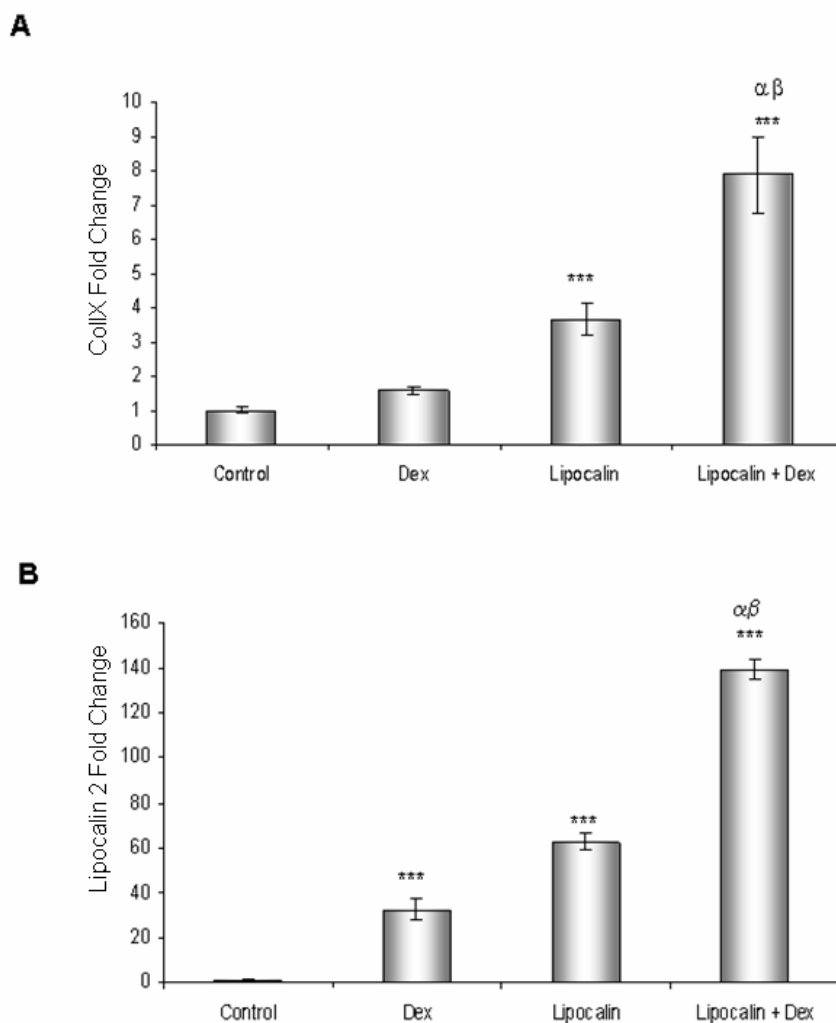


Figure 4.11 The combined effect of lipocalin 2 and Dex on ATDC5 cells. (A) Type X collagen expression in lipocalin 2 over-expressing ATDC5 cells incubated with or without 10^{-6} M Dex for 48h. (B) Effect of Dex on lipocalin 2 expression in ATDC5 cells over-expressing lipocalin 2. Cells were incubated with 10^{-6} M Dex for 48h, and lipocalin 2 expression was measured by qPCR ($n=3-6$ cell culture replicates run in triplicate; *** $p < 0.001$ vs. control; $^{\alpha}p < 0.05$ vs. Dex Empty; $^{\beta}p < 0.05$ vs. lipocalin only). All data are expressed as mean \pm SEM.

4.6 Discussion

Lipocalin 2, also known as Neutrophil-associated gelatinase lipocalin (NGAL), was originally identified as a 25kDa protein which binds to small lipophilic substances such as bacteria-derived lipopolysaccharide (LPS). Since then, the known actions of lipocalin 2 have spiralled, and lipocalin 2 has now been linked with a wide range of different functions, including partuition, inflammation, differentiation, apoptosis and acute phase immunity. Originally termed SIP24 (Superinducible-protein 24), lipocalin 2 is known to be induced by a number of factors and conditions, such as LPS, CHX, serum, FGF2, prostaglandin F2 α , oxidative stress, partuition, and, of course, Dex (Meheus *et al.*, 1993; Lui *et al.*, 1995).

In this study, it has been shown that lipocalin 2 expression is significantly increased with Dex treatment in murine chondrogenic ATDC5 cells. This increased expression was Dex-concentration dependent, and reached a plateau after 48h Dex. In primary murine costochondral chondrocytes isolated from the rib cages of 2-day-old mice, an increase in lipocalin 2 expression was also observed, and although significant, this increase was smaller than seen in ATDC5 cells. ATDC5 cells were originally isolated from a differentiating culture of AT805 teratocarcinoma cells, which display a fibroblast-like phenotype until the addition of insulin, which promotes their differentiation into chondrocytes (Atsumi *et al.*, 1990). These cells are a useful model for studying chondrogenesis due to the fact that their temporal sequence of maturation directly mirrors the maturational phases within the growth plate. In addition, the cell population differentiates collectively, so that all the cells are at the same stage of differentiation at the same time. However, because of this, they cannot be compared directly to primary costochondral chondrocytes, which are isolated as a population of

chondrocytes at all stages of differentiation. The fact that ATDC5 cells and primary costochondral chondrocytes comprise of 2 different phenotypes could explain the differences in the magnitude of lipocalin 2 expression observed in this study.

The expression of lipocalin 2 in primary chondrocytes was supported by the finding that lipocalin 2 was expressed in the metatarsals of embryonic mice. Lipocalin 2 has previously shown to be expressed in the liver, spleen, lung, muscle, heart and tibia of embryonic mice (Garay-Rojas *et al.*, 1996; Ulivi *et al.*, 2006), and within the tibia of embryonic rats, the rat homologue of lipocalin 2 neu-related lipocalin (NRL) is localised to the prehypertrophic chondrocytes (Zerega *et al.*, 2000), supporting the findings of this study. It has previously been found that ALP has a similar pattern of localisation within the growth plate (Maio and Scutt, 2002; Mushtaq *et al.*, 2004), suggesting that, like ALP, lipocalin 2 may be a marker for chondrocyte differentiation. Interestingly, in 10-day-old and 5-week-old mice in this study, it has been shown that lipocalin 2 is more prominent in the proliferative chondrocytes, suggesting the localisation of lipocalin 2 expression within the growth plate is age-dependent. Differences in lipocalin 2 expression between adult and foetal tissue have previously been described, with a general decline in expression in conjunction with ageing (Garay-Rojas *et al.*, 1996). This, together with similarities in expression to ALP, and previous studies showing the pro-differentiating effects of lipocalin 2 in epithelial cells (Yang *et al.*, 2002), further supports the hypothesis that lipocalin 2 may have a role in the regulation of chondrocyte differentiation. Interestingly, it has been shown that lipocalin 2 knock-out mice have no skeletal defects, the only obvious phenotype being an increased susceptibility to infection (Berger *et al.*, 2006). To date, there have been no studies documenting skeletal growth in these mice following

Dex treatment, and, it is possible that growth retardation in these mice could be reduced.

In an attempt to identify some of the mechanisms involved in Dex-induced lipocalin 2 expression, the GR antagonist RU486 was incubated alone or with Dex in ATDC5 cells. Results showed that, in the presence of RU486 alone, lipocalin 2 expression was increased to some extent. RU486 is a competitive antagonist for the GR, and, by nature, such antagonists often display some agonist activity at the receptor they competitively bind to, accounting for the increases in lipocalin 2 expression observed here. When RU486 and Dex were incubated together, lipocalin 2 expression could no longer be induced with Dex. Analysis of the lipocalin 2 sequence with 'MatInspector' (www.genomatix.de) confirmed previous reports of two GC response elements (GRE) in the 5' regulatory region of the lipocalin 2 promoter (Garay Rojas *et al.*, 1996; Cartharius *et al.*, 2005) (Figure 4.11). The presence of GRE in the promoter region of lipocalin 2 suggested that this gene could be a direct target of the GR complex. This was supported by the fact that the Dex-induced increase in lipocalin 2 mRNA levels was not inhibited by CHX, a protein synthesis inhibitor. Interestingly, CHX in fact caused a further increase in lipocalin 2 expression. This finding has been previously reported (Davis *et al.*, 1991) and could be due to CHX blocking the synthesis of a lipocalin 2 or Dex repressor.

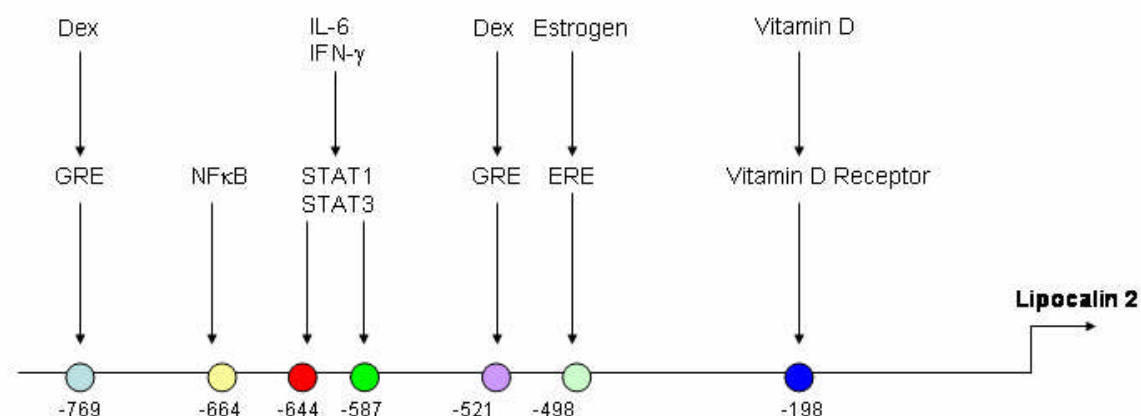


Figure 4.12 The Lipocalin 2 Promoter Analysis of the lipocalin 2 promoter sequence with ‘MatInspector’ (www.genomatix.de) confirmed previous reports of two GC response elements (GREs), suggesting that this gene could be a direct target of the GR complex. Other interesting binding sites include the estrogen response element (ERE), an NFκB binding site, Vitamin D receptor site, and binding sites for the pro-inflammatory transcription factors STAT1 and STAT3.

In addition to several GRE’s, the lipocalin 2 promoter region also contains a number of NFκB binding sites. Previous studies have reported IL-1-induced lipocalin 2 expression through NFκB signalling (Cowland *et al.*, 2006), and the presence of an NFκB binding site on the lipocalin 2 promoter supports a putative role for NFκB in this study (Figure 4.10). The NFκB/p38 pathway is suggested to be involved in LPS-induced lipocalin 2 expression in chondrocytes (Ulivi *et al.*, 2006), and is also involved in chondrocyte differentiation (Wen *et al.*, 2006), and in an attempt to further define the mechanisms by which Dex induces lipocalin 2 expression, the role of the p38/NFκB pathway was examined. The p38 inhibitor SB203580 had no effect on lipocalin 2 expression, although its activity was confirmed by a p38 MAPK assay, suggesting that p38 had no role in lipocalin 2 induction in this study. The NFκB inhibitor TLCK, a serine protease inhibitor, blocked Dex-induced lipocalin 2 expression and partly blocked the Dex effects on ATDC5 proliferation, initially

suggesting that NF κ B was involved in the Dex effects on lipocalin 2. To confirm this result, the experiment was repeated using another NF κ B inhibitor, SN50, a peptide inhibitor which selectively inhibits the translocation of NF κ B to the nucleus. Results using this inhibitor showed that blocking NF κ B activity had no effect on lipocalin 2 expression, suggesting that the initial results obtained with TLCK were due to the inhibition of other factors such as protein kinase C (PKC) (Solomon *et al.*, 1985), or cell cycle regulators such as pp70s6k (Grammer *et al.*, 1996). Consequently, the exact mechanisms by which Dex increases lipocalin 2 expression in ATDC5 cells are still unknown.

Interestingly, a recent study has found that there is a marked increase in lipocalin 2 in obese humans (Wang *et al.*, 2006). In addition, this study displayed a significant positive correlation between lipocalin 2 expression and several variables associated with obesity-related metabolic disorders, including hyperinsulinemia and fasting glucose concentrations. It is known that at pharmacological doses, Dex can cause an increase in fasting glucose concentrations, and due to the fact that lipocalin 2 expression is increased following exposure to insulin-resistance-inducing and inflammatory adipokines such as TNF α , IL6 and resistin (Berg *et al.*, 2005; Wellen *et al.*, 2005), it is possible that Dex is increasing lipocalin 2 expression through alterations the gluconeogenesis pathway.

The importance of lipocalin 2 in GC-induced growth retardation was further supported with the finding that its overexpression caused a reduction in ATDC5 proliferation and an increase in differentiation, an effect which is similar to that seen with GC-treated ATDC5 cells (Mushtaq *et al.*, 2002; Owen *et al.*, 2007). The effects

on proliferation were also reproduced with the addition of lipocalin 2 recombinant protein, supporting the hypothesis that lipocalin 2 is influencing chondrocyte dynamics in a similar way to GCs. Interestingly, the effects of lipocalin 2 overexpression on proliferation and differentiation were exacerbated with Dex, and lipocalin 2 expression in transfected cells was increased more than would be expected from the additive effects of Dex and lipocalin 2 expression alone. The synergistic effect of Dex and LPS on lipocalin 2 expression has previously been described (Vizzardelli *et al.*, 2006), however, these findings suggest that lipocalin 2 itself may play a role in mediating the effects of Dex. It is therefore possible that lipocalin 2 could be exacerbating Dex-induced growth retardation by interacting directly with Dex to inhibit chondrocyte proliferation and increase differentiation. As previously discussed, it has been reported that lipocalin 2 contains 2 GREs on the promoter. Due to this fact, it would be interesting to study the behaviour of Dex-treated ATDC5 cells transfected with a lipocalin 2 promoter, constructed with a GRE knock-out element.

4.7 Conclusions

Lipocalin 2 has previously been shown to be regulated by Dex in dendritic cells (Vizzardelli *et al.*, 2006) and fibroblast-derived murine L-cells (Garay-Rojas *et al.*, 1996), however, its stimulation in chondrocytes has not previously been reported. This study has shown that the acute-phase binding protein lipocalin 2 is markedly increased in chondrocytes in response to Dex, and that lipocalin 2 may mediate Dex effects on chondrocytes. This finding provides a potential novel mechanism for GC-induced growth retardation.

Chapter 5

The Role of p21^{WAF1/CIP1} in Glucocorticoid-Induced Growth Retardation

Chapter Contents

- 5.1 Introduction
- 5.2 Hypothesis
- 5.3 Aims
- 5.4 Materials and Methods
 - 5.4.1 *In Vitro* Studies
 - 5.4.1.1 Cell Culture
 - 5.4.1.2 Cell Counting
 - 5.4.1.3 PCR
 - 5.4.1.4 Western Blotting
 - 5.4.2 *In Vivo* Studies
 - 5.4.2.1 p21 Null Mice Genotyping
 - 5.4.2.2 *In Vivo* Treatment of Mice with Dex
 - 5.4.2.3 Measurement of Organ Weights
 - 5.4.2.4 Tissue Processing
 - 5.4.2.5 Toluidine Blue Analysis of Growth Plate
 - 5.4.2.6 Analysis of X-rays
 - 5.4.2.7 Calcein Labelling
 - 5.4.2.8 Laser Capture Microscopy
- 5.5 Results
 - 5.5.1 *In Vitro* Studies
 - 5.5.1.1 Analysis of p21 Expression during Chondrocyte Differentiation
 - 5.5.1.2 p21 Expression in ATDC5 Cells following Dex Treatment
 - 5.5.2 *In Vivo* Studies
 - 5.5.2.1 Growth in Dex-treated Mice

- 5.5.2.2 Effect of Dex on Organ Weight
 - 5.5.2.3 Effect of Dex on Growth Plate Morphology
 - 5.5.2.5 Growth in Dex-treated p21^{-/-} Mice
 - 5.5.2.6 Skeletal Growth in Dex-treated p21^{-/-} Mice
 - 5.5.2.7 Growth Plate Morphology in Dex-treated p21^{-/-} Mice
 - 5.5.2.8 Calcein Labelling in Dex-treated p21^{-/-} Mice
- 5.6 Discussion
 - 5.7 Conclusions

5.1 Introduction

Despite recent advances in the understanding of how GCs regulate growth and differentiation in a number of target tissues, the molecular mechanisms by which they exert these profound effects on bone growth and development have remained a mystery. It is generally accepted that proliferation and differentiation are mutually exclusive biological processes; therefore, a required step in the progression towards terminal differentiation is the withdrawal of a cell from the cell proliferation cycle. A growing body of evidence suggests that GCs may exert their effects on cell growth and differentiation in chondrocytes partly through regulation of this cell cycle (Robson *et al.*, 1998; Sanchez and He 2002; Mushtaq *et al.*, 2002; Siebler *et al.*, 2002; Schrier *et al.*, 2006).

Progression of the cell cycle is controlled primarily by cyclin dependent kinases (CDKs), and their repressors, the cyclin dependent kinase inhibitors (CDKIs). In mammals, there are two families of CDKIs; the CIP/KIP family composed of p21^{WAF1/CIP1}, p27^{KIP1}, and p57^{KIP1}, which bind to and inhibit G1 CDKs, and the INK4 proteins p16^{INK4A}, p15^{INK4B}, p18^{INK4C} and p19^{INK4D}, which inhibit CDK4 and to a lesser extent CDK6. The Cip/Kip family can act on most cyclin/CDK complexes and are essential for G1 progression and S1 entry (Johnson and Walker 1999). Increasing evidence

from murine gene knockout experiments, analysis of human dyschondroplasias, and in vitro studies suggest that these CDKIs play an important role in the control of bone growth at the level of the growth plate.

Disruption of the p57 gene has been shown to cause delayed chondrocyte differentiation, resulting in skeletal deformations and shortened limbs (Yan *et al.*, 1997; Zhang *et al.*, 1997). In these studies, chondrocytes showed increased proliferation and reduced expression of Coll X, suggesting that p57 may be required for chondrocyte differentiation. In contrast, however, mice deficient for p27 or p21 do not show any obvious skeletal phenotypes. However, p27-null mice are larger than wild-type mice (Fero *et al.*, 1996; Kiyokawa *et al.*, 1996; Nakayama *et al.*, 1996), and this increase in size appears to affect growth of all organs, suggesting that some growth plate effects are likely. p21 deficient mice do not display any developmental defects, although isolated cells do show altered cell cycle kinetics (Deng *et al.*, 1995; Missero *et al.*, 1996). Expression of p21 in differentiating rat growth plate chondrocytes has been examined in cells cultured as three-dimensional pellets (Ballock *et al.*, 2000), and has also been detected in rat costochondral growth plate chondrocytes and articular chondrocytes in pellet culture (Stewart *et al.*, 1997) (Figure 5.1). In addition, upregulation of Coll X and ALP activity in hypertrophic chondrocytes has been associated with increased expression of p21 but not p27 (Stewart *et al.*, 1997).

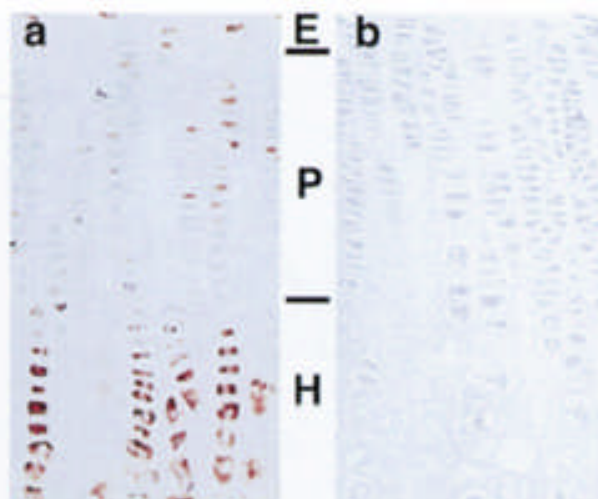


Figure 5.1 Immunohistochemical localisation of p21 in the rat growth plate. Sections (5 μm) were incubated with polyclonal, rodent-specific rabbit antibody to p21 (**A**), or to an equal concentration of ammonium acetate-precipitated rabbit non-immune serum (**B**). Reactive cells are dark red. Although staining is evident in a few proliferative cells, expression of p21 appears substantially increased in cells at the transition between the proliferative and hypertrophic zones, in hypertrophic cells, and in cells adjacent the epiphyseal ossification front. E = epiphyseal ossification front, P = proliferative zone, H = hypertrophic zone. *From Stewart et al., 1997.*

Other studies have also suggested that p21 may play a role in the regulation of growth plate chondrocyte proliferation and differentiation. Increased expression of p21 in cartilage has been demonstrated in thanatophoric dysplasia human embryos (a form of short-limbed dwarfism that usually causes death within the first few hours after birth) (Su *et al.*, 1997). In addition, in ATDC5 cells, p21 expression increases as the cells progress towards terminal differentiation, and this expression is blocked by p38 and MAPK inhibitors, suggesting that, in chondrocytes, p21 expression is p38/MAPK dependent (Negishi *et al.*, 2001; Nakajima *et al.*, 2004).

p21 expression is usually controlled at the transcriptional level by both p53-dependent and -independent mechanisms. The p53 tumour suppressor protein is a transcription factor required for the activation of a number of genes involved in growth control, and results from the γ -irradiation of p53-knockout and wild-type mice suggested that p53

dependent regulation of p21 is critical for the response to DNA damage (Macleod *et al.*, 1995). However, a variety of agents that promote differentiation activate p21 transcription by p53-independent mechanisms, primarily through transcription factors which bind to specific *cis*-acting elements located within the p21 promoter. Dex has been shown to induce the expression of p21 by acting through the CCAAT/enhancer binding protein- α (C/EBP α) transcription factor, which regulates p21 expression at the transcriptional level (Timchenko *et al.*, 1996; Cha *et al.*, 1998; Cram *et al.*, 1998). In osteoblasts, pharmacological concentrations of Dex induce p21 expression (Leclerc *et al.*, 2004), resulting in reduced osteoblast development. In addition, studies using rat hepatoma cells have shown that Dex causes a p53-independent increase in p21 mRNA and protein expression, whereas the expression of other CDKIs such as p27 remain unchanged (Cha *et al.*, 1998).

5.2 Hypothesis

In Chapter 3, microarray analysis suggested that Dex may cause growth retardation by causing premature differentiation of proliferative chondrocytes within the growth plate. Due to the previous finding that increased p21 expression is linked with chondrocyte differentiation, it is possible that Dex may promote p21 expression to cause a reduced proliferation in growth plate chondrocytes.

5.3 Aims

- I. Confirm p21 expression is increased in terminally differentiating ATDC5 cells through Western Blotting and qPCR.
- II. Analyse the effect of Dex on p21 expression in ATDC5 cells by Western Blotting and qPCR.
- III. Develop an effective *in vivo* protocol for measuring GC-induced growth retardation in mice.
- IV. Analyse the role of p21 in GC-induced growth retardation with p21^{-/-} mice using physiological and histological measures of bone growth.

5.4 Materials and Methods

5.4.1 *In Vitro* Studies

5.4.1.1 Cell Culture

For experiments measuring the role of p21 in chondrocyte differentiation, the ATDC5 chondrocyte cell line was maintained and differentiated as previously described (Section 2.2.3) for up to 15 days. For studies examining p21 expression with GCs, Dex (final concentration 10^{-6} M) was added to both chondrogenic and terminally differentiating cells for 6, 12, or 24h. Control cells received differentiation medium only.

5.4.1.2 Cell Counting

In order to measure the growth of ATDC5 cells progressing towards terminal differentiation, cells were trypsinised and counted on days 0, 3, 7, 11, 14, and 18 of differentiation as described in section 2.2.3. Six replicates were used for each timepoint.

5.4.1.3 PCR

To measure the expression of CDKIs during ATDC5 differentiation, RNA was isolated from the cells at days 0, 2, 4, 7, 9, 11 and 15, and extracted as previously described (2.5.1). For analysis of p21 expression following Dex treatment, RNA was isolated by the same method. All samples were then reverse transcribed (2.5.3), and both qPCR and Endpoint-PCR reactions were carried out as detailed in sections 2.5.4 and 2.5.5, respectively. The primers for the endpoint PCR analysis of different CDKIs and chondrocyte marker genes during ATDC5 differentiation were as detailed in Table 5.1. The cycling reaction for all primers was as follows: 1 cycle of 92°C for

2mins, 55°C for 1min and 72°C for 1min, followed by 30 cycles of 92°C for 1min, 55°C for 1min and 72°C for 1min.

Table 5.1 Primer Sequences and product sizes for CDKIs and chondrocyte marker genes analysed by PCR

Gene Name	Primer Sequences (5' – 3')	Product Size (bp)
p21	F AATCCTGGTGATGTCCGACC R TTGCAGAAGACCAATCTGCG	460
p27	F TATGGAAGAAGCGAGTCAGC R GCGAAGAAGAATCTTCTGCAG	334
p57	F GGATTGTGGAGGCTTTCTCC R CTTGGCGATCATGTCCTCAAAG	309
p18	F GGACACTGTACAGGCTTTGC R TTCCATAGAACCTGGCCAAG	197
p19	F GCGACGTGCAAGAGGTCCG R GCTGACCACGGAGCTATGGC	318
Coll X	F AGGCAAGCCAGGCTATGGAA R GCTGTCCTGGAAAGCCGTTT	583
Aggrecan	F CGAGAATGACACCTGCTAGG R AAGAAGACAGGACCAGGAAGG	218
18S	Unknown, purchased from Ambion	488
p21 qPCR	F TTGCACTCTGGTGTCTGAGC R F TCTGCGCTTGGAGTGATAGA R	112
Coll II qPCR	F GCCAAGACCTGAACTCTGC R F GGTGGGGTAGACGCAAGTC R	123

5.4.1.4 Western Blotting

For analysis of p21 protein expression, ATDC5 cells were scraped at days 0, 2, 4, 7, 9, 11 and 15, or after 6h Dex treatment (10^{-6} M) in PBS containing 1.6 mg/ml of Complete[®] protease inhibitor cocktail, and protein concentration measured as previously described (2.7.1). Proteins were then separated on a 4-12% Bis-Tris Gel (Invitrogen) by SDS-PAGE (2.7.2), and Western blotting carried out as previously described (2.7.3). For analysis of p21 expression, monoclonal mouse anti-p21 (BD Pharmingen; Appendix 4) was used at a 1:250 dilution, and this was detected with a goat anti-mouse IgG peroxidase secondary antibody, at a dilution of 1:8000 (Sigma;

Appendix 4). Beta-actin expression was also measured as a loading control (Anti beta-actin clone AC15; Sigma; 1:5000 dilution).

5.4.2 *In Vivo* Studies

5.4.2.1 p21 Null Mice Genotyping

Genotyping for transgenic mice was carried out on tail clippings from mice no younger than 3 weeks of age, as detailed in section 2.6.2. Heterozygous p21 null mice were identified by bands at 872bp and 700bp, wildtype mice by one band at 700bp, and mice homozygous for the p21^{-/-} allele by one band at 872bp (Figure 5.2)

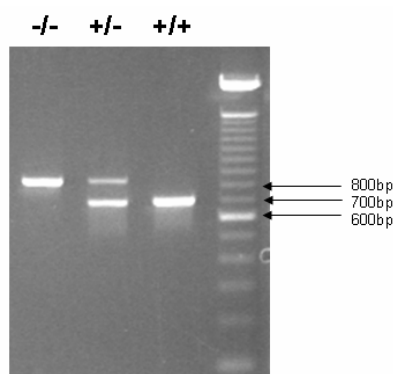


Figure 5.2 Genotyping of p21 null homozygous and heterozygous mice. Heterozygous p21 null mice were identified by bands at 872bp and 700bp, wildtype mice by one band at 700bp, and mice homozygous for the p21^{-/-} allele by one band at 872bp. Amplified products were loaded onto a 1.5% tris-acetate gel.

5.4.2.2 *In Vivo* Treatment of Mice with Dex

For all GC-growth retardation studies, 4-week-old mice underwent an injection regime of 5mg/kg subcutaneous (sc) Dex daily for 7 days (water soluble Dex; Sigma lot 105K1411; dissolved in 0.9% saline (NaCl)). Control mice received an equal volume of 0.9% NaCl. In addition, all mice received a single intra-peritoneal (ip) injection of calcein (10mg/kg in sodium bicarbonate (NaHCO₃)) on day 1, and BrdU (25mg/kg in NaCl; sc) exactly 1h before being culled. Although double calcein labelling (with one injection of calcein at the start of an experiment, and another just

before culling) is more common when measuring mineral apposition in skeletal tissue this was not necessary in this study due to the obvious demarcation of the chondro-osseous junction at the distal end of the growth plate. During the 7-day treatment period, mice were weighed daily, and crown-rump body lengths measured on days 1 and 7. Mice involved in the p21^{-/-} study also received x-rays at days 0, 3, and 6 of Dex treatment. In order to take the x-rays, the mice were placed into a Vet-Tech box where they were given Halothane gas. Once anaesthetised sufficiently, the mice were placed under the x-ray beam, and the x-ray taken at a setting of 5.0mas and 50Kv. All mice were culled by cervical dislocation at the end of the experiment.

5.4.2.3 Measurement of Organ Weights and Lengths

Directly following culling, left and right tibia were dissected, weighed, and measured using digital calipers. In addition, the spleen, heart, kidneys, and liver were also removed and weighed to analyse the effect of Dex.

5.4.2.4 Tissue Processing

As described above, both the left and right proximal tibiae were dissected from each mouse. The left tibia was decalcified and processed for embedding in paraffin wax and sectioned as described in section 2.4.1. The right tibia was left undecalcified, and frozen in a hexane freezing bath, before sections were cut using the CryoJane tape transfer system as previously described (2.4.2.1 – 2.4.2.4).

5.4.2.5 Toluidine Blue Analysis of Growth Plate Morphology

Paraffin sections of the proximal tibia were dewaxed through graded alcohol solutions as described in section 2.4.3, and stained for Toluidine blue as described in section

2.4.4. Stained sections were then examined under a Nikon Eclipse TE300 microscope, and the lengths of the proliferating and hypertrophic zones measured at 10 different sites along the length of the growth plate. The identification of sections were hidden with masking tape during analysis to avoid bias. However, it should be noted that this type of analysis is dependent on the angle at which tissues are embedded into the paraffin wax, as variations in the angle at which sections are cut can significantly alter the observed growth plate width. Consequently, when embedding, care was taken to ensure all tissues were embedded and cut at approximately the same angle.

5.4.2.6 Analysis of X-rays

X-rays of p21^{-/-} and wildtype mice were taken at days 0, 3, and 6 of Dex treatment as previously described (5.4.6). X-rays were scanned using the Kodak LS-75 film scanner, and images converted from DICOM to TIFF files using the programme IrfanView (www.irfanview.com). ImageJ was then used to measure the lengths of tibiae, femur, and tails from the TIFF x-ray files.

5.4.2.7 Measurement of Mineral Apposition Rate (MAR) with Calcein Labelling

Calcein labelling was used to measure the rate of bone formation in control and Dex treated mice during the 7-day treatment period. Mice were injected with a single dose of 10mg/kg Calcein fluorochrome on day 1 of Dex treatment as previously described (5.4.2.2). Tibia were dissected and frozen sections cut as previously described (2.4.2.1-2.4.2.4), and sections were examined for fluorescence using the Nikon Eclipse TE300 microscope. The distance between the chondro-osseous junction at the distal end of the growth plate and the fluorescing mineralisation front was

measured at 10 different points along the section, and an average taken. This was then divided by the number of days of treatment, to obtain a MAR for each section. Four sections per tibia were measured from 6 mice per treatment.

5.4.2.8 Laser Capture Microscopy

In an attempt to measure p21 gene expression within the proliferative and hypertrophic zones of the growth plate, sections (10 μ m) from undecalcified frozen proximal tibiae were cut using the CryoJane tape transfer system (2.4.2.6), and chondrocytes from both the proliferative and hypertrophic zones of 12 sections per mouse were isolated using LCM as previously described (2.4.2.7) (Figure 5.3). RNA was pooled, extracted from the chondrocytes (2.5.2), and amplified using the MessageAmp RNA amplification kit (2.5.3). The aRNA was then reverse transcribed, and qPCR for chondrocyte marker genes aggrecan and Coll II, and p21 carried out as previously described (2.5.4 and 2.5.6; primer details section 5.4.1.3).

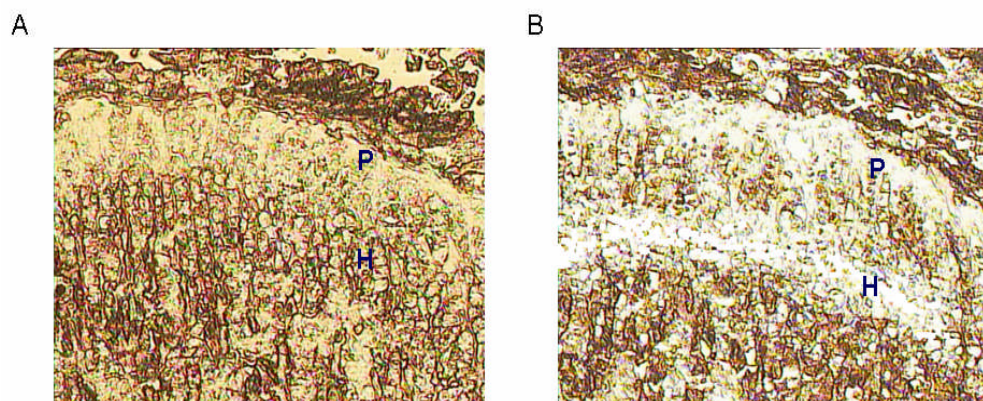


Figure 5.3 Laser Capture Microscopy (LCM) of proliferating and hypertrophic chondrocytes. (A) Proximal tibia growth plate section before LCM highlighting the proliferative (P) and hypertrophic (H) zones. (B) Proximal tibia growth plate section after LCM highlighting the removal of both zones, with only the prehypertrophic chondrocytes remaining.

5.5 Results

5.5.1 *In Vitro* Studies

5.5.1.1 Analysis of p21 Expression During ATDC5 Differentiation

During the 15 days of ATDC5 differentiation, expression of the hypertrophic chondrocyte marker gene aggrecan increase, as expected (Figure 5.4A). Of all the CDKIs analysed, only the expression of p21 increased as the cells progressed towards differentiation. The expression of p27, p27, p15 and p19 remained unchanged (Figure 5.4A). The increase in p21 expression during differentiation was confirmed by qPCR, with a 4-fold increase in expression by day 11 ($p < 0.01$; Figure 5.4B). p21 protein expression was also increased in ATDC5 cells at days 9 and 15 of differentiation (Figure 5.4C), at which point cell proliferation had ceased (Figure 5.4D).

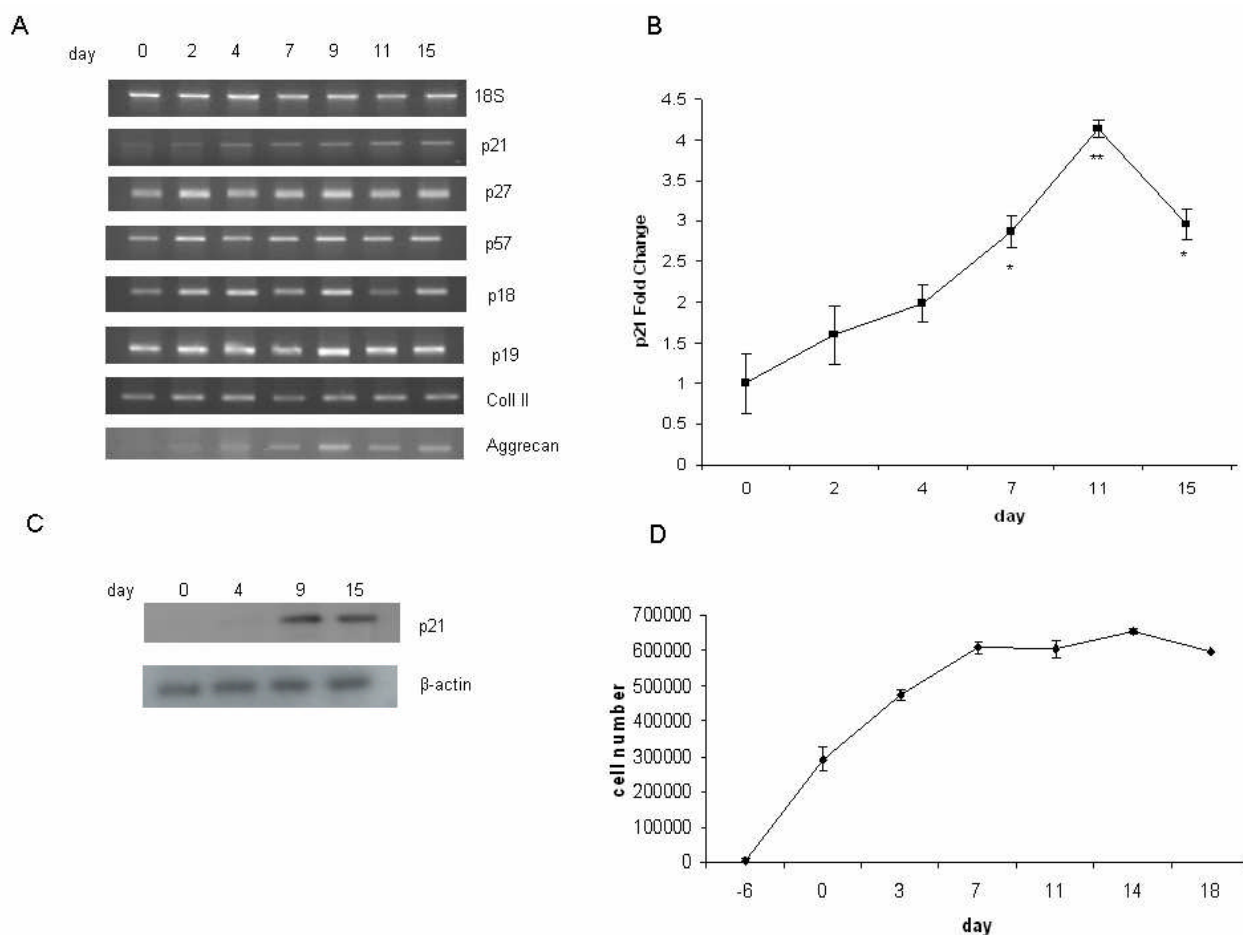


Figure 5.4 Expression of CDKIs during ATDC5 differentiation. (A) Of the CDKIs tested, only p21 expression increased as the cells progressed towards terminal differentiation. Expression of the chondrocyte marker gene, aggrecan, also increased. Samples were run on a 1.5% Tris-acetate gel. (B) p21 fold change in differentiating ATDC5 cells as measured by qPCR. (** $p < 0.01$; * $p < 0.05$ $n = 3$ separate cell replicates run in triplicate; all data are expressed as mean \pm SEM). (C) p21 protein expression in ATDC5 cells. β -actin was used as a loading control. (D) Proliferation in ATDC5 cells as measured by directly counting in a haemocytometer chamber.

5.5.1.2 p21 Expression in ATDC5 Cells Following Dex Treatment

Both p21 gene and protein expression were increased in ATDC5 cells following 1h and 6h Dex treatment, as measured by qPCR and Western Blotting, respectively (Figures 5.5A and B). qPCR revealed a 3.8-fold and 2-fold increase in p21 expression with 1h and 6h Dex treatment, respectively ($p < 0.01$; Figure 5.5A), although no change in expression was observed at 24h.

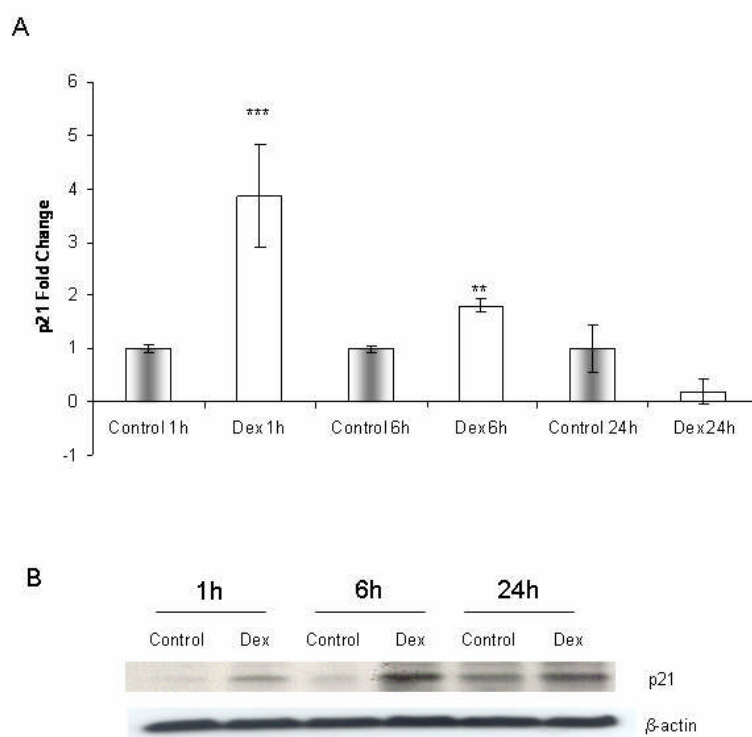


Figure 5.5 p21 expression with Dex treatment in ATDC5 cells. (A) qPCR analysis revealed a significant increase in p21 expression at 1h, and 6h Dex treatment. No change in expression was observed at 24h. (** $p < 0.01$; *** $p < 0.001$; $n = 3$ cell replicates run in triplicate; all data are expressed as mean \pm SEM). (B) p21 protein expression was also increased following 1h and 6h Dex treatment, but not at 24h. Expression of β -actin loading control remained unchanged.

5.5.2 *In Vivo* Studies

5.5.2.1 Growth in Dex-Treated Mice

In order to establish a dosing regime for future *in vivo* experiments, saline and Dex-treated mice were weighed daily for 7 days and crown-rump lengths measured. Dex-treated mice were significantly lighter than control mice from day 3 of treatment (14.5g and 17g, respectively; $p < 0.001$; Figure 5.6A), and by day 7, the body lengths of Dex-treated mice were also significantly shorter than control mice (7.6cm and 8.2cm, respectively; $p < 0.001$; Figure 5.6B)

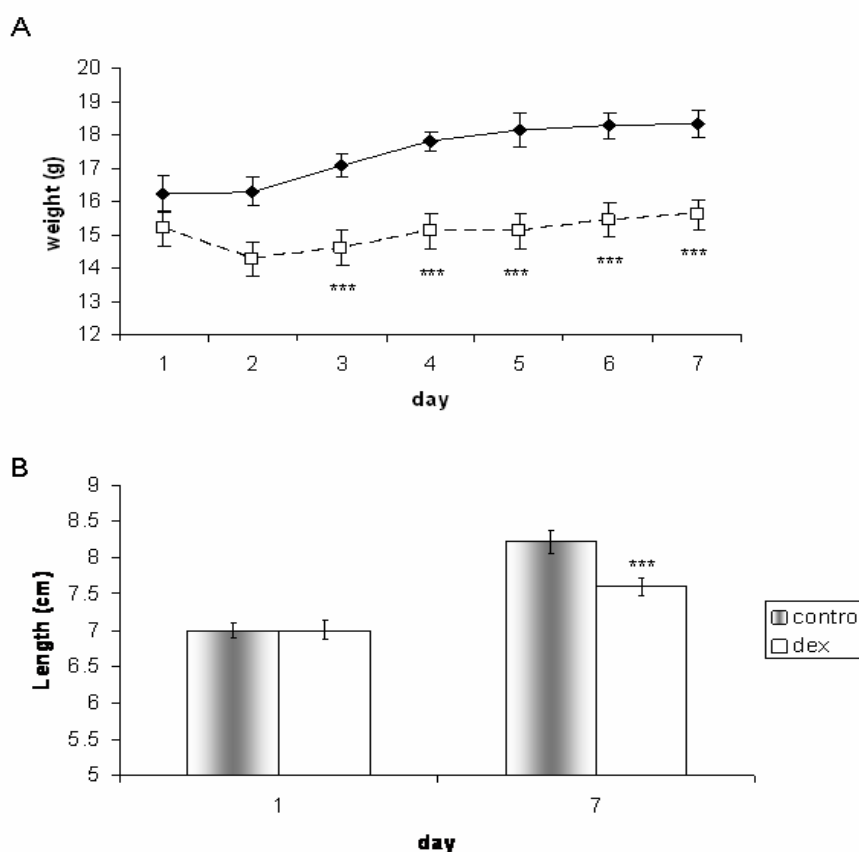


Figure 5.6 Skeletal growth in Dex-treated mice (A) 4-week-old mice were injected daily for 7 days with 5mg/kg Dex or 0.9% NaCl, and weighed each day. Dex-treated mice were significantly smaller from day 3 of treatment. (B) Dex-treated and control mice were measured from crown to rump at days 1 and 7 of treatment. The body lengths of Dex-treated mice were significantly shorter after 7 days (***) ($p < 0.001$; $n = 8$ mice; all data are expressed as mean \pm SEM).

5.5.2.2 Effect of Dex on Organ Weight

Organ weights were first normalised to the overall body weight for each mouse, and multiplied by 1000 for ease of data analysis. The weight of the liver and spleen were significantly reduced in Dex-treated mice compared to their control littermates ($p < 0.01$; Figure 5.7). Tibiae were also dissected from control and Dex-treated mice, and when weighed, the weights of Dex-tibiae were significantly reduced (39mg for

Dex-treated mice compared to 50mg for control mice; $p < 0.05$; Figure 5.7). Dex had no effect on the weight of the kidney or heart compared to control mice.

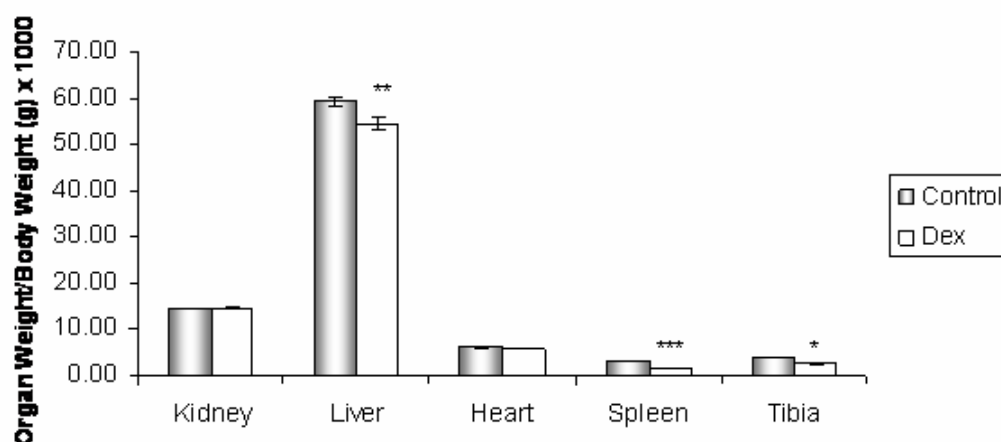


Figure 5.7 Effect of Dex on mouse organ weights. Organs were dissected, weighed, and normalised to the overall body weight for each mouse. Weights of the spleen, liver and tibia were significantly reduced with Dex treatment, whilst weights of the kidney and heart were unaffected ($***p < 0.01$; $**p < 0.01$; $*p < 0.05$; $n = 8$ organs; all data are expressed as mean \pm SEM).

5.5.2.3 Effect of Dex on Growth Plate Morphology

To analyse the effect of Dex on the growth plate, proximal tibia growth plate sections from control and Dex-treated mice were stained for Toluidine blue (Figure 5.8A and B, respectively). Dex significantly reduced the overall width of the growth plate, due to a reduction in the width of both the proliferative and hypertrophic zones ($p < 0.001$; Figure 5.8C).

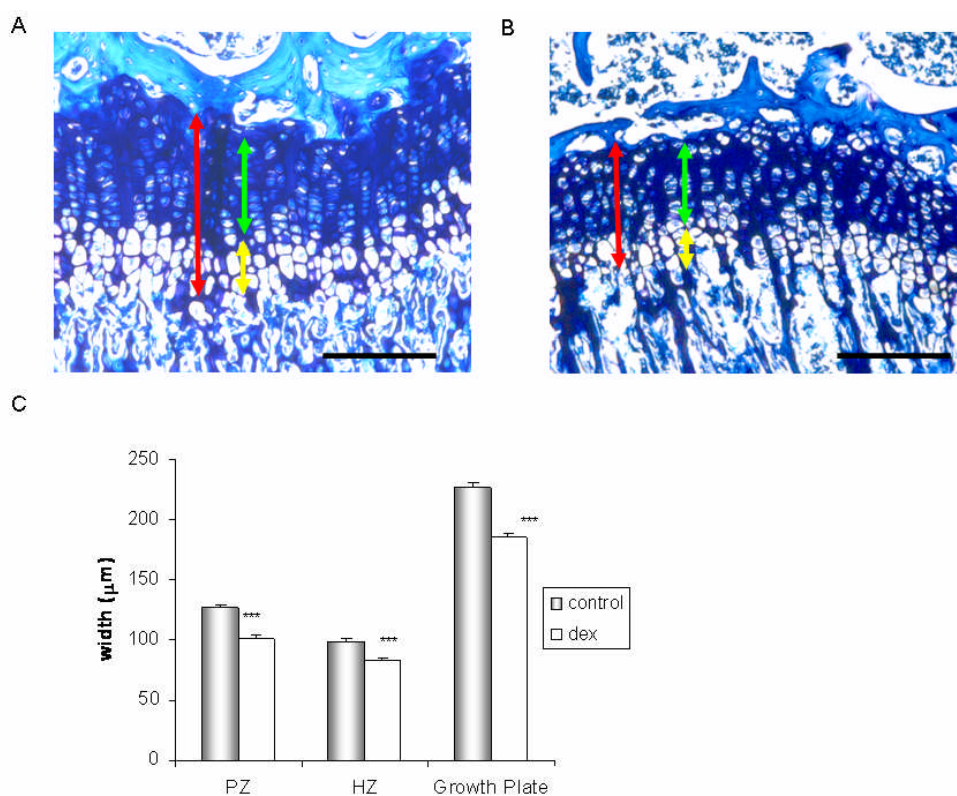


Figure 5.8 Toluidine Blue staining of the Growth Plate in Dex-treated mice Proximal tibia growth plate sections from control (A) and Dex-treated (B) mice were stained with toluidine blue for analysis of growth plate morphology and zone width. Scale bar = 200μm (C) The widths of both the proliferating and hypertrophic zones were significantly reduced in Dex-treated mice, resulting in a reduction in the overall growth plate width. (PZ = proliferating zone; HZ = hypertrophic zone) (***) $p < 0.01$ versus control; $n = 8$; all data are expressed as mean \pm SEM).

5.5.2.4 Analysis of p21 Expression in the Growth Plate

Due to the fact that p21 has previously been shown to be expressed at high levels in the hypertrophic zone of the growth plate (Stewart *et al.*, 1997), numerous attempts were made to confirm these findings, and to analyse the expression of p21 in the growth plate of Dex-treated mice. However, despite using various different antibodies against p21, I failed to show staining that was consistent with previous studies. Consequently, an attempt was made to compare the relative expression of p21 in the proliferative and hypertrophic zones in Dex-treated mice by qPCR. Chondrocytes were isolated from each zone by LCM, and the RNA was extracted and

amplified as described previously (5.4.2.8). Although chondrocytes were successfully isolated from each zone (Figure 5.3), the RNA obtained was of very poor quality, with 260/280 ratios varying between 0.29 and 2.42, and average total RNA yields of 20ng. In order for amplification to perform effectively, it is vital that the RNA is of good quality. Consequently, when amplification was carried out, although some samples were amplified successfully, others were not, making it impossible to analyse the expression of chondrocyte marker genes or p21 by endpoint or qPCR.

5.5.2.5 Growth in Dex-treated p21^{-/-} Mice

In order to study the role of p21 in GC-induced growth retardation, mice lacking the p21 gene were injected daily for 7 days with 5mg/kg Dex or 0.9% NaCl as previously described (5.4.2.2). Wildtype mice received identical treatments. By day 4, the growth of both p21^{-/-} and wildtype mice undergoing Dex treatment was significantly reduced compared to their control littermates ($p < 0.001$; Figure 5.9). This growth retardation was maintained until day 7.

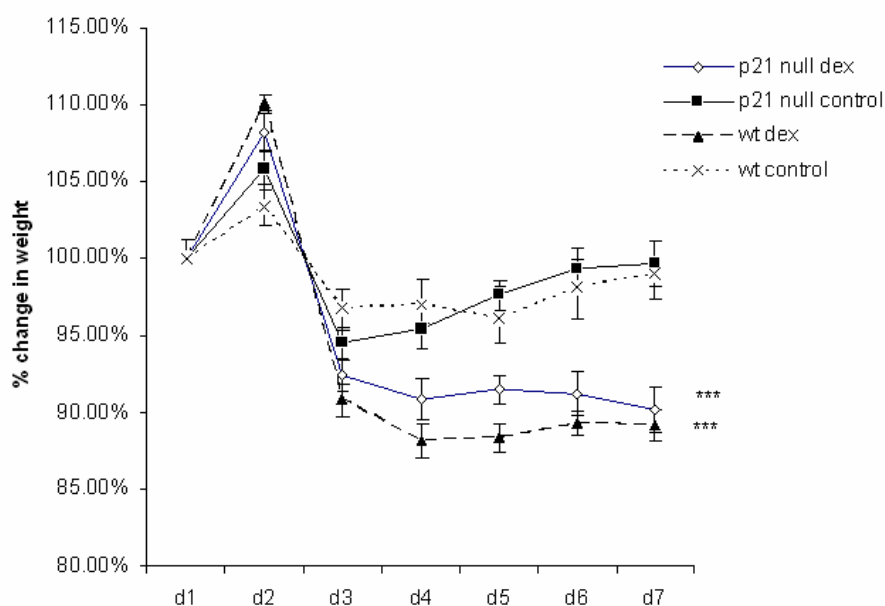


Figure 5.9 Growth in $p21^{-/-}$ Dex-treated mice $p21^{-/-}$ and wildtype mice were treated with 5mg/kg Dex for 7 days, and weighed daily. By day 4, the weights of both null and wildtype mice treated with Dex were significantly reduced compared to NaCl controls. (***) $p < 0.01$; $n = 8$; all data are expressed as mean \pm SEM).

5.5.2.6 Skeletal Growth of Dex-treated $p21^{-/-}$ mice – X-ray Analysis

X-rays of $p21^{-/-}$ and wildtype mice treated with 5mg/kg Dex were taken on days 0, 3 and 6 as described previously (5.4.2.2; Figure 5.10A). Lengths of the tibiae, femurs and tails for each day were measured with ImageJ (5.4.2.6). Tibia lengths in Dex-treated null and wildtype mice were slightly shorter than their respective controls, however this was not a significant change (Figure 5.10B). Similarly, when the lengths of the tibiae, femurs, and tails from each of the groups were combined, there did seem to be a reduction in bone growth in Dex-treated null and wildtype mice. However, this reduction was not significantly different (Figure 5.10C).

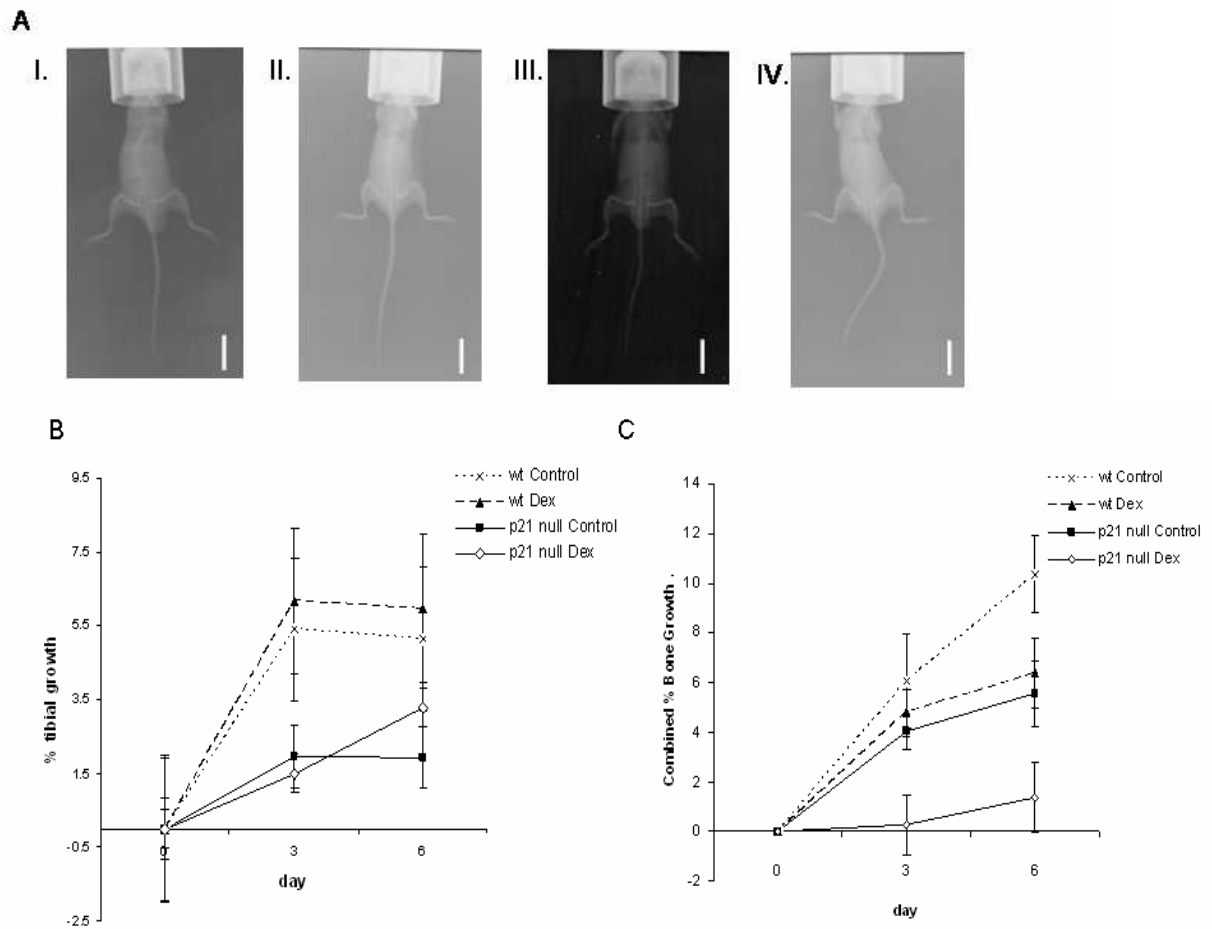


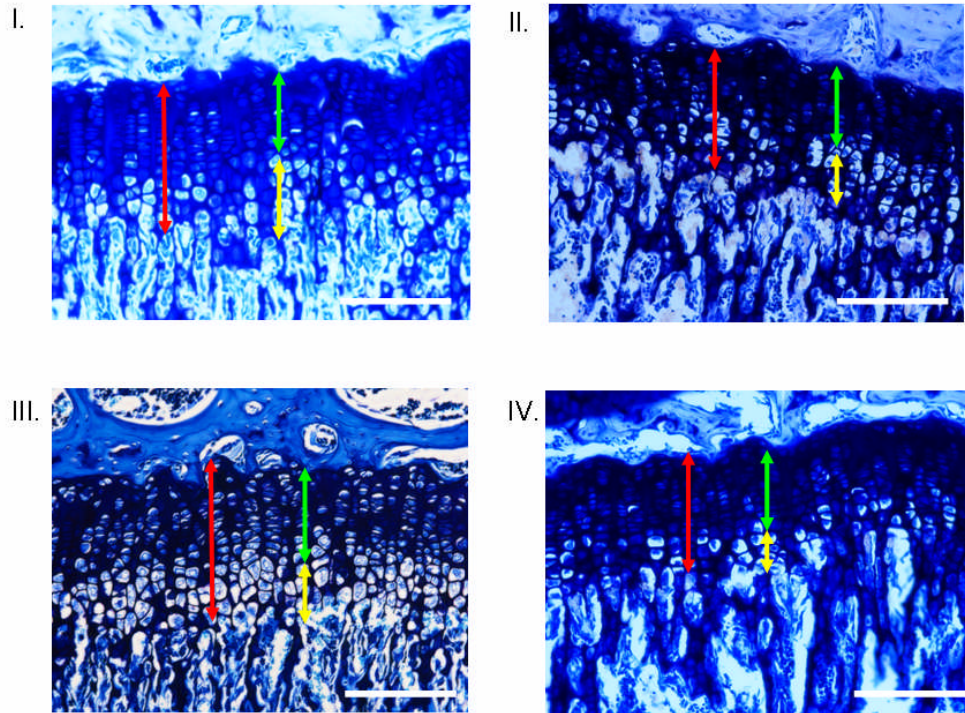
Figure 5.10 Skeletal growth of Dex-treated p21 null mice (A) Representative x-rays from (I) wildtype control, (II) wildtype Dex-treated, (III) p21^{-/-} control and (IV) p21^{-/-} Dex-treated mice on day 6. Scale bar = 2cm. **(B)** Percentage tibial growth from day 0 for p21^{-/-} and wildtype mice treated with or without Dex **(C)** Percentage growth of combined values from tibiae, femurs and tails of Dex-treated p21 null and wildtype mice (n = 8; all data are expressed as mean ± SEM).

5.5.2.7 Growth Plate Morphology in Dex-treated p21 Null Mice

As before, Dex significantly reduced the width of the growth plate in wildtype mice, due to a reduction in the width of both the proliferative and hypertrophic zones (p<0.001; Figure 5.11A I and II; Figure 5.11B). A similar response to Dex was observed in the growth plates of p21^{-/-} mice, with a significant reduction in the width of the proliferating and hypertrophic zones, leading to a reduction in overall growth plate width (p<0.001; Figure 5.11A III and IV; Figure 5.11B). Interestingly, the hypertrophic zone in p21^{-/-} control mice was also significantly smaller than the

hypertrophic zone in control wildtypes ($p < 0.05$; Figure 5.11A I and III; Figure 5.11B).

A



B

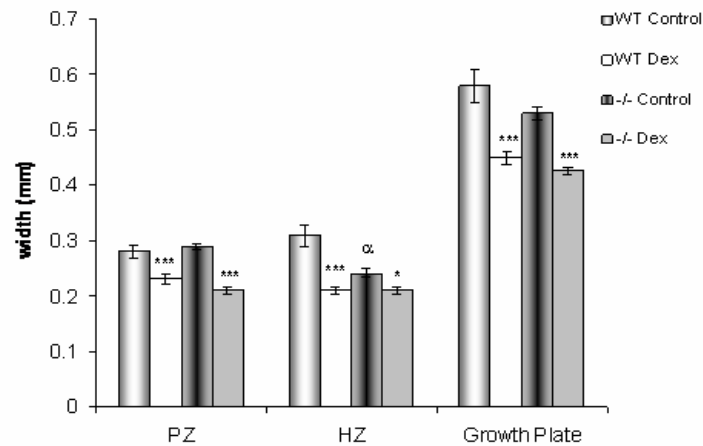


Figure 5.11 Toluidine Blue staining of growth plates from Dex-treated p21 null mice. (A) Proximal tibia growth plate sections from control wildtype (I), Dex-treated wildtype (II), p21 null control (III) and Dex-treated p21 null (IV) mice stained with toluidine blue for analysis of growth plate morphology and zone width. Scale bar = 200 μ m (B) The widths of both the proliferating and hypertrophic zones were significantly reduced in Dex-treated mice from both wildtype and p21 null strains, resulting in a reduction in the overall growth plate width. (PZ = proliferating zone; HZ = hypertrophic zone) (***) $p < 0.001$ versus respective control group; *) $p < 0.05$ versus respective control group; ^α $p < 0.05$ versus wildtype control HZ; $n = 8$; all data are expressed as mean \pm SEM).

5.5.2.8 Effect of Dex on Mineral Apposition in p21^{-/-} Mice

The daily rate of mineral formation (MAR) was measured using a Calcein fluorochrome label as previously described (5.4.2.7). The MAR in proximal tibiae from Dex-treated wildtype and null mice was significantly reduced compared to control mice (51% and 27% reduction, respectively; $p < 0.05$; Figure 5.12A and B). Interestingly, the MAR in p21^{-/-} control mice was also significantly reduced compared to wildtype controls (38%; $p < 0.05$; Figure 5.12A).

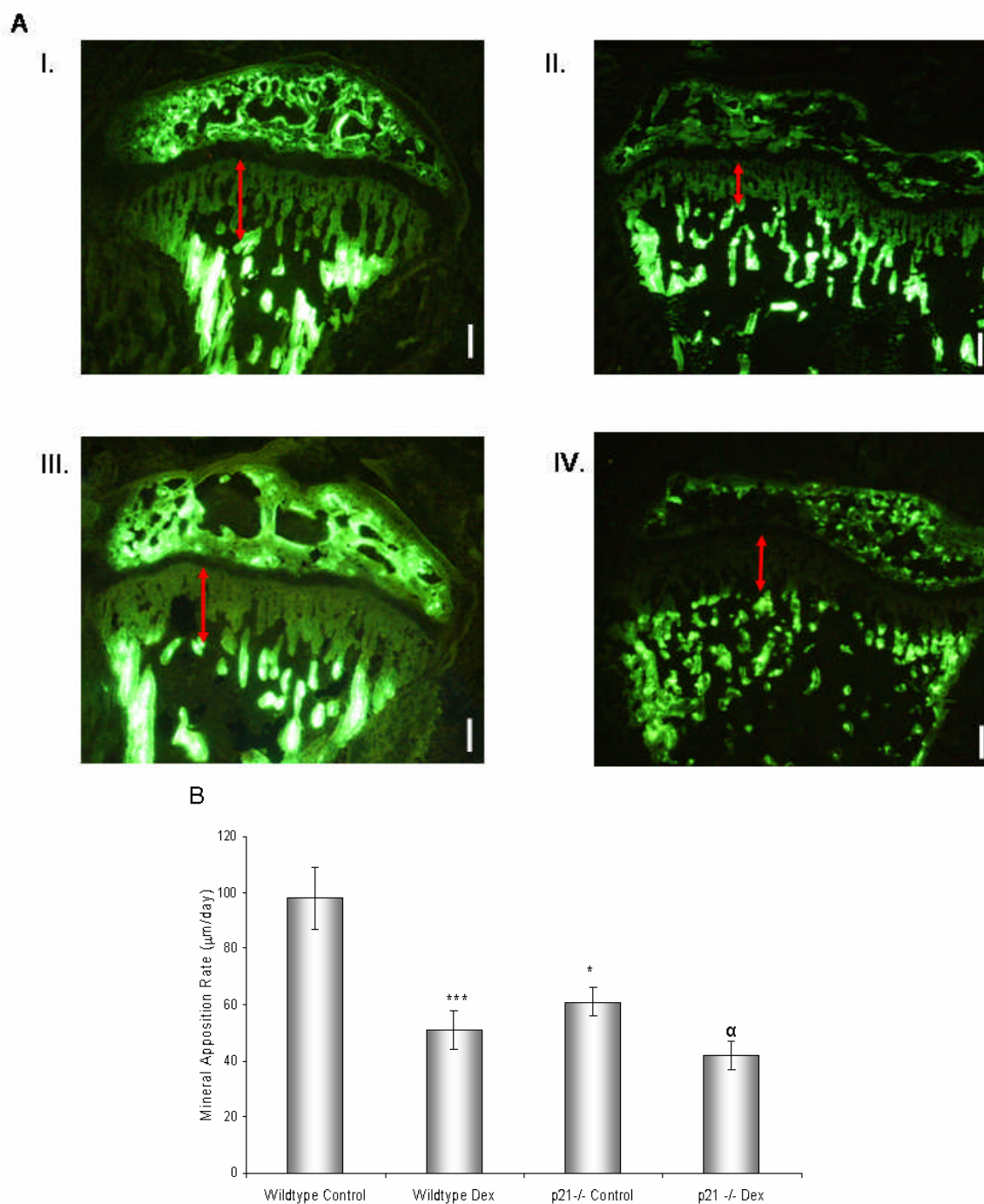


Figure 5.12 Calcein labelling in Dex-treated p21^{-/-} mice (A) Proximal tibia sections from control wildtype (I), Dex-treated wildtype (II), p21 null control (III) and Dex-treated p21 null (IV) mice examined under fluorescence for analysis of the mineral apposition rate. The MAR was calculated by measuring the distance between the distal end of the growth plate and the mineralisation front (green fluorescence), and dividing this by the number of treatment days. Scale bar = 500µm (B) MAR in wildtype and p21 null mice treated with Dex. The MAR was significantly reduced with Dex treatment in both wildtype and null mice (***) $p < 0.01$, (*) $p < 0.05$ vs. WT control; α $p < 0.05$ vs. p21^{-/-} control; all data are expressed as mean \pm SEM).

5.6 Discussion

Previous findings by us, and others, have suggested that GCs may act to inhibit bone growth by causing premature differentiation of growth plate chondrocytes (Mushtaq *et al.*, 2002; James *et al.*, 2007; Chapters 3 and 4). p21 is a CDKI that has previously been shown to increase in expression in differentiating chondrocytes (Negishi *et al.*, 2001; Stewart *et al.*, 1997), a finding that has been supported in this study. In ATDC5 cells, p21 gene and protein expression increased throughout the differentiation process, whereas the expression of all other CDKIs tested remained unchanged. As a CDKI, p21 controls the cell cycle by blocking the formation of Cyclin/CDK complexes which promote cell cycle progression through the phosphorylation of pocket proteins pRb (Retinoblastoma protein), p107 and p130. Once phosphorylated, these pocket proteins form complexes with E2F transcription factors, leading to the transcription of genes necessary for cell cycle progression and DNA replication.

Consequently, it is thought that the main function of p21 is the inhibition of cell proliferation and promotion of differentiation (Harper *et al.*, 1995). At high concentrations, p21 also acts as an inhibitor of proliferating cell nuclear antigen (PCNA) activity, a characteristic which is unique to p21, distinguishing it from other CDKIs (Luo *et al.*, 1995). A number of studies have correlated the expression of p21 with cell cycle arrest and/or differentiation in many cell types after treatment with extracellular growth regulators, exposure to particular environmental conditions, or by ectopic expression of intracellular modulators of the cell cycle (Sherr 1995; Harper and Elledge 1996). p21 is under transcriptional control by the p53 tumour suppressor gene, and the p21 promoter contains two p53 binding sites that are conserved in several species. For p53-dependent activation, at least one of these sites must be

functioning (El-Deiry *et al.*, 1995). p53 dependent activation of p21 has been shown to be critical in response to DNA damage, although during development, p21 expression is normal in p53^{-/-} mice. p21 activation can also occur independently of p53, and there are many factors involved in the activation of p21 at the transcriptional level. These include vitamin D receptor (Liu *et al.*, 1996), retinoic acid receptor (Liu *et al.*, 1996), TGF- β 1 and the AP2 (Zeng *et al.*, 1997), E2A (Prabhu *et al.*, 1997), Sp1, Sp3 and STAT1 transcription factors through their respective response elements on the p21 promoter (Figure 5.13) (El-Deiry *et al.*, 1993, 1994, 1995; Michieli *et al.*, 1994). Other factors include nerve growth factor (Erhardt *et al.*, 1998), platelet-derived-growth factor (Michieli *et al.*, 1994), progesterone (Owen *et al.*, 1998), and steroid hormones (Jiang *et al.*, 1994). In specific osteosarcoma and fibroblast cell lines, GCs have been shown to increase p21 expression through unknown mechanisms. GC inhibition of L929 mouse fibroblast proliferation was associated with an induction of p21 expression (Ramalingam *et al.*, 1997), and GCs were also shown to inhibit the entry of alveolar epithelial cells into the S-phase by inducing p21 expression (Corroyer *et al.*, 1997).

In this study, Dex significantly increased p21 gene and protein expression after 1 and 6 hours in ATDC5 cells. The rapid response in p21 expression with Dex is not surprising, as it has previously been shown that GCs stimulate p21 promoter activity. Although no GREs have been detected on the p21 promoter, it is thought that Dex acts through the C/EBP α transcription factor to directly increase p21 transcription (Figure 5.13) (Cha *et al.*, 1998; Cram *et al.*, 1998). It is possible that this increase in p21 expression with Dex-treatment could contribute to GC-induced growth retardation. In order to test this hypothesis, the effect of Dex on skeletal growth was

analysed in mice lacking the p21 gene. Before this, however, it was necessary to develop a Dex dosing regime that effectively caused growth retardation in 4-week-old mice.

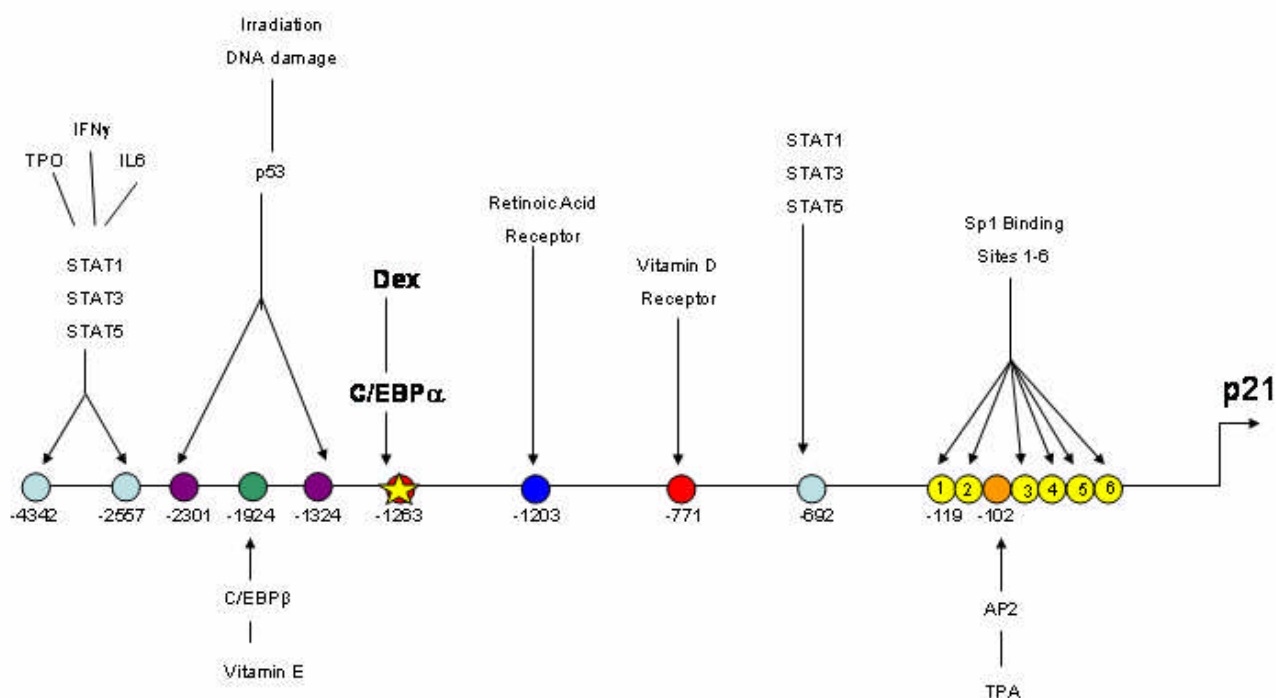


Figure 5.13 Factors acting on the p21 promoter A number of factors act to transcriptionally activate or repress p21 expression. The two p53 binding sites at positions 2301 and 1324 are critical for p21 expression during DNA damage and irradiation. Dex increases p21 expression through the transcription factor C/EBP α at position 1263. Figure adapted from Gartel *et al.*, 1999.

Injecting mice with 5mg/kg Dex daily for 7 days caused a significant reduction in growth by day 3 of treatment. The weights of the tibia, liver and spleen were significantly reduced in Dex treated mice, a finding that has previously been reported (Smink *et al.*, 2003a; Van Buul-Offers *et al.*, 2005). The reduction in spleen weight is most likely due to its known role in the immune response, and the effects on the liver may be due to its roles in drug metabolism. The reduction in weight of the tibia suggests that tibial growth was reduced, possibly due to a reduction in the width of the

proliferative and hypertrophic zones within the growth plate. This effect on the growth plate has been widely reported, (Smink *et al.*, 2003a; Smink *et al.*, 2003b; Van Buul-Offers *et al.*, 2005) and is probably due to a reduction in chondrocyte proliferation, as shown in Chapter 4, and by previous studies (Robson *et al.*, 1998; Klaus *et al.*, 2000; Mushtaq *et al.*, 2002; Owen *et al.*, 2007), in addition to an increase in chondrocyte apoptosis, and possibly a reduction in IGF-I expression (Smink *et al.*, 2003).

When this dosing regime was implemented in 4-week old mice lacking the p21 gene, significant growth retardation was still observed. As previously reported, p21^{-/-} mice have no obvious skeletal phenotype (Deng *et al.*, 1995), an interesting finding which has also been shown in mice lacking the p27 gene (Emons *et al.*, 2006). Although p21^{-/-} generally seemed smaller than their wildtype littermates, the width of the proliferating and hypertrophic zones within the growth plate were not significantly different. Interestingly, however, the MAR in p21^{-/-} control tibiae was significantly lower than wildtypes, suggesting that p21 may act on other factors involved in mineralisation. These findings suggest that p21 alone does not play a major role in longitudinal bone growth and endochondral ossification. It is possible that there may be considerable redundancy between the CDKIs, and that a number of CDKIs may act together to control chondrocyte dynamics in the growth plate. It would therefore be interesting to study skeletal growth in mice with numerous CDKI null mutations, such as p27^{-/-} and p21^{-/-} together.

When treated with Dex, the growth plate widths of p21^{-/-} mice were significantly reduced, due to a reduction in the width of both the proliferative and hypertrophic

zones, as observed in wildtype mice. Interestingly, when measuring longitudinal bone growth by x-rays throughout the treatment period, no significant changes in growth were observed in either mouse strain with Dex treatment. Previous studies have suggested that obvious skeletal differences are only observed after long-term GC treatment of up to 1 month (Smink *et al.*, 2003), although morphological cell changes within the growth plate are observed much earlier. Due to the size of the mice and the x-ray, it was difficult to accurately determine the beginning and end of the bone in question. Measuring skeletal growth using x-ray technology is also limited due to the large amount of variation in results that can arise from the distance between the mouse and the x-ray apparatus, differences in exposure between days, and similarly, differences in experimental procedure between the staff of the small animal unit between different days. An alternative measurement of skeletal growth during Dex treatment, such as tail length, may have highlighted changes between treatment groups, due to the large number of long bones, and hence growth plates present in murine tails. The mineral apposition rate was also reduced in Dex-treated mice from wildtype and p21^{-/-} groups, which is unsurprising when the reduction in growth plate width is taken into account. This finding has previously been shown (Fritz *et al.*, 1998), and an additional contributing factor is likely to be increased osteoblast apoptosis and increased survival of osteoblasts (Kim *et al.*, 2006).

5.7 Conclusions

The role of p21 in GC-induced growth retardation was studied due to the findings from this, and previous studies that p21 expression is increased in chondrocyte differentiation, and that p21 expression is increased with Dex. Findings from this study suggest that, although p21 seems to play a role in GC effects in ATDC5 cells, it

does not seem to be important in GC-induced growth retardation *in vivo*. A number of other cell cycle regulators have also been shown to be important in chondrocyte growth *in vitro*, such as p57 and p27, although their effects on skeletal growth *in vivo* are minimal. Although the cell cycle does play some role in the control of endochondral ossification, it is clear that a number of other factors are involved.

Chapter 6

The Growth Plate Sparing Effects of the Novel Glucocorticoid Receptor Ligand, AL-438

Chapter Contents

- 6.1 Introduction
 - 6.2 Hypothesis
 - 6.3 Aims
 - 6.4 Materials and Methods
 - 6.4.1 ATDC5 Proliferation in AL-438 treated cells
 - 6.4.2 Effect of AL-438 on Proteoglycan production in ATDC5 cells
 - 6.4.3 Alkaline Phosphatase Activity in AL-438 treated cells
 - 6.4.4 Expression of chondrocyte marker genes with AL-438
 - 6.4.5 Apoptosis in AL-438 treated ATDC5 cells
 - 6.4.6 Determination of anti-inflammatory efficacy of AL-438 in ATDC5s
 - 6.4.7 Foetal metatarsal organ culture
 - 6.4.8 Morphometric analysis
 - 6.4.9 Histological assessment of bromodeoxyuridine (BrdU) uptake
 - 6.4.10 Statistical Analysis
 - 6.5 Results
 - 6.5.1 Effect of AL-438 on ATDC5 cell number and proliferation
 - 6.5.2 Differentiation in AL-438 treated chondrocytes
 - 6.5.3 Effect of AL-438 on apoptosis in ATDC5 cells
 - 6.5.4 Chondrocyte Marker Gene Expression in AL-438 treated ATDC5 cells
 - 6.5.5 Anti-inflammatory efficacy of AL-438 in ATDC5 cells
 - 6.5.6 Longitudinal bone growth and assessment of chondrocyte maturational zone sites
 - 6.5.7 Effect of AL-438 on chondrocyte proliferation in metatarsals
 - 6.6 Discussion
 - 6.7 Conclusions
-
-

6.1 Introduction

Glucocorticoids (GC) are commonly used as anti-inflammatory or immunosuppressive treatments, and it has been estimated that 5-10% of children may require some form of GC therapy at some time in childhood (Warner 1995). Since the introduction of GCs in the treatment of rheumatoid arthritis over 50 years ago, the therapeutic applications of these drugs have greatly broadened to encompass a large number of non-endocrine and endocrine diseases (Hench *et al.*, 1949). Despite intense efforts in optimising therapy, adverse effects of GC medication are still common with growth impairment being one of the commonest in childhood (Mushtaq and Ahmed 2002).

Over the last several decades, attempts to improve the therapeutic window of GCs have focused on methods of limiting systemic exposure. These include the development of topical or inhaled agents such as budesonide, or the development of "antedrugs" such as fluticasone propionate that act at the site of administration but are transformed to inactive metabolites upon entry to the systemic circulation. Much effort has also been spent on modifying the steroid backbone of GCs in an attempt to reduce the side effect profile; however, these efforts have been met with little success. Deflazacort, a D-ring-substituted steroid otherwise similar to cortisol, was originally hyped as a powerful anti-inflammatory molecule exhibiting more selective activity, and therefore reduced adverse effects on bone and glucose metabolism. Initially, clinical data supported this notion (Markham *et al.*, 1995; Canalis *et al.*, 1992). However, subsequent trials that adjusted the steroid dose to maintain equivalent anti-inflammatory efficacy needed higher doses of Deflazacort that resulted in the re-occurrence of side effects (Markham *et al.*, 1995).

It has only been in the last 5-10 years, however, that an understanding of the molecular mechanism by which GCs elicit their biological effects has led to the development of structurally novel small molecule GR modulators that differentiate the anti-inflammatory properties from the metabolic side effects of GCs. The field was re-energised by the discovery that the likely mechanism of GR-mediated repression of pro-inflammatory genes involved the receptor binding directly to specific transcription factors (AP-1 and NFκB) involved in up-regulating inflammatory genes. This mechanism was genetically separable from transcriptional activation and led to the search of ligands that could induce transcriptional repression but impede transcriptional activation. In 1997, the first compounds that separated transactivation from transrepression were reported (Vayssiere *et al.*, 1997). These compounds (RU24858, RU40066 and RU24782) were steroidal in nature, were very efficient inhibitors of both AP-1 and NFκB-mediated gene induction, and were strong anti-inflammatory agents *in vivo*. However, subsequent *in vivo* studies revealed that, despite their promising *in vitro* profile, no therapeutic advantage could be demonstrated for these molecules. It was found that they were no better than Pred when side effects such as body weight, thymic involution and inhibitory effects at the growth plate of the femoral head were measured (Belvisi *et al.*, 2001).

The activation-repression hypothesis has also been used as an approach to discovering selective GR modulators. One such ligand discovered in this way was a compound created during a collaborative effort between Abbott Laboratories and Ligand Pharmaceuticals, named AL-438 (Abbott-Ligand 438) (Coghlan *et al.*, 2003). This ligand was shown to be a specific, non-steroidal ligand for the GR that exhibited a unique profile both *in vitro* and *in vivo*.

Although AL-438 possesses a tetracyclic core similar to classic GCs, there are several key structural differences that alter its functional activity. These include: the lack of a C-11-hydroxyl group mandatory for function in steroidal GR ligands; the absence of a C-3 ketone typically found in corticosteroids; the addition of a secondary amine function in AL-438 and the presence of a methoxy group in needed for GR selectivity and functional activity (Zhi *et al.*, 1998). These structural differences significantly alter the functional activity of AL-438 compared to other GCs such as Dex, allowing the activational properties to be separated from repression (Figure 6.1).

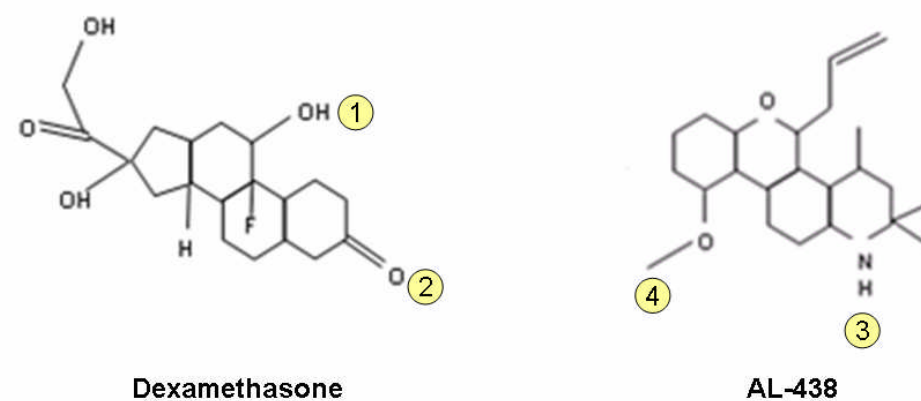


Figure 6.1 Structural differences between AL-438 and Dexamethasone Although AL-438 possesses a tetracyclic core similar to classic GCs, there are several key structural differences that alter its functional activity. (1) The lack of a C-11-hydroxyl group mandatory for function in steroidal GR ligands; (2) the absence of a C-3 ketone typically found in corticosteroids; (3) the addition of a secondary amine function in AL-438 and (4) the presence of a methoxy group in needed for GR selectivity and functional activity

AL-438 displayed similar affinity to Pred at the GR ($K_i = 2.5\text{nM}$ and 2.4nM , respectively), and was fully efficacious when repressing E-selectin activity compared to Dex (94% repression of activity compared to Dex). AL-438 is fully efficacious at the transcriptional repression of certain genes related to the anti-inflammatory aspect of GC activity (E-selectin and interleukin-6 (IL-6)), but is weaker (a partial agonist) for the transcriptional activation of certain genes linked to adverse side effects. This

activity seems to be cell-type specific, as, using other promoters in different cell backgrounds, AL-438 becomes more active as a transcriptional activator. In animal models, AL-438 was as efficacious as Pred at inhibiting inflammation, and importantly, AL-438 exhibited significantly reduced impact on fasting glucose levels compared with Pred, suggesting that this compound might not cause the diabetogenic effects of steroidal GCs (Coghlan *et al.*, 2003). Studies with AL-438 using the carrageenan-induced paw edema assay and the adjuvant arthritis models in rats have shown that it retains full anti-inflammatory efficacy but has reduced negative effects on bone compared to those elicited by Pred (Elmore *et al.*, 2001; Coghlan *et al.*, 2003,

6.2 Hypothesis

Due to the bone-sparing properties of AL-438 in osteoblasts, it is hypothesised that AL-438 will have reduced deleterious effects on growth plate chondrocyte dynamics compared with the effects of other commonly used GCs such as Dex and Pred.

6.3 Aims

- I. Compare the effect of AL-438 on chondrocyte proliferation and differentiation in ATDC5 cells with the commonly used GCs, Dex and Pred.
- II. Analyse the effect of AL-438 on longitudinal bone growth *in vitro* compared to Dex using the foetal mouse metatarsal culture model.
- III. Determine the anti-inflammatory efficacy of AL-438 in ATDC5 cells compared to Dex.

6.4 Materials and Methods

6.4.1 ATDC5 Proliferation in AL-438 Treated Cells

ATDC5 cells were maintained as previously described (2.2.3). Dex, Pred, AL-438 or 0.01% dimethyl sulphoxide (DMSO) (10^{-6} M, 10^{-7} M or 10^{-8} M) were added to the cells during both chondrogenesis (day 6) and terminal differentiation (day 13), and were incubated for 24h. Chondrocyte proliferation was measured using the [3 H]thymidine incorporation assay as previously described (2.9.1).

6.4.2 Effect of AL-438 on Proteoglycan production in ATDC5 cells

Dex, Pred and AL-438 (10^{-6} M) or 0.01% DMSO were added to ATDC5 cells at day 6 or day 13 for 96h. For analysis of proteoglycan production, ATDC5 cells were measured for alcian blue incorporation onto the monolayer as previously described (2.9.2).

6.4.3 Effect of AL-438 on Alkaline Phosphatase Activity

Dex, Pred and AL-438 (10^{-6} M) or 0.01% DMSO were added to ATDC5 cells at day 6 or day 13 for 96h. To measure ALP activity, cells were scraped and the supernatant was assayed for protein content and ALP activity as previously described (2.9.3).

6.4.4 Expression of Chondrocyte Marker Genes with AL-438

In order to study and compare the effects of AL-438 on chondrocyte marker gene expression, Dex, Pred and AL-438 were added to the cells during both chondrogenesis (day 6) and terminal differentiation phases (day 13) at a final concentration of 10^{-6} M in 0.01% (DMSO). Control cultures contained 0.01% DMSO only. Cells were grown in the presence of the compounds for 4 days, at which point

RNA was extracted, reverse transcribed and analysed for aggrecan gene expression by qPCR as previously described (2.5.5). Primers for aggrecan were obtained from SuperArray Bioscience (Maryland, USA; sequence unknown) and primers for GAPDH were designed using the software programme Primer3 (Whitehead Institute for Biomedical Research) (forward 5' TGAGGCCGGTGCTGAGTATGTCG 3', reverse 5'CCACAGTCTTCTGGGTGGCAGTG 3'). Briefly, cDNA (5ng) was amplified in triplicate using the Platinum SYBR Green qPCR SuperMix (Invitrogen, Paisley, UK) under the following conditions: cDNA was denatured for 2 minutes at 95 °C, followed by 40 cycles consisting of 15 s at 95°C and 30 s at 60°C and 1 cycle consisting of 1 min at 95°C and 30 s at 60 °C. Each reaction contained 10µl cDNA, 25µl Platinum SYBR Green qPCR Super-Mix, 1µl ROX Reference Dye, and 250nM primer in a total volume of 40µl. Fold changes, normalised for the expression of GAPDH, were calculated using the comparative method as previously described (2.5.5) (Livak *et al.*, 2001).

6.4.5 Apoptosis in AL-438 Treated ATDC5 Cells

Dex, Pred and AL-438 (10^{-6} M) were added to ATDC5 cells in a 6-well plate during chondrogenesis or terminal differentiation periods for 24h. As a positive control, cells were incubated as above with 10ng/ml TNF α (Autogen Bioclear, Wiltshire, UK). Apoptosis was then measured using the Caspase-3 Apoptosis assay, which was used according to the manufacturer's instructions (R&D Systems, Minneapolis, MN, USA). Caspase-3 is a cysteine protease that exists as a proenzyme, and is activated during apoptosis. Briefly, cells were scraped in their own medium and transferred to Eppendorfs. The cells were then centrifuged at 17,900 x g for 2mins, the supernatant removed and 75µl of lysis buffer added to the pellet. This was incubated for 10mins

at 4°C, and centrifuged again at 10000g for 1min. The supernatant was then transferred to a fresh Eppendorf and kept on ice. 50µl of this supernatant was added to wells in duplicate in a 96-well plate, along with 50µl reaction buffer plus DTT (10µl per 1ml reaction buffer), and 5µl substrate. The 96-well plate was then incubated for 2h at 37 °C and read at 405nm. Following this, the protein content of the cell lysates was measured as previously described (2.7.1).

6.4.6 Determination of Anti-inflammatory Efficacy of AL-438 in ATDC5 Cells

ATDC5 cells were grown in 10µg/ml LPS (Lot 104K4036; from EColi 0127:B8; Sigma) with or without Dex or AL-438 (10^{-6} M) for 24h. The medium was removed and analysed for levels of IL-1, IL-6 and TNF-α by Luminex technology (assay completed by Dr Alistair Gracie, Division of Immunology, Infection and Inflammation, University of Glasgow). Luminex technology utilises patented pre-dyed microsphere bead sets allowing up to 100 cytokines to be measured simultaneously in the one biological sample. By utilising the theory of a sandwich ELISA, a specific antibody against a cytokine of choice is coupled to an individual bead set. Combinations of these bead sets are then incubated with the sample and thereafter a cocktail of detection antibodies are labelled with a reporter fluorochrome. Detection of the beads and quantification of cytokines was then performed using a Multiplex system and Bio-Plex software (Bio-Rad Laboratories, Inc., Hemel Hempstead, Herts, UK). This technique has the advantage of allowing detection of multiple cytokines from a single small sample volume (typically 50µl). In addition, unlike a standard ELISA which gives one optical density value for each sample, Luminex will give the average value of at least 100 individual measurements per cytokine in each sample. All samples were assayed in duplicate and values determined

by comparison to standard curves run in parallel. Analysis was carried out as per manufacturer's instruction using preconfigured multiplex cytokine kits (Biosource, Nivelles, Belgium).

6.4.7 Foetal Metatarsal Organ Culture

The middle three metatarsals were aseptically dissected from 18-day-old embryonic Swiss mice that had been killed by decapitation (2.3.6). The experimental protocol was approved by Roslin Institute's Animal Users Committee and the animals were maintained in accordance with Home Office guidelines for the care and use of laboratory animals. Bones were individually cultured at 37°C in a humidified atmosphere in the conditions described in section 2.3.6. Dex or AL-438 were added at a final concentration of 10^{-6} M in 0.01% DMSO to the bones and the medium was changed every second or third day. The control groups (0.01% DMSO only) and experimental groups contained 6 metatarsals each.

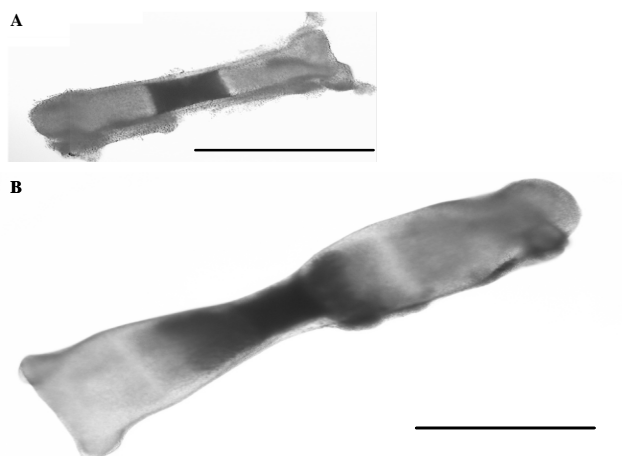


Figure 6.2 Murine foetal metatarsal culture model. (A) Metatarsals were dissected from the hind legs of 18-day-old foetal mice, and cultured for up to 10 days in the presence of Dex or AL-438. (B) Metatarsal after 10 days of culture (Scale bar = 1mm).

6.4.8 Morphometric Analysis

Images were taken of the metatarsals every second or third day of culture using a digital camera attached to a Nikon TE300 microscope. The total length of the bone was determined using Image Tool (Image Tool version 3.00, University of Texas Health Life Science Centre, San Antonio, TX). All results are expressed as a percentage change from harvesting length, which was regarded as baseline to demonstrate the rate of growth over time. For the determination of the size (in the direction of longitudinal growth) within the growth region of the distinct chondrocyte maturational zones, the 12-day-old metatarsals were fixed in 70% ethanol, dehydrated, and embedded in paraffin wax (Mushtaq *et al.*, 2004). Wax sections (10 μ m in thickness) were reacted for ALP activity for the demarcation of the hypertrophic and proliferating zones. Sections were also stained with von Kossa and haematoxylin and eosin using standard protocols to identify the zone of cartilage mineralisation (Mushtaq *et al.*, 2004). Images of the stained metatarsals were captured and the size of the ALP-negative proliferating zone was determined (proliferating zone = total length – (hypertrophic zone + mineralising zone). The size of the hypertrophic zone was determined by subtracting the von Kossa stained mineralising zone from the ALP-positive zone, and the size of the mineralising zone was determined directly from the von Kossa-stained sections.

6.4.9 Histological Assessment of Bromodeoxyuridine (BrdU) Uptake

BrdU was added to the culture medium of the metatarsals at a final concentration of 1mg/ml for the last 6h of culture on day 12. At the end of the incubation period, the tissue was washed in PBS and fixed in 70% ethanol, dehydrated, and embedded in paraffin wax. Sections 10 μ m in thickness were cut along the longitudinal axis, and

chondrocyte nuclei with incorporated BrdU were detected as described in section 2.4.5. To determine the proliferation index, the total number of BrdU positive cells was divided by the total area of the metatarsal section. Three sections from each of six bones from each treatment group were examined to obtain an aggregate value.

6.4.10 Statistical Analysis

Data were analysed by one-way analysis of variance. All data are expressed as the mean \pm S.E.M of at least 6 replicates within each experiment, and statistical analysis was performed using Minitab (Minitab 14; PA, USA). $P < 0.05$ was considered to be significant.

6.5 Results

6.5.1 Effect of AL-438 on ATDC5 Cell Number and Proliferation

During chondrogenesis exposure to Dex or Pred for 24h led to a concentration-dependent reduction in [^3H]-thymidine incorporation (54.5% and 29.2%, respectively, at 10^{-6}M ($p < 0.05$)), whereas exposure to AL-438 had no significant effect at any concentration tested (Figure 6.3A and 6.3B). Therefore, based on these data and previous observations that the affinity of AL-438 and Pred for the GC-receptor is similar (Elmore *et al.*, 2001), a saturating dose of 10^{-6}M was used for all compounds in future experiments. Counting the cells directly in a haemocytometer chamber supported these results, with Dex and Pred causing a significant reduction in cell number at 10^{-6}M (36.2% and 36.8% respectively ($p < 0.05$)), and AL-438 having no significant effect (Figure 6.3C). During the terminal differentiation phase (days 13-17), no compounds significantly altered chondrocyte proliferation or cell number (data not shown).

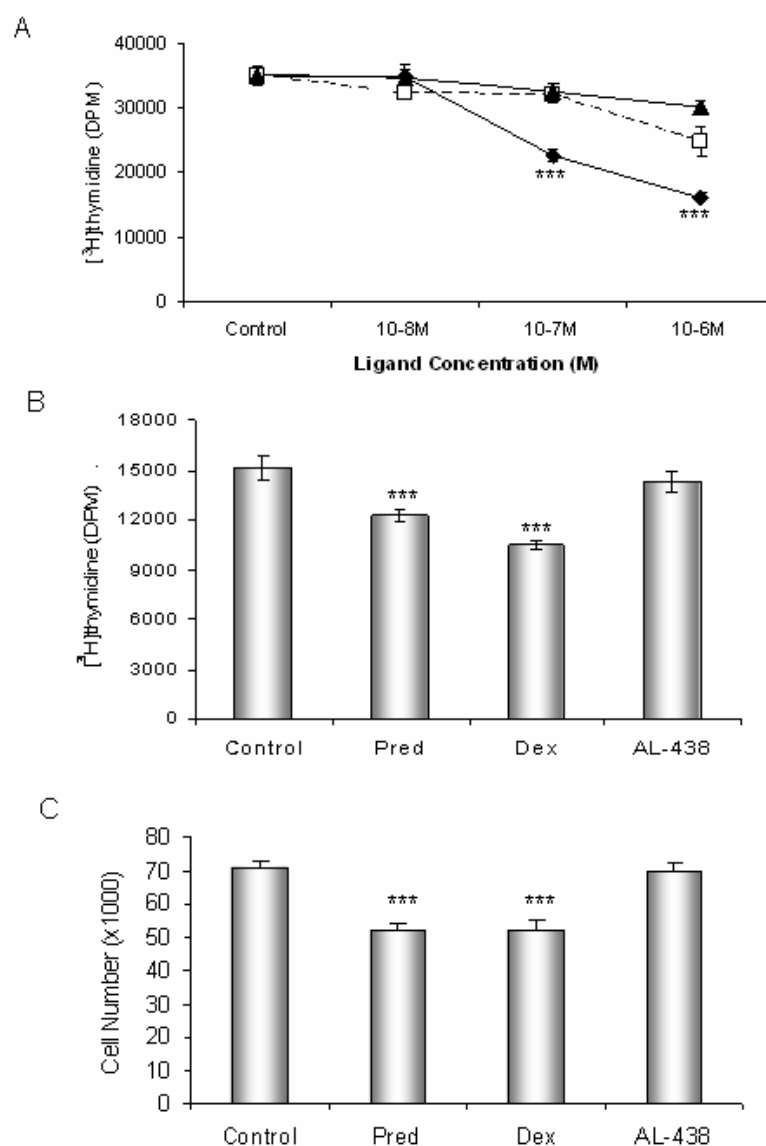


Figure 6.3 Effect of Dex, Pred and AL-438 on cell proliferation as assessed by [³H]-thymidine uptake. (A) Dex (♦ and solid line) and Pred (□ and dashed lines) caused a dose-dependent decrease in ATDC5 chondrocyte proliferation, whereas AL-438 (▲ and solid line) had no effect. (B) ATDC5 proliferation with 10⁻⁶M Dex, Pred and AL-438. (C) Cell proliferation as measured by counting the cells directly in a haemocytometer. Data are expressed as means ± SEM. (n = 6 separate cell culture replicates). ***p < 0.001 compared with control treated cells.

6.5.2 Differentiation in AL-438-treated Chondrocytes

In comparison with control cultures during the chondrogenesis period, exposure to 10^{-6} M Dex and Pred for 96h caused a significant reduction in proteoglycan synthesis, as measured by Alcian Blue staining of the ATDC5 cell monolayer (56% and 54%, respectively; $p < 0.001$), whereas exposure to AL-438 had no significant effect (Figure 6.4A). No significant differences between treatments were noted during terminal differentiation (data not shown). The effect of AL-438 on terminal chondrocyte differentiation was assessed by ALP activity. During chondrogenesis, ALP activity was significantly increased after exposure to Dex, Pred and AL-438 ($p < 0.001$) (Figure 6.4B), but no significant differences were observed during terminal differentiation (data not shown).

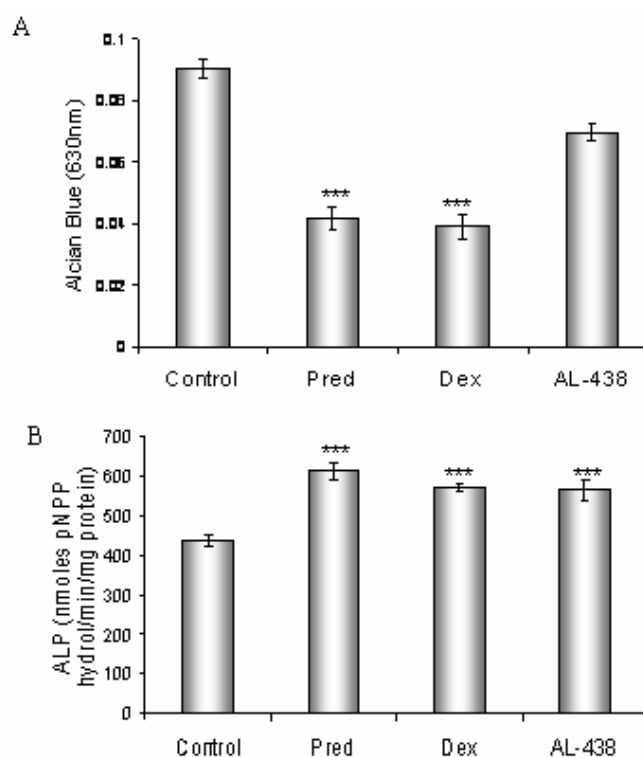


Figure 6.4 Effect of AL-438 on ATDC5 differentiation. A) Effect of Dex, Pred and AL-438 (all 10^{-6} M) on proteoglycan production as assessed by Alcian Blue staining in ATDC5 cells during chondrogenesis. Data are expressed as means \pm SEM ($n = 6$ cell culture replicates). *** $p < 0.001$ compared with control and AL-438 treated cells. B) Effect of Dex, Pred and AL-438 (all 10^{-6} M) on ALP activity in ATDC5 cells during chondrogenesis. Data are expressed as means \pm SEM ($n = 6$). *** $p < 0.001$ compared with control treated cells.

6.5.3 Effect of AL-438 on Apoptosis in ATDC5 Cells

Caspase-3 activity was unchanged in Dex, Pred and AL-438 treated cells compared to controls during both chondrogenesis and terminal differentiation, but TNF- α led to a significant increase in Caspase-3 activity, as expected (93% increase in Caspase-3 activity compared to control samples; $p < 0.001$) (Figure 6.5).

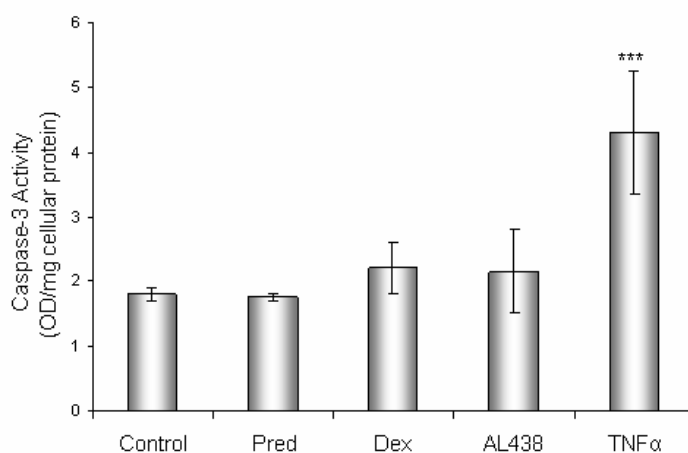


Figure 6.5 Effect of AL-438 on apoptosis in ATDC5 cells during chondrogenesis. Dex, Pred, AL-438 (10^{-6} M) and TNF α (10ng/ml) were added to ATDC5 cells for 24h and Caspase-3 activity measured at 405nm. Absorbances were then normalised to amount of protein per sample. Data are expressed as means \pm SEM (n = 6 cell culture replicates). * $P < 0.001$ compared with control and AL-438 treated cells.

6.5.4 Chondrocyte Marker Gene Expression in AL-438 treated ATDC5 Cells

Endpoint PCR of ATDC5 cDNA from Dex, Pred, and AL-438 treated cells revealed that the expression of chondrocyte marker genes Coll II, Coll X and aggrecan was reduced by Dex. Pred caused a small reduction in aggrecan expression, but no changes in expression were observed in AL-438 treated cells. Analysis by qPCR confirmed a significant reduction in aggrecan expression with Dex (3.5-fold reduction; $p < 0.001$), and with Pred (1.36-fold; $p < 0.001$), but no effect on aggrecan expression by AL-438 (Figure 6.6).

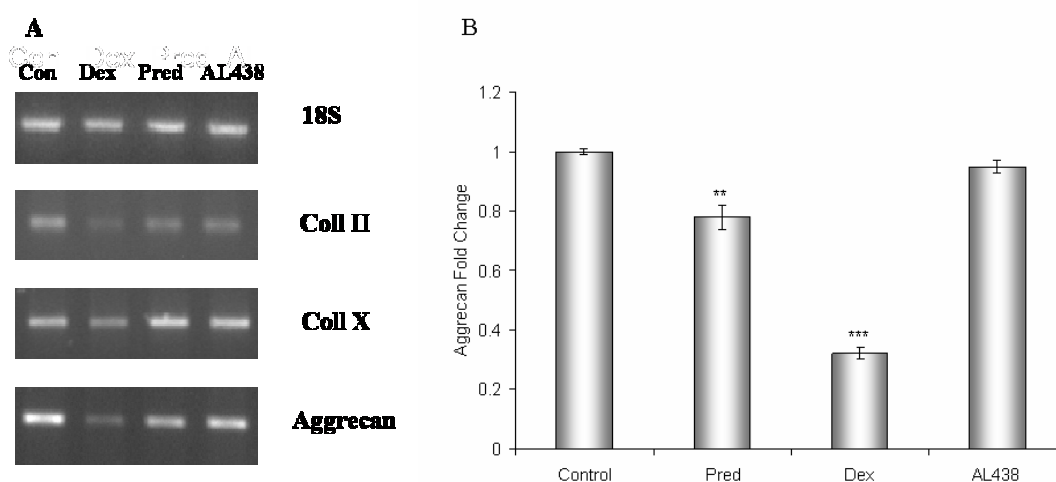


Figure 6.6 Chondrocyte marker gene expression in ATDC5 cells. A) RT-PCR of Coll II, Coll X, and aggrecan in ATDC5 cells treated with Dex, Pred or AL-438 (10^{-6} M) for 96h. (B) qRT-PCR of aggrecan gene expression in ATDC5 cells treated with Dex, Pred or AL-438 (10^{-6} M) for 96h. All data are shown as the mean relative gene expression \pm SEM ($n=6$ cell culture replicates run in triplicate) and normalised to GAPDH mRNA levels. *** $p < 0.001$; ** $p < 0.01$ compared with control treated cells.

6.5.5 Anti-inflammatory Efficacy of AL-438 in ATDC5 Cells

LPS induced IL-6 production in ATDC5 cells and this induction was reduced by the co-incubation of Dex or AL-438 by 58.1% and 55.4%, respectively. These results were significantly different from IL-6 levels in LPS-only treated cells ($p < 0.001$), but not significantly different from each other (Figure 6.7). Interestingly, levels of IL-1 β and TNF- α were undetected in control and test samples (data not shown). These results demonstrate that AL-438 has a similar anti-inflammatory efficacy to Dex in ATDC5 cells.

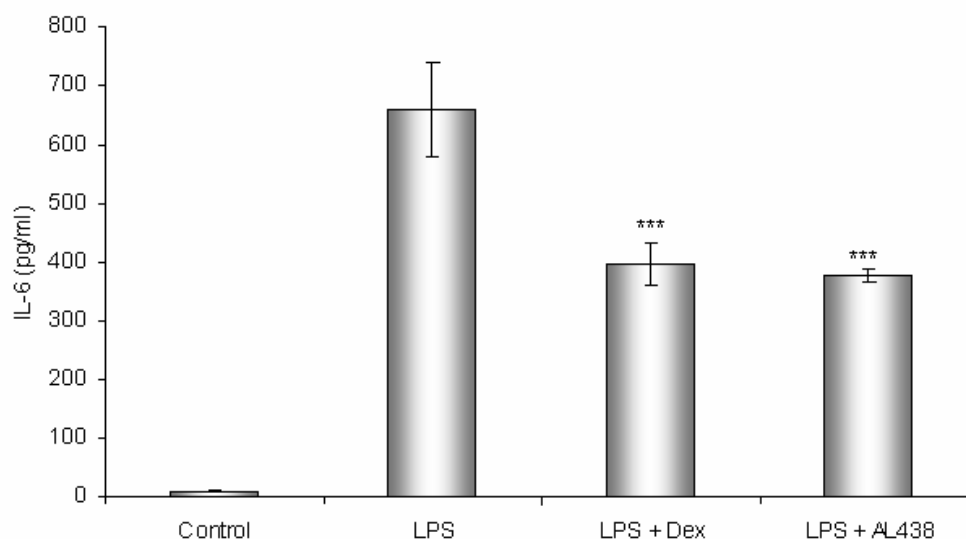


Figure 6.7 LPS-induced IL-6 production in ATDC5 cells. ATDC5 cells were grown in 10 μ g/ml lipopolysaccharide (LPS) (Lot 104K4036; from EColi 0127:B8; Sigma) with or without Dex or AL-438 (10⁻⁶M) for 24h. The medium was removed and analysed for levels of IL-1, IL-6 and TNF- α by Luminex technology. Data are expressed as means \pm S.E.M. (n = 6). *** $p < 0.001$ compared with LPS treated cells.

6.5.6 Longitudinal Bone Growth and Assessment of Maturational Zones

Until day 7 of culture, foetal mouse metatarsals treated with Dex or AL-438 grew at a similar rate to controls. After day 7, Dex treated metatarsals were significantly shorter than controls (18.5% shorter at day 10 ($p < 0.05$) and 22.2% shorter at day 12 ($p < 0.01$)), whereas the growth of the AL-438 treated metatarsals continued to parallel the growth of the controls (Figure 6.8A). The lengths of the proliferating, hypertrophic and mineralising zones were measured on histological sections of 12-day-old metatarsals (Table 6.1), using Von Kossa staining to identify mineralisation, and ALP staining to identify the hypertrophic and proliferating regions (Figure 6.8B and C). The lengths of the proliferating and hypertrophic zones did not significantly change between treatments, however, Dex significantly reduced the length of the mineralising zone (57% of control; $p < 0.05$).

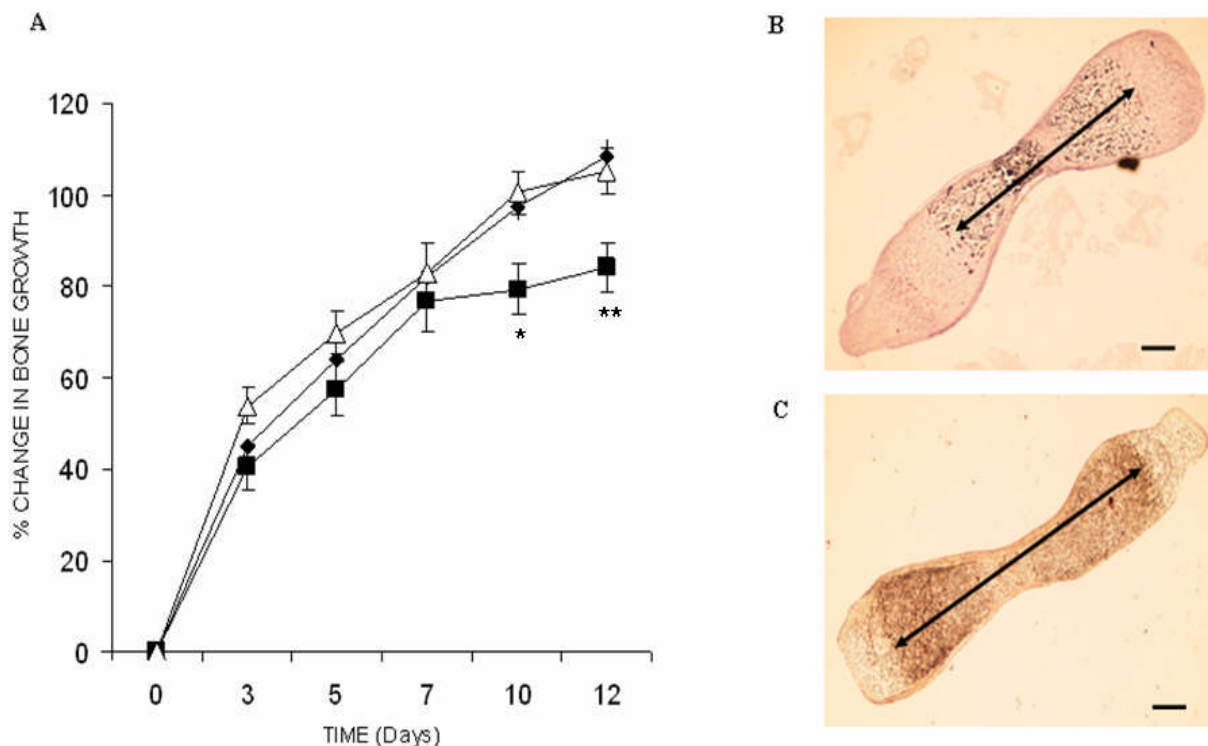


Figure 6.8 Effect of AL-438 on the growth of murine metatarsals (A) Effect of Dex or AL-438 (10^{-6} M) on the growth of metatarsals isolated from the hind legs of 18-day old foetal Swiss mice and cultured over a 12-day period (\triangle = Control; \blacklozenge = AL-438; \blacksquare = Dex) Data are expressed as mean \pm SEM (n = 6). **p<0.01 compared with controls; *p<0.05 compared with controls. (B) The mineralisation zone was measured by Von Kossa staining of 12-day old metatarsal sections. (C) The length of the hypertrophic and mineralising zone was defined by ALP staining, and the proliferating zone was deduced by subtracting the total length of ALP staining from the entire length of the bone (Scale bars = 200 μ m).

Treatment	Mineralising zone	Hypertrophic zone	Proliferating zone
Control	1.29 \pm 0.08	0.68 \pm 0.09	0.84 \pm 0.02
Dexamethasone	0.74 \pm 0.19 *	0.77 \pm 0.12	0.71 \pm 0.05 ^a
AL-438	1.30 \pm 0.07	0.56 \pm 0.06	0.80 \pm 0.03

Table 6.1 – Lengths of the proliferating, mineralising and hypertrophic zones in murine metatarsals treated with Dex or AL-438. Data are expressed in mm \pm SEM (n = 6). *P<0.05 compared with controls; ^aP = 0.06 compared with controls.

6.5.7 Effect of AL-438 on Chondrocyte Proliferation in Metatarsals

To study the effect of AL-438 on chondrocyte proliferation on a more physiological level, the number of proliferating cells in murine metatarsals was determined by BrdU incorporation analysis (Figure 6.9). The proliferation index in control metatarsals was significantly higher than metatarsals treated with either Dex (76%; $p < 0.001$) or AL-438 (80%; $p < 0.001$).

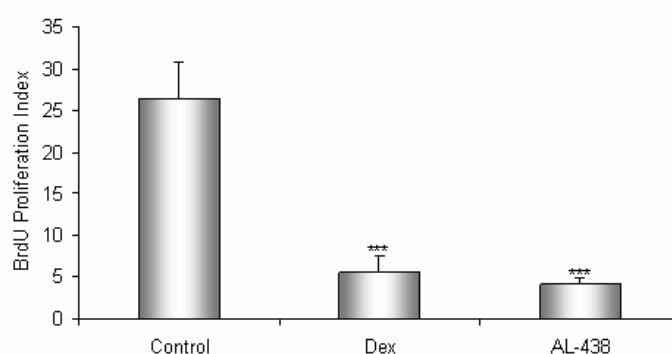


Figure 6.9 Histological assessment of chondrocyte proliferation in metatarsals treated with Dex or AL-438. BrdU-labeled cells in control, Dex-treated and AL-438-treated metatarsals cultured for 12d. Note the decreased number of proliferating cells in the Dex- and AL-438 treated metatarsals. The proliferation Index was calculated by dividing the total number of BrdU positive cells by the total section area in mm^2 . *** $p < 0.001$ compared with controls.

6.6 Discussion

Glucocorticoids are the most effective anti-inflammatory agents known. However, in children, their long-term use leads to growth retardation through a combination of GC-mediated effects on the systemic GH/IGF-1 axis as well as direct effects on the growth plate (Ahmed & Mushtaq, 2002). Infusion of GC directly into the growth plate results in a decrease in the ipsilateral tibial growth rate with no effects on the contralateral limb, suggest the possibility of a mechanism intrinsic to the epiphyseal growth plate (Baron *et al.*, 1992).

The search for a novel GC that has the anti-inflammatory properties of conventional steroids without one or more of the side-effects has been a long-standing goal. Previous efforts have concentrated primarily on modifying the steroid backbone, albeit with little success. Deflazacort, a D-ring substituted steroid, was originally hailed as a powerful anti-inflammatory molecule exhibiting reduced activity in bone and glucose metabolism (Miner 2002). Although, initial clinical data supported this notion (Canalis *et al.*, 1992), subsequent trials that adjusted the steroid dose to maintain equivalent anti-inflammatory efficacy resulted in the need for higher levels of deflazacort at which the advantages of deflazacort disappeared (Markham *et al.*, 1995). The discovery of specific transcription factors (NF κ B and AP-1) that bind to the GR and which can up- or down-regulate specific inflammatory genes initiated the search for ligands that could induce selective transcription (Diamond *et al.*, 1990; Jonat *et al.*, 1990).

AL-438 is a specific, non-steroidal ligand for the GR that exhibits a unique profile, both *in vivo* and *in vitro*. It retains full anti-inflammatory activity but has reduced negative effects on osteoblasts compared to Pred (Miner 2002; Coghlan *et al.*, 2003; Rosen and Miner, 2005). In this study, incubating ATDC5 cells with AL-438 had no effect on cell proliferation, cell number or proteoglycan synthesis, whereas, as found in previous studies, these factors were significantly reduced by both Dex and Pred (Mushtaq *et al.*, 2002; Fujita *et al.*, 2004). The finding that Dex and Pred promoted ALP activity is in concordance with the pro differentiating effects of Dex and Pred, and has previously been reported by us (Mushtaq *et al.*, 2002). The increase in ALP activity observed with AL-438 suggests that the bone-sparing effects seen with AL-

438 are not due to direct effects on chondrocyte differentiation, but may be due to reduced effects on chondrocyte proliferation compared to Dex and Pred. The lack of effect of Dex on ATDC5 apoptosis is in agreement with previous studies (Mushtaq *et al.*, 2002) but at variance with other chondrocyte studies (Chrysis *et al.*, 2005), suggesting a cell type dependent effect. Studies measuring the bone turnover marker osteocalcin in the human osteoblast-like cell line MG-63 have shown that AL-438 is unable to inhibit osteocalcin expression as efficiently as Pred (Coxam *et al.*, 1996). In addition, AL-438 has been shown to exhibit a weak inhibition of osteoprotegerin in MG-63 cells compared to other GCs (Coghlan *et al.*, 2003). The differential effect on ATDC5 cell progression between AL-438 and Dex and Pred may be due to the fact that AL-438 is qualitatively different in terms of its ability to activate or repress gene expression. Interestingly, none of the compounds had an effect on ATDC5 maturation in terms of proliferation, ALP activity or proteoglycan production during the terminal differentiation period, a finding that has been reported previously (Mushtaq *et al.*, 2002).

There are at least three distinct mechanisms by which GCs can regulate gene transcription. Firstly, GCs can bind to a cytosolic GR which translocates to the nucleus and, in the case of positive regulation, transactivates through *cis*-activating palindromic glucocorticoid response elements (GREs) located in the promoter region of responsive genes. Secondly, GCs are able to bind to negative GREs resulting in the repression of gene transcription. However, GCs decrease the transcription of genes involved in the inflammatory process that have no identifiable GREs in their promoter regions, suggesting that an alternative mechanism must mediate this inhibitory effect. There is now evidence to suggest that GCs may control inflammation predominantly

through the trans-repression of transcription factors that regulate inflammatory gene repression, such as activator protein-1 (AP-1), NF κ B, and nuclear factor of activated T-cells (NF-AT) (Belvisi *et al.*, 2001).

There is now increasing acceptance of the hypothesis that the side effects of steroids are likely to be due to the transactivation of genes (such as those involved in lipid and muscle metabolism) through binding of the GR dimers to DNA, whereas the anti-inflammatory effects may be due to the binding of a single GR to transcription factors or corepressors, resulting in the repression of pro-inflammatory genes such as IL-1, IL-6 and TNF- α (Figure 6.9). The proposed mechanism of action of AL-438 is based on this hypothesis, and is thought to result from changes in the interaction of the GR with gene-specific transcriptional cofactors.

Upon binding to the GR, AL-438 induces a unique change to its structural conformation, which is completely different than those induced by steroids such as Pred or Dex (Coghlan *et al.*, 2003). These structural changes lead to a reduction in co-factor interactions between the GR and co-factors such as PGC-1, which is involved in hepatic glucose production (Herzig *et al.*, 2001; Yoon *et al.*, 2001), but do not change the interactions between GR and GRIP-1, a co-factor which plays a role in the repression of pro-inflammatory genes (Rogastsky *et al.*, 2001; Coghlan *et al.*, 2003) (Figure 6.9). This hypothesis may explain the reported maintenance of anti-inflammatory activity with AL-438 but also its reduced effects on ATDC5 cells as found in this study.

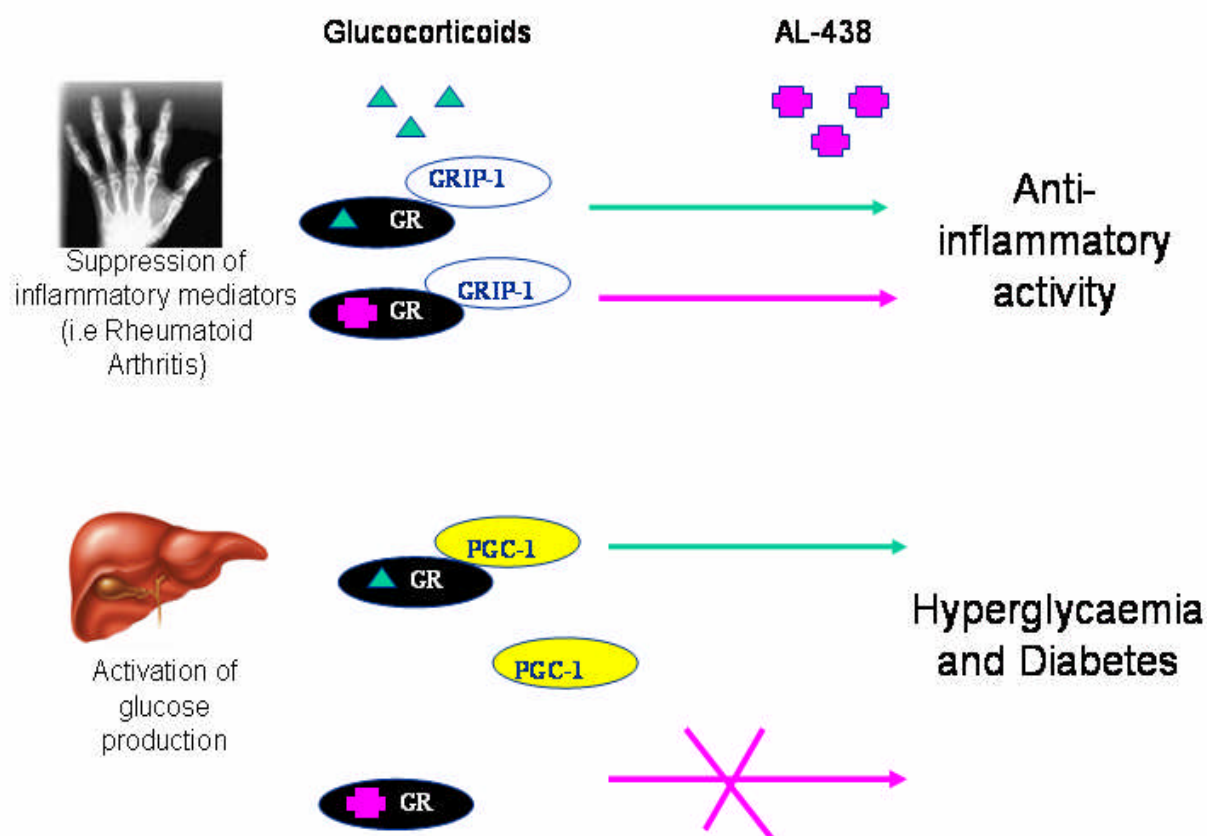


Figure 6.9 Proposed mechanism of action of AL-438 Upon binding to the GR, AL-438 induces a unique change to its structural conformation, which is different than that induced by Dex. These structural changes lead to a reduction in co-factor interactions between the GR and co-factors such as PGC-1, which is involved in hepatic glucose production, but do not change the interactions between the GR and cofactors involved in the inflammatory response, such as GRIP-1, a co-factor which plays a role in the repression of pro-inflammatory genes.

The proposed mechanism of action of AL-438 is also supported by the finding that as opposed to Dex, AL-438 does not have a detrimental effect on metatarsal bone growth. This finding confirms bone-sparing results from previous studies which used calcein and tetracycline labelling in rats to show that AL-438 treatment was not associated with the level of reduction in bone formation that was associated with Pred

(Coghlan *et al.*, 2003). This study also measured the expression of bone formation markers osteocalcin and osteoprotegerin, and found that these genes were not, or only weakly repressed by AL-438 compared to Pred. The fact that the length of the mineralising zone, but not the proliferating or hypertrophic zones, was significantly shorter in Dex treated bones suggests that Dex is acting directly on the terminally differentiated chondrocytes to reduce overall bone length. A similar finding has previously been found by our group (Mushtaq *et al.*, 2004) and others (Picherit *et al.*, 2000), and may be caused by Dex interfering with genes involved in the mineralisation process.

The finding that AL-438 maintains a similar anti-inflammatory efficacy to Dex in ATDC5 cells was important, as it proved that AL-438 was still fully efficacious as an anti-inflammatory agent in chondrocytes despite the fact that it was much less harmful than Dex or Pred. The anti-inflammatory efficacy of AL-438 has previously been demonstrated both *in vivo* using the rat carrageenan-induced paw edema assay and the adjuvant arthritis model in rats, and *in vitro* in HepG2 cells and human skin fibroblasts (Coghlan *et al.*, 2003). In these studies, AL-438 and Pred were equally effective at inhibiting an inflammatory response, although Pred was slightly more potent, with an ED₅₀ of 1mg/kg compared to 9mg/kg for AL-438 in the adjuvant arthritis model.

To compensate for the fact that AL-438 is slightly less potent than Pred, a saturating dose of 10⁻⁶M was used for all compounds in this study. In addition, this pharmacological concentration of Dex and Pred is similar to that found in chronic GC therapy and has been shown previously by us, and others, to inhibit both chondrocyte

proliferation and longitudinal bone growth (Mushtaq *et al.*, 2002 and 2004). At 10^{-6} M the compounds fully occupied the receptor (Elmore *et al.*, 2001; Coghlan *et al.*, 2003), therefore, allowing their full efficacy as anti-inflammatory agents to be measured. Although AL-438 has been shown to have similar affinity for the GC-receptor across a wide array of tested cell types (Elmore *et al.*, 2001; Coghlan *et al.*, 2003; plus unpublished data) it also exhibits some affinity for the mineralocorticoid receptor at this concentration. This affinity is comparable to that of 10^{-6} M Pred, and when tested against a variety of other nuclear and non-nuclear receptors, kinases and enzymes, AL-438 displayed no affinity up to a concentration of $10\mu\text{M}$ (Coghlan *et al.*, unpublished). In addition to interactions with its receptor, GCs are also known to have non-genomic effects that are not mediated by the GC-receptor (Song *et al.*, 2005). Although all indications are that AL-438 acts exclusively through the GC-receptor (Coghlan *et al.*, 2003), further studies are required to establish the precise cellular events involved in AL-438 actions. Nevertheless, the data from this study suggest that, when studied at a concentration (10^{-6} M) that fully occupies the GC-receptor, allowing its full efficacy as a GC-receptor agonist, AL-438 may separate anti-inflammatory activity from a number of bone growth-related side effects, including chondrocyte proliferation and longitudinal bone growth.

6.7 Conclusions

This study has used a well-established model of longitudinal bone growth to show that the non-steroidal anti-inflammatory agent, AL-438 is less detrimental to chondrocyte proliferation and bone growth at the level of the growth plate. Importantly, it has also been shown that AL-438 maintains a similar anti-inflammatory efficacy to Dex, thereby confirming that a non-steroidal anti-

inflammatory agent is capable of selectively maintaining its anti-inflammatory effects without negatively affecting bone growth. The reduced skeletal side-effect profile of this novel ligand could prove important in the search for new anti-inflammatory treatments for children, however, it should be emphasised that these studies are based on in vitro analysis in mouse, and it still remains to be shown whether these results will translate into the human.

Chapter 7

General Discussion and Future Directions

7.1 General Discussion

GCs have been used in the treatment of inflammatory and autoimmune conditions for over 50 years. However, their use is limited by the wide range of side effects associated with long term therapy. These can include hyperglycaemia, behavioural changes, weight redistribution, osteoporosis, and, in children, growth retardation. The precise mechanisms by which GCs cause growth retardation in the developing skeleton are still unclear, however, it is thought that they may act directly upon the chondrocytes of the epiphyseal growth plate to delay the process of endochondral ossification (Baron *et al.*, 1994), and consequently longitudinal bone growth.

The work within this thesis has attempted to further our understanding of the mechanisms by which GCs alter chondrocyte dynamics within the growth plate, through a range of *in vitro* and *in vivo* studies. Microarray analysis of the murine chondrogenic ATDC5 cell line treated with Dex highlighted the importance of ECM genes in the chondrocyte response to GCs. An interesting finding was the upregulation of SGCK following Dex treatment. SGCK has been shown to play an important role in the maintenance of cells within the cell cycle, by phosphorylating and consequently inhibiting the activation of Foxo3a, a member of the Forkhead family of transcription factors (Brunet *et al.*, 2001). Under normal circumstances, Foxo3a targets the activation of the CDKI p27, causing cells to exit the cell cycle and progress towards terminal differentiation and apoptosis. By inhibiting Foxo3a activity, SGCK causes the cells to continue proliferating, indicating that SGCK is a regulator of cell survival (Tessier *et al.*, 2006). SGCK has previously been shown to be upregulated in osteoblasts in response to Dex (Leclerc *et al.*, 2004), however, there have been no previous reports of SGCK expression within the growth plate. The fact

that SGCK expression is increased in response to environmental and toxicological stresses, and inactivates proteins involved in the exit from the cell cycle, suggests that SGCK may be acting as a survival factor in response to Dex in this study.

A number of ECM genes were significantly upregulated following Dex treatment, a finding which has previously been reported in Dex-treated primary chondrocytes (James *et al.*, 2007). This finding supports the recent hypothesis that GCs may be causing premature differentiation of proliferating chondrocytes, therefore preventing the accumulation of a sufficient proliferative pool of chondrocytes available for differentiation and subsequent hypertrophy (Mustaq *et al.*, 2002). The fact that expression of the binding protein lipocalin 2 was also increased after Dex treatment also supports this hypothesis.

In this study, lipocalin 2 expression was significantly increased in proliferating ATDC5 cells treated with Dex. Lipocalin 2 has previously been shown to be expressed at high levels in hypertrophic chondrocytes, and is known to be induced by a number of factors including LPS, FGF, PGE₂, and Dex (Ulivi *et al.*, 2006). This study confirmed that Dex was acting directly at the GRE on the lipocalin 2 promoter to increase lipocalin 2 expression and reduce chondrocyte proliferation. These findings, along with the fact that lipocalin 2 increased expression of the hypertrophic chondrocyte marker Coll X, suggests that lipocalin 2 could also be causing premature differentiation in chondrocytes. Interestingly, this effect was amplified synergistically with the addition of Dex, indicating the possibility that Dex may be acting through lipocalin 2 to reduce chondrocyte proliferation and cause growth retardation through the premature differentiation of proliferative chondrocytes.

The proliferation and differentiation of growth plate chondrocytes is ultimately under control of cell cycle regulators such as cyclins and CDKs, and their inhibitors, the CDKIs. The rate of chondrocyte proliferation and the size of the proliferative pool in the growth plate can vary widely between species at the same stage of development, between bones within a single animal, and even between the proximal and distal ends of the same bone (Beier *et al.*, 1999). In order to test the hypothesis that GCs reduced chondrocyte proliferation by causing them to differentiate prematurely, the expression of a number of CDKIs was analysed. Of all the CDKIs tested, only p21 expression increased during ATDC5 differentiation, and so was chosen for further analysis. As a CDKI, increased p21 expression causes cells to exit the cell cycle at the G1/S checkpoint, and progress towards terminal differentiation (Negishi *et al.*, 2001). Consequently, if the theory was correct, Dex should have caused an increase in p21 expression. In ATDC5 cells, both p21 protein and gene expression was increased following Dex treatment, adding further evidence to the theory that one possible mechanism of GC-induced growth retardation is an increase in chondrocyte differentiation. However, this hypothesis was not transferable to an *in vivo* model of growth in mice lacking a functional p21 gene, and p21^{-/-} mice injected with Dex experienced comparable growth retardation to their wildtype littermates. A similar finding has previously been reported in p27^{-/-} mice (Emons *et al.*, 2006), and suggests that, although control of the cell cycle may play an important role in GC effects at the cellular level, it is likely that many other factors are involved.

Although a number of mechanisms have been postulated for GC induced growth retardation, there are still many questions which must be answered before novel bone-

sparing therapies are clinically available. Over the last 20 years, however, an intense effort has been made by both science and industry to develop new drugs that maintain the efficacy of commonly used GCs such as Pred and Dex, but display reduced adverse effects. In the late 1990's, hopes were raised with the discovery of the steroid Deflazacort, which displayed reduced effects on bone and glucose metabolism both *in vitro* and *in vivo* (Canalis *et al.*, 1992). However, when used at a dose that displayed equal anti-inflammatory efficacy to Dex and Pred, these side-effects re-appeared. Since then, our increased knowledge of GR pharmacology has allowed us to develop more sophisticated ligands that are able to separate anti-inflammatory properties from adverse side effects. AL-438 is a selective glucocorticoid receptor modulator with a similar anti-inflammatory efficacy to Dex and Pred *in vivo* and *in vitro*, but with reduced negative effects on glucose metabolism, bone turnover, and as found in this study, bone growth (Coghlan *et al.*, 2003). The growth-sparing effects of AL-438 seemed to be due to reduced effects on chondrocyte proliferation and proteoglycan production, and were observed in both *in vivo* and organ culture models of bone growth. The mechanism of action of AL-438 is based on the theory that most GCs exert their anti-inflammatory properties through the repression of pro-inflammatory genes such as TNF- α and IL-1, and their negative properties through the activation of genes such as PGC-1, which is involved in glucose production. AL-438 causes a unique conformational change in the GR which permits the binding of co-repressors, but not co-activators. Consequently, AL-438 can successfully inhibit pro-inflammatory genes, but cannot activate many genes that are associated with the adverse effects of other GCs.

As discussed in this thesis, the effects of Dex on endochondral ossification and growth plate dynamics are severe. Long-term therapy in juveniles can ultimately lead to growth retardation, due to a reduction in growth plate width caused by decreased chondrocyte proliferation and possible premature differentiation of proliferative chondrocytes. Due to these effects, a concerted effort has been made to develop new anti-inflammatory agents with reduced effects on bone growth. As outlined herein, AL438, has reduced effects on bone growth compared to Dex, but maintains similar anti-inflammatory efficacy. However, AL-438 has not yet progressed to be clinically available, and therefore there is still a pressing need for novel ligands that maintain anti-inflammatory efficacy but have minimal effects on growth plate dynamics and longitudinal bone growth.

7.2 Future Directions

The results presented within this thesis suggest possible mechanisms by which GCs cause growth retardation at the level of the growth plate. However, much further work is necessary if these mechanisms are to be confirmed. The upregulation of ECM genes such as DMP1 and CTGF was an interesting finding, and suggests that GCs could inhibit skeletal growth through an increase in the differentiation of proliferative chondrocytes. Although this finding has previously been reported at the gene expression level (James *et al.*, 2007), the upregulation of DMP1 and CTGF protein has not yet been described. In addition, it is important to study the effects of increased DMP1/CTGF expression in chondrocytes, possibly through stable transfection techniques, and equally, the knock-down of DMP or CTGF by siRNA could give an insight into the role of these genes in mediating GC-effects in chondrocytes. The up-regulation of SGCK was also an interesting finding, and could

warrant further investigation, particularly due to the fact that the downstream target of SGCK, Foxo3a, has been linked to CDKI inhibition and cell survival. A potential future study would be to analyse Foxo3a and SGCK expression in ATDC5 cells and primary chondrocytes, both at different stages of differentiation, and following Dex treatment. The up-regulation of SGCK should cause an inhibition in Foxo3a expression, and provides a potential survival mechanism for chondrocytes following Dex treatment.

The role of lipocalin 2 in GC-induced growth retardation is also an interesting issue which requires further investigation. An obvious question is whether Dex maintains its anti-proliferative effects in ATDC5 cells lacking a functional lipocalin 2 gene. This could be addressed by siRNA knock-down studies, and if the hypothesis was correct, Dex-effects would be reduced in ATDC5 cells in the absence of lipocalin 2. Another area which should be investigated are the signalling mechanisms involved in lipocalin 2 induction. Work in this thesis has shown that p38 and NFκB signalling do not play a role in Dex-induced lipocalin 2 expression, but the finding that the serine protease inhibitor TLCK blocks lipocalin 2 induction suggests that other signalling pathways such as PI3-Kinase may be involved. Although lipocalin 2 seems to be important for GC effects on chondrocytes *in vitro*, it may also be interesting to analyse its role in growth retardation on a more physiological level. The murine foetal metatarsal model could be used to study the effects of recombinant lipocalin 2 on Dex-induced growth retardation, and following growth studies, histological analysis of chondrocyte dynamics and mineralisation could be carried out. If successful, these studies could be extended into an *in vivo* model of GC-induced growth retardation in lipocalin 2^{-/-} mice.

The lack of involvement of p21 in reduced skeletal growth was disappointing, and suggests that there may be considerable redundancy between the CDKIs. It is possible that a number of CDKIs and other cell cycle regulators may act together to control chondrocyte proliferation, and it would therefore be interesting to study the growth of mice with multiple null mutations such as p21^{-/-}/p27^{-/-}. Due to the importance of cell cycle regulation in the control of endochondral ossification it would be interesting to analyse the expression of other factors involved in the cell cycle, such as CDKs, which should be down-regulated following Dex treatment in chondrocytes.

Reference List

Abad V, Meyers JL, Weise M, Gafni RI, Barnes KM, Nilsson O, Bacher JD, Baron J (2002) The role of the resting zone in growth plate chondrogenesis. *Endocrinology* **143**: 1851-1857

Abu EO, Bord S, Horner A, Chatterjee VK, Compston JE (1997) The expression of thyroid hormone receptors in human bone. *Bone* **21**: 137-142

Abu EO, Horner A, Kusec V, Triffitt JT, Compston JE (2000) The localisation of the functional glucocorticoid receptor alpha in human bone. *J Clin Endocrinol Metab* **85**: 883-889

Abuzzahab MJ, Schneider A, Goddard A, Grigorescu F, Lautier C, Keller E, Kiess W, Klammt J, Kratzsch J, Osgood D, Pfaffle R, Raile K, Seidel B, Smith RJ, Chernauek SD (2003) IGF-I receptor mutations resulting in intrauterine and postnatal growth retardation. *N Engl J Med* **349**: 2211-2222

Adams CS, Shapiro IM (2002) The fate of the terminally differentiated chondrocyte: evidence for microenvironmental regulation of chondrocyte apoptosis. *Crit Rev Oral Biol Med* **13**: 465-473

Agoston H, Baybayan L, Beier F (2006) Dexamethasone stimulates expression of C-type Natriuretic Peptide in chondrocytes. *BMC Musculoskelet Disord* **7**: 87

Ahmed SF, Wallace WH, Crofton PM, Wardhaugh B, Magowan R, Kelnar CJ (1999) Short-term changes in lower leg length in children treated for acute lymphoblastic leukaemia. *J Pediatr Endocrinol Metab* **12**: 75-80

Ahmed SF, Tucker P, Mushtaq T, Wallace AM, Williams DM, Hughes IA (2002) Short-term effects on linear growth and bone turnover in children randomised to receive prednisolone or dexamethasone. *Clin Endocrinol (Oxf)* **57**: 185-191

Akiyama H, Kim JE, Nakashima K, Balmes G, Iwai N, Deng JM, Zhang Z, Martin JF, Behringer RR, Nakamura T, De CB (2005) Osteo-chondroprogenitor cells are derived from Sox9 expressing precursors. *Proc Natl Acad Sci U S A* **102**: 14665-14670

Alexander CM, Werb Z (1992) Targeted disruption of the tissue inhibitor of metalloproteinases gene increases the invasive behavior of primitive mesenchymal cells derived from embryonic stem cells in vitro. *J Cell Biol* **118**: 727-739

Allen DB, Mullen M, Mullen B (1994) A meta-analysis of the effect of oral and inhaled corticosteroids on growth. *J Allergy Clin Immunol* **93**: 967-976

Alvarez J, Horton J, Sohn P, Serra R (2001) The perichondrium plays an important role in mediating the effects of TGF-beta1 on endochondral bone formation. *Dev Dyn* **221**: 311-321

Anderson HC (2003) Matrix vesicles and calcification. *Curr Rheumatol Rep* **5**: 222-226

- Annefeld M (1992) Changes in rat epiphyseal cartilage after treatment with dexamethasone and glycosaminoglycan-peptide complex. *Pathol Res Pract* **188**: 649-652
- Arikoski P, Komulainen J, Riihonen P, Parviainen M, Jurvelin JS, Voutilainen R, Kroger H (1999) Impaired development of bone mineral density during chemotherapy: a prospective analysis of 46 children newly diagnosed with cancer. *J Bone Miner Res* **14**: 2002-2009
- Atsumi T, Miwa Y, Kimata K, Ikawa Y (1990) A chondrogenic cell line derived from a differentiating culture of AT805 teratocarcinoma cells. *Cell Differ Dev* **30**: 109-116
- Ballock RT, Zhou X, Mink LM, Chen DH, Mita BC, Stewart MC (2000) Expression of cyclin-dependent kinase inhibitors in epiphyseal chondrocytes induced to terminally differentiate with thyroid hormone. *Endocrinology* **141**: 4552-4557
- Barash Y, Dehan E, Krupsky M, Franklin W, Geraci M, Friedman N, Kaminski N (2004) Comparative analysis of algorithms for signal quantitation from oligonucleotide microarrays. *Bioinformatics* **20**: 839-846
- Barker DJ, Winter PD, Osmond C, Margetts B, Simmonds SJ (1989) Weight in infancy and death from ischaemic heart disease. *Lancet* **2**: 577-580
- Barker DJ, Eriksson JG, Forsen T, Osmond C (2002) Foetal origins of adult disease: strength of effects and biological basis. *Int J Epidemiol* **31**: 1235-1239
- Barnard R, Haynes KM, Werther GA, Waters MJ (1988) The ontogeny of growth hormone receptors in the rabbit tibia. *Endocrinology* **122**: 2562-2569
- Barnhill JG, Fye CL, Williams DW, Reda DJ, Harris CL, Clegg DO (2006) Chondroitin product selection for the glucosamine/chondroitin arthritis intervention trial *J Am Pharm Assoc (Wash DC)* **46**: 14-24
- Baron J, Huang Z, Oerter KE, Bacher JD, Cutler GB, Jr. (1992) Dexamethasone acts locally to inhibit longitudinal bone growth in rabbits. *Am J Physiol* **263**: E489-E492
- Baron J, Klein KO, Colli MJ, Yanovski JA, Novosad JA, Bacher JD, Cutler GB, Jr. (1994) Catch-up growth after glucocorticoid excess: a mechanism intrinsic to the growth plate. *Endocrinology* **135**: 1367-1371
- Barreto C, Wilsman NJ (1994) Hypertrophic chondrocyte volume and growth rates in avian growth plates. *Res Vet Sci* **56**: 53-61
- Bartek J, Lukas J (2001) Mammalian G1- and S-phase checkpoints in response to DNA damage. *Curr Opin Cell Biol* **13**: 738-747
- Baxter JD (1992) The effects of glucocorticoid therapy. *Hosp Pract (Off Ed)* **27**: 111-8, 123
- Beato M, Sanchez-Pacheco A (1996) Interaction of steroid hormone receptors with the transcription initiation complex. *Endocr Rev* **17**: 587-609

- Beier F, Taylor AC, LuValle P (1999a) The Raf-1/MEK/ERK pathway regulates the expression of the p21(Cip1/Waf1) gene in chondrocytes. *J Biol Chem* **274**: 30273-30279
- Beier F, Lee RJ, Taylor AC, Pestell RG, LuValle P (1999b) Identification of the cyclin D1 gene as a target of activating transcription factor 2 in chondrocytes. *Proc Natl Acad Sci U S A* **96**: 1433-1438
- Beier F, Ali Z, Mok D, Taylor AC, Leask T, Albanese C, Pestell RG, LuValle P (2001) TGFbeta and PTHrP control chondrocyte proliferation by activating cyclin D1 expression. *Mol Biol Cell* **12**: 3852-3863
- Belanger LF, Casas-Cordero M, Urist MR (1977) The effects of zinc deprivation on the host response to intramuscular bone matrix implants in the rat. *Clin Orthop Relat Res* 208-213
- Belvisi MG, Brown TJ, Wicks S, Foster ML (2001) New Glucocorticosteroids with an improved therapeutic ratio? *Pulm Pharmacol Ther* **14**: 221-227
- Bengtsson T, Aszodi A, Nicolae C, Hunziker EB, Lundgren-Akerlund E, Fassler R (2005) Loss of alpha10beta1 integrin expression leads to moderate dysfunction of growth plate chondrocytes. *J Cell Sci* **118**: 929-936
- Berg AH, Scherer PE (2005) Adipose tissue, inflammation, and cardiovascular disease. *Circ Res* **96**:939-949
- Bertani G (2004) Lysogeny at mid-twentieth century: P1, P2, and other experimental systems. *J Bacteriol* **186**: 595-600
- Blanchard O, Tsagris L, Rappaport R, Duval-Beaupere G, Corvol M (1991) Age-dependent responsiveness of rabbit and human cartilage cells to sex steroids in vitro. *J Steroid Biochem Mol Biol* **40**: 711-716
- Blodgett FM, Burgin L, Iezzoni D, Gribetz D, Talbot NB (1956) Effects of prolonged cortisone therapy on the statural growth, skeletal maturation and metabolic status of children. *N Engl J Med* **254**: 636-641
- Boersma B, Rikken B, Wit JM (1995) Catch-up growth in early treated patients with growth hormone deficiency. Dutch Growth Hormone Working Group. *Arch Dis Child* **72**: 427-431
- Boersma B, Wit JM (1997) Catch-up growth. *Endocr Rev* **18**: 646-661
- Bohensky J, Shapiro IM, Leshinsky S, Terkhorn SP, Adams CS, Srinivas V (2007) HIF-1 regulation of chondrocyte apoptosis: induction of the autophagic pathway. *Autophagy* **3**: 207-214
- Borregaard N, Cowland JB (2006) Neutrophil gelatinase-associated lipocalin, a siderophore-binding eukaryotic protein. *Biometals* **19**: 211-215

- Bradford MM (1976) A rapid and sensitive method for the quantitation of microgram quantities of protein utilizing the principle of protein-dye binding. *Anal Biochem* **72**: 248-254
- Breur GJ, Lapierre MD, Kazmierczak K, Stechuchak KM, McCabe GP (1997) The domain of hypertrophic chondrocytes in growth plates growing at different rates. *Calcif Tissue Int* **61**: 418-425
- Brunet A, Park J, Tran H, Hu LS, Hemmings BA, Greenberg ME (2001) Protein kinase SGK mediates survival signals by phosphorylating the forkhead transcription factor FKHRL1 (FOXO3a). *Mol Cell Biol* **21**: 952-965
- Bruyere O, Reginster JY (2007) Glucosamine and chondroitin sulfate as therapeutic agents for knee and hip osteoarthritis. *Drugs Aging* **24**: 573-580
- Buckwalter JA, Mower D, Schafer J, Ungar R, Ginsberg B, Moore K (1985) Growth-plate-chondrocyte profiles and their orientation. *J Bone Joint Surg Am* **67**: 942-955
- Buckwalter JA, Mower D, Ungar R, Schaeffer J, Ginsberg B (1986) Morphometric analysis of chondrocyte hypertrophy. *J Bone Joint Surg Am* **68**: 243-255
- Burger EH, Klein-Nulend J, Smit TH (2003) Strain-derived canalicular fluid flow regulates osteoclast activity in a remodelling osteon--a proposal. *J Biomech* **36**: 1453-1459
- Canalis E, Avioli L (1992) Effects of deflazacort on aspects of bone formation in cultures of intact calvariae and osteoblast-enriched cells. *J Bone Miner Res* **7**: 1085-1092
- Cancedda R, Descalzi CF, Castagnola P (1995) Chondrocyte differentiation. *Int Rev Cytol* **159**: 265-358
- Cancedda R, Castagnola P, Cancedda FD, Dozin B, Quarto R (2000) Developmental control of chondrogenesis and osteogenesis. *Int J Dev Biol* **44**: 707-714
- Caplan AI (1994) The mesengenic process. *Clin Plast Surg* **21**: 429-435
- Carlberg AL, Pucci B, Rallapalli R, Tuan RS, Hall DJ (2001) Efficient chondrogenic differentiation of mesenchymal cells in micromass culture by retroviral gene transfer of BMP-2. *Differentiation* **67**: 128-138
- Carlevaro MF, Albini A, Ribatti D, Gentili C, Benelli R, Cermelli S, Cancedda R, Cancedda FD (1997) Transferrin promotes endothelial cell migration and invasion: implication in cartilage neovascularization. *J Cell Biol* **136**: 1375-1384
- Cha HH, Cram EJ, Wang EC, Huang AJ, Kasler HG, Firestone GL (1998) Glucocorticoids stimulate p21 gene expression by targeting multiple transcriptional elements within a steroid responsive region of the p21waf1/cip1 promoter in rat hepatoma cells. *J Biol Chem* **273**: 1998-2007
- Chagin AS, Savendahl L (2007) Oestrogens and growth: review. *Pediatr Endocrinol Rev* **4**: 329-334

- Chrousos GP (2000) The HPA axis and the stress response. *Endocr Res* **26**: 513-514
- Chrysis D, Ritzen EM, Savendahl L (2003) Growth retardation induced by dexamethasone is associated with increased apoptosis of the growth plate chondrocytes. *J Endocrinol* **176**: 331-337
- Chrysis D, Zaman F, Chagin AS, Takigawa M, Savendahl L (2005) Dexamethasone induces apoptosis in proliferative chondrocytes through activation of caspases and suppression of the Akt-phosphatidylinositol 3'-kinase signalling pathway. *Endocrinology* **146**: 1391-1397
- Coffin JD, Florkiewicz RZ, Neumann J, Mort-Hopkins T, Dorn GW, Lightfoot P, German R, Howles PN, Kier A, O'Toole BA, . (1995) Abnormal bone growth and selective translational regulation in basic fibroblast growth factor (FGF-2) transgenic mice. *Mol Biol Cell* **6**: 1861-1873
- Coghlan MJ, Jacobson PB, Lane B, Nakane M, Lin CW, Elmore SW, Kym PR, Luly JR, Carter GW, Turner R, Tyree CM, Hu J, Elgort M, Rosen J, Miner JN (2003) A novel antiinflammatory maintains glucocorticoid efficacy with reduced side effects. *Mol Endocrinol* **17**: 860-869
- Cole TJ, Blendy JA, Monaghan AP, Kriegelstein K, Schmid W, Aguzzi A, Fantuzzi G, Hummler E, Unsicker K, Schutz G (1995) Targeted disruption of the glucocorticoid receptor gene blocks adrenergic chromaffin cell development and severely retards lung maturation. *Genes Dev* **9**: 1608-1621
- Cooper MS, Walker EA, Bland R, Fraser WD, Hewison M, Stewart PM (2000) Expression and functional consequences of 11beta-hydroxysteroid dehydrogenase activity in human bone. *Bone* **27**: 375-381
- Cooper MS, Blumsohn A, Goddard PE, Bartlett WA, Shackleton CH, Eastell R, Hewison M, Stewart PM (2003) 11beta-hydroxysteroid dehydrogenase type 1 activity predicts the effects of glucocorticoids on bone. *J Clin Endocrinol Metab* **88**: 3874-3877
- Corroyer S, Nabeyrat E, Clement A (1997) Involvement of the cell cycle inhibitor CIP1/WAF1 in lung alveolar epithelial cell growth arrest induced by glucocorticoids. *Endocrinology* **138**: 3677-3685
- Cowland JB, Borregaard N (1997) Molecular characterization and pattern of tissue expression of the gene for neutrophil gelatinase-associated lipocalin from humans. *Genomics* **45**: 17-23
- Cowland JB, Muta T, Borregaard N (2006) IL-1beta-specific up-regulation of neutrophil gelatinase-associated lipocalin is controlled by IkappaB-zeta. *J Immunol* **176**: 5559-5566
- Coxam V, Miller MA, Bowman MB, Miller SC (1996) Ontogenesis of IGF regulation of longitudinal bone growth in rat metatarsal rudiments cultured in serum-free medium. *Arch Physiol Biochem* **104**: 173-179

- Coxam V, Miller MA, Bowman MB, Miller SC (1996) Ontogenesis of IGF regulation of longitudinal bone growth in rat metatarsal rudiments cultured in serum-free medium. *Arch Physiol Biochem* **104**: 173-179
- Cram EJ, Ramos RA, Wang EC, Cha HH, Nishio Y, Firestone GL (1998) Role of the CCAAT/enhancer binding protein-alpha transcription factor in the glucocorticoid stimulation of p21waf1/cip1 gene promoter activity in growth-arrested rat hepatoma cells. *J Biol Chem* **273**: 2008-2014
- Crofton PM, Ahmed SF, Wade JC, Stephen R, Elmlinger MW, Ranke MB, Kelnar CJ, Wallace WH (1998) Effects of intensive chemotherapy on bone and collagen turnover and the growth hormone axis in children with acute lymphoblastic leukemia. *J Clin Endocrinol Metab* **83**: 3121-3129
- Curtin JJ, Sampson MA (1992) Need for open access non-screening mammography in a hospital with a specialist breast clinic service. *BMJ* **304**: 549-551
- D'Ercole AJ, Stiles AD, Underwood LE (1984) Tissue concentrations of somatomedin C: further evidence for multiple sites of synthesis and paracrine or autocrine mechanisms of action. *Proc Natl Acad Sci U S A* **81**: 935-939
- Damen GM, Boersma B, Wit JM, Heymans HS (1994) Catch-up growth in 60 children with celiac disease. *J Pediatr Gastroenterol Nutr* **19**: 394-400
- Daughaday WH (1992) Pituitary gigantism. *Endocrinol Metab Clin North Am* **21**: 633-647
- Deng C, Zhang P, Harper JW, Elledge SJ, Leder P (1995) Mice lacking p21CIP1/WAF1 undergo normal development, but are defective in G1 checkpoint control. *Cell* **82**: 675-684
- Dennis G, Jr., Sherman BT, Hosack DA, Yang J, Gao W, Lane HC, Lempicki RA (2003) DAVID: Database for Annotation, Visualisation, and Integrated Discovery. *Genome Biol* **4**: 3
- Devireddy LR, Teodoro JG, Richard FA, Green MR (2001) Induction of apoptosis by a secreted lipocalin that is transcriptionally regulated by IL-3 deprivation. *Science* **293**: 829-834
- Diamond MI, Miner JN, Yoshinaga SK, Yamamoto KR (1990) Transcription factor interactions: selectors of positive or negative regulation from a single DNA element. *Science* **249**: 1266-1272
- Drissi H, Hushka D, Aslam F, Nguyen Q, Buffone E, Koff A, van WA, Lian JB, Stein JL, Stein GS (1999) The cell cycle regulator p27kip1 contributes to growth and differentiation of osteoblasts. *Cancer Res* **59**: 3705-3711
- Drop SL, De Waal WJ, De Muinck Keizer-Schrama SM (1998) Sex steroid treatment of constitutionally tall stature. *Endocr Rev* **19**: 540-558
- Drop SL, Greggio N, Cappa M, Bernasconi S (2001) Current concepts in tall stature and overgrowth syndromes. *J Pediatr Endocrinol Metab* **14 Suppl 2**: 975-984

- Ducy P, Schinke T, Karsenty G (2000) The osteoblast: a sophisticated fibroblast under central surveillance. *Science* **289**: 1501-1504
- Dupont J, LeRoith D (2001) Insulin and insulin-like growth factor I receptors: similarities and differences in signal transduction. *Horm Res* **55 Suppl 2**: 22-26
- el-Deiry WS, Tokino T, Velculescu VE, Levy DB, Parsons R, Trent JM, Lin D, Mercer WE, Kinzler KW, Vogelstein B (1993) WAF1, a potential mediator of p53 tumor suppression. *Cell* **75** : 817-825
- el-Deiry WS, Harper JW, O'Connor PM, Velculescu VE, Canman CE, Jackman J, Pietenpol JA, Burrell M, Hill DE, Wang Y, . (1994) WAF1/CIP1 is induced in p53-mediated G1 arrest and apoptosis. *Cancer Res* **54**: 1169-1174
- el-Deiry WS, Tokino T, Waldman T, Oliner JD, Velculescu VE, Burrell M, Hill DE, Healy E, Rees JL, Hamilton SR, . (1995) Topological control of p21WAF1/CIP1 expression in normal and neoplastic tissues. *Cancer Res* **55**: 2910-2919
- Elmore SW, Coghlan MJ, Anderson DD, Pratt JK, Green BE, Wang AX, Stashko MA, Lin CW, Tyree CM, Miner JN, Jacobson PB, Wilcox DM, Lane BC (2001) Nonsteroidal selective glucocorticoid modulators: the effect of C-5 alkyl substitution on the transcriptional activation/repression profile of 2,5-dihydro-10-methoxy-2,2,4-trimethyl-1H-[1]benzopyrano[3,4-f]quinolines. *J Med Chem* **44**: 4481-4491
- Emons JA, Marino R, Nilsson O, Barnes KM, Even-Zohar N, Andrade AC, Chatterjee NA, Wit JM, Karperien M, Baron J (2006) The role of p27Kip1 in the regulation of growth plate chondrocyte proliferation in mice. *Pediatr Res* **60**: 288-293
- Erdmann S, Muller W, Bahrami S, Vornehm SI, Mayer H, Bruckner P, von der MK, Burkhardt H (1996) Differential effects of parathyroid hormone fragments on collagen gene expression in chondrocytes. *J Cell Biol* **135**: 1179-1191
- Erenpreisa J, Roach HI (1996) Epigenetic selection as a possible component of transdifferentiation. Further study of the commitment of hypertrophic chondrocytes to become osteocytes. *Mech Ageing Dev* **87**: 165-182
- Erhardt JA, Pittman RN (1998) Ectopic p21(WAF1) expression induces differentiation-specific cell cycle changes in PC12 cells characteristic of nerve growth factor treatment. *J Biol Chem* **273**: 23517-23523
- Evers BM, Ko TC, Li J, Thompson EA (1996) Cell cycle protein suppression and p21 induction in differentiating Caco-2 cells. *Am J Physiol* **271**: G722-G727
- Ezzat S (1997) Acromegaly. *Endocrinol Metab Clin North Am* **26**: 703-723
- Fantl V, Stamp G, Andrews A, Rosewell I, Dickson C (1995) Mice lacking cyclin D1 are small and show defects in eye and mammary gland development. *Genes Dev* **9**: 2364-2372
- Farnum CE, Wilsman NJ, Hilley HD (1984) An ultrastructural analysis of osteochondritic growth plate cartilage in growing swine. *Vet Pathol* **21**: 141-151

- Farnum CE, Wilsman NJ (1986) Ultrastructural histochemical evaluation of growth plate cartilage matrix from healthy and osteochondritic swine. *Am J Vet Res* **47**: 1105-1115
- Farnum CE, Wilsman NJ (1987) Morphologic stages of the terminal hypertrophic chondrocyte of growth plate cartilage. *Anat Rec* **219**: 221-232
- Farnum CE, Wilsman NJ (1993) Determination of proliferative characteristics of growth plate chondrocytes by labeling with bromodeoxyuridine. *Calcif Tissue Int* **52**: 110-119
- Farquharson C (2003), 'Bone Growth', in Scanes, C.G. (ed) *Biology of growth of domestic animals*. Iowa State Press, Iowa, 170-185
- Feng JQ, Ward LM, Liu S, Lu Y, Xie Y, Yuan B, Yu X, Rauch F, Davis SI, Zhang S, Rios H, Drezner MK, Quarles LD, Bonewald LF, White KE (2006) Loss of DMP1 causes rickets and osteomalacia and identifies a role for osteocytes in mineral metabolism. *Nat Genet* **38** : 1310-1315
- Fero ML, Rivkin M, Tasch M, Porter P, Carow CE, Firpo E, Polyak K, Tsai LH, Broudy V, Perlmutter RM, Kaushansky K, Roberts JM (1996) A syndrome of multiorgan hyperplasia with features of gigantism, tumorigenesis, and female sterility in p27(Kip1)-deficient mice. *Cell* **85**: 733-744
- Flower DR (1994) The lipocalin protein family: a role in cell regulation. *FEBS Lett* **354**: 7-11
- Forrest D, Hanebuth E, Smeyne RJ, Everds N, Stewart CL, Wehner JM, Curran T (1996) Recessive resistance to thyroid hormone in mice lacking thyroid hormone receptor beta: evidence for tissue-specific modulation of receptor function. *EMBO J* **15**: 3006-3015
- Frank GR (2003) Role of oestrogen and androgen in pubertal skeletal physiology. *Med Pediatr Oncol* **41**: 217-221
- Franz-Odendaal TA, Hall BK, Witten PE (2006) Buried alive: how osteoblasts become osteocytes. *Dev Dyn* **235**: 176-190
- Friedl A, Stoesz SP, Buckley P, Gould MN (1999) Neutrophil gelatinase-associated lipocalin in normal and neoplastic human tissues. Cell type-specific pattern of expression. *Histochem J* **31**: 433-441
- Fritz PC, Ward WE, Atkinson SA, Tenenbaum HC (1998) Tamoxifen attenuates the effects of exogenous glucocorticoid on bone formation and growth in piglets. *Endocrinology* **139**: 3399-3403
- Fujita T, Fukuyama R, Enomoto H, Komori T (2004) Dexamethasone inhibits insulin-induced chondrogenesis of ATDC5 cells by preventing PI3K-Akt signalling and DNA binding of Runx2. *J Cell Biochem* **93**: 374-383

- Gabrielsson BG, Carmignac DF, Flavell DM, Robinson IC (1995) Steroid regulation of growth hormone (GH) receptor and GH-binding protein messenger ribonucleic acids in the rat. *Endocrinology* **136**: 209-217
- Gafni RI, Baron J (2000) Catch-up growth: possible mechanisms. *Pediatr Nephrol* **14**: 616-619
- Gafni RI, Weise M, Robrecht DT, Meyers JL, Barnes KM, De-Levi S, Baron J (2001) Catch-up growth is associated with delayed senescence of the growth plate in rabbits. *Pediatr Res* **50**: 618-623
- Galotto M, Campanile G, Robino G, Cancedda FD, Bianco P, Cancedda R (1994) Hypertrophic chondrocytes undergo further differentiation to osteoblast-like cells and participate in the initial bone formation in developing chick embryo. *J Bone Miner Res* **9**: 1239-1249
- Garay-Rojas E, Harper M, Hraba-Renevey S, Kress M (1996) An apparent autocrine mechanism amplifies the dexamethasone- and retinoic acid-induced expression of mouse lipocalin-encoding gene 24p3. *Gene* **170**: 173-180
- Gartel AL, Serfas MS, Tyner AL (1996) p21--negative regulator of the cell cycle. *Proc Soc Exp Biol Med* **213**: 138-149
- Gerber HP, Vu TH, Ryan AM, Kowalski J, Werb Z, Ferrara N (1999) VEGF couples hypertrophic cartilage remodeling, ossification and angiogenesis during endochondral bone formation. *Nat Med* **5**: 623-628
- Gevers EF, van der Eerden BC, Karperien M, Raap AK, Robinson IC, Wit JM (2002) Localisation and regulation of the growth hormone receptor and growth hormone-binding protein in the rat growth plate. *J Bone Miner Res* **17**: 1408-1419
- Giustina A, Buffoli MG, Bussi AR, Doga M, Girelli A, Pizzocolo G, Pozzi A, Wehrenberg WB (1992) Comparative effect of clonidine and growth hormone (GH)-releasing hormone on GH secretion in adult patients on chronic glucocorticoid therapy. *Horm Metab Res* **24**: 240-243
- Giustina A, Veldhuis JD (1998) Pathophysiology of the neuroregulation of growth hormone secretion in experimental animals and the human. *Endocr Rev* **19**: 717-797
- Gong Y, Krakow D, Marcelino J, Wilkin D, Chitayat D, Babul-Hirji R, Hudgins L, Cremers CW, Cremers FP, Brunner HG, Reinker K, Rimoin DL, Cohn DH, Goodman FR, Reardon W, Patton M, Francomano CA, Warman ML (1999) Heterozygous mutations in the gene encoding noggin affect human joint morphogenesis. *Nat Genet* **21**: 302-304
- Gothe S, Wang Z, Ng L, Kindblom JM, Barros AC, Ohlsson C, Vennstrom B, Forrest D (1999) Mice devoid of all known thyroid hormone receptors are viable but exhibit disorders of the pituitary-thyroid axis, growth, and bone maturation. *Genes Dev* **13**: 1329-1341

- Grammer TC, Blenis J (1996) The serine protease inhibitors, tosylphenylalanine chloromethyl ketone and tosyllysine chloromethyl ketone, potently inhibit pp70s6k activation. *J Biol Chem* **271**: 23650-23652
- Green H, Morikawa M, Nixon T (1985) A dual effector theory of growth-hormone action. *Differentiation* **29**: 195-198
- Grigoriadis AE, Heersche JN, Aubin JE (1996) Analysis of chondroprogenitor frequency and cartilage differentiation in a novel family of clonal chondrogenic rat cell lines. *Differentiation* **60**: 299-307
- Grimsrud CD, Romano PR, D'Souza M, Puzas JE, Reynolds PR, Rosier RN, O'Keefe RJ (1999) BMP-6 is an autocrine stimulator of chondrocyte differentiation. *J Bone Miner Res* **14**: 475-482
- Grumbach MM (2000) Oestrogen, bone, growth and sex: a sea change in conventional wisdom. *J Pediatr Endocrinol Metab* **13 Suppl 6**: 1439-1455
- Guo K, Wang J, Andres V, Smith RC, Walsh K (1995) MyoD-induced expression of p21 inhibits cyclin-dependent kinase activity upon myocyte terminal differentiation. *Mol Cell Biol* **15** : 3823-3829
- Haaijman A, Karperien M, Lanske B, Hendriks J, Lowik CW, Bronckers AL, Burger EH (1999) Inhibition of terminal chondrocyte differentiation by bone morphogenetic protein 7 (OP-1) in vitro depends on the periarticular region but is independent of parathyroid hormone-related peptide. *Bone* **25**: 397-404
- Haigh JJ, Gerber HP, Ferrara N, Wagner EF (2000) Conditional inactivation of VEGF-A in areas of collagen2a1 expression results in embryonic lethality in the heterozygous state. *Development* **127**: 1445-1453
- Halevy O, Novitch BG, Spicer DB, Skapek SX, Rhee J, Hannon GJ, Beach D, Lassar AB (1995) Correlation of terminal cell cycle arrest of skeletal muscle with induction of p21 by MyoD. *Science* **267**: 1018-1021
- Hall BK (1987) Earliest evidence of cartilage and bone development in embryonic life. *Clin Orthop Relat Res* 255-272
- Hall BK, Miyake T (2000) All for one and one for all: condensations and the initiation of skeletal development. *Bioessays* **22**: 138-147
- Haller AC, Zimny ML (1977) Effects of hibernation on interradicular alveolar bone. *J Dent Res* **56**: 1552-1557
- Hamilton RT, Nilsen-Hamilton M, Adams G (1985) Superinduction by cycloheximide of mitogen-induced secreted proteins produced by Balb/c 3T3 cells. *J Cell Physiol* **123**: 201-208
- Han F, Adams CS, Tao Z, Williams CJ, Zaka R, Tuan RS, Norton PA, Hickok NJ (2005) Transforming growth factor-beta1 (TGF-beta1) regulates ATDC5 chondrogenic differentiation and fibronectin isoform expression. *J Cell Biochem* **95**: 750-762

- Hanahan D (1983) Studies on transformation of *Escherichia coli* with plasmids. *J Mol Biol* **166**: 557-580
- Harper JW, Elledge SJ (1996) Cdk inhibitors in development and cancer. *Curr Opin Genet Dev* **6**: 56-64
- Hatori M, Klatte KJ, Teixeira CC, Shapiro IM (1995) End labeling studies of fragmented DNA in the avian growth plate: evidence of apoptosis in terminally differentiated chondrocytes. *J Bone Miner Res* **10**: 1960-1968
- Havers, C (1691), 'Osteologia nova, or Some new observations of the bones, and the parts belonging to them, with the manner of their accretion, and nutrition, communicated to the Royal Society in several discourses. I. Of the membrane, nature, constituent parts, and internal structure of the bones. II. Of accretion, and nutrition, as also of the affections of the bones in the rickets, and of venereal nodes. III. Of the medulla, or marrow. IV. Of the mucilaginous glands, with the etiology or explication of the causes of a rheumatism, and the gout, and the manner how they are produced. To which is added a fifth discourse of the cartilages.', Printed for Samuel Smith, at the Princes Arms in St. Paul's Church-Yard, London
- Hench S, Kendall EC, Slocumb CH, Polley HF (1949) The effect of a hormone of the adrenal cortex (17-hydroxy-11-dehydrocorticosterone: compound E) and of pituitary adrenocorticotrophic hormone on rheumatoid arthritis. *Proc. Staff Meetings Mayo Clin.* **24**: 181-197
- Herzig S, Long F, Jhala US, Hedrick S, Quinn R, Bauer A, Rudolph D, Schutz G, Yoon C, Puigserver P, Spiegelman B, Montminy M (2001) CREB regulates hepatic gluconeogenesis through the coactivator PGC-1. *Nature* **413**: 179-183
- Hiraki Y, Inoue H, Iyama K, Kamizono A, Ochiai M, Shukunami C, Iijima S, Suzuki F, Kondo J (1997) Identification of chondromodulin I as a novel endothelial cell growth inhibitor. Purification and its localisation in the avascular zone of epiphyseal cartilage. *J Biol Chem* **272**: 32419-32426
- Hiraoka K, Zenmyo M, Komiya S, Kawabata R, Yokouchi M, Suzuki R, Hamada T, Kato S, Nagata K (2002) Relationship of p21 (waf1/cip1) and differentiation in chondrosarcoma cells. *Virchows Arch* **440**: 285-290
- Horner A, Shum L, Ayres JA, Nonaka K, Nuckolls GH (2002) Fibroblast growth factor signalling regulates Dach1 expression during skeletal development. *Dev Dyn* **225**: 35-45
- Horton WA (2003) Skeletal development: insights from targeting the mouse genome. *Lancet* **362**: 560-569
- Hulleman E, Boonstra J (2001) Regulation of G1 phase progression by growth factors and the extracellular matrix. *Cell Mol Life Sci* **58**: 80-93
- Hunziker EB, Schenk RK, Cruz-Orive LM (1987) Quantitation of chondrocyte performance in growth-plate cartilage during longitudinal bone growth. *J Bone Joint Surg Am* **69**: 162-173

- Hunziker EB (1994) Mechanism of longitudinal bone growth and its regulation by growth plate chondrocytes. *Microsc Res Tech* **28**: 505-519
- Hurley HM, Florkiewicz RA (1996), 'Fibroblast growth factor and vascular endothelial cell growth factor families', in Bilezikian JP, Raisz LG, Rodan GA (eds) *Principles of Bone Biology*. Academic Press, San Diego, 627-645
- Hutchison MR, Bassett MH, White PC (2007) Insulin-like growth factor-I and fibroblast growth factor, but not growth hormone, affect growth plate chondrocyte proliferation. *Endocrinology* **148**: 3122-3130
- Irizarry RA, Hobbs B, Collin F, Beazer-Barclay YD, Antonellis KJ, Scherf U, Speed TP (2003) Exploration, normalisation, and summaries of high density oligonucleotide array probe level data. *Biostatistics* **4**: 249-264
- Isaksson OG, Jansson JO, Gause IA (1982) Growth hormone stimulates longitudinal bone growth directly. *Science* **216**: 1237-1239
- Isaksson OG, Lindahl A, Nilsson A, Isgaard J (1987) Mechanism of the stimulatory effect of growth hormone on longitudinal bone growth. *Endocr Rev* **8**: 426-438
- Ishizaki Y, Burne JF, Raff MC (1994) Autocrine signals enable chondrocytes to survive in culture. *J Cell Biol* **126**: 1069-1077
- Itagane Y, Inada H, Fujita K, Isshiki G (1991) Interactions between steroid hormones and insulin-like growth factor-I in rabbit chondrocytes. *Endocrinology* **128**: 1419-1424
- Ivkovic S, Yoon BS, Popoff SN, Safadi FF, Libuda DE, Stephenson RC, Daluiski A, Lyons KM (2003) Connective tissue growth factor coordinates chondrogenesis and angiogenesis during skeletal development. *Development* **130**: 2779-2791
- James CG, Ulici V, Tuckermann J, Underhill TM, Beier F (2007) Expression profiling of Dexamethasone-treated primary chondrocytes identifies targets of glucocorticoid signalling in endochondral bone development. *BMC Genomics* **8**: 205
- Jantzen HM, Strahle U, Gloss B, Stewart F, Schmid W, Boshart M, Miksicek R, Schutz G (1987) Cooperativity of glucocorticoid response elements located far upstream of the tyrosine aminotransferase gene. *Cell* **49**: 29-38
- Jiang H, Lin J, Su ZZ, Collart FR, Huberman E, Fisher PB (1994) Induction of differentiation in human promyelocytic HL-60 leukemia cells activates p21, WAF1/CIP1, expression in the absence of p53. *Oncogene* **9**: 3397-3406
- Jilka RL, Weinstein RS, Bellido T, Parfitt AM, Manolagas SC (1998) Osteoblast programmed cell death (apoptosis): modulation by growth factors and cytokines. *J Bone Miner Res* **13**: 793-802
- Jingushi S, Scully SP, Joyce ME, Sugioka Y, Bolander ME (1995) Transforming growth factor-beta 1 and fibroblast growth factors in rat growth plate. *J Orthop Res* **13**: 761-768

- Johnson DG, Walker CL (1999) Cyclins and cell cycle checkpoints. *Annu Rev Pharmacol Toxicol* **39**: 295-312
- Jonat C, Rahmsdorf HJ, Park KK, Cato AC, Gebel S, Ponta H, Herrlich P (1990) Antitumor promotion and antiinflammation: down-modulation of AP-1 (Fos/Jun) activity by glucocorticoid hormone. *Cell* **62**: 1189-1204
- Jones CM, Lyons KM, Hogan BL (1991) Involvement of Bone Morphogenetic Protein-4 (BMP-4) and Vgr-1 in morphogenesis and neurogenesis in the mouse. *Development* **111**: 531-542
- Juul A (2001) The effects of oestrogens on linear bone growth. *Hum Reprod Update* **7**: 303-313
- Kanaan RA, Aldwaik M, Al-Hanbali OA (2006) The role of connective tissue growth factor in skeletal growth and development. *Med Sci Monit* **12**: RA277-RA281
- Karaplis AC, Luz A, Glowacki J, Bronson RT, Tybulewicz VL, Kronenberg HM, Mulligan RC (1994) Lethal skeletal dysplasia from targeted disruption of the parathyroid hormone-related peptide gene. *Genes Dev* **8**: 277-289
- Kember NF, Sissons HA (1976) Quantitative histology of the human growth plate. *J Bone Joint Surg Br* **58-B**: 426-435
- Kember NF (1978) Cell kinetics and the control of growth in long bones. *Cell Tissue Kinet* **11**: 477-485
- Kember NF (1993) Cell kinetics and the control of bone growth. *Acta Paediatr Suppl* **82 Suppl 391**: 61-65
- Kim HJ, Zhao H, Kitaura H, Bhattacharyya S, Brewer JA, Muglia LJ, Ross FP, Teitelbaum SL (2006) Glucocorticoids suppress bone formation via the osteoclast. *J Clin Invest* **116**: 2152-2160
- Kiyokawa H, Koff A (1998) Roles of cyclin-dependent kinase inhibitors: lessons from knockout mice. *Curr Top Microbiol Immunol* **227**: 105-120
- Klaus G, Weber L, Rodriguez J, Fernandez P, Klein T, Grulich-Henn J, Hugel U, Ritz E, Mehls P (1998) Interaction of IGF-I and 1 alpha, 25(OH)2D3 on receptor expression and growth stimulation in rat growth plate chondrocytes. *Kidney Int* **53**: 1152-1161
- Klaus G, Jux C, Fernandez P, Rodriguez J, Himmele R, Mehls O (2000) Suppression of growth plate chondrocyte proliferation by corticosteroids. *Pediatr Nephrol* **14**: 612-615
- Knutti D, Kralli A (2001) PGC-1, a versatile coactivator. *Trends Endocrinol Metab* **12**: 360-365
- Koedam JA, Smink JJ, van Buul-Offers SC (2002) Glucocorticoids inhibit vascular endothelial growth factor expression in growth plate chondrocytes. *Mol Cell Endocrinol* **197**: 35-44

- Kotaniemi A, Savolainen A, Kroger H, Kautiainen H, Isomaki H (1999) Weight-bearing physical activity, calcium intake, systemic glucocorticoids, chronic inflammation, and body constitution as determinants of lumbar and femoral bone mineral in juvenile chronic arthritis. *Scand J Rheumatol* **28**: 19-26
- Krohn K, Haffner D, Hugel U, Himmele R, Klaus G, Mehls O, Schaefer F (2003) 1,25(OH)₂D₃ and dihydrotestosterone interact to regulate proliferation and differentiation of epiphyseal chondrocytes. *Calcif Tissue Int* **73**: 400-410
- Kronenberg HM, Chung U (2001) The parathyroid hormone-related protein and Indian hedgehog feedback loop in the growth plate. *Novartis Found Symp* **232**: 144-152
- Kronenberg HM (2003) Developmental regulation of the growth plate. *Nature* **423**: 332-336
- Kubota S, Moritani NH, Kawaki H, Mimura H, Minato M, Takigawa M (2003) Transcriptional induction of connective tissue growth factor/hypertrophic chondrocyte-specific 24 gene by dexamethasone in human chondrocytic cells. *Bone* **33**: 694-702
- Kuhn JL, DeLacey JH, Leenellett EE (1996) Relationship between bone growth rate and hypertrophic chondrocyte volume in New Zealand white rabbits of varying ages. *J Orthop Res* **14**: 706-711
- Kwan KM, Pang MK, Zhou S, Cowan SK, Kong RY, Pfordte T, Olsen BR, Silience DO, Tam PP, Cheah KS (1997) Abnormal compartmentalisation of cartilage matrix components in mice lacking collagen X: implications for function. *J Cell Biol* **136**: 459-471
- Langille RM (1994) Chondrogenic differentiation in cultures of embryonic rat mesenchyme. *Microsc Res Tech* **28**: 455-469
- Laplantine E, Rossi F, Sahni M, Basilico C, Cobrinik D (2002) FGF signalling targets the pRb-related p107 and p130 proteins to induce chondrocyte growth arrest. *J Cell Biol* **158**: 741-750
- Le RD, Scavo L, Butler A (2001) What is the role of circulating IGF-I? *Trends Endocrinol Metab* **12**: 48-52
- Leach RM, Jr., Sokol C, McMurtry JP (1997) Immunolocalisation of basic fibroblast growth factor in porcine epiphyseal growth plate. *Domest Anim Endocrinol* **14**: 129-132
- Leclerc N, Luppen CA, Ho VV, Nagpal S, Hacia JG, Smith E, Frenkel B (2004) Gene expression profiling of glucocorticoid-inhibited osteoblasts. *J Mol Endocrinol* **33**: 175-193
- Lefebvre V, Garofalo S, Zhou G, Metsaranta M, Vuorio E, De CB (1994) Characterization of primary cultures of chondrocytes from type II collagen/beta-galactosidase transgenic mice. *Matrix Biol* **14**: 329-335

- Lefebvre V, De CB (1998) Toward understanding SOX9 function in chondrocyte differentiation. *Matrix Biol* **16**: 529-540
- Legeai-Mallet L, oist-Lasselain C, Munnich A, Bonaventure J (2004) Overexpression of FGFR3, Stat1, Stat5 and p21Cip1 correlates with phenotypic severity and defective chondrocyte differentiation in FGFR3-related chondrodysplasias. *Bone* **34**: 26-36
- Leong ML, Maiyar AC, Kim B, O'Keeffe BA, Firestone GL (2003) Expression of the serum- and glucocorticoid-inducible protein kinase, Sgk, is a cell survival response to multiple types of environmental stress stimuli in mammary epithelial cells. *J Biol Chem* **278** : 5871-5882
- Leonhardt SA, Edwards DP (2002) Mechanism of action of progesterone antagonists. *Exp Biol Med (Maywood)* **227**: 969-980
- Lettgen B, Jeken C, Reiners C (1994) Influence of steroid medication on bone mineral density in children with nephrotic syndrome. *Pediatr Nephrol* **8**: 667-670
- Lewinson D, Silbermann M (1992) Chondroclasts and endothelial cells collaborate in the process of cartilage resorption. *Anat Rec* **233**: 504-514
- Liu M, Iavarone A, Freedman LP (1996) Transcriptional activation of the human p21(WAF1/CIP1) gene by retinoic acid receptor. Correlation with retinoid induction of U937 cell differentiation. *J Biol Chem* **271**: 31723-31728
- Liu M, Lee MH, Cohen M, Bommakanti M, Freedman LP (1996) Transcriptional activation of the Cdk inhibitor p21 by vitamin D3 leads to the induced differentiation of the myelomonocytic cell line U937. *Genes Dev* **10**: 142-153
- Liu Q, Nilsen-Hamilton M (1995) Identification of a new acute phase protein. *J Biol Chem* **270**: 22565-22570
- Livak KJ, Schmittgen TD (2001) Analysis of relative gene expression data using real-time quantitative PCR and the 2(-Delta Delta C(T)) Method. *Methods* **25**: 402-408
- Loveridge N, Farquharson C (1993) Studies on growth plate chondrocytes in situ: cell proliferation and differentiation. *Acta Paediatr Suppl* **82 Suppl 391**: 42-48
- Lundberg AS, Weinberg RA (1999) Control of the cell cycle and apoptosis. *Eur J Cancer* **35**: 1886-1894
- Luo JM, Murphy LJ (1989) Dexamethasone inhibits growth hormone induction of insulin-like growth factor-I (IGF-I) messenger ribonucleic acid (mRNA) in hypophysectomised rats and reduces IGF-I mRNA abundance in the intact rat. *Endocrinology* **125**: 165-171
- Lyons KM, Pelton RW, Hogan BL (1989) Patterns of expression of murine Vgr-1 and BMP-2a RNA suggest that transforming growth factor-beta-like genes coordinately regulate aspects of embryonic development. *Genes Dev* **3**: 1657-1668

- Macias D, Ganan Y, Sampath TK, Piedra ME, Ros MA, Hurle JM (1997) Role of BMP-2 and OP-1 (BMP-7) in programmed cell death and skeletogenesis during chick limb development. *Development* **124**: 1109-1117
- Macleod KF, Sherry N, Hannon G, Beach D, Tokino T, Kinzler K, Vogelstein B, Jacks T (1995) p53-dependent and independent expression of p21 during cell growth, differentiation, and DNA damage. *Genes Dev* **9**: 935-944
- Macrae VE, Ahmed SF, Mushtaq T, Farquharson C (2007) IGF-I signalling in bone growth: Inhibitory actions of dexamethasone and IL-1beta. *Growth Horm IGF Res*
- Mancilla EE, De LF, Uyeda JA, Czerwiec FS, Baron J (1998) Effects of fibroblast growth factor-2 on longitudinal bone growth. *Endocrinology* **139**: 2900-2904
- Mansfield K, Rajpurohit R, Shapiro IM (1999) Extracellular phosphate ions cause apoptosis of terminally differentiated epiphyseal chondrocytes. *J Cell Physiol* **179**: 276-286
- Markham A, Bryson HM (1995) Deflazacort. A review of its pharmacological properties and therapeutic efficacy. *Drugs* **50**: 317-333
- Markowitz J, Grancher K, Rosa J, Simpser E, Aiges H, Daum F (1995) Highly destructive perianal disease in children with Crohn's disease. *J Pediatr Gastroenterol Nutr* **21**: 149-153
- Marotti G (1996) The structure of bone tissues and the cellular control of their deposition. *Ital J Anat Embryol* **101**: 25-79
- Martin EA, Ritman EL, Turner RT (2003) Time course of epiphyseal growth plate fusion in rat tibiae. *Bone* **32**: 261-267
- Masuyama A, Ouchi Y, Sato F, Hosoi T, Nakamura T, Orimo H (1992) Characteristics of steroid hormone receptors in cultured MC3T3-E1 osteoblastic cells and effect of steroid hormones on cell proliferation. *Calcif Tissue Int* **51**: 376-381
- McCarthy TL, Centrella M, Canalis E (1989) Effects of fibroblast growth factors on deoxyribonucleic acid and collagen synthesis in rat parietal bone cells. *Endocrinology* **125**: 2118-2126
- McKay LI, Cidlowski JA (1999) Molecular control of immune/inflammatory responses: interactions between nuclear factor-kappa B and steroid receptor-signalling pathways. *Endocr Rev* **20**: 435-459
- Meheus LA, Franssen LM, Raymackers JG, Blockx HA, Van Beeumen JJ, Van Bun SM, Van d, V (1993) Identification by microsequencing of lipopolysaccharide-induced proteins secreted by mouse macrophages. *J Immunol* **151**: 1535-1547
- Mehta A, Hindmarsh PC, Stanhope RG, Turton JP, Cole TJ, Preece MA, Dattani MT (2005) The role of growth hormone in determining birth size and early postnatal growth, using congenital growth hormone deficiency (GHD) as a model. *Clin Endocrinol (Oxf)* **63**: 223-231

- Michieli P, Chedid M, Lin D, Pierce JH, Mercer WE, Givol D (1994) Induction of WAF1/CIP1 by a p53-independent pathway. *Cancer Res* **54**: 3391-3395
- Mikic B, Van der Meulen MC, Kingsley DM, Carter DR (1996) Mechanical and geometric changes in the growing femora of BMP-5 deficient mice. *Bone* **18**: 601-607
- Mikuni-Takagaki Y (1999) Mechanical responses and signal transduction pathways in stretched osteocytes. *J Bone Miner Metab* **17**: 57-60
- Miner JN (2002) Designer glucocorticoids. *Biochem Pharmacol* **64**: 355-361
- Minina E, Kreschel C, Naski MC, Ornitz DM, Vortkamp A (2002) Interaction of FGF, Ihh/Pthlh, and BMP signalling integrates chondrocyte proliferation and hypertrophic differentiation. *Dev Cell* **3**: 439-449
- Missero C, Calautti E, Eckner R, Chin J, Tsai LH, Livingston DM, Dotto GP (1995) Involvement of the cell-cycle inhibitor Cip1/WAF1 and the E1A-associated p300 protein in terminal differentiation. *Proc Natl Acad Sci U S A* **92**: 5451-5455
- Missero C, Di CF, Kiyokawa H, Koff A, Dotto GP (1996) The absence of p21Cip1/WAF1 alters keratinocyte growth and differentiation and promotes ras-tumor progression. *Genes Dev* **10**: 3065-3075
- Mitchell N, Shepard N, Harrod J (1982) The measurement of proteoglycan in the mineralizing region of the rat growth plate. *J Bone Joint Surg Am* **64**: 32-38
- Morey JS, Ryan JC, Van Dolah FM (2006) Microarray validation: factors influencing correlation between oligonucleotide microarrays and real-time PCR. *Biol Proced Online* **8**: 175-193
- Mori-Akiyama Y, Akiyama H, Rowitch DH, De CB (2003) Sox9 is required for determination of the chondrogenic cell lineage in the cranial neural crest. *Proc Natl Acad Sci U S A* **100**: 9360-9365
- Muragaki Y, Mariman EC, van Beersum SE, Perala M, van Mourik JB, Warman ML, Hamel BC, Olsen BR (1996) A mutation in COL9A2 causes multiple epiphyseal dysplasia (EDM2). *Ann N Y Acad Sci* **785**: 303-306
- Murakami S, Kan M, McKeehan WL, De CB (2000) Up-regulation of the chondrogenic Sox9 gene by fibroblast growth factors is mediated by the mitogen-activated protein kinase pathway. *Proc Natl Acad Sci U S A* **97**: 1113-1118
- Mushtaq T, Ahmed SF (2002) The impact of corticosteroids on growth and bone health. *Arch Dis Child* **87**: 93-96
- Mushtaq T, Bijman P, Ahmed SF, Farquharson C (2004) Insulin-like growth factor-I augments chondrocyte hypertrophy and reverses glucocorticoid-mediated growth retardation in foetal mice metatarsal cultures. *Endocrinology* **145**: 2478-2486
- Mushtaq T, Farquharson C, Seawright E, Ahmed SF (2002) Glucocorticoid effects on chondrogenesis, differentiation and apoptosis in the murine ATDC5 chondrocyte cell line. *J Endocrinol* **175**: 705-713

- Nagahama H, Hatakeyama S, Nakayama K, Nagata M, Tomita K, Nakayama K (2001) Spatial and temporal expression patterns of the cyclin-dependent kinase (CDK) inhibitors p27Kip1 and p57Kip2 during mouse development. *Anat Embryol (Berl)* **203**: 77-87
- Nakajima M, Negishi Y, Tanaka H, Kawashima K (2004) p21(Cip-1/SDI-1/WAF-1) expression via the mitogen-activated protein kinase signalling pathway in insulin-induced chondrogenic differentiation of ATDC5 cells. *Biochem Biophys Res Commun* **320**: 1069-1075
- Nakanishi T, Yamaai T, Asano M, Nawachi K, Suzuki M, Sugimoto T, Takigawa M (2001) Overexpression of connective tissue growth factor/hypertrophic chondrocyte-specific gene product 24 decreases bone density in adult mice and induces dwarfism. *Biochem Biophys Res Commun* **281**: 678-681
- Nakayama K, Ishida N, Shirane M, Inomata A, Inoue T, Shishido N, Horii I, Loh DY, Nakayama K (1996) Mice lacking p27(Kip1) display increased body size, multiple organ hyperplasia, retinal dysplasia, and pituitary tumors. *Cell* **85**: 707-720
- Naski MC, Colvin JS, Coffin JD, Ornitz DM (1998) Repression of hedgehog signalling and BMP4 expression in growth plate cartilage by fibroblast growth factor receptor 3. *Development* **125**: 4977-4988
- Negishi Y, Ui N, Nakajima M, Kawashima K, Maruyama K, Takizawa T, Endo H (2001) p21Cip-1/SDI-1/WAF-1 gene is involved in chondrogenic differentiation of ATDC5 cells in vitro. *J Biol Chem* **276**: 33249-33256
- Nilsen-Hamilton M, Hamilton RT, Adams GA (1982) Rapid selective stimulation by growth factors of the incorporation by BALB/C 3T3 cells of [35S]methionine into a glycoprotein and five superinducible proteins. *Biochem Biophys Res Commun* **108**: 158-166
- Nilsson O, Baron J (2005) Impact of growth plate senescence on catch-up growth and epiphyseal fusion. *Pediatr Nephrol* **20**: 319-322
- Nishida T, Kubota S, Nakanishi T, Kuboki T, Yosimichi G, Kondo S, Takigawa M (2002) CTGF/Hcs24, a hypertrophic chondrocyte-specific gene product, stimulates proliferation and differentiation, but not hypertrophy of cultured articular chondrocytes. *J Cell Physiol* **192**: 55-63
- Noble BS, Stevens H, Loveridge N, Reeve J (1997) Identification of apoptotic changes in osteocytes in normal and pathological human bone. *Bone* **20**: 273-282
- Ohlsson C, Nilsson A, Isaksson O, Lindahl A (1992) Growth hormone induces multiplication of the slowly cycling germinal cells of the rat tibial growth plate. *Proc Natl Acad Sci U S A* **89**: 9826-9830
- Ohlsson C, Isgaard J, Tornell J, Nilsson A, Isaksson OG, Lindahl A (1993) Endocrine regulation of longitudinal bone growth. *Acta Paediatr Suppl* **82 Suppl 391**: 33-40

- oist-Lasselin C, Gibbs L, Heuertz S, Odent T, Munnich A, Legeai-Mallet L (2007) Human immortalised chondrocytes carrying heterozygous FGFR3 mutations: an in vitro model to study chondrodysplasias. *FEBS Lett* **581**: 2593-2598
- Onat T (1975) Prediction of adult height of girls based on the percentage of adult height at onset of secondary sexual characteristics, at chronological age, and skeletal age. *Hum Biol* **47**: 117-130
- Ornitz DM, Marie PJ (2002) FGF signalling pathways in endochondral and intramembranous bone development and human genetic disease. *Genes Dev* **16**: 1446-1465
- Ortega N, Behonick D, Stickens D, Werb Z (2003) How proteases regulate bone morphogenesis. *Ann N Y Acad Sci* **995**: 109-116
- Owen GI, Richer JK, Tung L, Takimoto G, Horwitz KB (1998) Progesterone regulates transcription of the p21(WAF1) cyclin- dependent kinase inhibitor gene through Sp1 and CBP/p300. *J Biol Chem* **273**: 10696-10701
- Owen HC, Miner JN, Ahmed SF, Farquharson C (2007) The growth plate sparing effects of the selective glucocorticoid receptor modulator, AL-438. *Mol Cell Endocrinol* **264**: 164-170
- Panda DK, Miao D, Lefebvre V, Hendy GN, Goltzman D (2001) The transcription factor SOX9 regulates cell cycle and differentiation genes in chondrocytic CFK2 cells. *J Biol Chem* **276** : 41229-41236
- Parfitt AM (1990) Interpretation of bone densitometry measurements: disadvantages of a percentage scale and a discussion of some alternatives. *J Bone Miner Res* **5**: 537-540
- Parfitt AM (2002) Misconceptions (1): epiphyseal fusion causes cessation of growth. *Bone* **30**: 337-339
- Parker SB, Eichele G, Zhang P, Rawls A, Sands AT, Bradley A, Olson EN, Harper JW, Elledge SJ (1995) p53-independent expression of p21Cip1 in muscle and other terminally differentiating cells. *Science* **267**: 1024-1027
- Peeke PM, Chrousos GP (1995) Hypercortisolism and obesity. *Ann N Y Acad Sci* **771**: 665-676
- Peters KG, Werner S, Chen G, Williams LT (1992) Two FGF receptor genes are differentially expressed in epithelial and mesenchymal tissues during limb formation and organogenesis in the mouse. *Development* **114**: 233-243
- Pfaffle RW, Parks JS, Brown MR, Heimann G (1993) Pit-1 and pituitary function. *J Pediatr Endocrinol* **6**: 229-233
- Picherit C, Coxam V, Oudadesse H, Martini B, Gaumet N, Davicco MJ, Lebecque P, Miller S, Irrigaray JL, Barlet JP (2000) Dihydrotestosterone prevents glucocorticoid-negative effects on foetal rat metatarsal bone in vitro. *Biol Neonate* **77**: 181-190

- Polinkovsky A, Robin NH, Thomas JT, Irons M, Lynn A, Goodman FR, Reardon W, Kant SG, Brunner HG, van dB, I, Chitayat D, McGaughran J, Donnai D, Luyten FP, Warman ML (1997) Mutations in CDMP1 cause autosomal dominant brachydactyly type C. *Nat Genet* **17**: 18-19
- Polito C, La MA, Papale MR, Villani G (1999) Delayed pubertal growth spurt and normal adult height attainment in boys receiving long-term alternate-day prednisone therapy. *Clin Pediatr (Phila)* **38**: 279-285
- Powell-Braxton L, Hollingshead P, Warburton C, Dowd M, Pitts-Meek S, Dalton D, Gillett N, Stewart TA (1993) IGF-I is required for normal embryonic growth in mice. *Genes Dev* **7**: 2609-2617
- Prabhu S, Ignatova A, Park ST, Sun XH (1997) Regulation of the expression of cyclin-dependent kinase inhibitor p21 by E2A and Id proteins. *Mol Cell Biol* **17**: 5888-5896
- PRADER A, TANNER JM, von HG (1963) Catch-up growth following illness or starvation. An example of developmental canalisation in man. *J Pediatr* **62**: 646-659
- Puigserver P, Adelmant G, Wu Z, Fan M, Xu J, O'Malley B, Spiegelman BM (1999) Activation of PPARgamma coactivator-1 through transcription factor docking. *Science* **286**: 1368-1371
- Ramalingam A, Hirai A, Thompson EA (1997) Glucocorticoid inhibition of fibroblast proliferation and regulation of the cyclin kinase inhibitor p21Cip1. *Mol Endocrinol* **11**: 577-586
- Reddi AH (2001) Interplay between bone morphogenetic proteins and cognate binding proteins in bone and cartilage development: noggin, chordin and DAN. *Arthritis Res* **3**: 1-5
- Rivkees SA, Bode HH, Crawford JD (1988) Long-term growth in juvenile acquired hypothyroidism: the failure to achieve normal adult stature. *N Engl J Med* **318**: 599-602
- Roach HI, Mehta G, Oreffo RO, Clarke NM, Cooper C (2003) Temporal analysis of rat growth plates: cessation of growth with age despite presence of a physis. *J Histochem Cytochem* **51**: 373-383
- Roberts S, Narisawa S, Harmey D, Millan JL, Farquharson C (2007) Functional involvement of PHOSPHO1 in matrix vesicle-mediated skeletal mineralisation. *J Bone Miner Res* **22**: 617-627
- Robson H, Anderson E, Eden OB, Isaksson O, Shalet S (1998) Chemotherapeutic agents used in the treatment of childhood malignancies have direct effects on growth plate chondrocyte proliferation. *J Endocrinol* **157**: 225-235
- Robson H, Siebler T, Shalet SM, Williams GR (2002) Interactions between GH, IGF-I, glucocorticoids, and thyroid hormones during skeletal growth. *Pediatr Res* **52**: 137-147

- Rogatsky I, Trowbridge JM, Garabedian MJ (1997) Glucocorticoid receptor-mediated cell cycle arrest is achieved through distinct cell-specific transcriptional regulatory mechanisms. *Mol Cell Biol* **17**: 3181-3193
- Rosen J, Miner JN (2005) The search for safer glucocorticoid receptor ligands. *Endocr Rev* **26**: 452-464
- Rossi L, Migliaccio S, Corsi A, Marzia M, Bianco P, Teti A, Gambelli L, Cianfarani S, Paoletti F, Branca F (2001) Reduced growth and skeletal changes in zinc-deficient growing rats are due to impaired growth plate activity and inanition. *J Nutr* **131**: 1142-1146
- Roudkenar MH, Kuwahara Y, Baba T, Roushandeh AM, Ebishima S, Abe S, Ohkubo Y, Fukumoto M (2007) Oxidative stress induced lipocalin 2 gene expression: addressing its expression under the harmful conditions. *J Radiat Res (Tokyo)* **48**: 39-44
- Ruoslahti E, Yamaguchi Y (1991) Proteoglycans as modulators of growth factor activities. *Cell* **64**: 867-869
- Saha MT, Ruuska T, Laippala P, Lenko HL (1998) Growth of prepubertal children with inflammatory bowel disease. *J Pediatr Gastroenterol Nutr* **26**: 310-314
- Sahni M, Ambrosetti DC, Mansukhani A, Gertner R, Levy D, Basilico C (1999) FGF signalling inhibits chondrocyte proliferation and regulates bone development through the STAT-1 pathway. *Genes Dev* **13**: 1361-1366
- Salmon WD, Jr., Daughaday WH (1990) A hormonally controlled serum factor which stimulates sulfate incorporation by cartilage in vitro. 1956. *J Lab Clin Med* **116**: 408-419
- Sambrook P, Kelly P, Eisman J (1993) Bone mass and ageing. *Baillieres Clin Rheumatol* **7**: 445-457
- Sanchez CP, He YZ (2002) Alterations in the growth plate cartilage of rats with renal failure receiving corticosteroid therapy. *Bone* **30**: 692-698
- Savage MO, Burren CP, Blair JC, Woods KA, Metherell L, Clark AJ, Camacho-Hubner C (2001) Growth hormone insensitivity: pathophysiology, diagnosis, clinical variation and future perspectives. *Horm Res* **55 Suppl 2**: 32-35
- Scheven BA, Hamilton NJ (1991) Longitudinal bone growth in vitro: effects of insulin-like growth factor I and growth hormone. *Acta Endocrinol (Copenh)* **124**: 602-607
- Schipani E, Ryan HE, Didrickson S, Kobayashi T, Knight M, Johnson RS (2001) Hypoxia in cartilage: HIF-1alpha is essential for chondrocyte growth arrest and survival. *Genes Dev* **15** : 2865-2876
- Schipani E (2006) Hypoxia and HIF-1alpha in chondrogenesis. *Ann N Y Acad Sci* **1068**: 66-73

- Schmidt A, Rodegerdts U, Buddecke E (1978) Correlation of lysozyme activity with proteoglycan biosynthesis in epiphyseal cartilage. *Calcif Tissue Res* **26**: 163-172
- Schrier L, Ferns SP, Barnes KM, Emons JA, Newman EI, Nilsson O, Baron J (2006) Depletion of resting zone chondrocytes during growth plate senescence. *J Endocrinol* **189**: 27-36
- Schwartz Z, Sylvia VL, Guinee T, Dean DD, Boyan BD (2002) Tamoxifen elicits its anti-oestrogen effects in growth plate chondrocytes by inhibiting protein kinase C. *J Steroid Biochem Mol Biol* **80**: 401-410
- Seinsheimer F, III, Sledge CB (1981) Parameters of longitudinal growth rate in rabbit epiphyseal growth plates. *J Bone Joint Surg Am* **63**: 627-630
- Sekiya I, Koopman P, Tsuji K, Mertin S, Harley V, Yamada Y, Shinomiya K, Nifuji A, Noda M (2001) Dexamethasone enhances SOX9 expression in chondrocytes. *J Endocrinol* **169**: 573-579
- SEMearo EJ, Stallings VA, Peck SN, Piccoli DA (1997) Vertebral compression fractures in pediatric patients with Crohn's disease. *Gastroenterology* **112**: 1710-1713
- SEMenza GL (1999) Regulation of mammalian O₂ homeostasis by hypoxia-inducible factor 1. *Annu Rev Cell Dev Biol* **15**: 551-578
- Shao YY, Wang L, Ballock RT (2006) Thyroid hormone and the growth plate. *Rev Endocr Metab Disord* **7**: 265-271
- Shapiro IM, Boyde A (1987) Mineralisation of normal and rachitic chick growth cartilage: vascular canals, cartilage calcification and osteogenesis. *Scanning Microsc* **1**: 599-606
- Shapiro IM, Adams CS, Freeman T, Srinivas V (2005) Fate of the hypertrophic chondrocyte: microenvironmental perspectives on apoptosis and survival in the epiphyseal growth plate. *Birth Defects Res C Embryo Today* **75**: 330-339
- Shaw NJ, Fraser NC, Weller PH (1997) Asthma treatment and growth. *Arch Dis Child* **77**: 284-286
- Sherr CJ (1995) Mammalian G1 cyclins and cell cycle progression. *Proc Assoc Am Physicians* **107**: 181-186
- Sicinski P, Donaher JL, Geng Y, Parker SB, Gardner H, Park MY, Robker RL, Richards JS, McGinnis LK, Biggers JD, Eppig JJ, Bronson RT, Elledge SJ, Weinberg RA (1996) Cyclin D2 is an FSH-responsive gene involved in gonadal cell proliferation and oncogenesis. *Nature* **384**: 470-474
- Siebler T, Robson H, Shalet SM, Williams GR (2002) Dexamethasone inhibits and thyroid hormone promotes differentiation of mouse chondrogenic ATDC5 cells. *Bone* **31**: 457-464

- Silvestrini G, Mocetti P, Ballanti P, Di GR, Bonucci E (1999) Cytochemical demonstration of the glucocorticoid receptor in skeletal cells of the rat. *Endocr Res* **25**: 117-128
- Skedros JG, Mason MW, Nelson MC, Bloebaum RD (1996) Evidence of structural and material adaptation to specific strain features in cortical bone. *Anat Rec* **246**: 47-63
- Smeets T, van Buul-Offers S (1986) Influence of growth hormone and thyroxine on cell kinetics in the proximal tibial growth plate of Snell dwarf mice. *Cell Tissue Kinet* **19**: 161-170
- Smink JJ, Koster JG, Gresnigt MG, Rooman R, Koedam JA, van Buul-Offers SC (2002) IGF and IGF-binding protein expression in the growth plate of normal, dexamethasone-treated and human IGF-II transgenic mice. *J Endocrinol* **175**: 143-153
- Smink JJ, Buchholz IM, Hamers N, van Tilburg CM, Christis C, Sakkers RJ, de MK, van Buul-Offers SC, Koedam JA (2003) Short-term glucocorticoid treatment of piglets causes changes in growth plate morphology and angiogenesis. *Osteoarthritis Cartilage* **11**: 864-871
- Smith EP, Boyd J, Frank GR, Takahashi H, Cohen RM, Specker B, Williams TC, Lubahn DB, Korach KS (1994) Oestrogen resistance caused by a mutation in the oestrogen-receptor gene in a man. *N Engl J Med* **331**: 1056-1061
- So CL, Kaluarachchi K, Tam PP, Cheah KS (2001) Impact of mutations of cartilage matrix genes on matrix structure, gene activity and chondrogenesis. *Osteoarthritis Cartilage* **9 Suppl A**: S160-S173
- Solomon DH, O'Brian CA, Weinstein IB (1985) N-alpha-Tosyl-L-lysine chloromethyl ketone and N-alpha-tosyl-L-phenylalanine chloromethyl ketone inhibit protein kinase C. *FEBS Lett* **190**: 342-344
- Sommerfeldt DW, Rubin CT (2001) Biology of bone and how it orchestrates the form and function of the skeleton. *Eur Spine J* **10 Suppl 2**: S86-S95
- Song IH, Gold R, Straub RH, Burmester GR, Buttgerit F (2005) New glucocorticoids on the horizon: repress, don't activate! *J Rheumatol* **32**: 1199-1207
- Spranger J, Menger H, Mundlos S, Winterpacht A, Zabel B (1994) Kniest dysplasia is caused by dominant collagen II (COL2A1) mutations: parental somatic mosaicism manifesting as Stickler phenotype and mild spondyloepiphyseal dysplasia. *Pediatr Radiol* **24**: 431-435
- St-Jacques B, Hammerschmidt M, McMahon AP (1999) Indian hedgehog signalling regulates proliferation and differentiation of chondrocytes and is essential for bone formation. *Genes Dev* **13**: 2072-2086
- Stanton LA, Underhill TM, Beier F (2003) MAP kinases in chondrocyte differentiation. *Dev Biol* **263**: 165-175

- Steinberg ME, Trueta J (1981) Effects of activity on bone growth and development in the rat. *Clin Orthop Relat Res* **156**: 52-60
- Stevens DA, Williams GR (1999) Hormone regulation of chondrocyte differentiation and endochondral bone formation. *Mol Cell Endocrinol* **151**: 195-204
- Stewart MC, Farnum CE, MacLeod JN (1997) Expression of p21CIP1/WAF1 in chondrocytes. *Calcif Tissue Int* **61**: 199-204
- Stewart MC, Kadlcek RM, Robbins PD, MacLeod JN, Ballock RT (2004) Expression and activity of the CDK inhibitor p57Kip2 in chondrocytes undergoing hypertrophic differentiation. *J Bone Miner Res* **19**: 123-132
- Storm EE, Kingsley DM (1999) GDF5 coordinates bone and joint formation during digit development. *Dev Biol* **209**: 11-27
- Su WC, Kitagawa M, Xue N, Xie B, Garofalo S, Cho J, Deng C, Horton WA, Fu XY (1997) Activation of Stat1 by mutant fibroblast growth-factor receptor in thanatophoric dysplasia type II dwarfism. *Nature* **386**: 288-292
- Sunters A, McCluskey J, Grigoriadis AE (1998) Control of cell cycle gene expression in bone development and during c-Fos-induced osteosarcoma formation. *Dev Genet* **22**: 386-397
- Tazawa K, Hoshi K, Kawamoto S, Tanaka M, Ejiri S, Ozawa H (2004) Osteocytic osteolysis observed in rats to which parathyroid hormone was continuously administered. *J Bone Miner Metab* **22**: 524-529
- Teixeira LT, Kiyokawa H, Peng XD, Christov KT, Frohman LA, Kineman RD (2000) p27Kip1-deficient mice exhibit accelerated growth hormone-releasing hormone (GHRH)-induced somatotrope proliferation and adenoma formation. *Oncogene* **19**: 1875-1884
- Tessier M, Woodgett JR (2006) Serum and glucocorticoid-regulated protein kinases: variations on a theme. *J Cell Biochem* **98**: 1391-1407
- Thomas JT, Lin K, Nandedkar M, Camargo M, Cervenka J, Luyten FP (1996) A human chondrodysplasia due to a mutation in a TGF-beta superfamily member. *Nat Genet* **12**: 315-317
- Thomas JT, Kilpatrick MW, Lin K, Erlacher L, Lembessis P, Costa T, Tsiouras P, Luyten FP (1997) Disruption of human limb morphogenesis by a dominant negative mutation in CDMP1. *Nat Genet* **17**: 58-64
- Timchenko NA, Wilde M, Nakanishi M, Smith JR, Darlington GJ (1996) CCAAT/enhancer-binding protein alpha (C/EBP alpha) inhibits cell proliferation through the p21 (WAF-1/CIP-1/SDI-1) protein. *Genes Dev* **10**: 804-815
- Uliivi V, Tutolo G, Mallein-Gerin F, Daga A, Cancedda R, Cancedda FD (2006) A common pathway in differentiation and inflammation: p38 mediates expression of the acute phase SIP24 iron binding lipocalin in chondrocytes. *J Cell Physiol* **206**: 728-737

- Unterman TG, Phillips LS (1985) Glucocorticoid effects on somatomedins and somatomedin inhibitors. *J Clin Endocrinol Metab* **61**: 618-626
- Vaananen HK, Zhao H, Mulari M, Halleen JM (2000) The cell biology of osteoclast function. *J Cell Sci* **113** (Pt 3): 377-381
- Vajo Z, Francomano CA, Wilkin DJ (2000) The molecular and genetic basis of fibroblast growth factor receptor 3 disorders: the achondroplasia family of skeletal dysplasias, Muenke craniosynostosis, and Crouzon syndrome with acanthosis nigricans. *Endocr Rev* **21** : 23-39
- van Buul-Offers SC, Smink JJ, Gresnigt R, Hamers N, Koedam J, Karperien M (2005) Thyroid hormone, but not parathyroid hormone, partially restores glucocorticoid-induced growth retardation. *Pediatr Nephrol* **20**: 335-341
- van der Eerden BC, Karperien M, Wit JM (2003) Systemic and local regulation of the growth plate. *Endocr Rev* **24**: 782-801
- van der Eerden BC, Lowik CW, Wit JM, Karperien M (2004) Expression of oestrogen receptors and enzymes involved in sex steroid metabolism in the rat tibia during sexual maturation. *J Endocrinol* **180**: 457-467
- Vayssiere BM, Dupont S, Choquart A, Petit F, Garcia T, Marchandeu C, Gronemeyer H, Resche-Rigon M (1997) Synthetic glucocorticoids that dissociate transactivation and AP-1 transrepression exhibit antiinflammatory activity in vivo. *Mol Endocrinol* **11**: 1245-1255
- Veldhuis JD (1998) Neuroendocrine control of pulsatile growth hormone release in the human: relationship with gender. *Growth Horm IGF Res* **8 Suppl B**: 49-59
- Vingron M (2001) Bioinformatics needs to adopt statistical thinking. *Bioinformatics* **17**: 389-390
- Vizzardelli C, Pavelka N, Luchini A, Zanoni I, Bendickson L, Pelizzola M, Beretta O, Foti M, Granucci F, Nilsen-Hamilton M, Ricciardi-Castagnoli P (2006) Effects of dexamethazone on LPS-induced activation and migration of mouse dendritic cells revealed by a genome-wide transcriptional analysis. *Eur J Immunol* **36**: 1504-1515
- Vortkamp A, Lee K, Lanske B, Segre GV, Kronenberg HM, Tabin CJ (1996) Regulation of rate of cartilage differentiation by Indian hedgehog and PTH-related protein. *Science* **273**: 613-622
- Vu TH, Shipley JM, Bergers G, Berger JE, Helms JA, Hanahan D, Shapiro SD, Senior RM, Werb Z (1998) MMP-9/gelatinase B is a key regulator of growth plate angiogenesis and apoptosis of hypertrophic chondrocytes. *Cell* **93**: 411-422
- Wakita R, Izumi T, Itoman M (1998) Thyroid hormone-induced chondrocyte terminal differentiation in rat femur organ culture. *Cell Tissue Res* **293**: 357-364
- Wallis GA (1996) Bone growth: coordinating chondrocyte differentiation. *Curr Biol* **6**: 1577-1580

- Wang J, Zhou J, Bondy CA (1999) Igf1 promotes longitudinal bone growth by insulin-like actions augmenting chondrocyte hypertrophy. *FASEB J* **13**: 1985-1990
- Wang W, Kirsch T (2002) Retinoic acid stimulates annexin-mediated growth plate chondrocyte mineralisation. *J Cell Biol* **157**: 1061-1069
- Wang Y, Middleton F, Horton JA, Reichel L, Farnum CE, Damron TA (2004) Microarray analysis of proliferative and hypertrophic growth plate zones identifies differentiation markers and signal pathways. *Bone* **35**: 1273-1293
- Wang Y, Lam KS, Kraegen EW, Sweeney G, Zhang J, Tso AW, Chow WS, Wat NM, Xu JY, Hoo RL, Xu A (2007) Lipocalin-2 is an inflammatory marker closely associated with obesity, insulin resistance, and hyperglycemia in humans. *Clin Chem* **53**: 34-41
- Warner JO (1995) Review of prescribed treatment for children with asthma in 1990. *BMJ* **311**: 663-666
- Weir EC, Philbrick WM, Amling M, Neff LA, Baron R, Broadus AE (1996) Targeted overexpression of parathyroid hormone-related peptide in chondrocytes causes chondrodysplasia and delayed endochondral bone formation. *Proc Natl Acad Sci U S A* **93**: 10240-10245
- Weise M, De-Levi S, Barnes KM, Gafni RI, Abad V, Baron J (2001) Effects of oestrogen on growth plate senescence and epiphyseal fusion. *Proc Natl Acad Sci U S A* **98**: 6871-6876
- Weksler NB, Lunstrum GP, Reid ES, Horton WA (1999) Differential effects of fibroblast growth factor (FGF) 9 and FGF2 on proliferation, differentiation and terminal differentiation of chondrocytic cells in vitro. *Biochem J* **342 Pt 3**: 677-682
- Wellen KE, Hotamisligil GS (2005) Inflammation, stress, and diabetes *J Clin Invest* **115**:1111-1119
- Wen D, Nong Y, Morgan JG, Gangurde P, Bielecki A, Dasilva J, Keaveney M, Cheng H, Fraser C, Schopf L, Hepperle M, Harriman G, Jaffee BD, Ocain TD, Xu Y (2006) A selective small molecule I κ B Kinase beta inhibitor blocks nuclear factor kappaB-mediated inflammatory responses in human fibroblast-like synoviocytes, chondrocytes, and mast cells. *J Pharmacol Exp Ther* **317**: 989-1001
- Wenke AK, Rothhammer T, Moser M, Bosserhoff AK (2006) Regulation of integrin alpha10 expression in chondrocytes by the transcription factors AP-2epsilon and Ets-1. *Biochem Biophys Res Commun* **345**: 495-501
- Werb Z (1997) ECM and cell surface proteolysis: regulating cellular ecology. *Cell* **91**: 439-442
- Werner S, Bronnegard M (1996) Molecular basis of glucocorticoid-resistant syndromes. *Steroids* **61**: 216-221

- Wikstrom L, Johansson C, Salto C, Barlow C, Campos BA, Baas F, Forrest D, Thoren P, Vennstrom B (1998) Abnormal heart rate and body temperature in mice lacking thyroid hormone receptor alpha 1. *EMBO J* **17**: 455-461
- Wilsman NJ, Farnum CE, Leiferman EM, Fry M, Barreto C (1996) Differential growth by growth plates as a function of multiple parameters of chondrocytic kinetics. *J Orthop Res* **14**: 927-936
- Wilsman NJ, Farnum CE, Green EM, Lieferman EM, Clayton MK (1996) Cell cycle analysis of proliferative zone chondrocytes in growth plates elongating at different rates. *J Orthop Res* **14**: 562-572
- Winnier G, Blessing M, Labosky PA, Hogan BL (1995) Bone morphogenetic protein-4 is required for mesoderm formation and patterning in the mouse. *Genes Dev* **9**: 2105-2116
- Woods A, Wang G, Beier F (2005) RhoA/ROCK signalling regulates Sox9 expression and actin organization during chondrogenesis. *J Biol Chem* **280**: 11626-11634
- Wu CW, Tchetina EV, Mwale F, Hasty K, Pidoux I, Reiner A, Chen J, Van Wart HE, Poole AR (2002) Proteolysis involving matrix metalloproteinase 13 (collagenase-3) is required for chondrocyte differentiation that is associated with matrix mineralisation. *J Bone Miner Res* **17**: 639-651
- Yakar S, Wu Y, Setser J, Rosen CJ (2002) The role of circulating IGF-I: lessons from human and animal models. *Endocrine* **19**: 239-248
- Yan Y, Frisen J, Lee MH, Massague J, Barbacid M (1997) Ablation of the CDK inhibitor p57Kip2 results in increased apoptosis and delayed differentiation during mouse development. *Genes Dev* **11**: 973-983
- Yang J, Goetz D, Li JY, Wang W, Mori K, Setlik D, Du T, Erdjument-Bromage H, Tempst P, Strong R, Barasch J (2002) An iron delivery pathway mediated by a lipocalin. *Mol Cell* **10**: 1045-1056
- Yoon JC, Puigserver P, Chen G, Donovan J, Wu Z, Rhee J, Adelmant G, Stafford J, Kahn CR, Granner DK, Newgard CB, Spiegelman BM (2001) Control of hepatic gluconeogenesis through the transcriptional coactivator PGC-1. *Nature* **413**: 131-138
- Zeng YX, Somasundaram K, el-Deiry WS (1997) AP2 inhibits cancer cell growth and activates p21WAF1/CIP1 expression. *Nat Genet* **15**: 78-82
- Zenmyo M, Komiya S, Kawabata R, Sasaguri Y, Inoue A, Morimatsu M (1996) Morphological and biochemical evidence for apoptosis in the terminal hypertrophic chondrocytes of the growth plate. *J Pathol* **180**: 430-433
- Zenmyo M, Komiya S, Hamada T, Hiraoka K, Suzuki R, Inoue A (2000) p21 and parathyroid hormone-related peptide in the growth plate. *Calcif Tissue Int* **67**: 378-381

Zerega B, Cermelli S, Michelis B, Cancedda R, Cancedda FD (2000) Expression of NRL/NGAL (neu-related lipocalin/neutrophil gelatinase-associated lipocalin) during mammalian embryonic development and in inflammation. *Eur J Cell Biol* **79**: 165-172

Zhang M, Wang Y, Middleton FA, Horton JA, Farnum CE, Damron TA (2007) Growth Plate Zonal Microarray Analysis Shows Upregulation of Extracellular Matrix Genes and Downregulation of Metalloproteinases and Cathepsins following Irradiation. *Calcif Tissue Int* **81**: 26-38

Zhang P, Liegeois NJ, Wong C, Finegold M, Hou H, Thompson JC, Silverman A, Harper JW, DePinho RA, Elledge SJ (1997) Altered cell differentiation and proliferation in mice lacking p57KIP2 indicates a role in Beckwith-Wiedemann syndrome. *Nature* **387**: 151-158

Zhi L, Tegley CM, Edwards JP, West SJ, Marschke KB, Gottardis MM, Mais DE, Jones TK (1998) 5-Alkyl 1,2-dihydrochromeno[3,4-f]quinolines: a novel class of nonsteroidal progesterone receptor modulators. *Bioorg Med Chem Lett* **8**: 3365-3370

Zou H, Wieser R, Massague J, Niswander L (1997) Distinct roles of type I bone morphogenetic protein receptors in the formation and differentiation of cartilage. *Genes Dev* **11**: 2191-2203

Appendix 1**Gene Ontology of Dex-Responsive Chondrocyte Genes****Table 1 Up-regulated Genes**

Affymetrix ID	Gene Name	Gene Ontology	Fold Change
1427747_a_at	lipocalin 2	transporter activity, binding	14.5
1448550_at	lipopolysaccharide binding protein	Transport, lipid transport, defense response to bacterium; LPS binding lipid binding; extracellular space membrane, integral to membrane	7.9
1428942_at	metallothionein 2	zinc ion homeostasis, nitric oxide mediated signal transduction, detoxification of copper ion; zinc ion binding, metal ion binding	5.1
1416125_at	FK506 binding protein 5	protein folding; peptidyl-prolyl cis-trans isomerase activity binding, protein binding, isomerase activity; cytoplasm, mitochondrial inner membrane	3.8
1442025_a_at	similar to promyelotic leukemia zfp		3.8
1434202_a_at	hypothetical protein MCG58343 (cDNA sequence BC055107)		3.6
1418187_at	calcitonin receptor activity modifying protein	intracellular protein transport, regulation of G-protein coupled receptor protein signalling pathway; receptor activity, protein transporter activity, coreceptor, soluble ligand activity; extracellular space, integral to membrane	3.5
1448881_at	haptoglobin	Proteolysis, acute-phase response; serine-type endopeptidase activity chymotrypsin activity, trypsin activity, hemoglobin binding; extracellular space	3.4
1416953_at	connective tissue growth factor	cartilage condensation, ossification, angiogenesis, regulation of cell growth, DNA replication, cell adhesion, cell-matrix adhesion, integrin-mediated signalling, pathway, fibroblast growth factor receptor signalling pathway, cell migration, cell differentiation; integrin binding, protein binding, insulin-like growth factor binding, heparin binding; extracellular region proteinaceous extracellular matrix	3.3
1425281_a_at	delta sleep inducing peptide (TSC22 domain family 3)	regulation of transcription, DNA-dependent anti-apoptosis; transcription factor activity;	3.1
1423233_at	CCAAT/enhancer binding	Transcription, regulation of	3.1

	protein delta	transcription, DNA-dependent; DNA binding, transcription factor activity protein binding, protein homodimerization activity sequence-specific DNA binding protein heterodimerization activity protein dimerization activity; nucleus	
1449851_at	chemokine ligand 2 (Period homolog 1)	two-component signal transduction system (phosphorelay) transcription regulation of transcription, DNA- dependent signal transduction, circadian rhythm, negative regulation of transcription, rhythmic process; signal transducer activity	3.0
1419874_x_at	promyelotic leukaemia zinc finger protein	protein binding; nucleus skeletal development, mesonephros development, regulation of transcription, DNA-dependent central nervous system development, negative regulation of cell proliferation, embryonic pattern specification, anterior/posterior pattern formation, hemopoiesis myeloid cell differentiation, embryonic limb morphogenesis, leg morphogenesis, embryonic hindlimb/forelimb morphogenesis, positive regulation of apoptosis, regulation of transcription, negative regulation of myeloid cell differentiation, negative regulation of transcription, DNA-dependent male germ-line stem cell division; nucleic acid binding, DNA binding protein binding, zinc ion binding specific transcriptional repressor activity, protein homodimerization activity, metal ion binding; intracellular, nucleus, nuclear speck	2.9
1422557_s_at	metallothionein 1	transcriptional repressor complex zinc ion homeostasis, nitric oxide mediated signal transduction, detoxification of copper ion; zinc ion binding, metal ion binding; lysosome, cytosol	2.8
1418091_at	transcription factor CP2 like 1	negative regulation of transcription, from RNA polymerase II promoter, cell morphogenesis, epithelial cell maturation, regulation of transcription, DNA-dependent cytoplasm organization and biogenesis, salivary gland development determination of adult life span positive regulation of	2.7

1440235_at	Integrin alpha 10	growth; DNA binding, general transcriptional repressor activity; nucleus, transcription factor complex, cytoplasm, membrane cell adhesion, integrin-mediated signalling pathway; integrin complex	2.6
1422878_at	synaptotagmin 12	transport; transporter activity; synaptic vesicle, membrane, integral to membrane, synapse	2.5
1416041_at	serum/glucocorticoid regulated kinase	protein amino acid phosphorylation, apoptosis, response to DNA damage stimulus; nucleotide binding, protein kinase activity	2.5
1428471_at	sorbin and SH3 domain containing 1	protein kinase activity, protein serine/threonine kinase activity, protein binding, ATP binding, kinase activity, transferase activity; nucleus, endoplasmic reticulum	2.5
1450826_a_at	serum amyloid A 3	Transport, insulin receptor signalling pathway, glucose transport, stress fiber formation, focal adhesion formation; insulin receptor binding	2.5
1455048_at	immunoglobulin superfamily member 2	protein binding, protein kinase binding; stress fiber nucleus, cell-cell adherens junction, cell-substrate adherens junction, membrane, lipid raft	2.4
1423274_at	integrator complex subunit 6	acute-phase response; lipid transporter activity; extracellular space	2.3
1443745_s_at	dentin matrix protein 1	snRNA processing; nucleic acid binding, protein binding, ATP binding, ATP-dependent helicase activity; extracellular space, nucleus, integrator complex	2.3
1426236_a_at	glutamate ammonia ligase	Ossification, extracellular matrix organization and biogenesis; proteinaceous extracellular matrix, extracellular space, nucleus	2.3
1422573_at	AMP deaminase 3	glutamine biosynthetic process nitrogen compound metabolic process; catalytic activity glutamate-ammonia ligase activity ligase activity; mitochondrion	2.1
1449254_at	secreted phosphoprotein 1	nucleotide metabolic process, purine ribonucleoside, monophosphate biosynthetic process; AMP deaminase activity hydrolase activity, deaminase activity	2.0
		Ossification, anti-apoptosis, inflammatory response, cell adhesion, cell-matrix adhesion. negative regulation of bone mineralisation, leukocyte	

		chemotaxis, T-helper 1 type immune response, positive regulation of T cell proliferation, regulation of myeloid cell differentiation, induction of positive chemotaxis; cytokine activity, integrin binding, protein binding	
1418269_at	lysyl oxidase-like 3	growth factor activity; extracellular region proteinaceous extracellular matrix, extracellular space, cytoplasm, apical part of cell protein-lysine 6-oxidase activity, scavenger receptor activity, copper ion binding, oxidoreductase activity, metal ion binding; extracellular space, membrane	2.0
1448830_at	dual specificity phosphatase 1	protein amino acid dephosphorylation, cell cycle dephosphorylation; phosphoprotein phosphatase activity protein tyrosine phosphatase activity, protein binding, protein tyrosine/serine/threonine, phosphatase activity, hydrolase activity, phosphoric monoester, hydrolase activity, MAP kinase phosphatase activity;	2.0
1417507_at	cytochrome b-561	electron transport; ferric-chelate reductase activity, transporter activity, iron ion binding, metal ion binding; nucleus	1.9
1434203_at	hypothetical protein MCG58343 (cDNA sequence BC055107)		1.9
1438953_at	c-fos induced growth factor		1.9
1435943_at	dipeptidase 1	Proteolysis; membrane dipeptidase activity, peptidase activity, metallopeptidase activity, dipeptidyl-peptidase activity, zinc ion binding, hydrolase activity, dipeptidase activity, metal ion binding, GPI anchor binding; extracellular space, endoplasmic reticulum, microsome membrane	1.9
1434642_at	hydroxysteroid (17-beta) dehydrogenase 11	steroid biosynthetic process, metabolic process, lipid biosynthetic process; oxidoreductase activity;	1.9
1448842_at	Cysteine dioxygenase 1	L-cysteine catabolic process to taurine, taurine metabolic process, L-cysteine metabolic process; iron ion binding, electron carrier activity oxidoreductase activity, oxidoreductase activity, acting on single donors with incorporation of molecular oxygen, incorporation of two atoms of oxygen, cysteine	1.8

1439755_at	signal-induced proliferation-associated 1 like 1	dioxygenase activity; cytosol	1.8
1416383_a_at	pyruvate carboxylase	Gluconeogenesis, metabolic process, lipid biosynthetic process; nucleotide binding, catalytic activity, pyruvate carboxylase activity, ATP binding, biotin binding, ligase activity, manganese ion binding; cytoplasm, mitochondrion, mitochondrial inner membrane	1.8
1451596_a_at	sphingosine kinase 1	blood vessel development, protein kinase C activation, intracellular signalling cascade, brain development, positive regulation of cell proliferation, negative regulation of apoptosis, sphingoid catabolic process, positive regulation of fibroblast proliferation; magnesium ion binding, DNA binding, diacylglycerol kinase activity, protein binding, calmodulin binding, sphinganine kinase activity, kinase activity, D-erythro-sphingosine kinase activity; membrane fraction, soluble fraction, cytoplasm, cytosol	1.8
1424051_at	procollagen type IV	phosphate transport, cell adhesion, negative regulation of angiogenesis; structural molecule activity, extracellular matrix structural constituent, conferring tensile strength; proteinaceous extracellular matrix, collagen type IV, basement membrane, extracellular space, cytoplasm	1.8
1436789_at	cyclin J-like	regulation of progression through cell cycle; nucleus	1.8
1460011_at	cytochrome p450	cell fate determination, electron transport, male meiosis, spermatogenesis, proximal/distal pattern formation, embryonic limb morphogenesis, retinoic acid metabolic process, retinoic acid receptor signalling pathway; monooxygenase activity, iron ion binding, oxidoreductase activity, heme binding, metal ion binding; endoplasmic reticulum, microsome, membrane	1.7
1452141_a_at	selenoprotein P	selenium metabolic process, brain development, locomotory behaviour, post-embryonic development, sexual reproduction growth; selenium binding; extracellular space	1.7
1433832_at	unc-84 homolog B (C. elegans)	nuclear membrane organization and biogenesis; nuclear membrane	1.7

1418932_at	nuclear factor, interleukin 3, regulated	organization and biogenesis; nuclear chromosome, telomeric region, nuclear chromosome, telomeric region, condensed nuclear chromosome, condensed nuclear chromosome, nucleus, nuclear envelope, nuclear envelope membrane, integral to membrane regulation of transcription, DNA-dependent regulation of transcription, DNA-dependent; DNA binding, transcription factor activity, sequence-specific DNA binding, protein dimerization activity; nucleus	1.7
1426195_a_at	Cystatin C	endopeptidase inhibitor activity, cysteine protease inhibitor activity; extracellular space;	1.7
1422620_s_at	phosphatidic acid phosphatase 2a	protein amino acid dephosphorylation, diacylglycerol biosynthetic process, sphingosine metabolic process, ceramide metabolic process, signal transduction, protein kinase C activation, negative regulation of cell proliferation, regulation of lipid metabolic process, androgen receptor signalling pathway, phospholipid dephosphorylation; phosphatidate phosphatase activity hydrolase activity; membrane fraction, plasma membrane integral to plasma membrane	1.7
1422478_a_at	acetyl coenzyme A synthetase 2	acetyl-CoA biosynthetic process, metabolic process; catalytic activity, acetate-CoA ligase activity, AMP binding, ligase activity; cytoplasm integral to membrane	1.6
1417936_at	chemokine ligand 9	Chemotaxis, immune response, signal transduction; cytokine activity chemokine activity; extracellular region, extracellular space	1.6
1454675_at	thyroid hormone receptor alpha	cartilage condensation, ossification, regulation of transcription, DNA-dependent regulation of heart contraction, organ morphogenesis, negative regulation of transcription; DNA binding, transcription factor activity, steroid hormone receptor activity, receptor activity, ligand-dependent nuclear receptor activity, ligand-dependent nuclear receptor activity, thyroid hormone receptor activity, thyroid hormone receptor activity, protein binding, zinc ion binding, transcriptional repressor activity, transcription regulator	1.6

1449731_s_at	nuclear factor of kappa light chain gene enhancer	activity, sequence-specific DNA binding, metal ion binding; nucleus protein import into nucleus, translocation, lipopolysaccharide-mediated signalling pathway, response to lipopolysaccharide, regulation of cell proliferation, response to exogenous dsRNA, negative regulation of myeloid cell differentiation, negative regulation of Notch signalling pathway; protein binding, nuclear localisation sequence binding, ubiquitin protein ligase binding, NF-kappaB binding; nucleus, cytoplasm, cytosol	1.6
1448489_at	platelet activating factor 2	lipid catabolic process; catalytic activity, 1-alkyl-2-acetylglycerophosphocholine esterase activity, hydrolase activity; 2-acetyl-1-alkylglycerophosphocholine esterase complex	1.6
1447602_x_at	sulfatase 2	sulfur metabolic process, metabolic process, heparan sulfate proteoglycan metabolic process; arylsulfatase activity, calcium ion binding, N-acetylglucosamine-6-sulfatase activity, sulfuric ester hydrolase activity, hydrolase activity	1.6
1424671_at	pleckstrin homology domain containing F	metal ion binding; extracellular space, endoplasmic reticulum cell surface	1.6
1437820_at	forkhead-like 18	Apoptosis, ,induction of apoptosis, regulation of mitochondrial, membrane permeability; zinc ion binding, metal ion binding; nucleus lysosome	1.6
1451939_a_at	sushi-repeat containing protein	Transcription, regulation of transcription, DNA-dependent positive regulation of body size, regulation of balance; DNA binding	1.6
1435254_at	plexin B1	transcription factor activity, sequence-specific DNA binding; nucleus, transcription factor complex	1.6
1456312_x_at	Gelsolin	extracellular space	1.6
		multicellular organismal development, positive regulation of axonogenesis; receptor activity protein binding; membrane integral	1.6
		vesicle-mediated transport, actin filament polymerization, actin filament severing; actin binding structural molecule activity, calcium ion binding, protein	1.6

		binding; extracellular space, cytoplasm, cytosol, cytoskeleton, actin cytoskeleton, actin cytoskeleton, lamellipodium	
1454849_x_at	clusterin	cell death; protein binding; extracellular space	1.6
1441926_x_at	transmembrane inner ear	sensory perception of sound, inner ear morphogenesis; membrane, integral to membrane	1.6
1448321_at	SPARC related modular calcium binding 1	calcium ion binding; proteinaceous extracellular matrix, baSEMent membrane	1.6
1455078_at	slingshot homolog 2	protein amino acid dephosphorylation; actin binding, phosphoprotein phosphatase activity, protein tyrosine phosphatase activity, protein tyrosine/serine/threonine phosphatase activity, hydrolase activity, phosphoric monoester hydrolase activity; cytoskeleton	1.6
1416825_at	synotrophin acidic 1	neuromuscular junction development; actin binding, calcium ion binding, protein binding, calmodulin binding	1.6
1450678_at	Integrin beta 2	cell adhesion, cell-matrix adhesion integrin-mediated signalling, pathway, integrin-mediated signalling pathway, multicellular organismal development, neutrophil chemotaxis, cellular extravasation	1.5
1425894_at	MAS-related GPR, member F	activated T cell proliferation; signal transduction, G-protein coupled receptor protein signalling pathway; rhodopsin-like receptor activity, signal transducer activity receptor activity, G-protein coupled receptor activity; membrane, integral to membrane	1.5
1452296_at	slit homolog 3	multicellular organismal development, nervous system development, axon guidance, organ morphogenesis, organ morphogenesis, cell differentiation; receptor binding, calcium ion binding, protein binding; extracellular space	1.5
1426947_x_at	procollagen type IV alpha 2	phosphate transport, cell adhesion; structural molecule activity, extracellular matrix structural constituent, protein binding extracellular matrix structural constituent conferring tensile strength; proteinaceous extracellular matrix, collagen	1.5
1417872_at	four and a half LIM domains	extracellular space, cytoplasm multicellular organismal	1.5

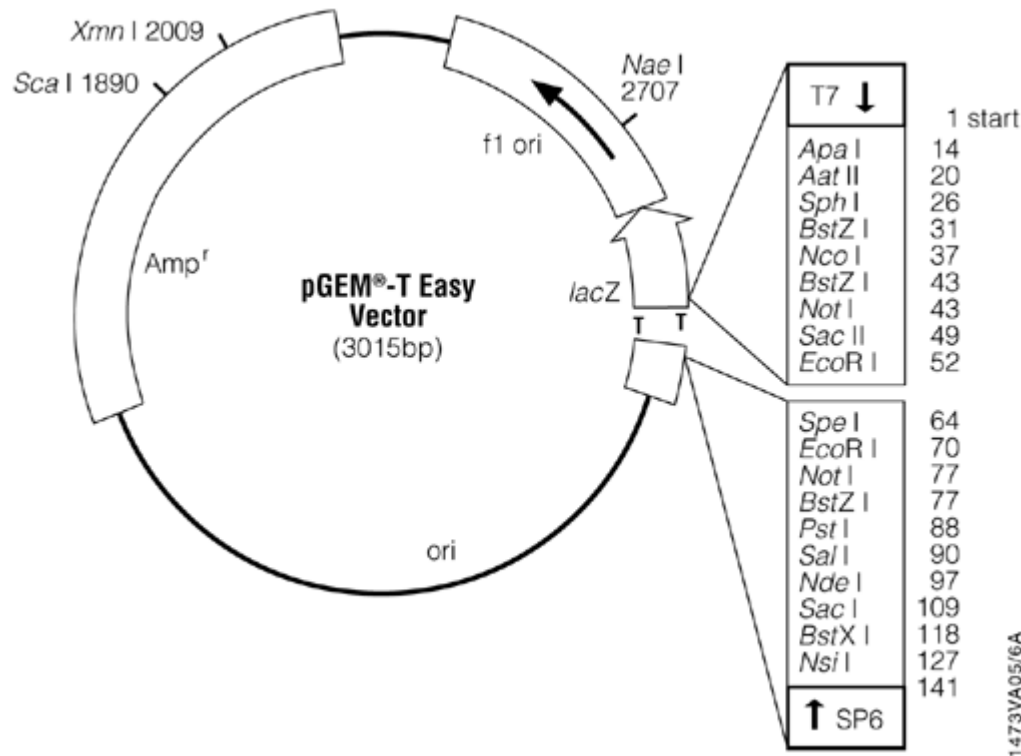
	1	development, cell differentiation; zinc ion binding, heme binding, metal ion binding; nucleus cation transport, ADP catabolic process, IDP catabolic process; magnesium ion binding, calcium activated cation channel activity, hydrolase activity, nucleoside-diphosphatase activity, ADP-sugar diphosphatase activity, manganese ion binding, ADP-ribose diphosphatase activity	1.5
1428164_at	nudix type motif 9		
1415874_at	sprouty homolog 1	ureteric bud development, induction of an organ, multicellular organismal development, regulation of signal transduction, negative regulation of MAPK activity, protein binding; membrane	1.5
1420834_at	vesicle-associated membrane protein 2	membrane fusion, synaptic vesicle exocytosis, vesicle-mediated transport, calcium ion-dependent exocytosis, calcium ion-dependent exocytosis, regulation of exocytosis; SNARE binding, protein binding, calmodulin binding, phospholipid binding; synaptic vesicle membrane, integral to membrane, integral to membrane synaptosome, secretory granule synaptic vesicle membrane, zymogen granule membrane synapse	1.5
1455768_at	Niemann pick type C2	cholesterol homeostasis; enzyme binding; extracellular space	1.5
1437865_at	spermatogenesis associated 13	intracellular signalling cascade, regulation of Rho protein signal transduction; guanyl-nucleotide exchange factor activity, Rho guanyl-nucleotide exchange factor activity; intracellular	1.5
1455158_at	Integrin alpha 3	neuron migration, cell adhesion integrin-mediated signalling pathway, fusion of sperm to egg, plasma membrane memory; receptor activity, protein binding; integrin complex membrane, integral to membrane, basolateral plasma membrane, synaptosome	1.5
1427038_at	preproenkephalin 1	behavioral fear response, neuropeptide signalling pathway, behaviour, sensory perception of pain; opioid peptide activity	1.5
1421037_at	neuronal PAS domain protein 2	two-component signal transduction system (phosphorelay)transcription, regulation of transcription, DNA-dependent signal transduction, circadian sleep/wake cycle,	1.5

1421921_at	Cysteine protease inhibitor	regulation of transcription, locomotor rhythm, rhythmic process; two-component sensor activity, DNA binding, transcription factor activity, signal transducer activity, transcription regulator activity; nucleus endopeptidase inhibitor activity serine-type endopeptidase inhibitor activity	1.5
------------	-----------------------------	--	-----

Table 2 Down-Regulated Genes

Affmetrix ID	Gene Name	Gene Ontology	Fold Change
1418174_at	D site albumin promoter binding protein	Transcription, regulation of transcription, DNA-dependent regulation of transcription, DNA-dependent, circadian rhythm, rhythmic process; DNA binding transcription factor activity, sequence-specific DNA binding, protein dimerization activity; nucleus	2.6
1423607_at	lumican	protein binding, collagen binding; proteinaceous extracellular matrix, fibrillar collagen, extracellular space	2.2
1451191_at	cellular retinoic acid binding protein II	Transport, embryonic forelimb morphogenesis, retinoic acid metabolic process; retinoic acid binding, lipid binding, retinal binding, cyclin binding; nucleus cytoplasm	1.9
1423294_at	mesoderm specific transcript	proteolysis	1.9
1449855_s_at	ubiquitin thiolesterase	ubiquitin-dependent protein, catabolic process, ubiquitin cycle, adult walking behaviour, protein deubiquitination, eating behaviour; ubiquitin thiolesterase activity, peptidase activity, cysteine-type, peptidase activity, hydrolase activity; intracellular	1.8
1449486_at	carboxylesterase 1	catalytic activity, carboxylesterase activity, serine esterase activity, hydrolase activity, carboxylic ester hydrolase activity; extracellular space, endoplasmic reticulum	1.8
1448201_at	secreted frizzled-related sequence protein 2	Somitogenesis, multicellular organismal development, multicellular organismal development, anterior/posterior pattern formation, Wnt receptor signalling pathway, cell differentiation; transmembrane receptor activity; membrane	1.7
1450243_a_at	down syndrome critical region gene 1	calcium-mediated signalling	1.6
1428950_s_at	nucleolar protein 8	nucleotide binding, nucleic acid binding, RNA binding, protein binding; nucleus, nucleolus	1.6
1454888_at	prefoldin 4	protein folding, chaperonin-mediated tubulin folding; protein binding, unfolded protein binding; cytosol, prefoldin complex	1.6
1425357_a_at	gremlin 1	cell-cell signalling, organ morphogenesis, proximal/distal pattern formation, embryonic limb morphogenesis; cytokine activity; extracellular space	1.6

1450756_s_at	cullin 3	ubiquitin cycle, cell cycle; nucleus	1.6
1425806_a_at	SRB7(suppressor of RNA polymerase B)	regulation of transcription, DNA-dependent regulation of transcription from RNA polymerase II promoter, positive regulation of transcription from RNA polymerase II promoter; RNA polymerase II transcription factor activity transcription coactivator activity DNA-directed RNA polymerase activity, protein binding; mediator complex, nucleus DNA-directed RNA polymerase II, core complex	1.5
1417394_at	Kruppel-like factor 4 (gut)	Transcription, regulation of transcription, DNA-dependent negative regulation of transcription; nucleic acid binding, DNA binding, transcription factor activity, zinc ion binding, transcriptional activator activity, transcriptional repressor activity, metal ion binding; intracellular, nucleus	1.5
1431056_a_at	lipoprotein lipase	lipid metabolic process; catalytic activity, lipoprotein lipase activity, lipid transporter activity, heparin binding, hydrolase activity, GPI anchor binding; extracellular space membrane, chylomicron	1.5
1436993_x_at	profilin 2	cytoskeleton organization and biogenesis; actin cytoskeleton organization and biogenesis; actin binding, protein binding; cytoskeleton, actin cytoskeleton	1.5
1437401_at	IGF-1	Growth factor activity, hormone activity, IGF-IR activity, protein binding; anti-apoptosis, cell development, glial cell differentiation, IGF-IR pathway; nervous system development; organ morphogenesis; extracellular region, extracellular space, IGF-IR binding protein complex	1.5

Appendix 2 - Vector Diagrams**pGEM-T-Easy Vector (Promega)****Vector Features**

T7 RNA Polymerase transcription initiation site: 1

SP6 RNA Polymerase transcription initiation site: 141

T7 RNA Polymerase promoter (-17 to +3): 2999-3

SP6 RNA Polymerase promoter (-17 to +3): 139-158

Multiple cloning region: 10-128

LacZ start codon: 180

Lac operon sequences: 2996, 166-395

Lac operator: 200-216

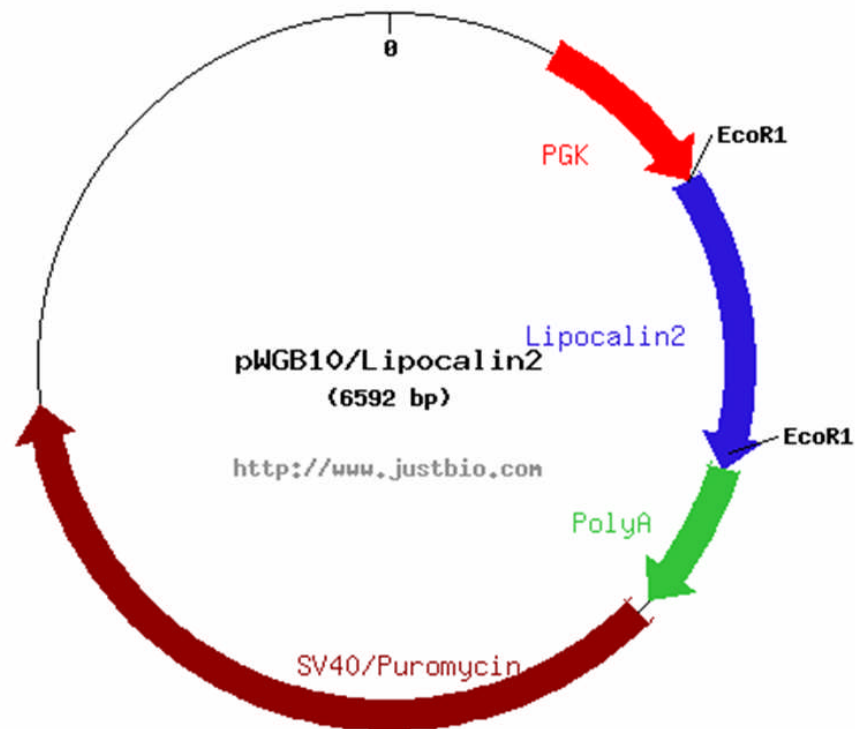
Beta-lactamase coding region: 1337-2197

Phage f1 region: 2380-2835

Binding site of pUC/M13 Forward Sequencing Primer: 2956-2972

Binding site of pUC/M13 Reverse Sequencing Primer: 176-192

pWGB10/Lipocalin 2 Expression Construct



Vector Features

pWGB10 contains a phosphoglycerate kinase (PGK) promoter to drive Lipocalin 2 expression, simian virus 40 (SV40) small t intron/polyA and SV40/Puromycin to allow cell selection. The plasmid Backbone is composed of pBluescript.

Appendix 3 - Antibodies Used**A - Primary Antibodies**

Antibody	Source	Catalogue ID	Dilution
phospho-p38 MAPK (Thr-180/Tyr-182)	Cell Signalling Technology	9211	1:50 (IP)
total-p38 MAPK	Cell Signalling Technology	9212	1:1000 (WB)
Phospho-ATF2 (Thr76)	Cell Signalling Technology	9820	1:1000 (WB)
goat anti-lipocalin 2	R & D Systems	AF1857	1:500 (WB) 1:50 (IHC)
mouse anti beta-actin	Sigma	A5441	1:5000 (WB)
mouse anti-p21	BD Pharmingen	556431	1:250 (WB)
mouse anti-BrdU	DAKO	M0744	1:100 (IHC)

B - Secondary Antibodies

Antibody	Source	Catalogue ID	Dilution
Rabbit anti-goat peroxidase	DAKO	P0449	1:2000 (WB) 1:100 (IHC)
goat anti-mouse IgG peroxidase	Sigma	A9917	1:8000 (WB)
goat anti-mouse IgG FITC	Sigma	F0257	1:50 (IHC)

Appendix 4 - Primer Locations

Murine GAPDH

CCTCCCTGTTCCAGAGACGGCCGCATCTTCTTGTGCAGTGCCAGCTCGTCCCCTAGACAAAATGGTGAA
 GGTCCGGTGTGAACGGATTTGGCCGTATTGGGCGCCTGGTCACCAGGGCTGCCATTTGCAGTGGCAAAGT
 GGAGATTGTTGCCATCAACGACCCCTTCATTGACCTCAACTACATGGTCTACATGTTCCAGTATGACTC
 CACTCACGGCAAATTC AACGGCACAGTCAAGGCCGAGAATGGGAAGCTTGTTCATCAACGGGAAGCCCAT
 CACCATCTTCCAGGAGCGAGACCCCACTAACATCAAATGGGGT**TGAGGCCGGTGCTGAGTATGTCG**TGGA
 GTCTACTGGTGTCTTACCACCATGGAGAAAGGCCGG**GC**CCCACTTGAAGGGTGGAGCCAAAAGGGTCAT
 CATCTCCGCCCTTCTGCCGATGCCCCCATGTTTGTGATGGGTGTGAACCACGAGAAATATGACAACCTC
 ACTCAAGATTGTCAGCAATGCATCCTGCACCACCAACTGCTTAGCCCCCTGGCCAAGGTCATCCATGA
 CAACTTTGGCATTGTGGAAGGGCTCAT**GA**CCACAGTCCATGCCAT**CACTGCCACCCAGAAGACTGTGGA**
 TGGCCCCCTTGAAAGCTGTGGCGTGATGGCCGTGGGGCTGCCAGAACATCATCCCTGCATCCACTGG
 TGCTGCCAAGGCTGTGGGCAAGTCAATCCAGAGCTGAACGGGAAGCTCACTGGCATGGCCTTCCGTGT
 TCCTACCCCAATGTGTCCGTGGATCTGACGTGCCCTGGAGAAACCTGCCAAGTATGATGACAT
 CAAGAAGGTGGTGAAGCAGGCATCTGAGGGCCCACTGAAGGGCATCTTGGGCTACACTGAGGACCAGGT
 TGTCTCCTGCGACTTCAACAGCAACTCCCACTCTTCCACCTTCGATGCCGGGGCTGGCATTGCTCTCAA
 TGACAACCTTTGTCAAGCTCATTTCTGGTATGACAATGAATACGGCTACAGCAACAGGGTGGTGGACCT
 CATGGCCTACATGGCCTCCAAGGAGTAAGAAACCTGGACCACCCACCCAGCAAGGACACTGAGCAAG
 AGAGGCCCTATCCCAACTCGGCCCAACTGAGCATCTCCTCACAATTTCCATCCAGACCCCAT
 AATAACAGGAGGGCCTAGGGAGCCCTCCCTACTCTTGAATACCATCAATAAAGTTCGCTGCACC

Accession number: NM_008084
 Green highlights: Primers for qPCRs (302bp)
 Yellow highlights: Location of introns 3 and 4

Lipocalin 2

CCATGGCCCTGAGTGTCATGTCTGGGCCTTGCCCTGCTTGGGGTCTGCAGAGCCAGGCCAGGACT
 CACTCAGAACTTGATCCCTGCCCCATCTCTGCTCACTGTCCCCCTGCAGCCAGACTTCCGGAGCGATCA
 GTTCCGGGGCAGGTGGTACGTTGTGGGCCTGGCAGGCAATGCGGTCCAGAAAAAA**CAGAAGGCAGCTT**
TACGATGTACAGCACCATCTATGAGCTACAAGAGAACAATAGCTACAATGTCACCTCCATCCTGGTCA**G**
CGACCAGGACCAGGGCTGTGCTACTGGATCAGAA**CATTTGTTCCAAGCTCCAGG**GCTGGCCAGTTCAC
 TCTGGGAAATATGCACAGGTATCCTCAGGTACAGAGCTACAATGTGCAAGTGGCCACCACGGACTACAA
 CCAGTTCCGCATGGTATTTTTCCGAAAGACTTCTGAAAAACAAGCAATACTTCAAAATTACCCTGTATGG
 AGAACCAAGGAGCTGTCCCCTGAACTGAAGGAACGTTTCACCCGCTTTGCCAAGTCTCTGGGCCTCAAG
 GACGACAACATCATCTTCTGTCCCACCGACCAATGCATTGACAACCTGAATGGGTGGTGGTGGTGGC
 TGACTGGGATGCGCAGAGACCCAATGGTTCAGGCGCTGCCTGTCTGTCTGCCACTCCATCTTCTTATTTGG
 GCCAGAGAGCCACCTGGCTGCCCCACCAGCCACCATACCAAGGAGCATCTGGAGCCTCTTCTTATTTGG
 CCAGCACTCCCCATCCACCTGTCTTAACACCACCAATGGCGTCCCCTTCT**TGCTGAATAAAATACATGCC**
CAAGCTCGAC

Red highlights: Primers for cDNA amplification for cloning (834bp)
 Yellow highlights: Primers for qPCR analysis (137bp)
 Green highlights: Location of intron 2-3
 Accession number: X81627

CTGF

ATGCTCGCCTCCGTTCGCAGGTCCCATCAGCCTCGCCTTGGTGCTCCTCGCTCTCTGCACCCGGCCTGCT
 ATGGGCCAGGACTGCAGCGCGCAATGTGAGTGCAGCCGAAGCAGCGCCGCACTGCCCGCCGGCGTG
 AGCCTGGTGCTGGACGGCTGCGGCTGCTGCCGCTGCTGCCAAGCAGCTGGGAGAACTGTGTACGGAG
 CGTGACCCCTGCGACCCACACAAGGGCCTCTTCTGCGATTTTCGGCTCCCCCGCAACCGCAAGATCGGA
 GTGTGCACTGCCAAAGATGGTGCACCCCTGTGTCTTCGGTGGGTGCGGTGTACCGCAGCGGTGAGTCCCTC
 CAAAGCAGCTGCAAATACCAATGCACTTGCCTGGATGGGGCCGTGGGCTGCGTGCCCTGTGCAGCATG
 GACGTGCGCCTGCCAGCCCTGACTGCCCTTCCCGAGAAGGGTCAAGCTGCCTGGGAAATGCTGCGAG
 GAGTGGGTGTGTGACGAGCCCAAGGACCGCACAGCAGTTGGCCCTGCCCTAGCTGCCTACCGACTGGAA
 GACACATTTGGCCAGACCCAATATGATGCGAGCCAACCTGGTCCAGACCACAGAGTGGAGCGCC
 TGTTCTAAGACCTGTGGGATGGGCATCTCCACCCGAGTTACCAATGACAATACCTTCTGCAGACTGGAG
 AAGCAGAGCCGCTCTGCATGGTCAGGCCCTGCGAAGCTGACCTGGAGGAAAAATTAAAGAGGGCAAA
 AAGTGCATCCGGACACTTAAAAATCGCCAAGCCTGTCAAGTTTGTAGCTTTCTGGCTGCACCAGTGTGAAG
 ACATACAGGGCTAAGTTCTGCGGGGTGTGCACAGACGGCCGCTGCTGCACACCGCACAGAACCACCACT
 CTGCCAGTGGAGTTCAAATGCCCGATGGCGAGATCATGAAAAAGAATATGATGTTTCATCAAGACCTGT
 GCCTGCCATTACAACCTGTCTGGGGACAATGACATCTTTGAGTCCCTGTACTACAGGAAGATGTACGGA
 GACATGGCGTAA

Yellow highlights: Primers for qPCR analysis (146bp)

Green highlights: Location of intron 4-5

Accession number: NM_010217

IGF-I

ATGACCGCACCTGCAATAAAGATACACATCATGTTCGCTTTCACACCTCTTCTACCTGGCGCTCTGCTTC
 TCACCTTCACCAGCTCCACCACAGCTGGACCAGAGACCTTTGCGGGGCTGAGCTGGTGGATGCTCTTA
 GTTCGTGTGTGGACCCGAGGGGCTTTTACTTCAACAAGCCACAGGCTATGGCTCCAGCATTCGGAGGA
 CCTCAGACAGGCATTGTGGATGAGTGTGCTTCCGGAGCTGTGATCTGAGGAGACTGGAGATGTACTGG
 CCCCCTGAAGCCTACAAAAGCAGCCCGCTCTATCCGTGCCAGCGCCACACTGACATGCCCAAGACTA
 GAAGTCCCCGTCCCTATCGACAAACAAGAAAAACGAAGCTGCAAAAGGAGAAGGAAAGGTGAGCCAAAGAA
 CACCCAGAAGGGGAACAGGAGGAGGTAACGGAGGCAACTCGGAAAAATCAGAGGTCCAGAGAAAAAAGC
 TGGGCTAG

Yellow highlights: Primers for qPCR analysis (242bp)

Green highlights: Location of intron 3-4

Accession number: NM_010512

SFRP2

ATGCCGCGGGGCCCTGCCTCGCTGCTGCTGCTAGTCCCTCGCCTCGCACTGCTGCCTGGGCTCGGCGCGG
GGCTCTTCTCTTCGCCCAGCCCCGACTTCTCCTACAAGCGCAGCAACTGCAAGCCCATCCCCGCCAACT
GCAGCTGTGCCACGGCATCGAGTACCAGAACATGCGGCTGCCAACCTGCTGGGCCACGAGACCATGAG
GAGGTGCTGGAGCAGGCGGGCGCCTGGATTCCGCTGGTCATGAAGCAGTGCCACCCGGACACCAAGAAT
TCCTGTGCTCGCTCTTCGCCCTGTCTGTCTCGACGACCTAGATGAGACCATCCAGCCGTGTCACTCGT
CTGCGTGCAGGTGAAGGACCGCTGCGCCCCGGTCATGTCCGCTTCGGCTTCCCCTGGCCAGACATGCC
GAGTGCAGCCGTTTCCCGCAGGACAACGACCTCTGCATCCCCCTCGCTAGTAGCGACCACCTCCTGCCG
CCACAGAGGAACTCCCAAGGTGTGTGAAGCCTGCAAAACCAAGAA TGAGGACGACAACGACATCATGA
AACCTTTGTAAAAATGACTTCGCACTGAAAATCAAAGTGAAGGAGATAACGTACATCAACAGAGACAC
AAGATCATCCTGGAGACAAAGAGCAAGACCATTTACAAGCTGAACGGCGTGTCCGAAAGGGACCTGAAA
AATCCGTGCTGTGGCTCAAAGACAGCCTGCAGTGCACCTGTGAGGAGATGAACGACATCAACGCTCCGA
TCTGGTCATGGGACAGAAGCAGGGCGGCGAGCTGGTGATCACCTCCGTGAAACGGTGGCAGAAGGGCCG
AGAGAGTTCAAGCGCATCTCCCGCAGCATCCGCAAGCTGCAATGCTAG

Yellow highlights: Primers for qPCR analysis (97bp)

Green highlights: Location of intron 1-2

Accession number: NM_009144

Lumican

ATGAATGTATGTGCGTTCTCTCTTGCCTTGGCATTAGTCGGTAGTGTCACTGGCCAATACTACGATTAG
ACATCCCTCTTTCATGTATGGGCAAATATCACCCAAGTGTGCACCAGAATGTAAGTGCACCCACAGCA
CCCAACTGCCATGTACTGTGATGACCTCAAGTTGAAGAGTGTGCCAATGGTTCCCTCCTGGCATCAAGTC
CTTTACCTGAGGAATAACCAAATCGACCATATTGATGAGAAGGCCCTTTGAGAACGTCACAGACCTGCAT
GGCTCATTCTTGACCACAACCTTCTAGAAAACCTCAAGATCAAAGGAAAGGTTTTCTCTAAGCTGAAAA
ACTGAAGAACTGCATATAAACTACAACAACCTGACCGAGTCCGTCGGTCCACTTCCAAAGTCCCCTGCA
GACCTACAGCTGACCAATAATAAAATCAGCAAGCTCGGCTCCTTCGACGGGCTGGTCAACTTGACCTTA
TTTATCTTCAACACAACCAGCTCAAAGAGGATGCTGTCTCGGCTTCTCTGAAAGTCTCAAATCACTAA
GTACCTGGATTTGAGCTTCAATCAGATGAGCAAGCTGCCTGCTGGTCTACCTACATCTCTTCTAATCC
TACCTAGACAATAATAAGATCAGCAACATTCCGGATGAGTACTTCAAGCGCTTCACTGGGCTGCAATAC
TGCGTTTATCTCACAATGAACTGGCTGATAGTGGGGTACCTGGAACTCGTTTAAATATATCATCCTTGT
CGAGCTTGATCTCTCC TATAATAAGCTTAAAGAGTATACCAACAGTTAATGAAAATCTTGAAAATTATTC
CTGGAGGTCAATGAACTTGAAA GTTTGATGTGAAGAGCTTC TGTAAAGATCCTGGGACCACTG TCTTAT
CCAAGATCAAGCATCTGCGCTTGATGGCAATCCTCTCACTCAGAGCAGTCTGCCCTCTGACATGTATA
GTGTCTACGTGTAGCAAATGAAATCACCGTTAACTAA

Yellow highlights: Primers for qPCR analysis (135bp)

Green highlights: Location of intron 2-3

Accession number: NM_008524

Integrin alpha 10

ATGGAGTCTCTCTCCATCCCTCACCTGCTCCTGCCCTGGCGTTGCTGACAGGTCTCTGCTCCTCCTTT
 AATCTGGATGAACACCACCCACGACTCTTACAGGGCCACCAGAGCCGAATTTGGATACAGTGTCTTA
 CAGCATGTTGGGGGTGGACAGCGATGGATGCTGGTGGGTGCCCTTGGGATGGGCCATCAGGTGACCGG
 AGAGGGGATGTTTATCGTTGCTCTATAGGGGGATTCCACAGTGCTCCATGTACCAAAGGCCACCTGGGT
 GACTATCAACTTGGAAATTCCTCTCAGCCTGCTGTGAATATGCACCTAGGGATGTCTCTACTAGAGACA
 GATGCTGATGGGGGATTTCATGGCCTGTGCCCTCTTTGGTCTCGTGCCTGCGGCAGCTCTGTCTTCACT
 TCTGGAATATGTGCCCGTGTGGATGCTTCATTCCGGCCCCAGGGAAGCTGGCACCCACCGCCAACGC
 TGTCCACATACATGGATGTCGTCAATTGTTTTGGATGGCTCCAACAGTATCTATCCCTGGTCAGAAGTT
 CAGACTTTCCTTCGGAGGCTGGTAGGAAGACTGTTTCATCGATCCGGAGCAGATACAGGTAGGACTGGTA
 CAGTACGGGGAGAACCCTGTGCATGAGTGGTCCCTGGGAGACTTCCGAACAAAGGAAGAAGTTGTGAGA
 GCAGCAAGGAACCTAAGTCGGAGGGAAGGGCGAGAAAACGAGAACCCGCCAAGCGATCATGGTGGCATGC
 ACAGAAGGGTTCACTCAGTCCCGGGGGGACGACCAGAGGCCGCTAGGCTGCTGGTAGTTGTCACTGAT
 GGAGAGTCCCATGATGGAGAGGAACCTCCAGCAGCGCTAAAGGCCGTGTGAGGCTGGCAGAGTGACACGT
 TATGGGATTGCGGTCTTGGTCACTATCTCCGGCAGCAGAGAGACCCAGCTCTTTTCTTCGGGAAATC
 AGAGCTATTGCTAGTGAATCCAGATGAGCGATTCTTCTTCAATGTACCGATGAAGCTGCGCTGACAGAC
 ATTTGGATGCACCTGGGGACCGAATTTTTGGTCTTGAAGGGTCCCGTGGAGAAAAATGAAAGCTCCTTTT
 GGGCTAGAAATGTCTGAGATTGGCTTCTCCATCCAGGACTACAGGATGGGATTCTCTTTGGGATGGTG
 GGGCCTATGACTGGGGGGCTCCGTGCTATGGCTTGAAGAAGGTCGCCCTTTTCCACCACAAGCT
 GCCCTGGAAGATGAGTTCCCCCTGCGTTGCAGAACCATGCGGCCACCTGGGTTACTCTGTTTTCTCC
 ATGCTTCTTCCCGGTGGACGCCGCTCTTTCTCTCAGGGGCACCGAGGTTTAGACATCGAGGAAAAGTT
 ATCGCCTTCCAGCTAAAGAAAAGATGGGGTTGTGAGGGTCGCCAGAGCTCCAGGGGGATCAGATTGGC
 TCATACTTTGGCAGCGAGCTCTGCCCGTTGGATACAGATAAGGACGGAATAACTAATATCTTACTTGTG
 GCGGCTCCCATGTTTCTGGGTCCCAGAACAAAGGAGACCGGACGCGTTTATGTGTACATGGTGGGCCAG
 CAAAATTTGCTAATGCTCCAAGGAACCCCTCAGCCAGACCGTTCCAGGATTCTCGTTTTGGCTTTGCC
 ATGGCTGCTCTTCTGATCTGAACCATGATGGTTTCACTGATGTAGCGGTGGGGGCACCCCTGGAGGAT
 GGACACCGGGGAGCGTTGTACCTGTATCATGGAACCCAGACTGGAATCAGGCCGATCCTACCCAGAGG
 ATTGCTGCTGTCTCCATGCCACAGGCCCTCCGATACTTCCGCCGAAGTGTGGATGGCCGCTTAGATCTG
 GATGGAGATGATCTTGTAGATGTTGCCGTGGGTGCCACGGGGCAGCCGTTCTGTTCCAGCTCCCAGCCC
 ATCATCCACCTGATTCCAACCCTGGATGTGATGCCTCCCCACATCAGTGTGGTTCCAGAAGGACTGTA
 AGACGAGGCCAGGAAGCAGCCTGTCTGACCGCAGCCCTTTGCTTCCAAGTAGTGTCTCAAACCTCCTGGG
 CGTTGGGATAGAAGATTCTACATAAGATTCTCAGCATCACTGGATGAGTGGACCGCTGGGGCAGTGCA
 GTATTTCGATGGCTCTGGTCAGCGCCTGTCCCCTCGGCAGCTCCAGCTTAGTGTGGCAATGTCACTTGT
 GAACAGCTGCACCTTCCATGCACTGGATACATCGGATTACCTCCGGCCAGTGGCCTTGACTTTTT
 GCTTTGGACAACACCACGAAGCCAGGGCCTGTGCTGGCGGAAGGATCCTCTACGATAATACGGAAGCTG
 ATCCCCTTCTCAAAGGACTGTGGCCCTGACAATGAATGTGTACAGACCTGGTGTCTTCAAGCTGACATG
 GACATCAGAGGCTCCAGGAAGTCCCCATTTGTGGTTCAAGGTGGACGACAGAAAGTGTGGTGTCTGCG
 ACCCTGGAGAACAAGAAGGAGAATGCCTACAACACTAGCCTGAGTCTCAGCTTTTTCTAGAAACCTCCAC
 CTGGCCAGTCTTACTCCTCAGAAGGCCAAATCAGTGAAGGTGGAGTGCAGTCCCTTCCCCCATAACC
 CGGCTCTGCACCGTGGGGCATCCGGTCTTCCAGACTGGGGCCAAGGTGAGCTTCCCTGTTAGAGTTTGAA
 TTTAGCTGCACCTTCCCTCCTGAGCCAGGTCTTTGTGAGGCTGACTGCCAGTAGCAGTAGCCTAGAGATG
 AATGAGACCCCTTCAAGATAACACAGCTCAGACCTCTGCCTACATCCGGTACGAACCTCACCTCGTGTTC
 TCCAGTGAGTCCACTCTGCATCGGTATGAGGTTACCCTTATAGGACTCTCCCAATGGTCTCTGGCCCT
 GAATTC AAGACCACTCTTAGGGTT CAGAATCTTGGTTGCCATGTGGT CAGTGGTCTCGTCATCTCCGCC
 CTCCTTCCAGCTGTAGCCCATGGGGGTA ACTACTTCTCTGCTACTATCTCAAGT CATCTCTGGCAATGCA
 AGCTGCACGGTGCAGAACCTGACTGAGCCCCGGGCTTCCCTGTGCACCCAGAGGAGCTTCAGCATGCA
 AGCAGACTGAATGGGAGTAACAGTGCATGTCAGGTGGTAAGGTGCCACCTTGGACTGCTGGCAAAGGGG
 ACTGAGATCTCTGT CAGGCTG **CTGAGGCTGGTTCACAATGA** ATTCTTTTCGGAG **GC** CCAAGTTCAAGTCT
 GTGACAGTGGT CAGCACCTTCAAGTTAGGAACTGAGGAGGGCAGTGTCTTA **CTACTGAATGAAGCCTCC**
CGCTCGAGTGAGAGTCACTTGGAGGTGATT CAGACCCACCCGACCCTCATCTCCCTGTGGATCCTCGTT
 GGCAGTGTCTGGGGGGCTGCTCCTGCTTGTCTCTCTTGTCTTCTGCTGTGGAAGCTTGGCTTCTTT
 ACCCGTAAGAAAATCCCCAAGAAGAGAAAGT GAGGAGAAGTTGGAGCAGTGA

Yellow highlights: Primers for qPCR analysis (119bp)

Green highlights: Location of intron 27-28

Accession number: NM_001081053

Dentin Matrix Protein 1

ATGAAGACTGTCAATTCTCCTTGTGTTCCCTTTGGGGGCTGTCTGTGCTCTCCCAGTTGCCAGATACCAA
 ATACTGAATCTGAAAGCTCTGAAGAGAGGACGGGTGATTTGGCTGGGTCAACCACCACCACCACGAACG
 TGAGTCATCAGAAGAAAGTCAAGCTAGCCCAGAGGACAGCAAATAGTGACCACACGGACAGCAGTGA
 TCTGGAGAGGAGCTGGGCTACGACAGAGGCCAGTACAGACCCGGCTGGTGGACTCTCTAAGAGTACGGGA
 CCGGCGCCGATAAAGGAGGATGATGAAGACGACAGTGGAGATGATACCTTTGGCGATGAGGACAATGATT
 AGGGCCCCGAAGAAGGACAGTGGGGAGGACCTCCAAACTGGACAGTGTGAGGACTCCACAGACACCAA
 CAGTCCAGTGAAGACAGCACCTCTCAAGAAAAAGTGCCTAAGATAACCCAGCGACAGCAAAGACCAG
 ACAGTGGAGGATGAGGCAGACAGCCGGCCTGAGGCAGGCGACTCCACTCAGGACAGTGTGAGAGTGGAGAA
 GCGGGTGGGAGGTGGCAGCGAGGGGGAGAGTAGCCACGGGGACGGTTCTGAGTTCGATGATGAAGGGAG
 CAGAGCGACGACCCCGAGAGTACCAGGAGCGATCGAGGCCACGCCAGAATGAGCAGCGCTGGTATCAGT
 CGGAAGAATCTAAAGGGGACCACGAGCCCACGAGCACTCAGGATTCAGATGACAGCCAGTCTGTGGAAT
 TTCAAGCAGGAAGTCTTCAGAAAGTCCCACGTCTCTGAGGAAGACTACAGAGGTGAGCTTACTGACAC
 AACAGCAGGGAAACCCAGAGCGACTCCACGGAGGATACGGCCTCCAAGGAGGAAAGCAGGAGCGAGTCC
 AGGAGGACACAGCCGAGAGCCAGTCCCAGGAAGATAGCCAGAGGGGCAAGACCCAGCAGTGTGAGTCCG
 CGAAGAGGCTGGTGTAGCCATCCCAGGAAAGCAGCAGCGAATCTCAGGAAGGGGTGACCAGCGAGTCCAG
 GGTGACAACCCAGATAACACAAGTCAAGCAGGAGACCAAGAAGACAGTGTGAGTCCAGTGTGAGGAGGACAGC
 TGAACACATTCTCCAGCTCAGAAAGCCAGTCCACCGAGGAGCAAGCTGACAGCGAGTCCAACGAGAGCT
 CAGCCTCTCCGAGAGGATCAGGAGTCGGCCAGGATGGTGACAGCTCCAGCCAGGAAGGCCCTGCAGTC
 CAGAGCGCATCCACTGAGAGCAGGAGCCAGGAGCCAGTCTGAGCAGGACAGCCGTTCTGAGGAAGAA
 GTGACTCTCAGGACAGTAGCCGATCCAAAGAAGAGAGCAACTCCACAGGGAGCGCTTCCAGCAGCGAGA
 GGACATCCGTCCCAAGAACATGGAAGCTGACAGTAGGAACTAATAGTTGATGCTTACCACAACAAACC
 ATCGGGGACCAAGATGACAATGACTGTGACAGGACGGCTACTAG

Yellow highlights: Primers for qPCR analysis (120bp)

Green highlights: Location of intron 5-6

Accession number: NM_94910

SGCK

ATGACCGTCAAAGCCGAGGCTGTCTGAAGCACCTTACCTACTCCAGAATGAGGGGAATGGTAGCGATC
 TCATCGCTTTTATGAAACAGAGAAGGATGGGCTGAACGATTTTATTCAGAAGATTGCCAGCAACACCA
 TGCATGCAAACAGCTGAAGTTCAGTCCATTTTGAATAATGTCCCATCCTCAGGAGCCGGAGCTTATGAC
 GCTAACCCTCTCCTCCGCAAGTCCCTCTCAACAAAATCAACCTGGGTCCGTCCCTCCAACCCTCACGCA
 AACCTCCGACTTTCACTTCTTGAAGTGTATCGGAAAAGGCAGTTTTGGAAAGGTTCTTCTGGCTAGGA
 CAAGGCAGAAGAAGTATTCTATGCAGTCAAAGTTTTACAGAAGAAAGCCATCCTGAAGAAGAAAGAGGG
 AAGCATATTATGTGAGAGCGGAATGTTCTGTTGAAGAATGTGAAGCACCTTTCTCGTGGTGGCCCTTCAT
 TCTCATTCCAGACCGCTGACAAGCTCTACTTTGTCTGGACTACATTAATGGTGGAGAGCTGTTCTACA
 TCTCCAGAGGGAGCGCTGCTTCTGGAACCACGGGCTCGATTCTACGCAGCTGAAATAGCCAGTGCCCG
 GGCTATCTGCACTCCCTAAACATCGTTTATAGAGACTTAAAACCTGAGAATATTCTCCTAGACTCCCAG
 GGCACATCGTCCCTCACTGACTTTGGGCTCTGCAAAGAGAATATTGAGCATAACGGGACAACATCTACCT
 CTGTGGCAGCCTGAGTATCTGGCTCCTGAGGTCTCCATAAGCAGCCGTATGACCCGACGGTGGACTG
 TGGTGTCTTGGGGCTGTCTGTATGAGATGCTCTACGGCCTGCCCCGTTTTATAGCCGGAACACGGCG
 AGATGTACGACAATATTCTGAACAAGCCTCTCCAGTTGAAACCAAATATTACAAACTCGGCAAGGCACT
 CCTGGAAGGCCTCCTGCAGAAGGACCGGACCAAGAGGCTGGGTGCCAAGGATGACTTTATGGAGATTAG
 AGTCATATTTTCTTCTTTAATTAAGTGGGATGATCTCATCAATAAGAAGATTACACCCCATTTAAC
 CAAATGTGAGTGGGCCAGTGACCTTCGGCACTTCGATCCCAGTTTACCGAGGAGCCGGTCCCCAGCC
 CATCGGACAGTCCCCTGACAGCATCCTTGTACGGCCAGTGTGAAGGAAGCAGCAGAAGCCTTCTCTCG
 TTCTCCTATGCACCTCCTGTGGATTCTTCTCTGA

Yellow highlights: Primers for qPCR analysis (129bp)

Green highlights: Location of intron 2-3

Accession number: NM_340062

Collagen type X

ATGCTGCCTCAAATACCCCTTTCTGCTGCTAATGTTCTTGACCCCTGGTTCATGGGATGTTTTATGCTGAC
 GGTACCAAACGCCACAGGCATAAAGGGCCCACTTGGCTAGCCCCAAGACACAATACTTCATCCCATAACC
 CATAAAGAGTAAAGCGGATTCCAGTAAGAGGAGAACAAGGCATTCCTGGTCCACCAGGCCAACCGGACT
 CGAGGACACCCAGGTCCCTCAGGACCGCCAGGCAAGCCAGGCTATGGAAAGTCTGGACTCCAAGGAGAC
 CAGGGTTGCCAGGACCACCAGGAATATCAGCCACGGGGAAAGCCAGGCCTGCCAGGCCCCGAGGCAAAC
 AGGGGAGAGAGGACCATATGGACACAAAGGAGATATTGGCCAGCTGGCTTACCCGGACCTCGGGGCCCT
 CCAGGGCCCCCTGGAATTCCTGGCCAGCTGGAATTTCTGTGCCAGGAAAACCTGGACAGCAGGGACTA
 CAGGTGCCCCAGGACCTAGGGGCTTTCTGGAGAGAAGGGTGCACAAGGAGCCCCCTGGTGTGAATGGGG
 GAAAGGGGAAACAGGATATGGCTCTCTGGCCGTCCAGGTGAGAGGGTCTTCCAGGCCCTCAAGGTCC
 ATAGGACCCCTGGCCCCCTCTGGAGTGGGAAGAAGAGGTGAAAACGGCTTTCCAGGACAGCCGGGCATA
 AAGGTGACCGGGGTTTCCCAGGAGAAATGGGACCATCAGGTCCACCAGGTCCCCAAGGTCCCTCCCGGGA
 GCAAGGACGAGAAGGTATTGGGAAGCCAGGAGCCATTGGATCCCTGGTCAGCCAGGTATCCCAGGAGA
 AAAGGCCACCCAGGGGCTCCAGGAATAGCTGGTCCCTCCAGGAGCTCCTGGCTTTGGAAAACAAGGCTTC
 CAGGTTTGGAGGGGACAAAGGGGACCTGCTGGTCTTCTGGGGCTCCAGGTGCCAAAGGGGAACGAGGGC
 AGCAGGTATCCTGGAGAACCAGGGTCTGCCTGGATCCCTGGGAATATGGGACCCCAAGGACCTAAAGA
 ATCCCAGGGAACCATGGCATTCCAGGCGCTAAAGGTGAGATAGGTCTAGTTGGCCCTGCAGGCCCCCG
 GGGCTAGAGGAGCAAGGGGTCCACCTGGGTAGATGGAAAAACAGGGTATCCTGGGGAGCCAGGTCTCA
 TGGTCCCTAAGGGTAACCCAGGGTTACCAGGACAAAAAGGTGATCCTGGAGTGGGAGGAACCCCTGGTCT
 CGAGGTCTGTTGGCCCTGTAGGAGCTAAAGGAGTGCCTGGACACAATGGTGGAGCAGGTCCAAGAGGG
 AACCTGGAATACCAGGTACCAGGGGCCCCACTGGGCCACCAGGTGTCCAGGATTCCCTGGATCTAAGG
 TGACCCTGGAAACCCAGGTGCTCCAGGCCCAGCTGGCATAAGCAACTAAGGGCCTCAATGGGCCACTGT
 CCTCCAGGCCCTCCTGGTCCAAGAGGCCACAGTGGAGAACCCTGGTCTCCAGGTCCCTCCGGGTCCCCCG
 GACCCCCCGCCAAGCAGTCATGCCTGATGGCTTCATAAAGGCAGGCCAGAGGCCAGGCTTTCTGGGT
 GCCGCTTGTGAGTGTAAACACGGGGTAAACAGGTATGCCCGTGTCTGCTTTTACTGTCAATCTCTCTAA
 GCTTACCCAGCAGTAGGTGCCCCATCCCATTTGATGAGATTCTGTACAATAGGCAGCAGCATTACGAC
 CAAGATCTGGTATCTTTACCTGTAAGATCCCAGGCATATACTATTTCTCCTACCACGTGCATGTGAAAG
 GACTCACGTTTGGGTAGGCCTGTATAAGAACGGCACGCTACGATGTACACGTATGATGAGTACAGCAA
 GGCTACCTGGATCAGGCTTCAGGGAGTGCAATCATGGAGCTCACAGAAAATGACCAGGTATGGCTCCAT
 TGCCCAATGCAGAATCAAACGGCCTCTACTCCTCTGAGTACGTCCACTCGTCTTCTCAGGATTCCTAT
 GGCTCCCATGTGA

Yellow highlights: Primers for qPCR analysis (97bp)

Green highlights: Location of intron 1-2

Accession number: NM_84455

p21

ATGTCCAATCCTGGTGTGATGTCGACCTGTTCCGCACAGGAGCAAAGTGTGCCGTTGTCTCTTCGGTCCG
 TGGACAGTGAGCAGTTGCGCCGTGATTGCGATGCGCTCATGGCGGGCTGTCTCCAGGAGGCCCGAGAAG
 GTGGAACCTTTGACTTCGTACCGGAGACGCCGCTGGAGGGCAACTTCGTCTGGGAGCGGTTCCGGAGCCT
 AGGGCTGCCAAGGTCTACCTGAGCCCTGGGTCCCGCAGCCGTGACGACCTGGGAGGGGACAAGAGGCC
 AGTACTTCTCTGCCCCTGCTGCAGGGGCCAGCTCCGGAGGACCACGTGGCCTTGTGCTGCTTGGCACC
 TGGTGTCTGAGCGCCCTGAAGATTCCCCGGGTGGGGCCGAACATCTCAGGGCCGAAAACGGAGGCAGC
 CAGCCTGACAGATTCTATCACTCCAAGCGCAGATTGGTCTTCTGCAAGAGAAAACCCCTGA

Yellow highlights: Primers for qPCR analysis (113bp)

Green highlights: Location of intron 1-2

Accession number: NM_104556